# รายงานวิจัยฉบับสมบูรณ์

# การดัดแปรฟิล์มแอมโมนิโอเมธาคริเลตโคพอลิเมอร์โดยใช้แมกนีเซียมอะลูมินัมซิลิเคตและโซเดียมอัลจิเนต: การศึกษาคุณลักษณะทางเคมีฟิสิกส์และการใช้ประโยชน์สำหรับการเคลือบยาเม็ด

# Modification of ammonio-methacrylate copolymer films using magnesium aluminum silicate and sodium alginate: physicochemical characterization and application for tablet film coating

โดย

ศาสตราจารย์ ดร. ธเนศ พงศ์จรรยากุล และคณะ
สาขาวิชาเทคโนโลยีเภสัชกรรม
คณะเภสัชศาสตร์ มหาวิทยาลัยขอนแก่น

สิงหาคม 2558

สัญญาเลขที่ BRG5580016

# รายงานวิจัยฉบับสมบูรณ์

# การดัดแปรฟิล์มแอมโมนิโอเมธาคริเลตโคพอลิเมอร์โดยใช้แมกนีเซียมอะลูมินัมซิลิเคตและโซเดียมอัลจิเนต: การศึกษาคุณลักษณะทางเคมีฟิสิกส์และการใช้ประโยชน์สำหรับการเคลือบยาเม็ด

# Modification of ammonio-methacrylate copolymer films using magnesium aluminum silicate and sodium alginate: physicochemical characterization and application for tablet film coating

**คณะผู้วิจัย**

**ศาสตราจารย์ ดร. ธเนศ พงศ์จรรยากุล**

**นางสาวฐิติพร รองทอง**

**นางสาวณัฐนิชา เกื้อทาน**

**สาขาวิชาเทคโนโลยีเภสัชกรรม**

**คณะเภสัชศาสตร์ มหาวิทยาลัยขอนแก่น**

**สนับสนุนโดย**

**สำนักงานกองทุนสนับสนุนการวิจัย**

(ความเห็นในรายงานนี้เป็นของผู้วิจัย สกว. ไม่จำเป็นต้องเห็นด้วยเสมอไป)

## บทคัดย่อ

วัตถุประสงค์ของงานวิจัยนี้เพื่อศึกษาคุณลักษณะของฟิล์มผสมแอมโมนิโอเมธาคริเลตโคพอลิเมอร์ (ควอเทอร์นารีพอลิเมธาคริเลต) และแมกนีเซียมอะลูมินัมซิลิเคต หรือโซเดียมอัลจิเนต สำหรับใช้ในการเคลือบฟิล์มยาเม็ด ฟิล์มผสมสามารถเตรียมด้วยวิธีการหล่อแบบและระเหยตัวทำละลาย จากนั้นศึกษาคุณสมบัติเคมีฟิสิกส์ คุณสมบัติเชิงกล ความเหนอะ และสภาพให้ซึมผ่านได้ของยา และยังศึกษารูปแบบการปลดปล่อยยาจากยาเม็ดที่เคลือบด้วยฟิล์มผสม ผลการศึกษาพบว่า ประจุบวกของควอเทอร์นารีพอลิเมธาคริเลต สามารถเกิดอันตรกิริยากับประจุลบของหมู่ไซลานอลของแมกนีเซียมอะลูมินัมซิลิเคต หรือหมู่คาร์บอกซิลของโซเดียมอัลจิเนต อันตรกิริยาระดับโมเลกุลของควอเทอร์นารีพอลิเมธาคริเลตและแมกนีเซียมอะลูมินัมซิลิเคต ทำให้เกิดฟิล์มผสมนาโนแบบสอดแทรก การผสมแมกนีเซียมอะลูมินัมซิลิเคตหรือโซเดียมอัลจิเนต สามารถลดความเหนอะของฟิล์มควอเทอร์นารีพอลิเมธาคริเลตทั้งในสถานะแห้งและเปียก ความต้านแรงเจาะและการยืดของฟิล์มผสมแห้งลดลงเมื่อเพิ่มอัตราส่วนของแมกนีเซียมอะลูมินัมซิลิเคตหรือโซเดียมอัลจิเนต ในขณะที่ฟิล์มเปียกมีความแข็งแรงเพิ่มขึ้น การดูดน้ำของฟิล์มผสมลดลงเมื่อเพิ่มอัตราส่วนของแมกนีเซียมอะลูมินัมซิลิเคตหรือโซเดียมอัลจิเนต ซึ่งนำไปสู่การลดลงของสภาพให้ซึมผ่านได้และสภาพแพร่ของยา การใช้ชนิดของบล็อกโซเดียมอัลจิเนตที่แตกต่างกันมีผลต่อคุณลักษณะของฟิล์มผสม เช่น ความแข็งแรง การดูดน้ำและสภาพให้ซึมผ่านได้ของยา นอกจากนี้ ชนิดของยาและมวลโมเลกุล (สายโซ่ไฮโดรคาร์บอน) ของยามีอิทธิพลต่อคุณลักษณะการซึมผ่านฟิล์มผสม ฟิล์มผสมที่ได้จากการศึกษานี้สามารถใช้ในการเคลือบยาเม็ดได้ การดูดน้ำและการปลดปล่อยยาของยาเม็ดเคลือบฟิล์มผสมขึ้นกับอัตราส่วนของแมกนีเซียมอะลูมินัมซิลิเคตหรือโซเดียมอัลจิเนตที่เติม และระดับการเคลือบฟิล์ม กระบวนการบ่มยาเม็ดเคลือบฟิล์มผสมมีความจำเป็นต่อการเกิดฟิล์มที่เป็นเนื้อเดียวกันหลังจากกระบวนการเคลือบ ซึ่งมีผลให้การปลดปล่อยยาจากยาเม็ดเคลือบที่ผ่านการบ่มช้าลง การศึกษานี้ชี้ให้เห็นว่า การผสมแมกนีเซียมอะลูมินัมซิลิเคตหรือโซเดียมอัลจิเนต สามารถลดความเหนอะของฟิล์มควอเทอร์นารีพอลิเมธาคริเลต และเพิ่มความแข็งแรงของฟิล์มเปียก นอกจากนี้ ฟิล์มผสมทั้งสองสามารถใช้เป็นวัสดุเคลือบฟิล์มยาเม็ดสำหรับการดัดแปรรูปแบบการปลดปล่อยยาของยาเม็ด

**คำสำคัญ:** ควอเทอร์นารีพอลิเมธาคริเลต, แมกนีเซียมอะลูมินัมซิลิเคต, โซเดียมอัลจิเนต, ฟิล์มผสมนาโน, ความเหนอะ, การเคลือบฟิล์มยาเม็ด, การบ่ม

## Abstract

The objective of this research was to characterize the composite films of ammonio-methacrylate copolymer, quaternary polymethacrylate (QPM), and magnesium aluminum silicate (MAS) or sodium alginate (SA) for use in tablet film coatings. The composite films were prepared using a casting/solvent evaporation method. Physicochemical properties, mechanical properties, tackiness, and drug permeability were investigated, and drug release pattern of tablets coated with the composite films was examined as well. The results showed that the positively charged QPM could interact with the negatively charged silanol groups of MAS or the carboxyl groups of SA. The molecular interaction between QPM and MAS caused intercalated nanocomposite films. Incorporation of MAS or SA reduced a tackiness of the QPM films in both dry and wet states. The puncture strength and elongation of the dry composite films decreased with increasing MAS or SA ratio in the films, whereas increase of wet film strength was found. The water uptake of the composite films decreased with increasing MAS or SA ratio, leading to lower drug permeability and diffusivity. Different block types of SA used also affected composite film characteristics, such as strength, water uptake and drug permeability. Additionally, drug type and molecular weight (hydrocarbon side chain) of drug influenced permeation characteristic of the QPM-MAS films. Both composite films could be used for tablet coating. The water uptake and drug release of the coated tablets were dependent on MAS or SA ratio added, and film coating level. Curing process in the QPM-MAS coated tablets was also necessary to produce the homogeneous film formation after coating process, which caused slower drug release of the coated tablets with curing. This study indicates that incorporation of MAS or SA can reduce tackiness of the QPM films and can also strengthen the films in the wet state. Moreover, the QPM-MAS or QPM-SA films can be used as a tablet film coating material for modifying drug release pattern of tablets.

**Keyword:** quaternary polymethacrylate, magnesium aluminum silicate, sodium alginate, nanocomposite film, film coating, curing

## Executive summary

การเคลือบฟิล์มยาเม็ดมีความสำคัญในอุตสาหกรรมยาเป็นอย่างมาก แอมโมนิโอเมธาคริเลตโคพอลิเมอร์ (ควอเทอร์นารีพอลิเมธาคริเลต) เป็นพอลิเมอร์ที่ใช้เป็นวัสดุเคลือบยาเม็ดอย่างแพร่หลาย รูปแบบสารกระจายในน้ำของควอเทอร์นารีพอลิเมธาคริเลตเป็นที่นิยมมาก เพราะสามารถลดการใช้ตัวทำละลายอินทรีย์ที่ใช้ในการละลายพอลิเมอร์ได้ อย่างไรก็ตาม พอลิเมอร์ชนิดนี้มีข้อจำกัดของสภาพให้ซึมผ่านได้ของยาและความเหนอะของฟิล์ม ด้วยสาเหตุนี้ ทำให้เกิดงานวิจัยด้านวัสดุศาสตร์เพื่อค้นหาวัสดุที่จะนำมาผสมกับฟิล์มชนิดนี้และสามารถดัดแปรคุณสมบัติของฟิล์มให้ดีขึ้น สารที่มีประจุลบที่สามารถใช้เพื่อวัตถุประสงค์นี้ ได้แก่ แมกนีเซียมอะลูมินัมซิลิเคตซึ่งเป็นสารกลุ่มดินเหนียว และโซเดียมอัลจิเนตซึ่งเป็นพอลิแซ็กคาไรด์ ผลการศึกษา พบว่า ประจุบวกของควอเทอร์นารีพอลิเมธาคริเลต สามารถเกิดอันตรกิริยากับประจุลบของหมู่ไซลานอลของแมกนีเซียมอะลูมินัมซิลิเคตหรือหมู่คาร์บอกซิลของโซเดียมอัลจิเนต ฟิล์มผสมสามารถเตรียมด้วยวิธีการหล่อแบบและระเหยตัวทำละลาย อันตรกิริยาระดับโมเลกุลของควอเทอร์นารีพอลิเมธาคริเลตและแมกนีเซียมอะลูมินัมซิลิเคต ทำให้เกิดฟิล์มผสมนาโนแบบสอดแทรก การผสมแมกนีเซียมอะลูมินัมซิลิเคตหรือโซเดียมอัลจิเนต สามารถลดความเหนอะของฟิล์มควอเทอร์นารีพอลิเมธาคริเลตทั้งในสถานะแห้งและเปียก ความต้านแรงเจาะและการยืดของฟิล์มผสมแห้งลดลงเมื่อเพิ่มอัตราส่วนของแมกนีเซียมอะลูมินัมซิลิเคตหรือโซเดียมอัลจิเนต ในขณะที่ฟิล์มเปียกมีความแข็งแรงเพิ่มขึ้น การดูดน้ำของฟิล์มผสมลดลงเมื่อเพิ่มอัตราส่วนของแมกนีเซียมอะลูมินัมซิลิเคตหรือโซเดียมอัลจิเนต ซึ่งนำไปสู่การลดลงของสภาพให้ซึมผ่านได้และสภาพแพร่ของยา การใช้ชนิดของบล็อกโซเดียมอัลจิเนตที่แตกต่างกันมีผลต่อความแข็งแรง การดูดน้ำและสภาพให้ซึมผ่านได้ของฟิล์มผสม นอกจากนี้ ชนิดของยาและมวลโมเลกุลของยามีอิทธิพลต่อคุณลักษณะการซึมผ่านฟิล์มผสม ฟิล์มผสมที่ได้จากการศึกษานี้สามารถใช้ในการเคลือบยาเม็ดได้ การดูดน้ำและการปลดปล่อยยาของยาเม็ดเคลือบฟิล์มผสมขึ้นกับอัตราส่วนของแมกนีเซียมอะลูมินัมซิลิเคตหรือโซเดียมอัลจิเนตที่เติม และระดับการเคลือบฟิล์ม กระบวนการบ่มยาเม็ดเคลือบฟิล์มผสมมีความจำเป็นต่อการเกิดฟิล์มที่เป็นเนื้อเดียวกันหลังจากกระบวนการเคลือบ ซึ่งมีผลให้การปลดปล่อยยาช้าลง ผลลัพธ์ของการศึกษานี้ คือ การได้องค์ความรู้พื้นฐานของการเกิดอันตรกิริยาระดับโมเลกุลระหว่างควอเทอร์นารีพอลิเมธาคริเลตและแมกนีเซียมอะลูมินัมซิลิเคตหรือโซเดียมอัลจิเนต และนำมาซึ่งความรู้ใหม่ของคุณสมบัติของฟิล์มผสม นอกจากนี้ ยังได้ต้นแบบของยาเม็ดเคลือบฟิล์มผสมที่สามารถเตรียมได้ด้วยเครื่องมือจำลองในระดับอุตสาหกรรมยา และฟิล์มผสมสามารถใช้ประโยชน์ในการดัดแปรรูปแบบการปลดปล่อยยาของยาเม็ดได้

# Contents

# Introduction

Film coating of oral solid dosage forms provides many advantages in pharmaceutical manufacturing since it can overcome problems of unpleasant taste and odor of drugs, increase drug stability, and protect degradation of drugs from light, moisture, and oxidation processes (Nagai et al., 1997). Most importantly however, film coating can provide sustained release of drugs and protect the drugs from acid degradation in the gastro-intestinal tract (Wu et al., 1997). Pharmaceutically acceptable polymers used in the film coating are primarily based on acrylic or cellulose polymers. Many of these polymers have been formulated into aqueous colloidal dispersions in order to solve problems involved with the use of organic polymer solutions.

Polymethacrylates, which are known as Eudragit polymer, were the first synthetic polymers used in pharmaceutical coating. Ammonio-methacrylate copolymers or quaternary polymethacrylate QPM are polymethacrylate containing quaternary ammonium groups in the form of aqueous colloidal dispersion, namely Eudragit RS30D (EuRS) and Eudragit RL30D (EuRL) (Lehmann, 1997). Normally, EuRS film gave lower drug permeability than EuRL films. EuRS and EuRL have been used for controlled drug release of pellets, beads and tablets (Bodmeier et al., 1996; Wu and McGinity, 2000). The tablets coated with these polymers presented pH-independent drug release behavior (Bodmeier et al., 1996). The problems of the use of EuRS/RL films are a limitation of film permeability and a tackiness of the films. The blend of EuRS and EuRL at various ratios could modify the drug permeability, but it is limited in the narrow range of drug permeability. To overcome this problem, blending of EuRS or EuRL with some polymers such as pectin (Semdé et al., 1998; Semdé et al., 2000), chitosan (Wittaya-areekul et al., 2006), and hydroxyethylcellulose (Zheng et al., 2005) were investigated. The tackiness of EuRS/RL films caused a film defect, sticking and picking, of the coated tablets. Incorporation of insoluble materials, which were called antitackiness agent such as talc and glyceryl monostearate, is necessary to reduce tackiness of the coated films.

It is interesting to seek biomaterials for improving the properties of QPM films and leading to a high efficiency of the film coating process for pharmaceutical industry. Generally, anionic materials can interact with cationic QPM particles in the dispersion. This may cause a change of film formation of QPM that lead to a change of drug

permeability, tackiness and other physicochemical properties of QPM films. The feasible materials are sodium alginate (SA) and magnesium aluminum silicate (MAS).

SA is an anionic water soluble polysaccharide. It can form a rigid matrix structure in acidic condition. It has been used to produce sustained release drug delivery systems. The electrostatic interaction between SA and cationic polymers such as gelatin (Dong et al., 2006) and chitosan (Remuñán-López and Bodmeier, 1997) can improve mechanical properties of film and modify drug release. The QPM-SA blended film may reduce drug permeability in an acidic medium because SA can enhance the rigid structure of polymeric film due to formation of water-insoluble alginic acid. However, the drug permeation may potentially increase in a neutral pH due to pore formation in the film matrix by leaching of water-soluble SA. Consequently, the QPM-SA blended films are interesting to be used as a novel coating material for sustained release drug dosage form in gastrointestinal tract.

MAS is a mixture of colloidal montmorillonite and saponite clay (Rowe et al., 2006). It is composed of three-lattice layers, a central octahedral sheet of aluminum or magnesium and two external silica tetrahedron layers (Alexandre and Dubois, 2000). The silicate layer surface of clay has a negative charge, but weakly positive charges are present on the edges of the silicate layers. Electrostatic interactions between MAS and chitosan (CS) could form a nanocomposite material that the CS-MAS films showed lower drug permeability and high film flexibility than the CS films (Khunawattanakul et al., 2010). Moreover, the CS-MAS coated tablets gave lower film defect, higher acid stability, and lower drug release rate than the CS coated tablets (Khunawattanakul et al., 2011). From these reasons, incorporation of MAS into the QPM films may form nanocomposites and physicochemical properties of the blended films may be changed when compared with the QPM films. Moreover, it may reduce the tackiness of the QPM films and decrease film defects of the coated tablets during a coating process.

In this research project, the characteristics of QPM -SA and QPM -MAS dispersions at different ratios, such as zeta potential and particle size, were investigated in order to know the interaction between both QPM and SA or MAS in the dispersion form. Then, the blended dispersions were cast to the film using a casting/solvent evaporation method. Physicochemical properties, such as surface and internal structure morphology, thermal behavior, molecular interaction, mechanical properties, tackiness, water uptake, erosion, water vapor permeability, and drug permeability of the blended films were examined. Finally, the QPM-SA and QPM-MAS dispersions were used as a tablet film coating

material. The effect of QPM-SA ratios and QPM-MAS ratios, coating level, and curing condition on water uptake and drug release was also carried out. The QPM-SA and QPM-MAS blended films may be potentially used in tablet film coating intended for modifying drug release in pharmaceutical industry.

## Literature review

### General properties of quaternary polymethacrylates

EuRS and EuRL is synthetic polymer. They are cationic polymers that contain quaternary ammonium group in the structure as shown in Figure 1. They are copolymer of acrylic and methacrylic esters, which are prepared by copolymerization of ethyl acrylate, methyl methacrylate and trimethyl-ammonioehyl methacrylate chloride with a mole ratio of 1:2:0.1 for EuRS and 1:2:0.2 for EuRL. EuRL (10QPM) has 10% of quaternary ammonium functional groups whereas 5% of quaternary ammonium functional groups are found in EuRS (5QPM) (Lehmann, 1997; Rowe et al., 2006). Thus, EuRL provides higher hydrophilicity than EuRS.

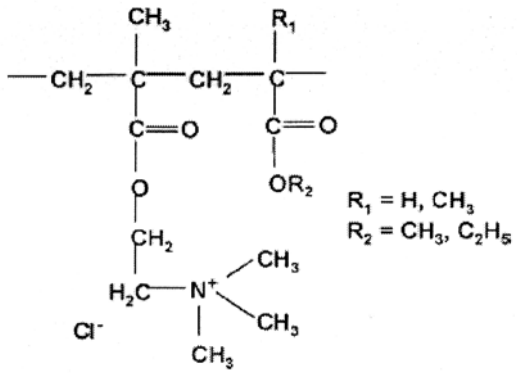


**Figure 1.** Chemical structure of EuRS or EuRL (Sipos et al, 2008).

EuRS and EuRL dispersions contain 30% w/w solid contents of acrylic copolymers. The color of dispersion is milky white liquid. The mean particle size was determined by photon correlation spectroscope was about 158 nanometer and pH of the dispersion was about 5.0. The dispersion contains 0.25% w/w sorbic acid as a preservative and small quantity of sodium hydroxide (Nyamweya et al., 2001). Because of colloidal size and Brownian movement of EuRS/RL30D, the particles in the dispersion do not precipitate. The quaternary ammonium groups are in the chloride salt form and responsible for the

permeability of films. EuRS is miscible with acetone, alcohol, dichloromethane, ethyl acetate, and water. It is insoluble in 1 N sodium hydroxide and petroleum ether (Rowe et al., 2006). EuRS films showed lower permeability than EuRL films, indicating hydrophobic properties of EuRS. However, it can swell in water because of the presence of quaternary ammonium groups in the structure (Knop, 1996). Properties of EuRS/RL films could be improved by addition 10-30% of plasticizers (Bodmeier and Paeratakul, 1997).

EuRS and EuRL have been used in pharmaceutical industry as a tablet film coating for controlled drug release. Drug permeability is the different property between EuRS and EuRL that affected drug release from the coated tablets. The coated tablets using ammonio-methacrylate copolymers gave pH-independent drug release behavior. Then, the applications have been used for controlled drug delivery in oral route in the form of pellets, bead and tablet (Wang et al., 1997; Wu and McGinity, 2000). Additionally, the advantage of aqueous dispersions is environmental protection, and avoidance of organic solvent that used to dissolve (Ghebre-Sellassie et al., 1997).

**Film formation mechanism**

Film formation of colloidal dispersion is an unique mechanism. The particles in dispersion are separated by electrostatic repulsion. During drying process, a strong driving force was necessary to overcome repulsive force and induced coalescence of the particles, which referred to compaction, deformation, cohesion, and polymer chains inter-diffusion of the individual particles. This resulted in a fusion of the particles. High interfacial surface tension of water provided the driving forces to fuse the particles together, the particles coalescence during drying process are shown in Figure 2. The film formation was also depended upon the minimum film formation temperatures (MFT) of the polymer. If the drying temperature was higher than the MFT, polymeric film could be formed. Film formation on the substrate had three stages of drying process as shown in Figure 3. In the first stage of drying process, water evaporated from the dispersion until the concentration of particles increased. This was the longest stage of film formation and the polymer reached approximately 60-70% of volume fraction. The polymeric particles were close to one another and fused together to form a dense sphere. During continued drying process in the second stage, the polymeric particles came into irreversible contact. Then, particle deformation occurred and the particle coalescence happened in the end of this stage. The final stage was the formation of continuous film. The remaining water was

removed from the film and the polymer chains inter-diffusion occurred, resulting in homogeneous film (Wheatley and Steuernagel, 1997).

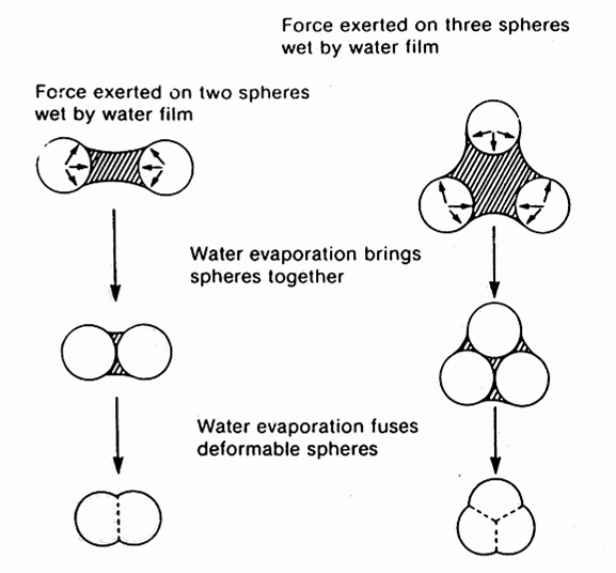


**Figure 2.** Polymeric particle coalescence during the evaporation (Wheatley and Steuernagel, 1997).

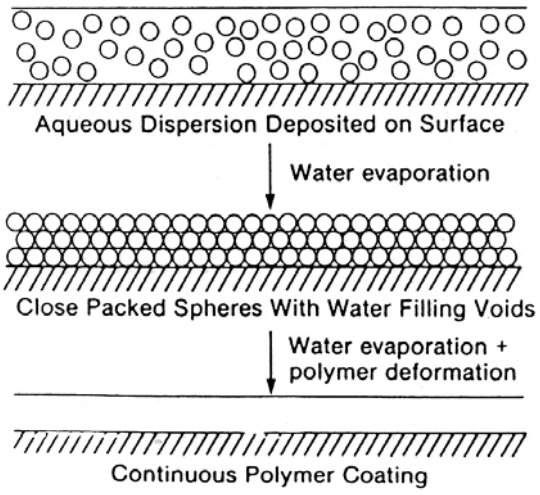


**Figure 3.** Model of the film formation mechanism of aqueous polymer dispersions. (Wheatley and Steuernagel, 1997).

## Characteristics of QPM films

Effect of plasticizers

Plasticizers are film additive, which soften the colloidal polymer particles and enhance coalescence and film formation. These substances often add into Eudragit

dispersion for promoting film formation by decreasing MFT and glass transition temperature. These effects caused a film formation at lower temperature. EuRS dispersions with plasticizer gave more continuous film than those without plasticizer (Bodmeier and Paeratakul, 1990). Thus, films with plasticizers had good flexibility and distensibility.

Plasticizers can be classified into two types; water soluble and water insoluble substances. The thermal properties of acrylic film influenced by amount and types of plasticizers added. MFT was reduced when increasing amount of both types of plasticizers because plasticizer could interact with polymer chains and decrease the intermolecular force between polymer chains, resulting in lower glass-rubber transition temperature. These effects caused the film formation at lower temperature when compared with the film without plasticizer (Saettone et al., 1995; Lehmann, 1997). Water soluble plasticizers could reduce the MFT more than water insoluble plasticizers because they could soluble in the water and rapidly diffuse into the particles (Bodmeier and Paeratakul, 1994), which contained quaternary ammonium groups in the chains.

Mechanical properties

Eudragit films without plasticizer were more brittle and easier to break (Lecomte et al., 2004). Plasticizers added could improve the mechanical properties of film, leading to increase of elongation and decreasing tensile strength. Dry films plasticized with water soluble plasticizers (triethyl citrate and triacetin) gave higher elongation and lower puncture strength than those plasticized with water insoluble plasticizers. The difference in mechanical properties explained with the different plasticizing efficiencies of plasticizer on the polymer particles. However, wet films had lower puncture strength than dry film because of hydration of Eudragit polymer (Bodmeier and Paeratakul, 1994). The puncture strength of dry EuRS and EuRL films did not different but the difference founded in wet films. EuRL films gave lower puncture strength and higher elongation than EuRS films. This was due to more water hydration of EuRL films with higher quaternary ammonium groups (Bodmeier and Paeratakul, 1994)

Thermal properties

The thermal properties of Eudragit are presented as glass transition temperature and minimum film formation temperatures (MFT). The MFT of the dispersion is over the range of 40-50 °C (Lehmann, 1997) and film formation occurred when temperature above

from the MFT approximately 10 °C. The MFT reduced in both EuRL and EuRS when adding plasticizers. The plasticizer is necessary in the film formation because it can reduce the MFT below 25 °C. This suggested that the film formation of the dispersion with plasticizers was faster than that without plasticizer because it can soften the particles by reduce intermolecular attraction forces and increasing the flexibility of polymeric chains (Mendoza-Romero et al., 2009).

Swelling properties

Swelling properties of EuRS and EuRL films depended on anionic type in medium. The structure of these polymers contains quaternary ammonium groups and the anionic counterions are chloride ions. Therefore, anion in the medium could exchange and replace with chloride counterions of quaternary ammonium groups in EuRS and EuRL by electrostatic interaction (Bodmeier et al., 1996; Narisawa et al., 1996). The degree of hydration and swelling depended on interaction between the quaternary ammonium groups and the counterions. Stronger interaction decreased polymer hydration and swelling because polymer chains are cross-linked with anion, resulting in reduction of polymer mobility and formation of rigid structures (Bodmeier et al., 1996; Wagner and Gruetzmann, 2005). The selective anion in the medium for ion exchangers were in following orders: sulfate > nitrate > chloride > formate > acetate (Bodmeier et al, 1996; Wagner and Gruetzmann, 2005) and dibasic succinate > acetate > mono-succinate (Wagner and McGinity, 2002). However, the swelling properties cannot explain by the extent of the ion exchange but it may be related to water binding capacities of exchanged anions (Knop, 1996).

The swelling property of film was determined by the water content of swollen polymeric film in the medium. Plasticized EuRS film had the highest swell in distilled water followed by in phosphate buffer. Film exposed the medium that contained chloride ion in the form of HCl or NaCl decreased in water content because chloride ions are strong interaction with quaternary ammonium groups. In phosphate buffer at pH 4.4 (Knop, 1996) 6.0 and 7.4, the swelling properties of EuRS films without plasticizer did not difference because EuRS is pH-independent polymer, which quaternary ammonium groups could ionized in the wide range pHs (Ghaffari et al., 2007).

Tackiness

In the film coating of solid dosage form by aqueous polymeric dispersion, the attachment of the coated substrates always occurs during the coating process. The attachment results from the tackiness of polymeric film. Tack is the ability of two materials to resist separation after bringing their surfaces into contact for a short time under light pressure. The common problem of coating process is the sticking of coating substrates. Type of polymer affected the tackiness that EuRS film was stickier than EuRL film. This result could possibly be explained by the different number of quaternary ammonium groups that EuRL had more quaternary ammonium groups than EuRS. The repulsive force of these groups may be occurred, resulting in lower attachment of EuRL films than that of EuRS films. Moreover, increasing the temperature in coating process caused high sticking of polymeric films (Wesseling et al., 1999).

Thus, anti-tacking agents are necessary in polymeric coating formulation in order to prevent the coating substrate agglomeration. There are many materials that can be used as anti-taking agents such as talc (Wesseling et al., 1999; Maejima and McGinity, 2001; Nimkulrat et al., 2004), magnesium stearate (Fernández-Cervera et al., 2004), titanium dioxide (Fernández-Cervera et al., 2004), colloidal silica (Vecchio et al., 1995; Fernández-Cervera et al., 2004), glyceryl monostearate (Wesseling et al., 1999; Nimkulrat et al., 2004), and surfactants such as Span 60 and Span 40 (Nimkulrat et al., 2004).

Talc is most commonly used as anti-tacking agent in polymer coating formulation at concentrations ranging from 25-100% based on the weight of dry polymer. Nevertheless, talc had some adverse effects such as the variation of quality, high amounts used, and incompatibility with some drug. Additionally, high amount of dispersion pigments resulted in nozzle clogging and sedimentation. The high concentration of talc could reduce the release rate of the drug from the formulation (Maejima and McGinity, 2001). Glyceryl monostearate had major advantage on lower amount used and more effective than talc. The concentration of this anti-tackiness was approximately 5-10% for prevention the sticking of EuRS films (Wesseling et al., 1999). Moreover, hydrophobic surfactant, such as Span60 and Span40 could use as anti-tackiness for EuRS films. (Nimkulrat et al., 2004)

Effect of curing

An incomplete film formation of aqueous polymeric dispersion may occur during coating process. Curing process is the essential step after coating. Curing can enhance the coalescence of the polymer particles to form a homogeneous film. The homogeneous films are occurred if the film is subjected to storage at the temperature above glass transition temperature of film polymers. At this temperature, inter-diffusion of polymer chains are occurred, resulting in continuous and complete films. The curing process is dependent on time, temperature, and relative humidity. These factors promoted particle fusion during curing process. These occurrences affected drug release pattern from coated formulation with different curing condition. Thus, many researches were studied about the curing condition that suitable for each polymer. The tensile strengths of EuRS films increased with increasing the curing time at 50 °C. On the other hand, the films showed slightly increase of tensile strength in the first 4 h and reached a maximum at 4 h of curing at 70-90 °C. After the maximum, tensile strengths decreased when increasing the curing time to 6 h. The elongation of EuRS film was slightly decreased when increasing the temperature and curing time within the first 2 h, and after that the elongation were a sudden decrease. These results can be explained that the film formation was completed under these conditions, within the first 4 h of curing at 70 and 90°C. The loss of plasticizers was occurred in a longer curing time, leading to increasing in glass transition temperature of polymeric films. This resulted in an increase in brittleness and weakness of the films (Bhattacharjya and Wurster, 2008).

The influences of curing condition on drug release from coated pellets were also studied. Ibuprofen release profiles were investigated in simulated intestinal fluid from EuRS coated pellets cured at 50, 70, and 90°C. The drug release rate decreased when increasing curing time at 50°C. In fact, longer curing time resulted in the greater coalescence of polymeric particles and promoting the continuous film formation. Moreover, the lag time of drug release was longer when increasing the curing time. These results can be described that higher curing times affected more fusion of the polymeric particles, leading to more complete and dense film coating. However, drug release profile of coated pellets curing at 70 and 90°C were different from the drug release profile at 50°C. The drug release rate decreased with increasing curing time to 4 h, after that the higher drug release rate was found for the curing time of 6 and 8 h. The decreasing of drug release rate resulted from high degree of polymer film coalescence, leading to

complete and dense coated films. The increasing of drug release rate brought about the over curing that relate to the loss of plasticizer, which is water soluble plasticizer, triethyl citrate (TEC). The loss of plasticizer can create the small pores in the coated films, leading to the higher drug release rate. Moreover, curing at the high temperature also caused the moisture loss from the coated film. The water in the film acts as a plasticizer that helped the fusion of the particles. Thus, the loss of the moisture led to an increase in tensile strength and a decrease in percent elongation of the polymeric film (Wu and McGinity, 2000; Bhattacharjya and Wurster, 2008).

Drug permeability

Drug permeability of EuRS and EuRL films is independent on pH of medium because they contain many quaternary ammonium groups. The degree of ionization of these groups did not affect by pH level within the physiological range (Bodmeier et al., 1996) but depended on the nature of drug molecules, such as molecular size, steric structure effects, and interactions with the solvent or polymeric film structures (Lehmann, 1997). The drug permeability was also controlled by the anionic species in the medium similar to the swelling properties. Strong affinity of anion to cationic quaternary ammonium groups of polymeric chains decreased permeability of the drug. These suggested that the permeability relate to ion exchange, which depended on electrostatic interaction and ion mobility. The ion's mobility decreased when increasing the concentration of anionic in the mediums (Wagner and McGinity, 2002). Generally, the mechanism of drug permeated through polymeric film had two mechanisms, the pore mechanism and the partition mechanism. In the pore mechanism, drug permeated through the pore by diffusion and permeation rate was controlled by molecular size of drug and pore size of membrane. In the part of partition mechanism, the dissolution of drug in polymer and the diffusion of drug through between polymer segments in the membrane were the important process. Normally, drug permeation occurred by two mechanisms but the most one is predominate (Ghaffari et al., 2007).

The permeability of phenylpropanolamine (PPA) and chlorpheniramine (CPA) did not different in EuRS films. However, PPA had higher permeability than CPA in EuRL films due to the larger structure of CPA. EuRL films gave higher drug permeability than EuRS films because of higher quaternary ammonium groups. (Lehmann, 1997) Moreover, the permeability of theophylline as a model basic drug was very low in pH 7.4

phosphate buffer. This was due to the hydrophobic and low water permeability of EuRS (Ghaffari et al., 2007).

**QPM-aqueous polymer blended films**

The blended films can be prepared by mixing EuRS/RL with water soluble polymer. EuRS/RL is in particle form and water soluble polymer is long chain molecule hydrated in water. The polymer molecules were mixed and located between EuRS/RL particles. This caused a change in film formation of EuRS/RL. The water soluble polymer could dissolve and leach out from the blended film, leading to aqueous channel formation. This resulted in an increase of drug permeability of the blended films. Moreover, the EuRS/RL remained in the blended film could control drug release from the coated tablets. The EuRS/RL could be mixed with anionic, cationic and nonionic polymer.

Nonionic polymer

Hydroxyethylcellulose (HEC) is a nonionic water-soluble polymer. It is widely used in pharmaceutical formulations as a thickening agent, coating agent, suspending agent, and tablet binder (Rowe et al., 2006). HEC was blended into EuRS dispersion without phase separation even if it is water soluble polymer and EuRS is water insoluble polymer. Addition of HEC in EuRS films provided an advantage on improvement of stability of coated film during storage. In general, “aging” phenomenon is major problem of coated film prepared using the dispersion form of polymer. It is a result from further coalescence and inter-diffusion of polymeric particles. This phenomenon caused a decrease in permeability and drug release when increasing storage time (Maejima and McGinity, 2001; Lecomte et al., 2004). Mechanical properties and drug release rate of pellets coated with EuRS-HEC films did not change after storage. This suggested that HEC acted as a coalescence-blocking agent when it was added into water insoluble polymer. It located surround the polymer particle and hinder coalescence of polymeric particles during storage. However, EuRS films with HEC gave higher drug permeability and faster drug release rate from coated pellets when compared with EuRS films (Zheng et al., 2005)

Cationic polymer

EuRS and EuRL can be blended with chitosan to modify the film properties. Chitosan is a positively charged polysaccharide that consists of N-acetyl-D-glucosamine and D-glucosamine. Its application in pharmaceutical technology is a film forming agent

and a gelling agent. The amino groups in chitosan structure can cross-link with anionic substances. This cross-linking can be used to prepare drug delivery systems such as beads and microspheres. Even though EuRS is in particle form and chitosan is presented as molecular chains, the blending of them did not show any incompatibility because chitosan and EuRS were dispersed in aqueous medium. EuRS was mixed with chitosan in the different ratios to modify the properties of chitosan films. Addition of EuRS could improve the mechanical properties, but reduced bioadhesiveness of chitosan films (Wittaya-areekul et al., 2006).

Anionic polymer

Anionic polymer that used to blend with EuRS or EuRL was pectin. EuRS/RL and pectin can be blended to modify drug release of controlled drug release dosage form. Pectin is a linear polysaccharide mainly extracted from cell wall dry substance of higher plants. It consists mainly of D-galacturonic acid units joined in chains by means of α-(1-4) glycosidic linkage. The presence of uronic acid group in the structure of pectin results anionic charges of this polysaccharide. Blending pectin with EuRS or EuRL was a choice to prevent the swelling and the solubilization of pectin during transit from mouth to caecum because of the complexation of EuRS or EuRL and pectin that was formed via electrostatic interaction. The blended film reduced ionic charge, hydrophilicity and swelling properties of both pectin and EuRS or EuRL. The interaction of EuRS and pectin could prevent the pectin leaching from the film coated on tablets into pH 4.5 acetate-phosphate buffer without pectinolytic enzyme. In the buffer containing enzyme, the rate and extent of pectin leaching from the blended films were dependent on pectin content in the film. Pectin leaching from the blended films containing 5% of pectin in the absence and presence of enzyme were not significant difference because the proportion of pectin molecule was very low and pectin was entrapped in the film structure, resulting in lower porosity of the film generated by leaching of pectin. The film containing more than 10% of pectin gave higher leaching of pectin in presence of pectinolytic enzyme when compared to that observed in the medium without enzyme (Semdé et al., 1998). The leaching of pectin also affected drug release from the coated formulation. Normally, the leaching of the coating substance could increase drug release rate from the coated formulation due to higher pore formation. Nevertheless, The EuRS containing 10% pectin films showed different results. The leaching of pectin from the coated films was high in the presence of pectinolytic enzyme because of rapid enzyme degradation and leaching of

pectin. This lead to decrease of water uptake and swelling of the coated films and also EuRS could restructure and plug up the channels created by pectin leaching because of decrease of glass transition temperature of EuRS. Thus, the lower drug release rate was obtained. On the other hand, pectin in the coated films could rapidly absorb water, swell and hydration, and subsequently leaching of pectin, leading to large pore formation in the film structure. This caused higher drug release from the coated formulation (Semdé et al., 2000).

**Sodium alginate (SA)**

SA is a water soluble polysaccharide extracted from brown seaweed. It is composed of alternating blocks of 1-4 linked α-L-guluronic and β-D-mannuronic acid residues as shown in Figure 4. There are three types of SA depends on the ratio of α-L-guluronic acid and β-D-mannuronic acid residues in the structure. SA can be divided as M-block, G-block, and MG-block, which depends on the amount of each residue in the structure. Specifically, the G-blocks are buckled while the M-blocks have a shape referred to an extended ribbon. Physical properties of SA were affected by composition, extent of the sequences and molecular weight. SA is anionic polymer due to the carboxyl group in its structure. SA has been widely used in pharmaceutical technology as a tablet binder, disintegrant, viscosity-increasing agent, and suspending agent (Rowe et al., 2006).

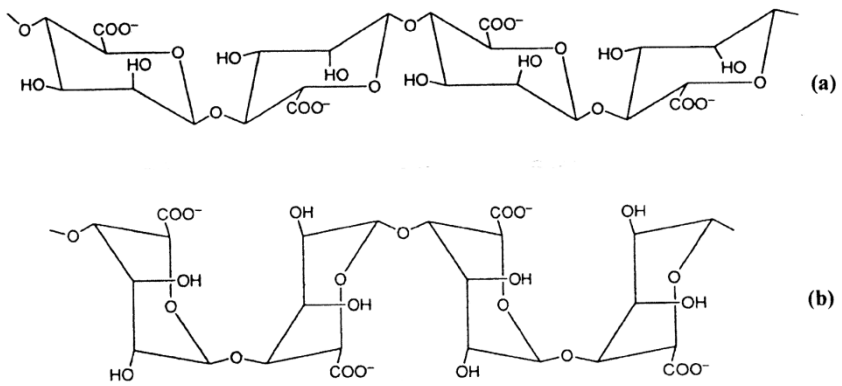


**Figure 4.** Chemical structure of β-D-manuronic acid (a) and α-L-guluronic acid of alginate (b) (Pongjanyakul, 2009).

SA can be used to fabricate drug delivery systems such as matrix dosage forms (Liew et al., 2006; Sriamornsak et al., 2007), film coated dosage forms (Sriamornsak et al., 2006), beads (Lee et al., 1999), and controlled release capsules (Pongjanyakul and

Puttipipatkhachorn, 2007a). It has been regarded as an excellent polysaccharide for drug delivery system because of its unique biocompatibility, biodegradability, low immunogenicity, and non-toxicity. SA can be prepared as a film for controlled drug release but it was not preferred to use alone due to its solubility in aqueous medium. However, addition of other substances into SA film had been done to solve this problem and to modify drug release pattern. Various ratios gelatin were mixed with SA to modify the properties of film. The blended films were prepared and cross-linked with calcium chloride to enhance the strength of films. Ciprofloxacin hydrochloride was incorporated into the films and the drug release was tested. The results showed that drug release increased when increasing amount of gelatin in the blended films (Dong et al., 2006). SA films have been modified by incorporation of magnesium aluminum silicate (MAS), which is anionic clay. The addition of MAS into SA film could improve the physicochemical, mechanical, and modify release properties of SA films that depended on the ratios of MAS (Pongjanyakul et al, 2005a; Pongjanyakul and Puttipipatkhachorn, 2008). Type of SA affected the physicochemical properties and permeability of the composite films. Composite films with high G-block SA had higher crystalline than that with high M-block SA due to higher density of the matrix structure of composite films, resulting in lower water uptake and permeability than that of composite films with high G-block SA (Pongjanyakul, 2009).

Moreover, Eudragit E (EuE) is a cationic polymer with dimethylamino groups. EuE is high solubility with organic solvents and can slightly dissolve in acid medium. EuE in the form of solution could interact with SA to form EuE-SA complexes (Moustafine et al., 2005). The interaction of Eudragit E and SA depended on pH of the solution because EuE is soluble in acid condition up to pH 6.0 and the $pK_a$ of SA was in the range of 3.38 - 3.65. Thus, the interaction between both compounds could be occurred in the pH range between 2.5 and 6.0. This was a limitation of the formation of EuE-SA complexes. However, the EuE and SA was used to prepare a matrix tablets. The interaction of EuE and SA influenced swelling and drug release of the matrix tablets (Moustafine and Zakharov, 2004; Moustafine et al., 2009).

**Magnesium aluminum silicate (MAS)**

MAS is a mixture of colloidal montmorillonite and saponite (Rowe et al., 2006) that has been washed with water to optimize purity and performance and is employed as a pharmaceutical excipient due to its non-toxicity and non-irritation at levels used in drug

formulations (Rowe et al., 2006). MAS is composed of three-lattice layers, a central octahedral sheet of aluminum or magnesium and two external silica tetrahedron layers as shown in Figure 5 (Alexandre and Dubois, 2000). The silicate layer surface of clay has a negative charge, but weakly positive charges are present on the edges of the silicate layers. The silicate layers of clay can be separated and form three-dimensional structures when they are hydrated in water. The positively charged edges of MAS could interact with anionic polymers, such as xanthan gum (Ciullo, 1981), carbomer (Ciullo and Braun, 1991), and sodium alginate (Pongjanyakul et al., 2005b; Pongjanyakul and Puttipipatkhachorn, 2007b), which resulted in viscosity synergism. Moreover, the negatively charged faces brought about a strong electrostatic interaction with amine drugs (Suksri and Pongjanyakul, 2008; Pongjanyakul et al., 2009; Rojtanatanya and Pongjanyakul, 2010), leading to a prolonged release of drug.

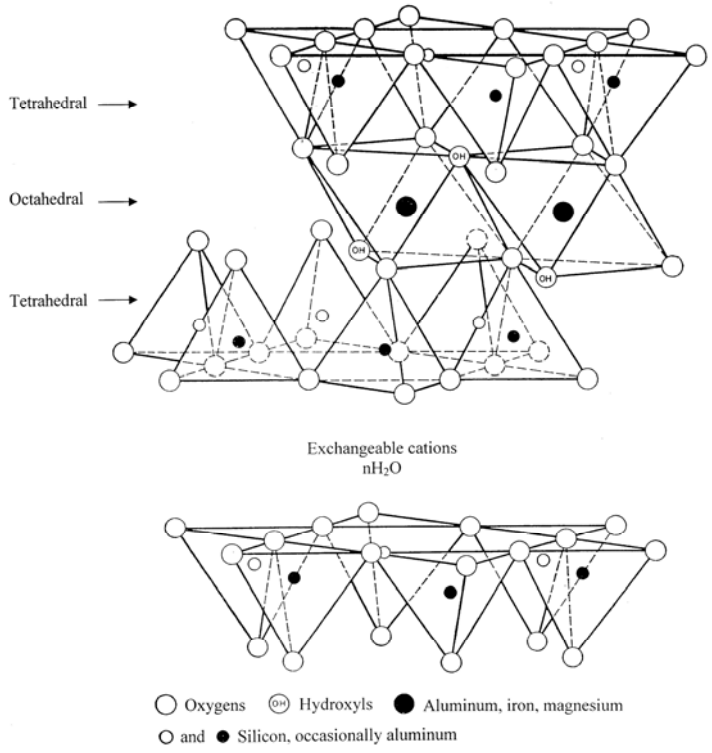


**Figure 5.** Strucrture of montmorillonite clays (Alexandre and Dubois, 2000).

Additionally, MAS could also interact with a positively charged polysaccharide, such as chitosan (CS), resulting in an improvement of rheology of composite dispersions and a formation of positively charged flocculates (Khunawattanakul et al., 2008). Recently, CS-MAS composite films were successfully prepared and characterized (Khunawattanakul et

al., 2010). The CS-MAS composite films presented exfoliated and intercalated nanocomposites with properties dependent on the CS-MAS ratio used. For nanocomposite film formation it was not necessary to use heat treatment on the composite dispersion before film casting. The mechanical properties, particularly % elongation, of the CS films could be improved by nanocomposite formation of CS and MAS. Additionally, the CS-MAS films provided lower drug permeability than CS films. The drug permeation across the CS-MAS nanocomposite films occurred by diffusion processes through microchannels. In addition, the CS-MAS coated tablets showed lower film defects, slower drug release, higher acid stability, and lower enzymatic degradation than the CS coated tablets. Drug release from the coated tablets could be modified by varying CS-MAS ratios and coating levels (Khunawattanakul et al., 2011).

From these reviews, it is known that the basic knowledge about the interaction of SA or MAS with QPM in the form of dispersions and characteristics of the QPM-SA and QPM-MAS blended films are not available in the literatures. The quaternary ammonium groups of QPM possibly interact with the carboxyl groups of SA or negative charge on the silicate layers of MAS via an electrostatic force. The film formation mechanism of QPM may alter when SA or MAS located between particles of QPM, leading to a change in physicochemical properties, mechanical properties, tackiness, drug permeability of the QPM films. Moreover, the QPM-SA and QPM-MAS blended films have a strong potential to use in tablet coating.

## Objectives of this study

### General objective

-To investigate physicochemical properties and application of QPM-SA and QPM-MAS blended film for use in pharmaceutical industry intended for tablet film coatings.

### Specific objective

-To investigate effect of SA and MAS amounts on particle size and zeta potential of QPM in the dispersion form.

-To prepare and characterize physicochemical properties of QPM-SA and QPM - MAS blended films at various ratios of both substances.

-To prepare and investigate the QPM-SA and QPM-MAS film coated tablets for modifying drug release.

## Methodology

### Preparation of QPM-MAS or QPM-SA composite dispersions

MAS or SA dispersions were prepared and kept at room temperature overnight. Different volumes of this dispersion were slowly poured into appropriate amounts of QPM dispersions (30 %w/w polymer solids content) containing 4 g of copolymer. The resulting QPM-MAS or QPM-SA ratios were 4:0, 4:0.1, 4:0.25, 4:0.5, 4:0.75, or 4:1 by weight. The mixtures were stirred using a magnetic stirrer and distilled water was added to reach a final volume of 100 mL in each case. The QPM-MAS or QPM-SA composite dispersions were further stirred at room temperature for 30 min and then shaken in a water bath at 75 oscillations $min^{-1}$ for 24 h at 37°C.

### Characterization of QPM-MAS or QPM-SA composite dispersions

Particle size measurements

The particle sizes of the samples were determined using a laser diffraction particle size analyzer (Mastersizer2000 Model Hydro2000SM, Malvern Instrument Ltd., UK). The samples were dispersed in 70 mL distilled water in a sample dispersion unit and stirred at 50 Hz for 30 s prior to the measurements. The volume weighted mean diameters are reported.

Zeta potential measurements

The zeta potential was measured using a laser Doppler electrophoresis analyzer (Zetasizer Model ZEN 2600, Malvern Instrument Ltd., UK). The samples were diluted to obtain appropriate concentrations (count rates > 20,000 counts $s^{-1}$) prior to the measurements.

**Preparation of QPM-MAS or QPM-SA films**

QPM, QPM-MAS or QPM-SA films were prepared by casting and subsequent water evaporation. Twenty g QPM dispersions (30 %w/w polymer solids content) were mixed with 0.9 g diethyl sebacate (15% w/w plasticizer referred to the QPM dry mass), and stirred for 30 min. Then, appropriate amounts of MAS or SA dispersions were added to obtain QPM-MAS or QPM-SA ratios of 4:0, 4:0.1, 4:0.25, 4:0.5, 4:0.75, or 4:1 by weight. These composite dispersions were stirred for 30 min, and then adjusted to a final volume of 150 mL with distilled water before shaking in a water bath at 75 oscillations $min^{-1}$ for 24 h at 37°C. Subsequently, the dispersions were degassed, poured into Teflon® plates (17 cm × 18 cm) and dried at 50 °C for 48 h. The dry films were peeled off and kept in desiccators prior to characterization.

**Characterization of QPM-MAS or QPM-SA films**

Thickness measurement

The film thicknesses were measured at twenty different positions using a microprocessor coating thickness gauge (Minitest 600B, ElektroPhysik, Germany). The films were placed on a control plate. The probe was connected to the measurement gauze and calibrated using a reference film.

Scanning electron microscopy (SEM)

The external and internal morphology of the films were studied using SEM. Cross-sections were obtained by cutting with a knife. The samples were mounted onto holders, coated with gold in a vacuum evaporator, and analyzed with a scanning electron microscope (Joel Model JSM-6480LV, Tokyo, Japan).

ATR-FTIR spectroscopy

The spectra (4000 to 650 $cm^{-1}$ at a resolution of 4 $cm^{-1}$) of the samples were recorded using an ATR-FTIR spectrophotometer (Spectrum One, Perkin Elmer, Norwalk, CT). Each sample was cut and placed on a ZnSe prism of a sample holder.

Powder X-ray diffractometry (PXRD)

PXRD patterns of the samples were recorded using a powder X-ray diffractometer (Philips PW3710 mpd control, The Netherlands). A Cu radiation with a wavelength of 1.54 Å was used (30 kV, 20 mA, 2θ = 1-30°, step angle = 0.02° 2θ $s^{-1}$). The thickness of the silicate MAS layers was calculated using Bragg's equation:

$$n\lambda = 2d \sin\theta \qquad \text{(Eq. 1)}$$

where n is 1 (the first order reflection was used), λ is the X-ray wavelength (1.54 Å), θ is the angle of the basal spacing peak of MAS, and d is the thickness of the MAS silicate layer.

Differential scanning calorimetry (DSC)

DSC thermograms were recorded using a differential scanning calorimeter (DSC822, Mettler Toledo, Switzerland). The samples (2-3 mg) were accurately weighted into 40 µL open aluminum pans. The temperature was increased from 30 to 450 °C at 10 °C $min^{-1}$.

Determination of the mechanical properties

The puncture strength and % elongation at break of the films in the dry and wet state were determined using a texture analyzer (TA-XT2, Stable Micro systems, Ltd., UK), equipped with a 500 N load cell. Films were cut into 2 cm × 2 cm pieces and kept at 55 % relative humidity and 25 ○C for 3 d prior to testing. If measured in the wet state, films were exposed to 0.1 M HCl or pH 6.8 phosphate buffer (under occasional shaking) at 37 ○C for 1 h prior to the measurements. Excess water was removed by blotting. Dry and wet film samples were fixed using a film holder between two mounting plates. A 5 mm diameter spherical stainless puncturing probe was fixed at the load cell and moved downwards at 0.1 mm $s^{-1}$. The applied force and displacement were recorded. The puncture strength and % elongation at break were calculated as follows:

$$\text{Puncture strength} = \frac{F}{A} \qquad \text{(Eq. 2)}$$

where F is the maximum force and A is the cross-sectional area of the edge of the film located in the path of the cylindrical opening of the film holder.

$$\text{\% Elongation at break} = \frac{\sqrt{r^2 + D^2} - r}{r} \times 100\,\% \qquad \text{(Eq. 3)}$$

where r is the radius of the film exposed in the cylindrical hole of the film holder and D is the displacement of the probe from the point of probe-film contact to the point of film puncture.

Tackiness measurement

A modification of the method reported by Wesseling et al. (1999) was applied, using a texture analyzer (TA-XT2), equipped with a 50 N load cell. The films were cut into pieces of 2 cm × 7 cm. The samples were kept at 75% relative humidity and 25 °C for 3 d prior to testing. In case of wet films, the latter were exposed to distilled water for 10 min prior to the measurements. Excess water was removed by blotting. The films were tightly placed together and compressed with 500 g weights for 1 h. One end of each film was placed in the upper and lower clamps of tensile grips. The upper clamp was attached to the load cell, which was driven upwards at a cross-head speed of 15 mm min$^{-1}$; whereas the lower clamp was stationary. The detachment force needed to separate the films was recorded. The average detachment forces were obtained from twenty measurement points of the linear parts of the force-displacement curves.

Water uptake studies

Water uptake of films was carried out using a gravimetric method. The films were cut and weighted before the test. The films were soaked in 0.1 M HCl or pH 6.8 phosphate buffer, and shaken in incubator at 37 °C for 15, 30, and 60 min. The samples were taken from the test solution at the predetermined times and blotted to remove excess water. The wet films were immediately weighted ($W_t$) and dried at 50 °C for 3 days until a constant weight ($W_d$) was obtained. The water uptake of the films was calculated from the following equation (Ritthidej et al., 2002):

$$\text{Water uptake (\%)} = \left( \frac{W_t - W_d}{W_d} \right) \times 100 \qquad \text{(Eq. 4)}$$

$$\text{Erosion (\%)} = \left( \frac{W_0 - W_d}{W_0} \right) \times 100 \qquad \text{(Eq. 5)}$$

where $W_0$, $W_t$ and $W_d$ are the original, wet and dry weights of the films, respectively.

Determination of water vapor permeability (WVP)

The films, which had been cut into disc shape with 1 cm-diameter, were placed on open 5 ml glass vials containing 3.5 g silica gel beads, and held in place with a screw lid having 0.58 cm$^2$ of test area. The vials were placed in a chamber containing saturated solution of sodium chloride (75% RH). The chamber was kept in the room temperature at 27 ± 1 °C and 55 ± 3% RH. The weight change of vials was recorded periodically over 120 h. WVP rate was obtained from the slope of relationship between water vapor

permeated per area and time. WVP coefficient was calculated from the following equation (Pongjanyakul et al., 2005):

$$WVP\ coefficient = \frac{Mh}{A\Delta P_{\upsilon}} \qquad \text{(Eq. 6)}$$

where $M$ is WVP rate, $h$ is the mean thickness of the films, $A$ is the area of the exposed film, and $\triangle P_{\upsilon}$ is the vapor pressure difference.

Drug permeability studies

Drug permeability of the films was conducted using a horizontal side-by-side diffusion cell (Crown Glass Co., Inc., Someville, NJ). The permeation medium was 0.1 M HCl or pH 6.8 phosphate buffer. The films were cut and immersed in the medium for 30 min before permeation test. The wet film was clamped between donor and receptor compartments with a volume of 3 ml and diffusion area of 0.66 $cm^2$. Solution of propranolol HCl (PPN) or acetaminophen (ACT) in the concentration of 4 mg $ml^{-1}$ was placed in donor compartment and 3 ml of the fresh medium was placed in receptor compartment. Both compartments were stirred at 600 revolution $min^{-1}$ by magnetic stirrer during the test. At predetermined interval times, 2.6 ml of sample was taken from the receptor compartment and replaced with an equal volume of fresh medium. The amount of permeated drugs was analyzed using UV-visible spectrophotometer (Shimadzu UV1201, Japan) at the wavelength of 265 and 289 nm for ACT and PPN, respectively.

For paraben group, paraben suspensions with saturated concentration were prepared by adding an excess amount of paraben into the Erlenmeyer flask containing 20 ml of 0.1 M HCl. The suspensions were shaken at 37 °C for 3 days until a saturated solution of paraben was obtained. The concentration of parabens in the supernatant was analyzed using UV-visible spectrophotometer (Shimadzu UV1201, Japan) at the wavelength of 256 nm. Then, the paraben suspensions were added into the donor compartment and the concentration of saturated solution was used to calculate the permeability coefficient of the films.

Drug permeation across the films was calculated under steady state following Fick's first law, which can be demonstrated as (Flynn et al., 1974):

$$\frac{dQ}{Adt} = P_C C_0 \qquad \text{(Eq. 7)}$$

where $dQ/dt$ is permeation flux that calculated using linear regression analysis of the linear relationship between cumulative amount of drug permeated and time, $A$ is the diffusion area of the film that the drug permeated, $C_0$ is the concentration of the drug in

donor compartment, and $P_C$ is permeability coefficient. The apparent diffusion coefficient ($D_C$) elucidating the diffusivity of drug molecules across the film without thickness effects was calculated using the following equation:

$$t_L = \frac{h^2}{6D_C} \qquad \text{(Eq. 8)}$$

where $t_L$ is lag time, and $h$ is the mean thickness of the wet films.

**Preparation and evaluation of core tablets**

Core tablets (400 mg each), which were prepared using a direct compression method, consisted of 20 % active ingredient (PPN, ACT, or diclofenac sodium (DFS)), 49.7 % spray-dried lactose monohydrate, 28.0 % microcrystalline cellulose, 0.3 % colloidal silicon dioxide, and 2 % magnesium stearate. Drug powder, spray-dried lactose monohydrate, microcrystalline cellulose, and colloidal silicon dioxide were mixed using a Y-shape mixer for 45 min. Then, the mixtures were blended with magnesium stearate, lubricant, for 5 min before tabletting. The core tablets were prepared using a single punch machine with a 10-mm diameter biconvex punch. The mean surface area of the core tablets was approximately 2.55 $cm^2$/tablet. The average weight of the core tablets were over the range of 401.2-404.9 mg. The tablet hardnesses were found to be 104.3 ± 9.8, 117.8 ± 9.0, and 122.9 ± 8.3 N in the case of PPN, ACT, and DFS, respectively. The friability of the core tablets was less than 0.2 %. The core tablets could be completely disintegrated within 4 min in deionized water, 0.1 M HCl, or pH 6.8 phosphate buffer. The drug content of the PPN core tablets was extracted in 0.1 M HCl, whereas the ACT and DFS core tablets were extracted in pH 6.8 phosphate buffer. The amount of drug content was analyzed using a UV-spectrophotometer (Shimadzu UV1201, Japan) at the wavelength of 289, 265, and 260 nm, respectively. The drug content of the PPN, ACT, and DFS core tablets were 79.46 ± 0.70, 81.61 ± 2.19, and 78.99 ± 1.17 mg/tablet (n=3).

**Film coating of core tablets**

QPM dispersion and QPM-MAS or QPM-SA dispersions with various ratios were prepared and used as a film coating material. Diethyl sebacate (15 %w/w of QPM content) was added into the QPM dispersion and the mixed dispersion was stirred for 30 min. After mixing, the dispersion was adjusted to the final volume with distilled water. For the QPM-MAS or QPM-SA dispersions, accurate amount of MAS or SA which had

been prehydrated with water, was slowly added into the plasticized QPM dispersion and adjusted to the final volume using distilled water. The composite dispersion was continuously mixed with a propeller stirrer (Wisestir®, Daihan Scientific Co., Ltd, Korea) for overnight.

The film coating of the core tablets was conducted by using a side-vented coating pan (Thai Coater Model FC15, Pharmaceuticals and Medical Supply Ltd., Thailand). PPN, ACT, or DFS core tablets (1000 g) were warmed in a coating pan with an inlet temperature at 55-60 °C for 30 min before coating. The dispersions was continuously stirred during coating process. The rotation rate of coating pan was 6-7 revolutions $min^{-1}$. The spray rate and spray pressure of the dispersion was controlled at 6 ml $min^{-1}$ and 0.38 MPa, respectively. The coating level was calculated from weight gained of coating films by total surface area of the core tablet (Bauer et al., 1998). After the coating process, the obtained coated tablets were further dried in the coating pan for 30 min before storing in desiccators at ambient condition.

**Evaluation of coated tablets**

Surface and matrix morphology of coated tablets

Surface morphology and cross-sectional morphology of coated tablets was observed by using scanning electron microscope (Joel Model JSM-6480LV, Tokyo, Japan). The coated tablets and the cross-sectional coated tablets were mounted on the stubs and coated with gold in a vacuum evaporator. The surface and cross-sectional morphology of coated tablets were observed with different magnification.

Water uptake of coated tablets

Water uptake of the coated tablets was performed using a USP dissolution apparatus I (basket method) (Vankel VK7000, North Carolina, USA). The media used were 0.1 M HCl or pH 6.8 phosphate buffer at 37 °C. The coated tablet was weighted before placing in the basket and immersing in the medium. The rotation rate of the baskets was controlled at 50 revolutions $min^{-1}$. At the predetermined intervals times, the sample was collected and carefully blotted to remove an excess water at the surface of coated tablet and immediately weighed. After weighing, the sample was placed back in the basket and tested up to the time. The % water uptake of the coated tablets at different time points was calculated as follows:

$$\text{Water uptake (\%)} = \left( \frac{W_t - W_i}{W_i} \right) \times 100 \qquad \text{(Eq. 9)}$$

where $W_i$, and $W_t$ are the initial and wet weight at time point of the coated tablet, respectively.

Drug release study

*In vitro* drug release studies were performed using the USP dissolution apparatus I (basket method) (Vankel VK7000, North Carolina, USA). The dissolution media (900 ml) were 0.1 M HCl or pH 6.8 phosphate buffer at 37 °C. The coated tablet was placed into the basket which was rotated at a rate of 50 revolutions $min^{-1}$. At predetermined interval time, samples (7 ml) were collected and an equal volume of fresh medium was replaced into the vessel. The concentration of drug in the medium was analyzed using a UV-visible spectrophotometer (Shimadzu UV1201, Japan) at the wavelength of 289, 265, or 260 nm for PPN, ACT, or DFS, respectively. The release mechanism of the coated tablets was defined by fitting the obtained release data with the zero order kinetics (Eq. 9).

$$F = K_0 t + B \qquad \text{(Eq. 10)}$$

where $F$ is fraction of drug released, $t$ is time, $K_0$ is the zero-order rate constant and $B$ is a constant value.

# Results and discussion

## Part I: QPM-MAS films

### Characteristics of QPM-MAS dispersions

Aqueous colloidal dispersions of 5QPM and 10QPM are white liquid milky without sedimentation of the particles. The mean particle size of 5QPM and 10QPM was found to be 0.187 and 0.194 μm, respectively (Fig. 5a). Moreover, the particles of 5QPM and 10 QPM presented a positive charge, which the values of zeta potential were 44.90 and 50.93 mV, respectively (Fig. 5b). The zeta potential of 10QPM was higher than that of 5QPM because of greater content of quaternary ammonium groups in molecular structure of 10QPM (Kibbe, 2000). MAS dispersion was opaque in nature. The MAS particle size was 3.92 ± 0.02 μm and zeta potential of MAS was -38.17 ± 0.59 mV. In the preparation of QPM-MAS composite dispersion, whilst the MAS dispersion was slowly added and mixed into QP dispersion, sedimentation of the dispersed phase of the QPM-MAS dispersion was visibly observed. It is possibly to expect that the QPM-MAS flocculates may be formed. This is likely to be due to electrostatic interactions between the negatively charged silanol groups ($-SiO^-$) on the silicate layers of MAS and the positively charged quaternary ammonium groups ($-N(CH_3)_3^+$) of QPM.

The particle size and zeta potential of the dispersed phase of the QPM-MAS dispersions are shown in Fig. 5. The dispersed phase of QPM-MAS dispersions presented significantly greater particle sizes than those of the QPM and MAS dispersions. These results suggested that the QPM-MAS flocculates were formed after MAS was incorporated into the QPM dispersion. The particle sizes of the 5QPM-MAS flocculates were statistically smaller than those of the 10QPM-MAS flocculates. Moreover, the QPM-MAS flocculate sizes decreased with increasing ratio of MAS in the composite dispersions. The zeta potential of the QPM-MAS flocculates significantly reduced with higher ratio of MAS in the composite dispersion, but the flocculates still had positive charge. However, the 10QPM dispersions presented higher reduction of zeta potential when compared with the 5QPM dispersion after incorporating MAS.

Interaction between QPM and MAS could immediately occur after mixing. The positively charged quaternary ammonium groups of QPM could electrostatically interact with the negatively charged silanol groups of MAS. The smaller particle size of QPM

could adsorb and completely cover around the surface of the silicate layer of MAS. This phenomenon caused a reduction of zeta potential of QPM and an induction of flocculation of QPM via MAS. This reason can explain why the QPM-MAS flocculate size being remarkably greater than the particle sizes of QPM and MAS. Increasing MAS ratio brought about a decrease of particle size of the QPM-MAS flocculates. This indicated that the higher the MAS ratio, the greater the surface area for QPM adsorption, leading to a reduction of QPM particles ratio interacted with a particle of MAS, and a decrease of the QPM-MAS flocculate size.

**Appearance, thickness and morphology of the films**

QPM films without plasticizer were hard and brittle structure. Plasticizer is an important additive to improve flexibility, and promote particle coalescence that is the mechanism of film formation of aqueous colloidal dispersion polymer (Lehmann, 1997). Insoluble plasticizers in the range of 10-40%w/w were recommended for QPM films (Bodmeier and Paeratakul, 1997; Siepmann et al., 1997). For these reasons, diethyl sebacate (15 %w/w of QPM) was used as a plasticizer of the QPM films in this study. The QPM dispersion could form a transparent film. The QPM-MAS dispersions at the ratios of 4:0.1, 4:0.25, 4:0.5 and 4:0.75 could form an opaque film. On the other hand, a continuous film did not occur when using the QPM-MAS (4:1) dispersion. This is a limitation of the film formation of the QPM-MAS dispersion at higher MAS ratio. It could be explain that higher amount of MAS could insert between the QPM particles, and disturb the QPM particle coalescence, resulting in an incomplete film formation. Moreover, it was also suggested that the content of MAS could be used not more than 18.8 % (based on polymer content) in the QPM films for achieving film formation.

The thickness of the QPM-MAS composite films slightly increased with increasing ratio of MAS (Table 1). This is likely to be due to higher solid content in the composite dispersion for film casting. The microscopic surface and matrix morphology of the 5QMP and 5QMP-MAS composite films are shown in Fig. 6. The 5QPM films had smooth surface, whereas a rougher surface was found in the 5QPM-MAS composite films. Moreover, the matrix morphology of the 5QPM films showed denser structure than that of the 5QPM-MAS composite films. The similar results were obtained with the 10QPM and 10QPM-MAS composite films.

**Molecular interaction between QPM and MAS**

Molecular interaction between QPM and MAS in the films was investigated using ATR-FTIR spectroscopy and powder X-ray diffractometry. The ATR-FTIR spectra of MAS powder, QPM films, and QPM-MAS composite films are presented in Fig. 7. MAS showed a O–H bending of residue water at 1630 $cm^{-1}$, and a Si–O–Si stretching at 981 $cm^{-1}$ (Fig. 7a). The spectra of the 5QPM film presented a C–H stretching around 2857-2983 $cm^{-1}$, a C=O stretching of at 1722 $cm^{-1}$, a $CH_2$ symmetric bending at 1446 $cm^{-1}$, a $CH_3$ asymmetric bending at 1380 $cm^{-1}$, a C–CO–C stretching at 1143 $cm^{-1}$, and a C-N stretching at 1095 $cm^{-1}$ (Fig. 7b). The 10QPM film spectra (Fig. 7c) were similar with the spectra of the 5QPM film. Incorporation of MAS into the QPM films caused an obvious peak and shift of the C–N stretching to 1080 $cm^{-1}$ (Fig. 7d and 7e). Moreover, the Si–O–Si stretching of MAS moved to higher wavenumber at around 991-1006 $cm^{-1}$. These results suggested that the interaction between the silanol groups of MAS and quaternary ammonium groups of QPM was occurred via electrostatic force. This interaction may cause a formation of nanocomposite material that can be proved by using PXRD.

The PXRD patterns of MAS, QPM film and QPM-MAS composite films are shown in Fig. 8. MAS showed the basal spacing peak at 7.0° 2θ, indicating 1.26 nm of the thickness of the MAS silicate layers when calculated using Eq.1 (Pongjanyakul et al., 2005). The 5QPM and 10QPM films presented the similar broad peak at around 15° 2θ. This suggested an amorphous form of the QPM films. The results were in agreement with the previous study (Aceves and Hernandez, 2000). The MAS basal spacing peak of the 5QPM-MAS film at the ratio of 4:0.1 was not found, but this peak of MAS was moved to 6.6 ° 2θ in the 10QPM-MAS films at the same ratio. The basal spacing peak of MAS disappeared, suggesting that the MAS silicate layers could be completely separated in the 5QPM matrix. This is an exfoliated nanocomposite (Alexandre and Dubois, 2000). This type of nanocomposite could be possibly occurred when lower MAS ratio was used. However, the 10QPM-MAS (4:0.1) films still presented this peak, indicating that MAS could also form the layer structure. Incorporating MAS at higher ratios caused a shift to lower 2θ of the MAS basal spacing peak. The basal spacing peaks of the 5QPM- and 10QPM-MAS films was located at around 6.6 and 6.3 ° 2θ, respectively, representing that the thicknesses of MAS silicate layer were 1.34 and 1.40 nm, respectively. These results suggested a formation of intercalated nanocomposite which QPM could intercalate into

the MAS silicate layers. Thus, these findings suggested that QPM could electrostatically interact with MAS, leading to formation of the exfoliated nanocomposite films at very low MAS ratio, and of the intercalated nanocomposite films at higher ratio of MAS.

Thermal behavior of the films

MAS presented an endothermic peak at 77.7 °C, corresponding to evaporation of residue water, after that no peak presented in the DSC thermogram of MAS (Fig. 9). This result suggested that MAS had good stability at temperature range used in this study. The 5QPM and 10 QPM films showed an exothermic degradation peak at 386.5 and 383.4 °C, respectively (Fig. 9 in left and right panels, respectively). It can be seen that the intensity of exothermic degradation peak of the QPM films increased with increasing MAS ratio in the films. Moreover, the degradation peak of the films was shifted to higher temperature, especially the highest ratio of MAS in the composite films. These results were similar with the nanocomposite films of chitosan with MAS prepared using heat treatment (Khunawattanakul et al., 2010). This finding suggested that interaction of QPM with MAS in the films could enhance film thermal stability at high temperature.

**Mechanical properties of the films**

The mechanical properties are important characteristics of the films intended for using as tablet coating materials. Hard and brittle films could not be used to coat the formulation because the coated film was broken during coating process. The mechanical properties of the QPM films were dependent on type of polymer, and type and amount of plasticizer (Bodmeier and Paeratakul, 1994). The 5QPM and 10 QPM films without plasticizer were hard and brittle, thus plasticizer (diethyl sebacate) was used. Puncture strength and elongation of the QPM and QPM-MAS films in dry and wet state were determined, and the results are listed in Table 1. In dry state, the 10QPM films showed higher puncture strength than the 5QPM films. This result was on the contrary with the previous study that the puncture strength of both films was comparable (Bodmeier and Paeratakul, 1994). This was likely to be due to difference of plasticizer used. However, %elongation of the 5QPM films was higher than that of the 10QPM films. Incorporation of MAS into the QPM films caused a decrease of puncture strength and % elongation, and both parameters decreased with increasing MAS ratio in the films. It is possible to describe that MAS particles interacted with the QPM particles could partially obstruct the coalescence process of QPM particles.

The QPM films in the wet state presented lower puncture strength than those in the dry state, but higher % elongation of the wet films was obtained (Table 1). This result suggested that water molecules could be absorbed and inserted into the polymeric matrix, which caused a reduction of the film strength. Moreover, water molecules could also act as a plasticizer, leading to higher flexibility of the films (Bodmeier and Paeratakul, 1993). The wet 5QPM films showed higher puncture strength and lower %elongation than the wet 10QPM films (Table 1). It was indicated that the 5QPM films contained lower quaternary ammonium groups had a less affinity with counter ions in the medium and water molecules. This may lead to lower water uptake and denser matrix structure of the films when compared with the wet 10QPM films.

Incorporation of MAS into the QPM films showed an increase tendency of puncture strength in wet state when increasing MAS ratio, and the QPM-MAS films at the ratios of 4:0.5 and 4:0.75 gave statistically higher puncture strength than the QPM films in the wet state when using both 0.1 M HCl and pH 6.8 phosphate buffer (Table 1). On the other hand, %elongation of the wet QPM-MAS films significantly decreased with increasing MAS ratio. It was pointed out that interaction of QPM with MAS brought about a stronger film matrix in the wet state. This was an advantage of the QPM-MAS films for use as tablet coated films intended for sustained-release of drug. The stronger films could control drug release from the tablets throughout the gastro-intestinal tract.

The puncture strength and %elongation of the wet films were not obviously different in 0.1 M HCl and pH 6.8 phosphate buffer. However, it was observed that the strength of the films in 0.1M HCl was slightly greater than that in pH 6.8 phosphate buffer due to the stronger interaction of chloride ions than phosphate ions, resulting in lower hydration and swelling of films in an acidic medium (Wagner and Gruetzmann, 2005).

**Tackiness of the films**

The common trouble of QPM is tackiness of film during tablet coating process. Consequently, anti-tacking agent was used in order to prevent the coating substrate agglomeration. In this study, the tackiness of the films was measured in the form of detachment force as shown in Fig. 10. The detachment force of the 5QPM films was significantly higher than that of the 10QPM films in both dry and wet states, and the wet films gave greater detachment force when compared with the dry films. This result

indicated that the 5QPM films had higher tackiness property in nature than the 10QPM films. This finding was an agreement with the previous study (Wesseling et al., 1999). It is possible to describe that the 10QPM had more quaternary ammonium groups than the 5QPM. This led to stronger repulsive force of these groups of the 10QPM, resulting in lower detachment force of the 10QPM films. The QPM films could absorb a lot of water and film swelling could be occurred, leading to a large pore channels between QPM chains. The inter-diffusion process of QPM was occurred when applying the force to the films before detachment force measurement. For this reason, the wet films showed higher tackiness property than the dry films.

The detachment force of the 5QPM films decreased with increasing MAS ratio and could not be determined in the 5QPM-MAS (4:0.75) films in both dry and wet states (Fig. 10a). The dry 10QPM films gave a decrease of the detachment force when MAS was incorporated. However, the detachment force of the wet 10QPM-MAS films was not reduced until the 10QPM-MAS (4:0.75) ratio was used. The 10QPM-MAS (4:0.75) films possessed a small detachment force in wet state. These results suggested that incorporation of MAS could reduce film tackiness property of the QPM films via decreasing contact area of the QPM on the film surface (Nimkulrat et al., 2004). Moreover, interaction of QPM and MAS could possibly reduce water uptake and swelling of the films, resulting in hindrance of inter-diffusion of QPM chains, and lower attractive force of QPM was obtained. However, the wet 10QPM-MAS films at lower ratio of MAS still had detachment force because 10QPM possessed very high water uptake and swelling in water. Thus, the free 10QPM chain possibly presented an inter-diffusion process, leading to higher tackiness property (Voyutskii, 1971). The 10QPM-MAS (4:0.75) films presented the lowest detachment force, suggesting that this MAS ratio could retard inter-diffusion of 10QPM chain. These findings suggested that MAS could be used as a anti-tacking agent for QPM films.

Due to the potential use of MAS as anti-tacking agents for QPM films, the tackiness studies of the QPM-MAS films were compared with traditional anti-tacking agents, namely talcum and GMS. Comparative detachment forces of the QPM films added various anti-tacking agents at the QPM-anti-tacking agent ratio of 4:0.25 (6.25%w/w of QPM content) are shown in Fig. 8. The 5QPM-talcum films could not reduce the detachment force in both dry and wet states. On the other hand, MAS incorporated could remarkably decrease the detachment force in both states, and the lowest detachment

forces was found in the 5QPM-GMS films (Fig. 8a). For the 10QPM films, all anti-tacking agents could obviously reduce the detachment forces in dry films (Fig. 8b), and the 10QPM-MAS films gave the most effective for decreasing tackiness of the films. However, the 10QPM films containing MAS or talcum still had the detachment force in wet state, which was not different with the free 10QPM films. The 10QPM-GMS films showed the smallest detachment force. This study suggested that MAS could be used as an alternative anti-tacking agent for the QPM films that it had lower effective anti-tacking agent than GMS, but better than talcum at the same content added in the films.

**Thickness and water uptake of the films**

Dry and wet thicknesses of the films are listed in Table 2. Dry thickness of the QPM-MAS films tended to increase with increasing MAS ratios (Table 2). This is likely to be due to an increase of solid content for film casting. The films had slight increase in wet thickness after immersing in the media for 30 min (Table 2), leading to low values of the percentage of thickness increase after hydration, which was not related to MAS ratio added, quaternary ammonium content or anion type in the medium. These results suggested that the QPM and QPM-MAS films had low swelling properties in both media used and MAS did not remarkably affect film swelling of the QPM films.

Water uptake of the films determined using the gravimetric method in both media is presented in Fig. 12. It can be seen that the water uptake of the 10QPM films was significantly higher than that of the 5QPM films in both media. This was due to the higher content of quaternary ammonium group in the 10QPM structure, leading to higher hydration capacity of the 10QPM films. The water uptake of the QPM and QPM-MAS films increased with increasing immersed time, especially in 10QPM-MAS films. Additionally, incorporation of MAS could reduce water uptake of the 5QPM and 10QPM films in both media (Fig. 12a-12d).

At 30 min of the water uptake testing, the QPM-MAS films in the ratios of 4:0.1 and 4:0.25 were not significant difference with comparison to the QPM films. In contrast, the QPM films showed statistically higher water uptake than the QPM-MAS films in the ratios of 4:0.5 and 4:0.75. These results indicated that the water uptake of the QPM films occurred because water molecules could interact with quaternary ammonium groups of the QPM films via intermolecular hydrogen bonding. Consequently, water-filled channels could be formed in the film matrix. Incorporation of MAS with lower contents in the

QPM films did not affect on the water uptake of the films. Increasing MAS content could promote the electrostatic interaction between silanol groups of MAS and quaternary ammonium groups of QPM. These interactions brought about denser matrix structure of the QPM-MAS films, resulting in the formation of smaller water-filled channels with possibly higher tortuosity in the film matrix, and therefore lower water uptake was found. The results were in agreement with the previous studies when addition of MAS into natural polymeric films (Pongjanyakul et al, 2005; Khunawattanakul et al., 2010).

All ratios of the 10QPM-MAS films showed significantly higher water uptake in pH 6.8 phosphate buffer at 30 min when compared with those using acidic medium. This result was similar to the previous study that the water uptake of the QPM film in pH 6.8 phosphate buffer was higher than that in 0.1 M HCl (Knop, 1996). Thus, the water uptake of QPM films depended on anion types in the surrounding medium. Valency of anion involved ion-exchange selectivity and attraction force with quaternary ammonium groups of QPM (Narisawa et al., 1996; Wagner and McGinity, 2002; Wagner and Gruetzmann, 2005). In 0.1 M HCl, the presence of numerous chloride ions could not induce ion-exchange process with counterion (chloride ion) of quaternary ammonium groups of QPM. On the other hand, phosphate ion, a high valency anion, could exchange with counterion of quaternary ammonium groups of QPM. This process led to higher water flux into the QPM films because phosphate ions possessed higher water binding capacity than chloride ions (Knop, 1996). Therefore, the higher water uptake of the QPM and QPM-MAS films in pH 6.8 phosphate buffer was obtained in this study.

**Water vapor permeability of the films**

WVP coefficient of the films is shown in Fig. 13. It can be seen that the WVP coefficient values of the 5QPM and 10QPM films were comparable. Incorporation of MAS into the QPM films brought about a decrease of WVP coefficient with increasing MAS content. Moreover, the QPM-MAS films in the ratio of 4:0.5 and 4:0.75 presented significantly lower WVP coefficient than the QPM films. Form these results, it was suggested that MAS added into the QPM films could change an internal matrix structure of the films. The formation of exfoliated and intercalated nanocomposites between QPM and MAS may increase density and tortuosity of microchannels in the film matrix structure. This resulted in an increase of internal pathlength of water vapor diffusion

across the films. Thus, the QPM-MAS films at higher ratios of MAS gave lower WVP coefficient than the QPM films.

The 5QPM and 10QPM films had similar WVP coefficient values due to the similar film formation of these polymers in dry state. However, the WVP coefficient values of the 10QPM-MAS films at all ratios seem to higher than those of the 5QPM-MAS films. This result suggested that the 5QPM-MAS films had denser film matrix structure than the 10QPM-MAS films. This may involve the particle size of the QPM-MAS flocculates formed in the dispersion before film casting that the 5QPM-MAS flocculates were smaller than the 10QPM-MAS flocculates. In fact, the smaller size of QPM showed higher driving force to form particle fusion during drying process than the bigger size of OPM (Lehmann, 1997). Moreover, the grater size of the 10QPM-MAS flocculates may form many small voids during particle fusion of QPM particles. By these reasons, the 5QPM-MAS films may have smaller free volume of the films in dry state, leading to lower WVP coefficient values.

**Drug permeability of the films**

PPN was selected as a model drug to study the permeability of the QPM films and the QPM-MAS films with various ratios of MAS in both acid and neutral media. PPN is a basic drug with molecular weight of 295.84 g $mol^{-1}$. It can ionize in acid and alkaline conditions with pH less than 9.5 ($pK_a$ = 9.5). Figure 14 shows PPN permeation profiles across the films using 0.1 M HCl that the drug permeation reached a steady state, which could be described using Fick's first law. Relationship between cumulative amount of PPN permeated and time presented a good linearity ($R^2$ > 0.98) with a lag time. It was obviously seen that the permeation of PPN through the 5QPM films was statistically lower than that through the 10QPM films because of high hydrophobicity and very low water uptake of the 5QPM films. From this result, the 5QPM-MAS films could not be done drug permeation testing in this study. Moreover, the lag time of the 10QPM film in acidic medium was longer than that in pH 6.8 phosphate buffer (Fig. 15a), whereas the opposite result was found in the $P_C$ and $D_C$ values (Fig. 15b and 15c, respectively), suggesting that lower water uptake of the 10QPM films in acidic medium caused slower permeation of PPN.

The PPN permeation across the 10QPM-MAS films decreased with increasing MAS ratio in the films (Fig. 14). The lag time of PPN permeation tended to increase with

higher ratio of MAS (Fig. 15a), whereas decrease of $P_C$ values was found, and the 10QPM-MAS films at the ratios of 4:0.5 and 4:0.75 gave statistically lower $P_C$ values than the 10QPM film (Fig. 15b) in both acidic and neutral media. The $D_C$ values of PPN across the 10QPM-MAS films were statistically decreased in neutral medium when increasing MAS ratios (Fig. 15c). On the other hand, the $D_C$ value of PPN through the 10QPM film in acid medium was lower than that through the 10QPM-MAS films with lower MAS contents. However, the $D_C$ value tended to decrease when higher ratios of MAS (4:0.5 and 4:0.75) added. The addition of MAS in the 10QPM films caused longer lag time and slower drug permeation through the films because PPN, a positively charges molecule, could interact with silanol groups of MAS (Rojtanatanya and Ponjanyakul, 2010), resulting in a high affinity of PPN with MAS embedded in the 10QPM-MAS films. Additionally, the 10QPM-MAS films had smaller water-filled channels with higher tortuosity of the matrix structure, which could be observed from the decreasing of water uptake when the MAS content increased. Therefore, lower $P_C$ and $D_C$ values were found. Furthermore, anion in the medium also affected PPN permeation across the 10QPM-MAS films. The $P_C$ values of the 10QPM-MAS films in pH 6.8 phosphate buffer were higher than those in acidic medium. This was mainly attributed to higher water uptake of the films in neutral medium used.

At higher ratios (4:0.5 and 4:0.75) of MAS, the 10QPM-MAS films showed longer lag time in pH 6.8 phosphate buffer when compared with using acidic medium, although higher water uptake of the films was found in pH 6.8 phosphate buffer. In fact, MAS showed lower zeta potential of negative charge in low pH medium because hydrogen ions could rapidly interact with the silanol groups of MAS (Suksri and Pongjanyakul, 2008). So, the adsorption of hydrogen ions onto the silicate layers of MAS in the 10QPM-MAS films could be occurred, leading to a reduction of PPN affinity of the films. This resulted in shorter lag time and higher $D_C$ values in acidic medium.

The effect of drug types on permeability of the 10QPM and 10QPM-MAS films was studied using PPN and ACT (MW=151.16 $g.mol^{-1}$) as cationic and non-electrolyte drugs, respectively, and the drug permeation parameters in 0.1 M HCl are presented in Fig. 16. The lag time of ACT was significantly shorter than that of PPN when using the 10QPM films, whereas the $P_C$ and $D_C$ values of ACT were statistically higher than those of PPN. This was due to smaller molecule of ACT, and the charge of drug molecules did not involve the diffusion process across the 10QPM films. The 10QPM-MAS films gave

longer lag time, lower $P_C$ and $D_C$ values with increasing MAS ratios in both ACT and PPN. It was also found that all parameters of PPN and ACT were comparable when the 10QPM-MAS (4:0.75) films were used, although ACT was 1.96-fold smaller MW than PPN. As discussed previously, the 10QPM-MAS films at higher ratio of MAS had lower affinity with PPN in acidic medium due to adsorption of hydrogen ions onto MAS, resulting in lower lag time and D values. On the other hand, small molecule of ACT could possibly form hydrogen bonding with silanol groups of MAS, when increasing MAS ratio in the films because silanol groups of MAS also had hydrogen bonding potential with drug molecules (Gupta et al., 2003). Moreover, molecular structure of ACT consisted of OH and $NHCOCH_3$ groups that could potentially form hydrogen bonding with other substances (Wen et al., 2005), particularly silanol groups of MAS in this study. For these reasons, ACT had greater affinity on the 10QPM-MAS films with higher ratios of MAS as well, leading to slower drug diffusion of ACT.

The effect of MWs of parabens on permeability of the 10QPM and the 10QPM-MAS (4:0.75) films was also investigated in this study. MP, EP, and PP were selected because they were non-electrolytes and possessed the main structure with different numbers of hydrocarbon side chains as shown in Table 3. The solubility of parabens in 0.1 M HCl is reported in Table 3, and their saturated solutions were used as a donor compartment. The results showed that increasing MW of parabens provided longer lag time in both the 10QPM and 10QPM-MAS films. The 10QPM film had a slight change of the $P_C$ value, whereas the $D_C$ values were significantly decreased with increasing MW of parabens. These results suggested that increasing MW of parabens caused slower diffusion mobilities of permeants in water-filled channels of the matrix films due to the steric effect of hydrocarbon side chain of paraben molecules. QPM, which is composed of ethyl acrylate, methyl methacrylate and trimethyl-ammonioehyl methacrylate chloride, has greater hydrophobic segments than hydrophilic parts. Non-electrolyte compounds with longer hydrocarbon side chain may have greater partition effect to hydrophobic parts of QPM. Moreover, there was a report about good miscibility of MP with polymethacrylate because intermolecular hydrogen bonding of ester groups of polymethacrylate with hydroxyl groups of MP could be formed in the films (Wu and McGinity, 2003). Thus, the higher the hydrocarbon side chain of parabens, the lower the $D_C$ values was obtained. In the case of the 10QPM-MAS film, the slower permeation of parabens across the films occurred because the composite films, which had lower water uptake than the 10QPM

films, possessed smaller water-filled channels with higher tortuousity of the films. Besides, the relationship between MW of parabens and $D_C$ values was examined as shown in Fig. 17. The MW of parabens showed a good linearity with $D_C$ values for the 10QPM and 10QPM-MAS films that $R^2$ were 0.986 and 0.964, respectively. It can be seen that a molecular diffusivity of parabens across the films decreased with an increasing number of hydrocarbon side chains (Flynn et al., 1974; Pongjanyakul, 2009)

**Appearance and morphology of QPM-MAS coated tablets**

The appearance of the PPN tablets coated with QPM and QPM-MAS films are shown in Fig. 18. The obtained QPM-MAS coated tablets had yellowish color when compared with the QPM coated tablets. The microscopic surface and matrix morphologies of the coated tablets (uncuring) using SEM are also presented in Fig. 18. The QPM coated tablets had smoother surface than the QPM-MAS coated tablets, whereas matrix morphology of the QPM-MAS films appeared to be looser structure than that of the QPM films. These morphologies were similar to the free QPM and QPM-MAS films that were prepared using a casting/solvent evaporation method.

All coated tablets did not have a sticking problem during coating process. After 3-months storage, the sticking of the QPM coated tablets occurred because the QPM films had a tackiness in nature. The QPM-MAS coated tablets at the ratios of 4:0.1 and 4:0.25 gave a few sticking of the coated tablets. However, incorporation of MAS into the QPM films in the ratios of 4:0.5 and 4:0.75 brought about a lack of the sticking problem of the coated tablets that the tackiness of the QPM-MAS films decreased with increasing MAS content when tested using a texture analyzer.

**Effect of QPM-MAS ratio on coated tablets**

The water uptake of the PPN tablets coated with QPM-MAS films with different ratios (13.1 mg $cm^{-2}$ coating level) were investigated in 0.1 M HCl and pH 6.8 phosphate buffer as shown in Fig. 19a and 19b, respectively. The results showed that the water uptake of the QPM-MAS coated tablets tended to decrease with increasing MAS content in the films. It was suggested that electrostatic interaction between the silanol groups of MAS and the quaternary ammonium groups of QPM, which resulted in the nanocomposite formation, caused a denser network matrix with higher tortuosity. This led to a reduction of film hydration and retardation of water transport through the coated

films. Additionally, the water uptakes of the coated tablets in acidic medium were greater than those in pH 6.8 phosphate buffer at the same time points. For observation, the QPM-MAS coated tablets in neutral medium displayed higher film strength and could be handled for longer immersing time when compared to the test in 0.1 M HCl.

Drug release profiles of the PPN tablets coated with QPM and QPM-MAS films in 0.1 M HCl and pH 6.8 phosphate buffer are shown in Fig. 19c and 19d, respectively. The PPN core tablets showed a fast release in both media. The pattern of PPN release from the coated tablets was similar in acidic and neutral media. The zero-order release model could be used to analyze and calculate drug release rate constant ($K_0$) and lag time. It was found that drug release data could be fitted to the zero-order release model with $R^2$ higher than 0.99 when drug released was less than 60 %. Increase of MAS into the QPM film caused longer lag time and lower $K_0$ value that are shown in Table 4. This was due to slower water uptake of the QPM-MAS coated tablets that may cause a lower PPN dissolution rate in the core tablets before PPN permeation across the films. In addition, PPN, a positively charged molecule, could electrostatically interact with a negatively charged MAS (Rojtanatanya and Pongjanyakul, 2010), resulting in a lower diffusivity of PPN across the QPM-MAS films. This reason could be explained why the longer lag time was found in the QPM-MAS coated tablets using higher ratios of MAS.

The release medium used in this study also influenced the PPN release from the coated tablets. The lag time of the QPM coated tablets in pH 6.8 phosphate buffer was longer than that in 0.1 M HCl (Table 4), This is likely to be due to lower water uptake of the QPM coated tablets in neutral medium (Fig. 19b). However, the PPN release rate constant in neutral medium tended to higher than that in acidic medium (Table 4). It can be explained that PPN had higher solubility in neutral medium when compared with in acidic medium (Khunawattanakul et al., 2011). This led to higher concentration gradient of PPN in the core tablets, which caused a faster PPN release in neutral medium. This phenomenon also found in the QPM-MAS coated tablets in the ratios of 4:0.1 and 4:0.25. At higher ratio of MAS, the longer lag time was observed in neutral medium because the slower water uptake occurred when increasing MAS in the films. However, the PPN release rate constant was quite similar in both media (Table 4). The result suggested that the lower permeability of the QPM-MAS films at higher MAS ratios was observed, irrespective of type of medium that resulted in denser network matrix of the swollen films and higher PPN affinity onto the films. It was indicated that the QPM-MAS coated tablets

gave zero-order release kinetic with lag time and good efficiency for controlling drug release were obtained when using higher ratios of MAS.

**Effect of coating level on coated tablets**

The water uptake of the PPN tablets coated with QPM and QPM-MAS (4:0.75) films at various coating levels is shown in Fig. 20. The results showed that the water uptake of the coated tablets continuously increased with testing time. The water uptake of the QPM coated tablets at the lowest coating level (13.1 mg $cm^{-2}$) in acid condition was rapidly increased within 30 min, and the coated tablets could not be handled thereafter. The coated tablets at coating levels of 19.8 and 25.3 mg $cm^{-2}$ were not difference, but they had slower uptake of the water at the same time points comparing with the coated tablets with coating level of 13.1 mg $cm^{-2}$. Using neutral medium, the similar pattern of water uptake profile was found in the QPM coated tablets with different coating levels. However, the coated tablets with higher coating level could be handled at longer time of the test when compared to those with lower coating level. The water uptake of the QPM-MAS (4:0.75) coated tablets increased with increasing coating level in both media. The water uptake of the coated tablets in neutral medium was lower than that in acidic medium. Apart from water uptake studies, the PPN release profiles of the QPM and QPM-MAS coated tablets are presented in Fig. 21. The QPM-MAS coated tablets provided significantly longer lag time and lower drug release rate constant with increasing coating level (Table 4). On the other hand, the lag time and PPN release rate constant of the QPM coated tablets had no relation to the coating level. This was due to the similar of water uptake in some coating levels.

These results indicated that increasing coating level of the coated tablets could modify the drug release pattern from the QPM-MAS coated tablets. Increasing the coated film thickness caused longer path length of water penetration into the core tablets and drug diffusion across the film, resulting in longer lag time and slower rate of drug release (Khunawattanakul et al., 2011). This study also showed that the QPM-MAS films were superior to the QPM films. The first was the higher strength and denser matrix of the QPM-MAS film, which could retard water uptake, sustain drug release and offer stable films during the tests. Secondly, the release parameters of the QPN-MAS coated tablets could be possibly predicted by varying coated level of the coated tablets.

**Effect of drug types on coated tablets**

Effect of drug types on water uptake of the QPM and QPM-MAS (4:0.75) coated tablets in pH 6.8 phosphate buffer are shown in Fig. 22a. PPN, ACT, and DFS were selected to use as cationic, nonionic, and anionic drugs, respectively. The coated tablets were prepared at the same coating level of 13.1 mg $cm^{-2}$. The water uptake of the PPN coated tablets was greater than that of the ACT coated tablets, and the lowest water uptake of the DFS coated tablets was found. The similar results were obtained in the case of the QPM and QPM-MAS coated tablets. The drug release of the coated tablets was tested in pH 6.8 phosphate buffer because of water insoluble of DFS in acidic medium. However, the DFS coated tablets showed very small amount of drug released (less than 10%) that could not calculate lag time and release rate constant. It could be described that this coated tablets had very low water uptake and the negative charge of DFS could possibly interact with QPM, leading to remarkable retardation of DFS release. Thus, the lag time and release rate constant of the PPN and ACT coated tablets could be compared in Fig. 22b. The lag time of the PPN coated tablets was longer than that of the ACT coated tablets. Moreover, the PPN coated tablets had higher $K_0$ values than the ACT coated tablets.

This study suggested that drug characteristics, such as molecular weight, charge, and water solubility, affected the release pattern of drug from the QPM and QPM-MAS coated tablets. The PPN coated tablets showed higher water uptake than the ACT coated tablets because PPN could induce water penetration into the core tablets due to greater water solubility of PPN when compared with ACT (Khunawattanakul et al., 2011). However, the longer lag time of the PPN tablets coated with QPM films was observed. This resulted from bigger molecule of PPN that also showed lower diffusivity across the coated films. In the case of the QPM-MAS coated films, incorporation of MAS caused longer lag time when compared with the QPM films. However, the PPN coated tablets gave insignificantly longer lag time than the ACT coated tablets. It could be possibly explained that PPN and ACT could interact with MAS in the films with different mechanisms, namely electrostatic force and hydrogen bonding, respectively. The higher affinity of PPN with MAS via electrostatic interaction may cause longer lag time of the coated tablets. Additionally, the $K_0$ value of the PPN coated tablets was higher than that of the ACT coated tablets. The greater water uptake of the PPN coated tablets was sufficient for dissolving the drug particles in the core tablets, leading to a rapidly high

PPN concentration gradient for drug diffusion when compared to ACT. Thus, faster PPN release was obtained.

**Curing effect on coated tablets**

The surface and matrix morphologies of the QPM and QPM-MAS (4:0.75) coated tablets (13.1 mg $cm^{-2}$ coating level) cured at 45, 60, and 80 °C for 12 hr are shown in Fig. 18. The smoother surface of the QPM-cured tablets could be observed at higher temperature when compared to the QPM-uncured tablets (Fig. 18). In contrast, the surface of the QPM-MAS-cured tablets did not different with the uncured tablets (Fig. 18). Moreover, the curing temperature did not affect the internal structure morphology of the QPM and QPM-MAS tablets when observing using SEM. However, some of the QPM coated tablets were swollen at an edge of the coated tablets when curing at 80 °C. This phenomenon was slightly found in the case of the QPM-MAS coated tablets. This may be due to a vapor pressure inside the core tablets that occurred from evaporation of remaining water at high temperature (Bley et al., 2009).

The water uptake of the QPM and QPM-MAS coated tablets decreased with increasing curing temperature and the lower water uptake could be found in the QPM-MAS coated tablets (Fig. 23a and 23b). For the PPN release, the curing process brought about a remarkable increase of lag time of the QPM coated tablets when compared to the uncured tablets, but was not dependent on curing temperature (Fig. 24a). The slightly longer lag time of the QPM-MAS coated tablets was found after curing. The PPN release rate constant of both coated tablets was unchanged when curing at 45 and 60 °C (Fig. 24b). However, the coated tablets cured at 80 °C provided lower PPN release rate than those cured at lower temperatures.

The curing process could induce the further fusion of QPM particles in the QPM coated tablets at investigation temperatures, even though the temperature of 45 °C was lower than glass transition temperature ($T_g$) of QPM, approximately 55 °C (Hasanzadeh et al., 2009). This temperature (45 °C) was higher than the minimum film formation temperature of QPM that was reported to be 38.3 ± 0.4 °C (Mendoza-Romero et al., 2009), leading to a continue deformation of QPM particles in the coated films during curing period and partial homogeneous matrix of the films may be formed. This may lead to lower film permeability. Thus, a longer lag time of PPN release was obtained. At 60 and 80 °C, these curing temperatures were greater than $T_g$ of QPM and caused the further

fusions of QPM particles. Furthermore, polymer chain flexibility usually increased with increasing curing temperature. For these reasons, the homogeneous matrix of the coated films could be occurred (Azarmi et al., 2002; Heckötter et al., 2011; Yang et al., 2010), resulting in lower film permeability at higher curing temperature. This led to restriction of water absorption and slower drug release with longer lag time (Wurster et al., 2007; Williams III and Liu, 2000).

For the QPM-MAS coated tablets, the curing process did not change the appearance of surface and matrix morphology when compared with the QPM coated tablets. This result suggested that MAS interacted electrostatically with QPM could obstruct deformation and fusion of QPM particles during curing. However, the water uptake of the QPM-MAS coated tablets cured at 60 and 80 °C was slower than that of the uncured and cured tablets at 45 °C. This suggested that some of QPM particles still had a deformation and denser matrix formation may be occurred, leading to the slowest PPN release of the QPM-MAS coated tablets cured at 80 °C.

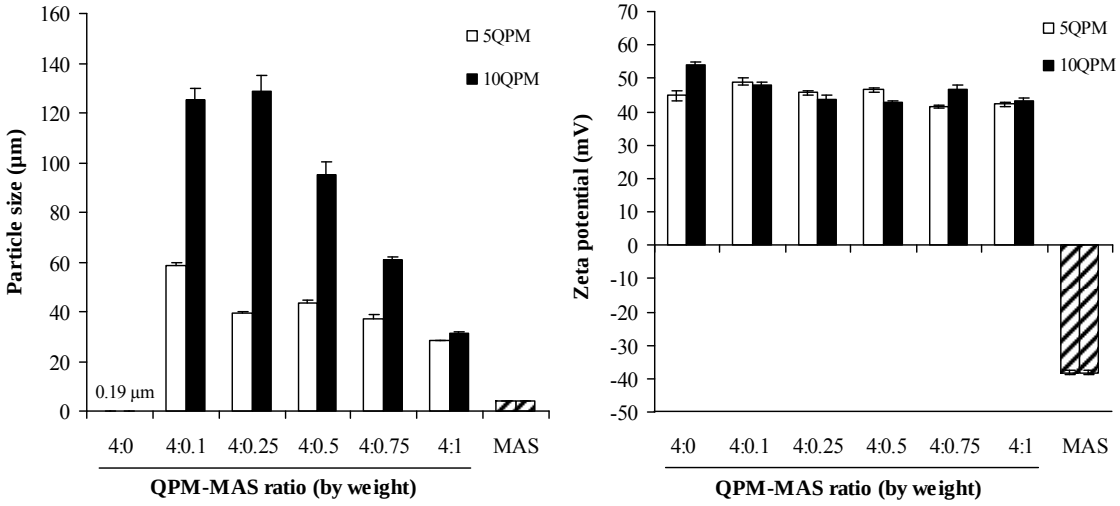


**Figure 5.** Particle size (a) and zeta potential (b) of QPM dispersions, MAS dispersions, and QPM-MAS composite dispersions. Data are mean ± S.D., n=3.

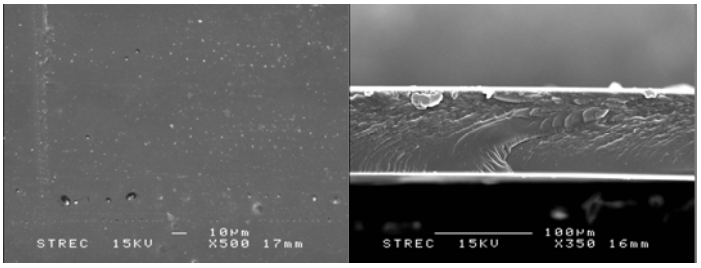


(a)

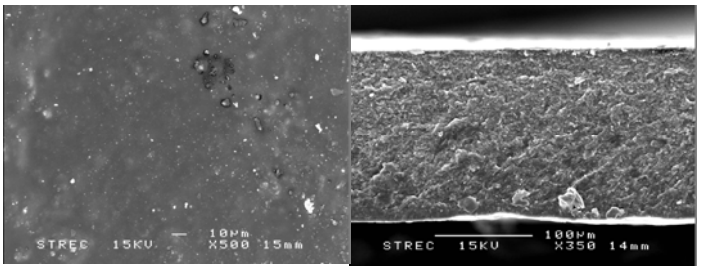


(b)

**Figure 6.** SEM pictures of surfaces and cross-sections of 5QPM films (a), and 5QPM-MAS (4:0.75) films (b).

**Table 1.** Thickness and mechanical properties of QPM films and QPM-MAS films.

| Film | Thickness [a] (μm) | Dry film | | Wet film using 0.1 M HCl | | Wet film using pH 6.8 PB | |
|---|---|---|---|---|---|---|---|
| | | Puncture strength [b] (MPa) | Elongation [b] (%) | Puncture strength [b] (MPa) | Elongation [b] (%) | Puncture strength [b] (MPa) | Elongation [b] (%) |
| 5QPM-MAS | | | | | | | |
| 4:0 | 162.5 ± 24.1 | 7.10 ± 0.29 | 113.89 ± 9.12 | 1.69 ± 0.19 | 118.80 ± 7.93 | 1.36 ± 0.08 | 131.88 ± 16.40 |
| 4:0.1 | 187.4 ± 34.4 | 5.97 ± 0.45 | 48.31 ± 7.18 | 1.45 ± 0.14 | 59.96 ± 5.30 | 1.13 ± 0.08 | 65.74 ± 8.56 |
| 4:0.25 | 216.4 ± 27.7 | 5.67 ± 0.19 | 33.90 ± 6.24 | 1.97 ± 0.20 | 32.92 ± 1.81 | 1.72 ± 0.10 | 35.85 ± 3.39 |
| 4:0.5 | 202.4 ± 21.3 | 5.58 ± 0.23 | 21.27 ± 4.02 | 1.90 ± 0.07 | 22.09 ± 2.10 | 1.78 ± 0.11 | 23.77 ± 3.34 |
| 4:0.75 | 226.9 ± 22.7 | 4.36 ± 0.37 | 18.62 ± 3.15 | 2.73 ± 0.20 | 15.58 ± 1.38 | 2.54 ± 0.27 | 15.60 ± 2.06 |
| 10QPM-MAS | | | | | | | |
| 4:0 | 182.4 ± 25.7 | 13.63 ± 1.06 | 58.01 ± 10.49 | 0.41 ± 0.14 | 320.35 ± 78.86 | 0.35 ± 0.09 | 245.14 ± 44.03 |
| 4:0.1 | 186.4 ± 22.0 | 10.56 ± 0.54 | 45.62 ± 7.31 | 0.70 ± 0.04 | 88.81 ± 1.70 | 0.52 ± 0.03 | 69.17 ± 5.98 |
| 4:0.25 | 204.4 ± 25.1 | 8.79 ± 0.47 | 37.15 ± 7.73 | 0.49 ± 0.04 | 57.62 ± 5.82 | 0.48 ± 0.02 | 45.18 ± 5.23 |
| 4:0.5 | 199.8 ± 37.1 | 7.48 ± 0.59 | 23.14 ± 3.52 | 0.78 ± 0.05 | 23.62 ± 2.21 | 0.73 ± 0.08 | 20.65 ± 1.40 |
| 4:0.75 | 209.5 ± 8.32 | 6.77 ± 1.38 | 24.08 ± 5.00 | 1.36 ± 0.14 | 22.16 ±1.16 | 1.50 ± 0.15 | 19.79 ± 1.50 |

[a] Data are mean ± S.D., n=20.

[b] Data are mean ± S.D., n=5.

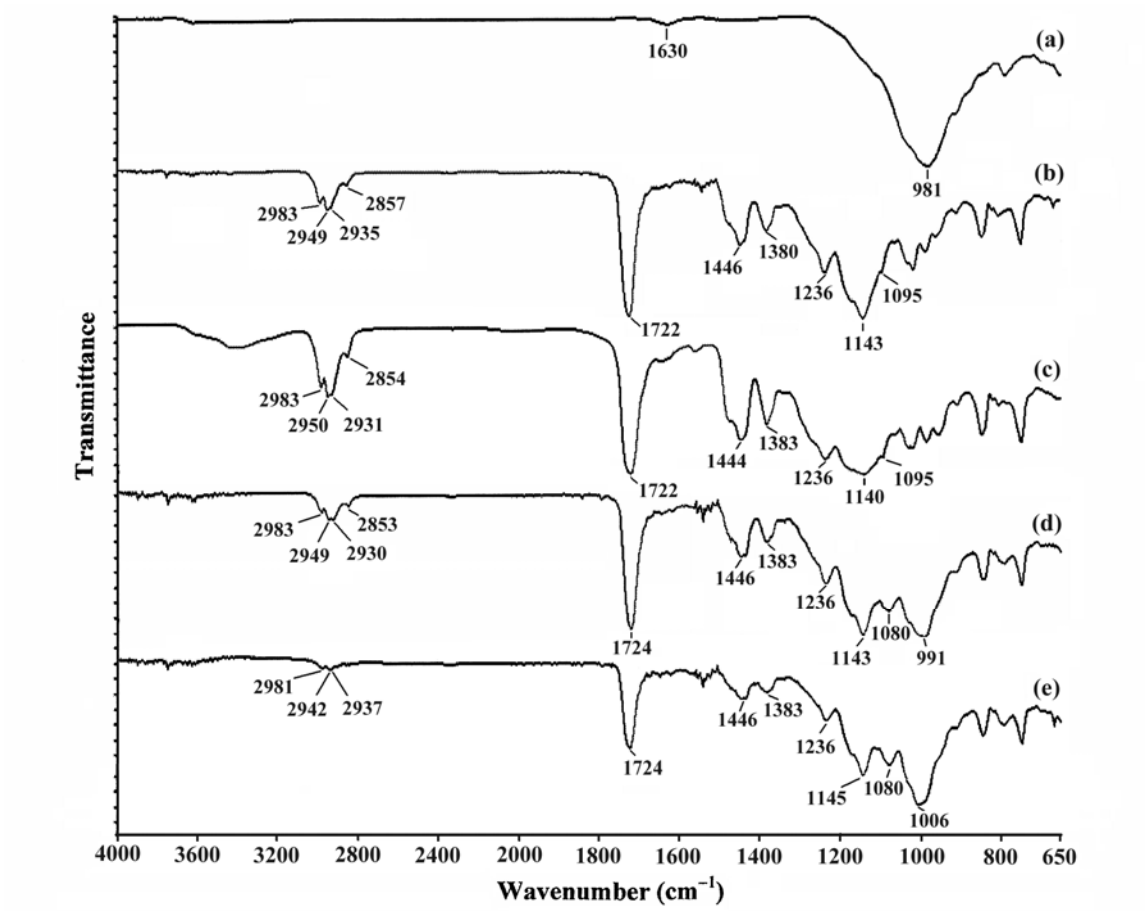


**Figure 7.** ATR-FTIR spectra of MAS powder (a), 5QPM films (b), 10QPM films (c), 5QPM-MAS (4:0.75) films (d), and 10QPM-MAS (4:0.75) films (e).

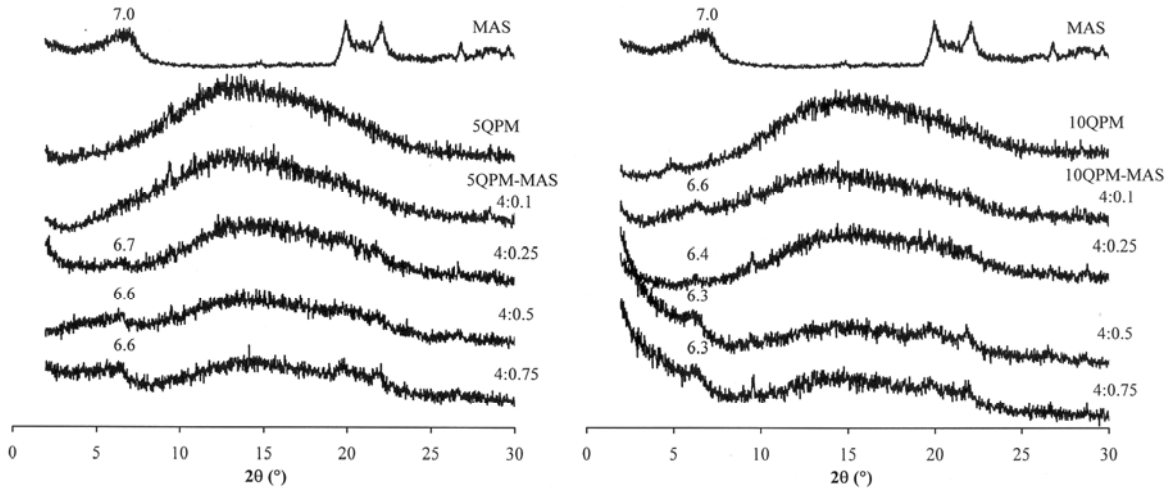


**Figure 8.** PXRD patterns of MAS powder, QPM films, and QPM-MAS composite films.

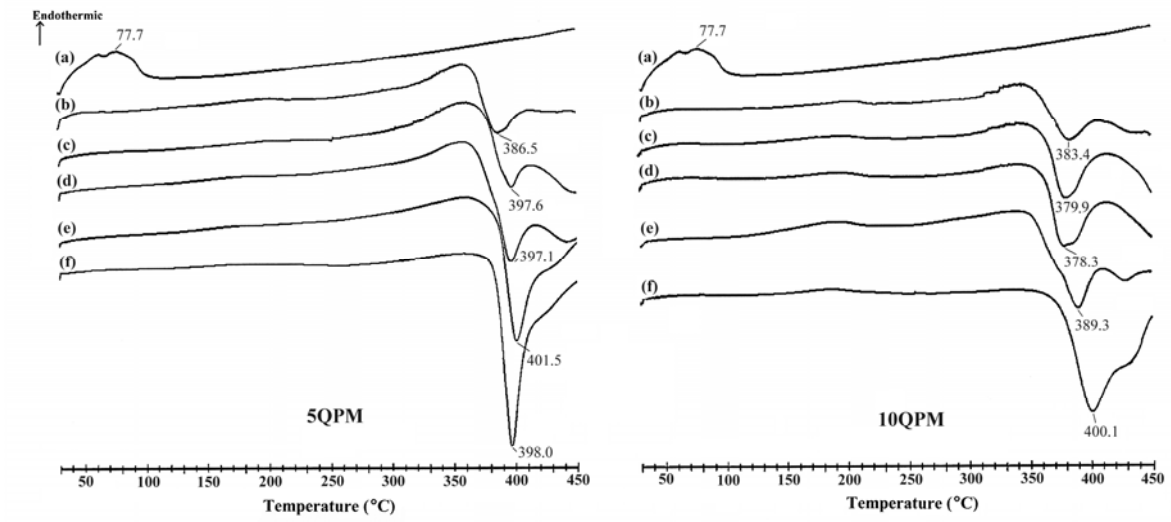


**Figure 9.** DSC thermograms of MAS powder (a), QPM films (b), and QPM-MAS composite films at the ratios of 4:0.1 (c), 4:0.25 (d), 4:0.5 (e), and 4:0.75 (f).

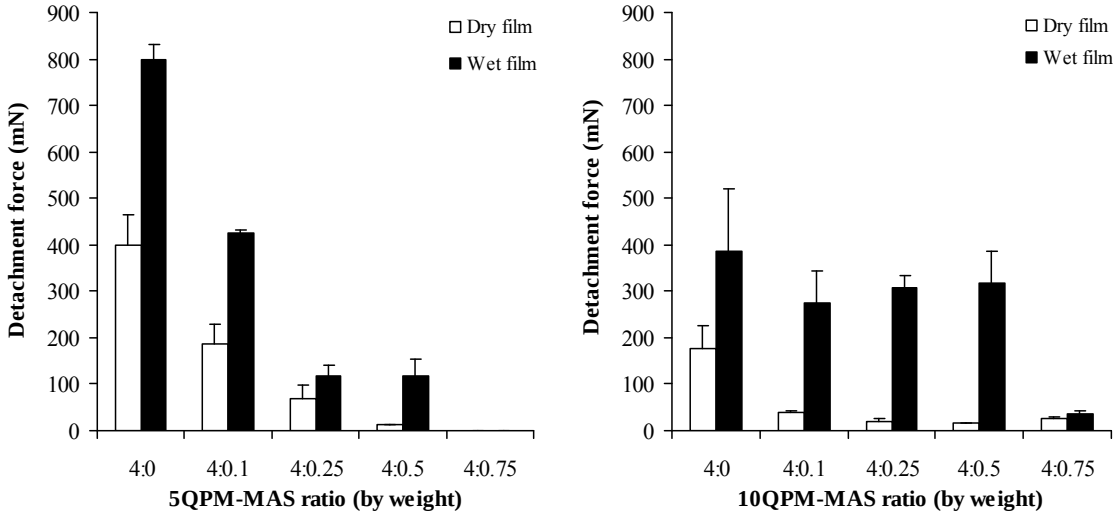


**Figure 10.** Effects of the addition of MAS on the tackiness of 5QPM films (a), and 10QPM films (b) in the dry and wet state. Data are mean ± S.D., n=5.

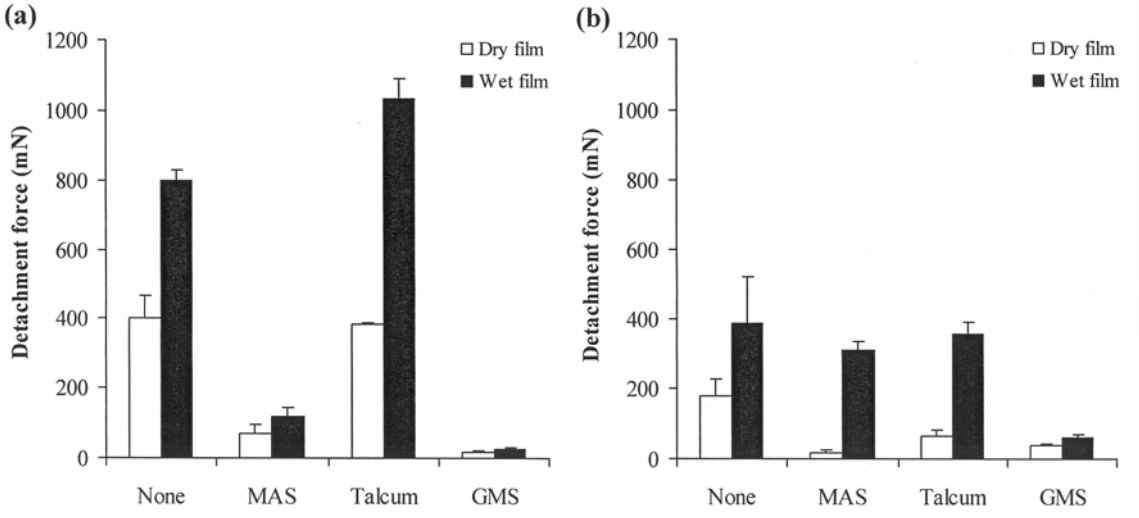


**Figure 11.** Comparative tackiness of 5QPM (a) and 10QPM (b) films added with various anti-tacking agents at QPM-anti-tacking agent ratio of 4:0.25. Data are mean ± S.D., n=5.

**Table 2.** Dry and wet thicknesses of QPM-MAS films.

| Film component | Dry thickness (μm) | Wet thickness (μm) | |
|---|---|---|---|
| | | 0.1M HCl | pH 6.8 phosphate buffer |
| 5QPM-MAS | | | |
| 4:0 | 162.50 ± 24.14 | 209.85 ± 22.35 (29.17%) | 193.90 ± 11.82 (19.32%) |
| 4:0.1 | 187.35 ± 34.44 | 195.55 ± 14.64 (4.38%) | 201.50 ± 12.33 (7.55%) |
| 4:0.25 | 216.435± 27.71 | 225.85 ± 17.54 (4.39%) | 219.30 ± 9.04 (1.36%) |
| 4:0.5 | 202.35 ± 21.33 | 223.80 ± 9.34 (10.60%) | 222.30 ± 12.37 (9.86%) |
| 4:0.75 | 226.95 ± 22.74 | 227.05 ± 9.67 (0.044%) | 239.40 ± 13.44 (5.49%) |
| 10QPM-MAS | | | |
| 4:0 | 182.45 ± 25.70 | 199.30 ± 24.34 (9.24%) | 185.95 ± 25.03 (1.52%) |
| 4:0.1 | 186.35 ± 22.04 | 193.65 ± 21.76 (3.92%) | 201.50 ± 18.48 (8.13%) |
| 4:0.25 | 204.45 ± 25.12 | 220.00 ± 30.83 (7.61%) | 249.30 ± 21.10 (21.94%) |
| 4:0.5 | 199.85 ± 37.09 | 253.68 ± 33.88 (26.94%) | 269.40 ± 60.34 (34.80%) |
| 4:0.75 | 209.50 ± 8.32 | 248.50 ± 19.69 (18.62%) | 238.90 ± 21.55 (14.03%) |

Data are mean ± SD, n = 20
Thickness increase after hydration (%) is shown in parentheses and calculated using the equation: ((mean wet thickness–mean dry thickness)/mean dry thickness) × 100.

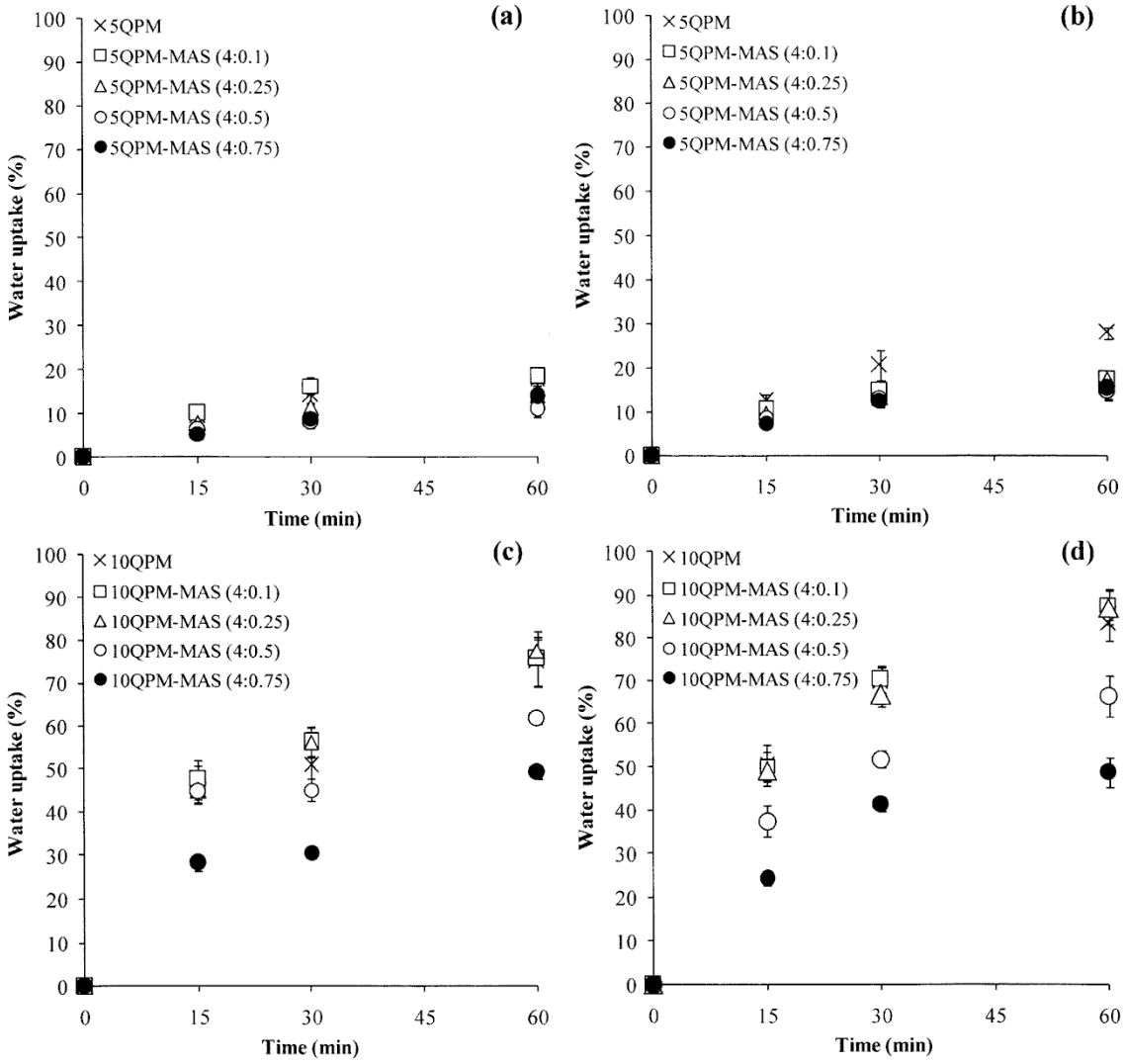


**Figure 12.** Water uptake profiles of 5QPM-MAS (a,b) and10QPM-MAS (c,d) films in 0.1 M HCl (a,c) and pH 6.8 phosphate buffer (b,d). Each point is the mean ± SD, n = 5

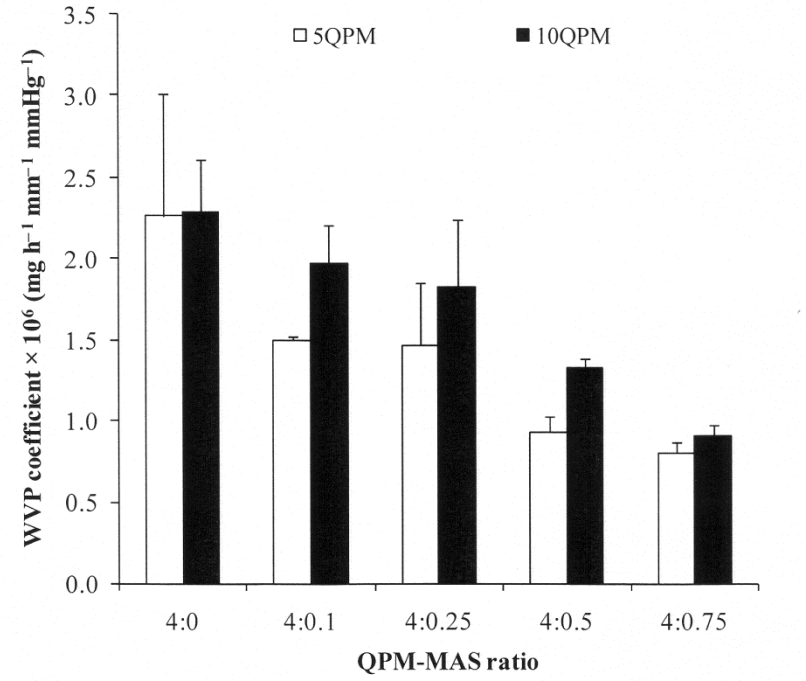


**Figure 13.** Water vapor permeability (WVP) coefficient of QPM-MAS films. Each value is the mean ± SD, n =3

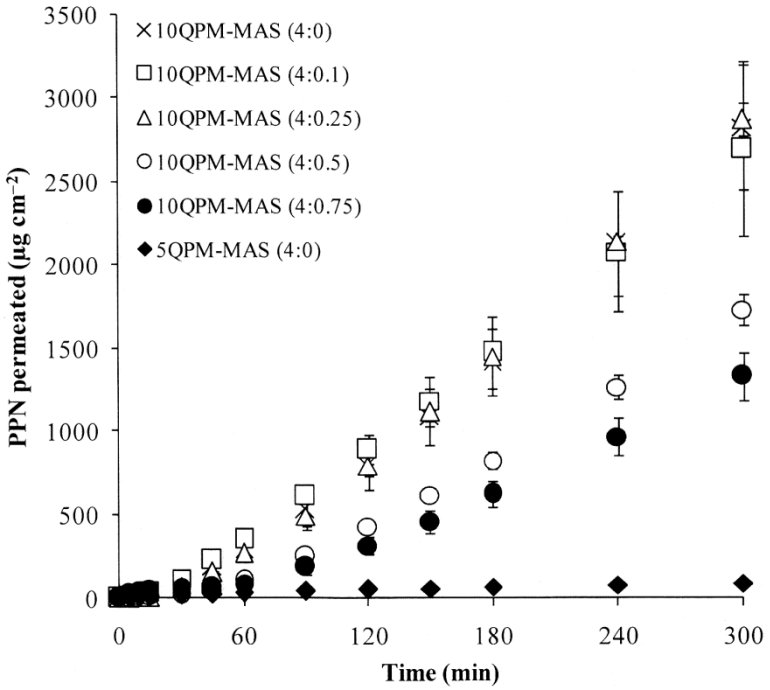


**Figure 14.** PPN permeation profiles of QPM and QPM-MAS films in 0.1 M HCl. Each value is the mean ± SD, n = 3.

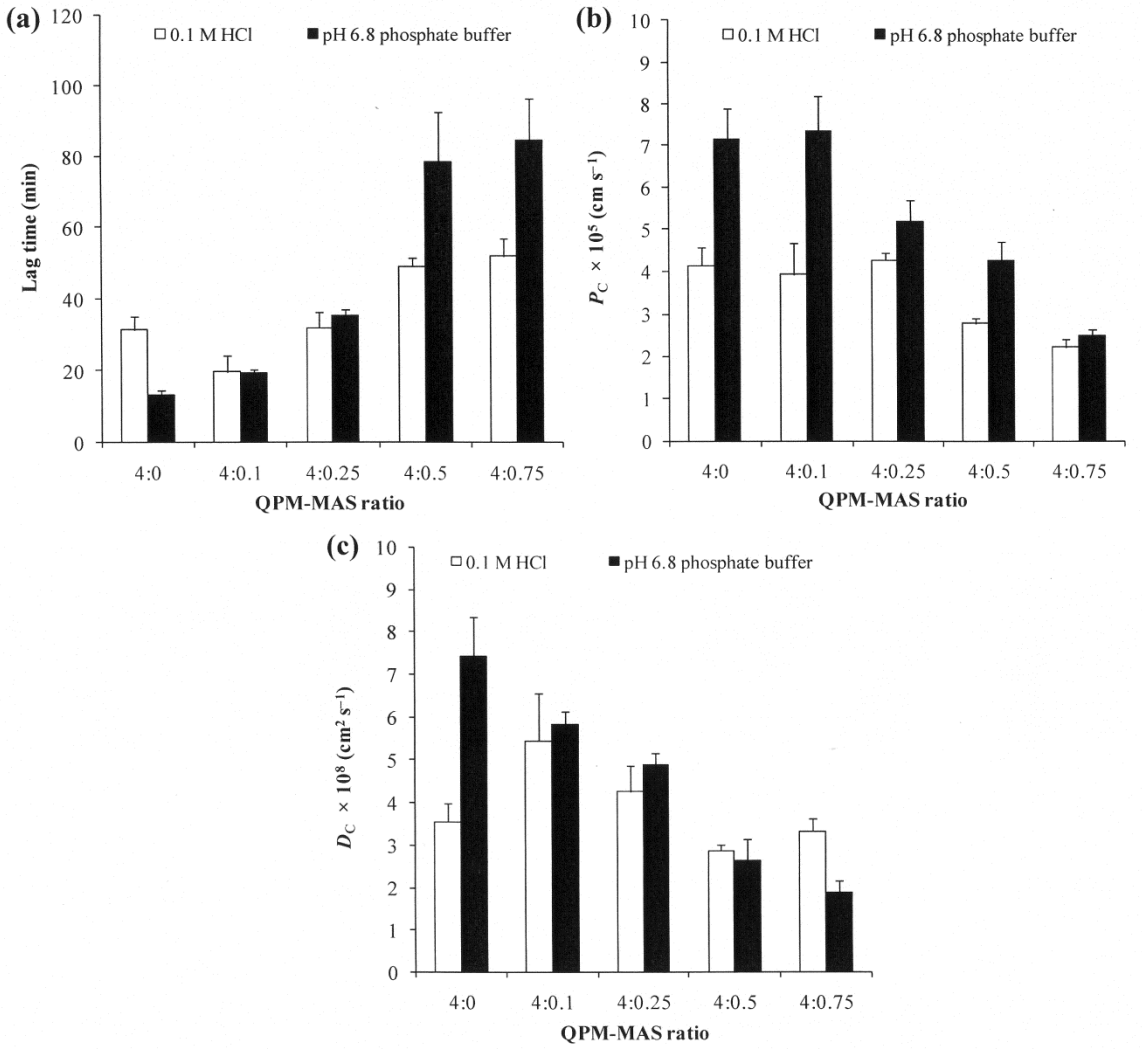


**Figure 15.** Lag time (a), permeability coefficient (b), and diffusion coefficient (c) of PPN permeation across 10QPM and 10QPM-MAS films in 0.1 M HCl and pH 6.8 phosphate buffer. Each value is the mean ± SD, n = 3.

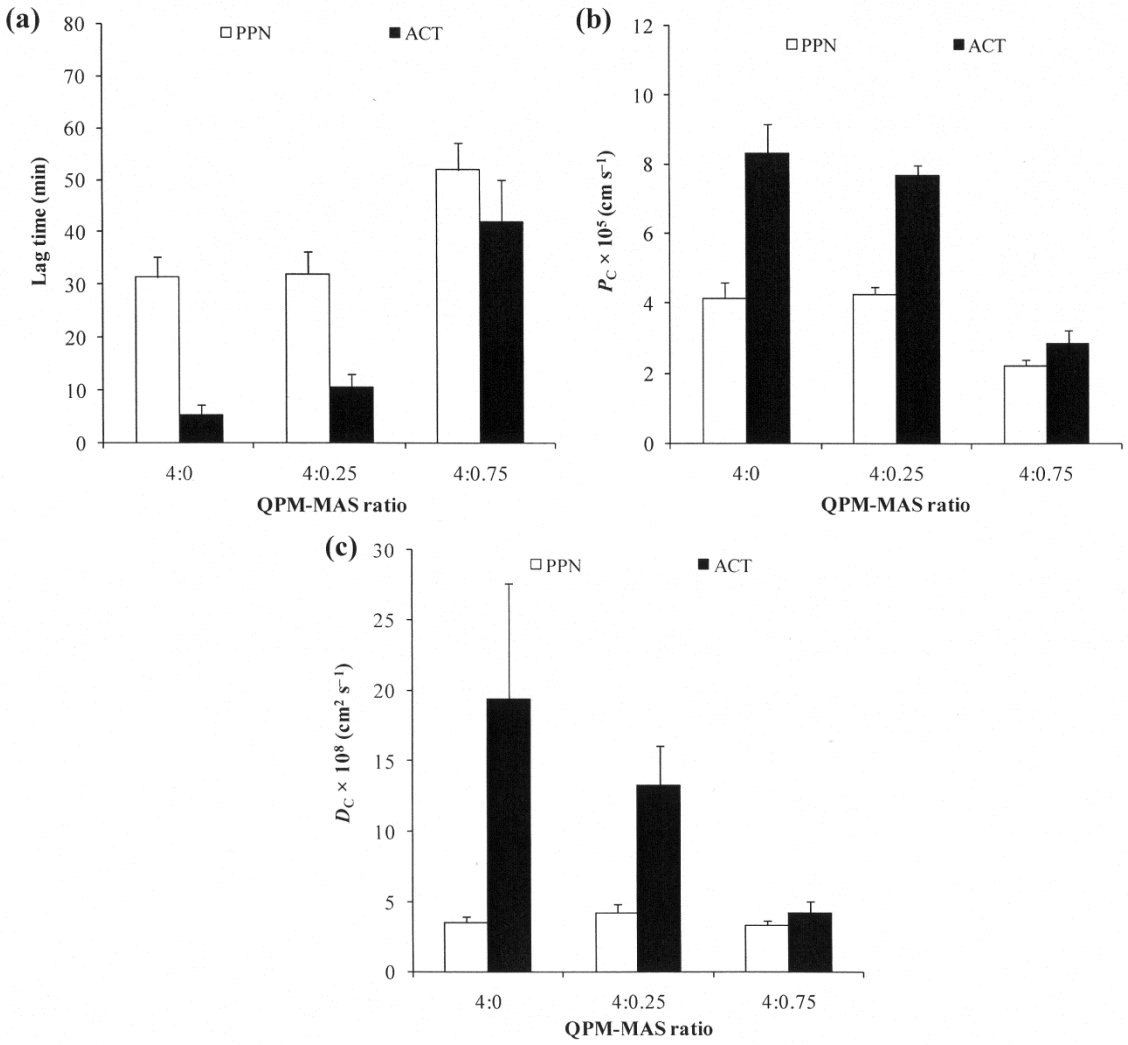


**Figure 16.** Lag time (a), permeability coefficient (b), and diffusion coefficient (c) of PPN and ACT permeation across 10QPM and 10QPM-MAS films in 0.1 M HCl. Each value is the mean ± SD, n = 3.

**Table 3.** Permeation parameters of parabens across 10QPM and 10QPM-MAS films in 0.1 M HCl.

| Structure and MW | Solubility ($mg\ ml^{-1}$) | 10QPM film | | | 10QPM-MAS film | | |
|---|---|---|---|---|---|---|---|
| | | Lag time (min) | $P_C \times 10^5$ ($cm\ s^{-1}$) | $D_C \times 10^8$ ($cm^2\ s^{-1}$) | Lag time (min) | $P_C \times 10^5$ ($cm\ s^{-1}$) | $D_C \times 10^8$ ($cm^2\ s^{-1}$) |
| MP (152.15 Da) 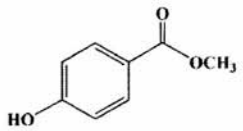 | 3.54 ± 0.05 | 23.20 ± 0.03 | 12.02 ± 1.86 | 3.89 ± 0.01 | 56.92 ± 4.34 | 4.64 ± 0.27 | 3.03 ± 0.24 |
| EP (166.18 Da) 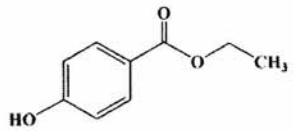 | 1.53 ± 0.04 | 31.90 ± 0.64 | 13.96 ± 1.30 | 2.83 ± 0.06 | 81.52 ± 6.49 | 3.63 ± 0.24 | 2.11 ± 0.18 |
| PP (180.20 Da) 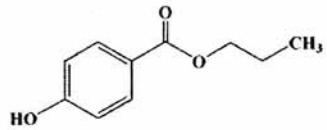 | 0.59 ± 0.02 | 73.41 ± 4.35 | 10.66 ± 1.72 | 1.23 ± 0.07 | 109.30 ± 30.62 | 1.77 ± 0.48 | 1.66 ± 0.48 |

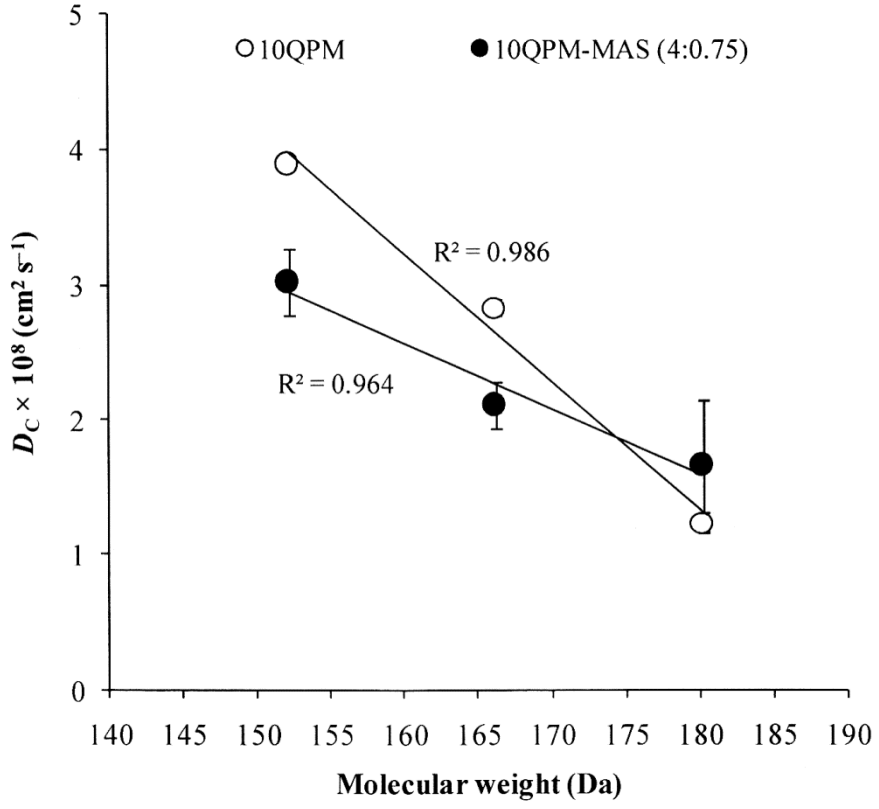


**Figure 17.** Relationship between diffusion coefficient and molecular weight of paraben group using 10QPM and 10QPM-MAS (4:0.75) films in 0.1 M HCl. Each value is the mean ± SD, n = 3.

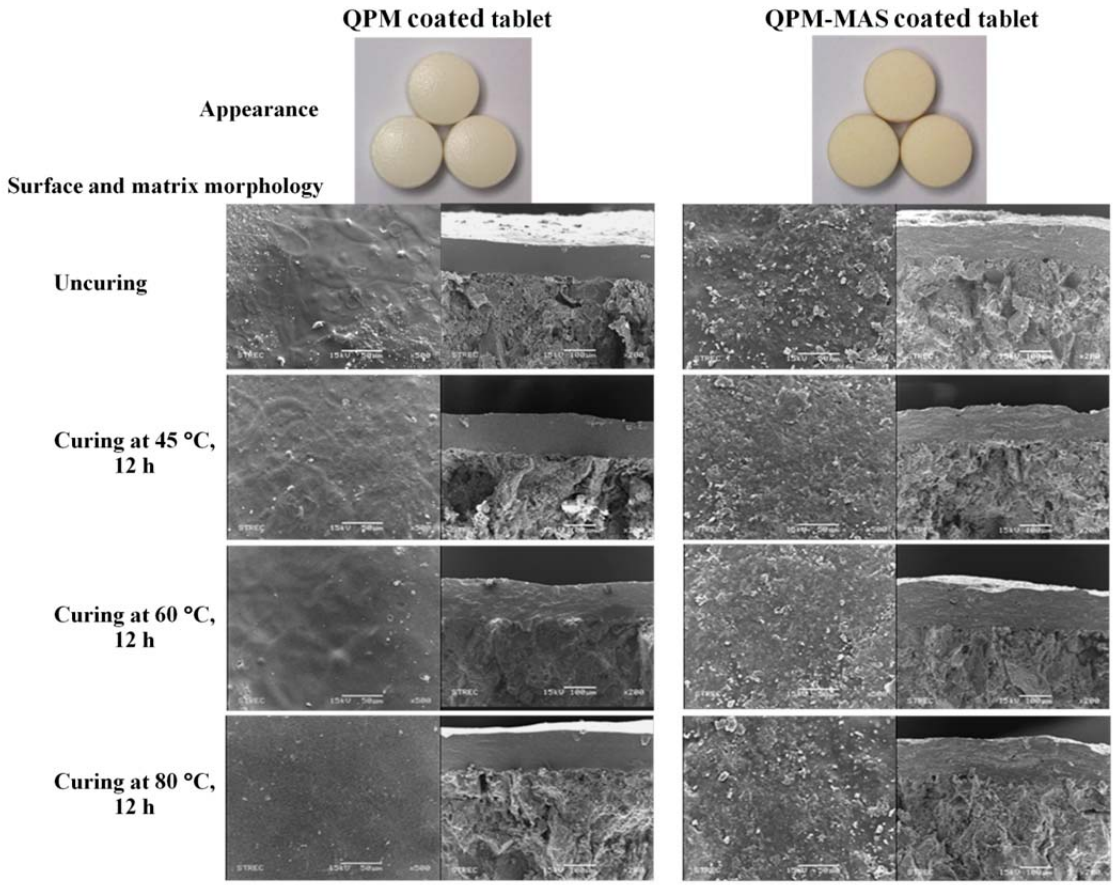


**Figure 18.** Appearance, and surface and matrix morphology of the PPN tablets coated with QPM and QPM-MAS (4:0.75) films with uncuring or curing at different temperatures.

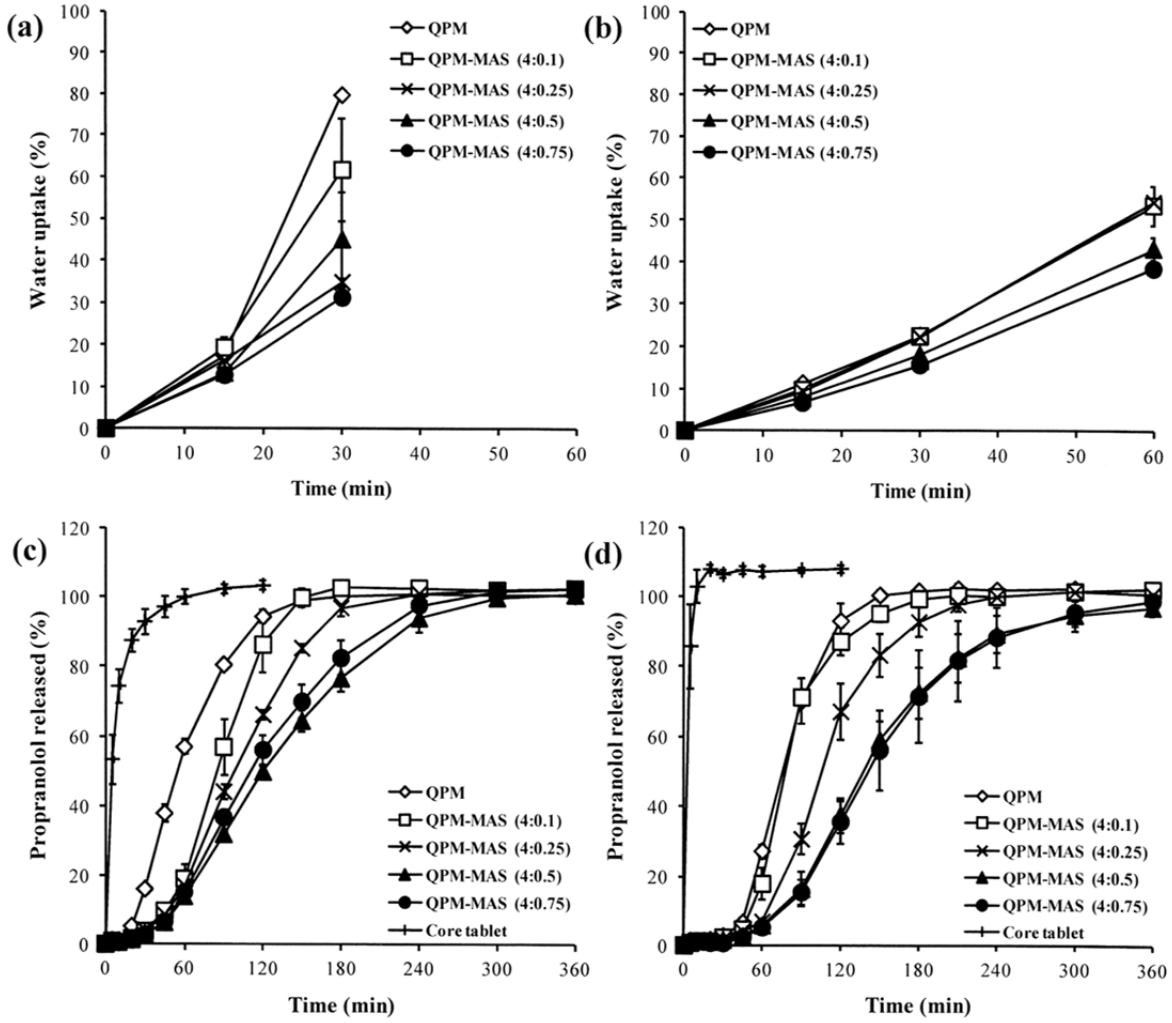


**Figure 19.** Effect of the QPM-MAS ratio on water uptake (a,b) and drug release (c,d) of PPN coated tablets at coating level of 13.1 ± 0.94 mg $cm^{-2}$ in 0.1 M HCl (a,c) and pH 6.8 phosphate buffer (b,d). Mean values ± SD are indicated, n=3.

**Table 4.** PPN release parameters of QPM and QPM-MAS coated tablets at different QPM-MAS ratios and coating levels.

| Investigation factors | 0.1 M HCl | | pH 6.8 phosphate buffer | |
|---|---|---|---|---|
| | Lag time (min) | $K_0$ ($min^{-1}$) | Lag time (min) | $K_0$ ($min^{-1}$) |
| Effect of QPM-MAS ratio | | | | |
| 4:0 | 16.63 ± 1.00 | 1.31 ± 0.08 | 40.47 ± 0.06 | 1.41 ± 0.12 |
| 4:0.1 | 31.54 ± 0.65 | 0.91 ± 0.15 | 44.42 ± 1.41 | 1.52 ± 0.04 |
| 4:0.25 | 35.49 ± 4.94 | 0.79 ± 0.05 | 55.05 ± 1.69 | 1.00 ± 0.14 |
| 4:0.5 | 34.01 ± 1.67 | 0.56 ± 0.03 | 67.04 ± 6.77 | 0.71 ± 0.01 |
| 4:0.75 | 35.85 ± 2.56 | 0.67 ± 0.07 | 65.66 ± 10.32 | 0.68 ± 0.21 |
| Effect of coating level | | | | |
| QPM | | | | |
| 13.1 mg $cm^{-2}$ | 16.63 ± 1.00 | 1.31 ± 0.08 | 40.47 ± 0.06 | 1.41 ± 0.12 |
| 19.8 mg $cm^{-2}$ | 78.91 ± 1.61 | 0.95 ± 0.20 | 91.75 ± 2.18 | 1.11 ± 0.09 |
| 25.3 mg $cm^{-2}$ | 77.92 ± 4.72 | 0.68 ± 0.07 | 116.03 ± 1.88 | 1.18 ± 0.13 |
| QPM-MAS (4:0.75) | | | | |
| 13.1 mg $cm^{-2}$ | 35.85 ± 2.56 | 0.67 ± 0.07 | 65.66 ± 10.32 | 0.68 ± 0.21 |
| 19.8 mg $cm^{-2}$ | 60.18 ± 4.37 | 0.53 ± 0.06 | 96.49 ± 5.09 | 0.51 ± 0.10 |
| 25.3 mg $cm^{-2}$ | 89.89 ± 7.80 | 0.35 ± 0.05 | 133.63 ± 2.58 | 0.41 ± 0.04 |

Data are mean ± SD, n=3.

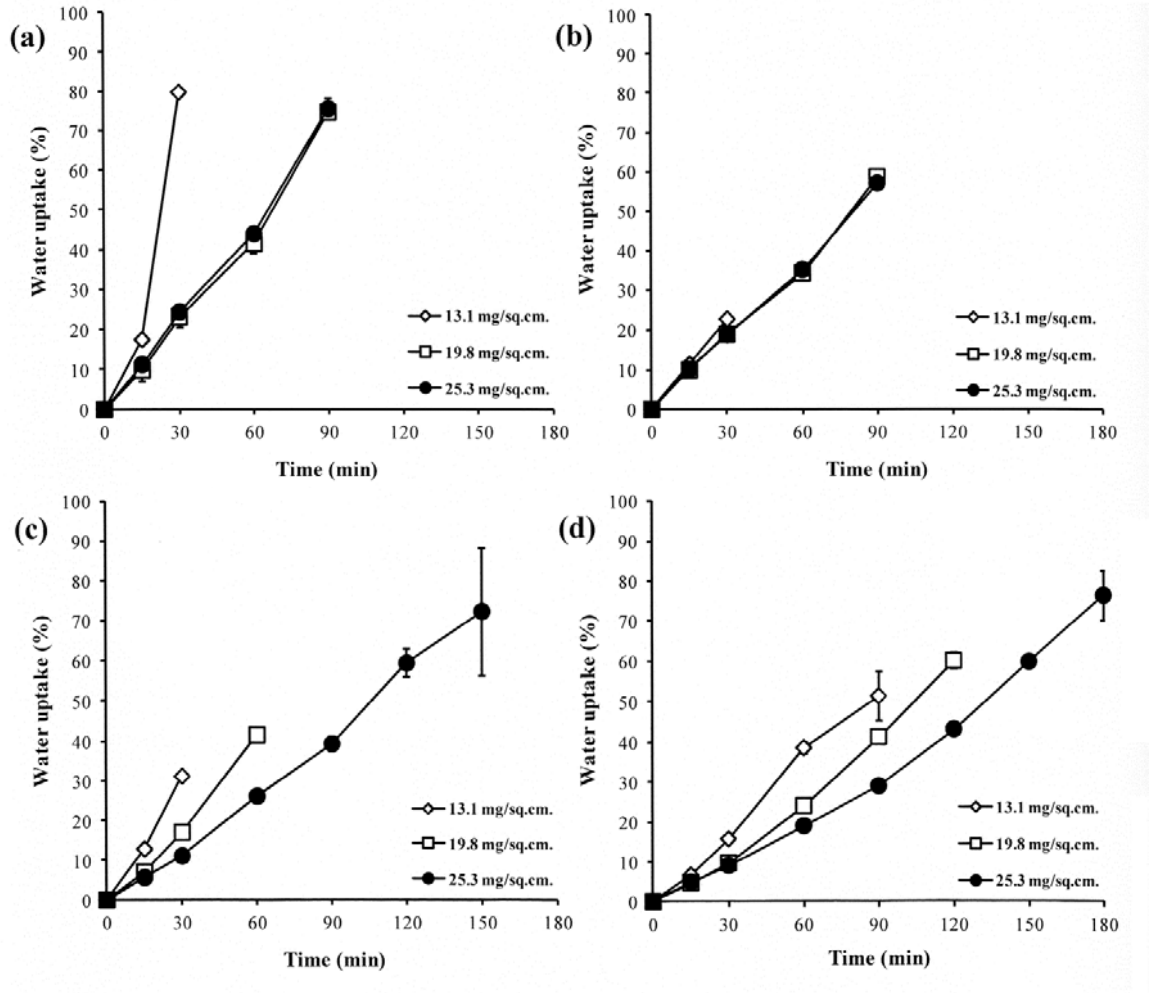


**Figure 20.** Effect of coating level on water uptake of PPN tablets coated with QPM film (a,b) and QPM-MAS (4:0.75) films (c,d) in 0.1 M HCl (a,c) and pH 6.8 phosphate buffer (b,d). Mean values ± SD are indicated, n=3.

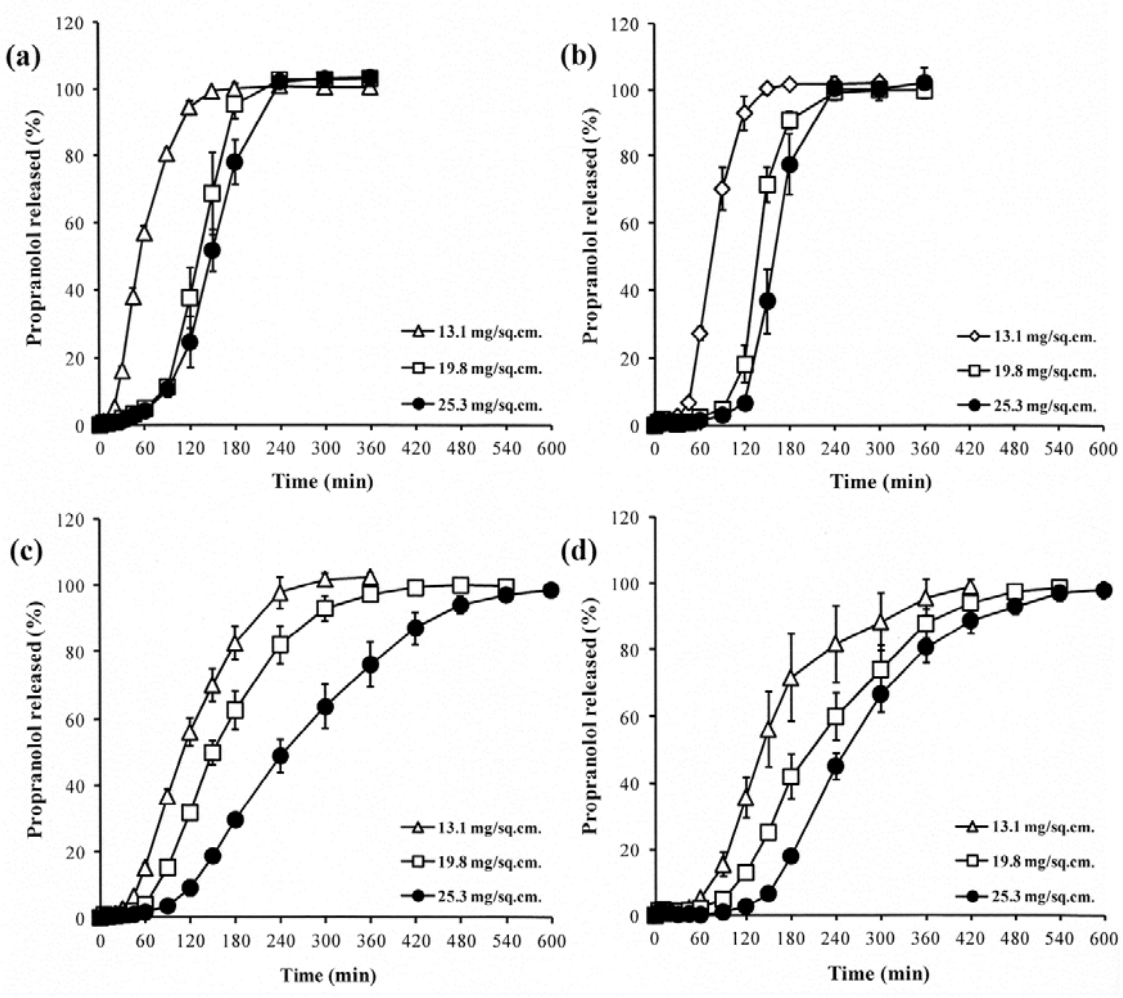


**Figure 21.** Effect of coating level on drug release of PPN tablets coated with QPM film (a,b) and QPM-MAS (4:0.75) films (c,d) in 0.1 M HCl (a,c) and pH 6.8 phosphate buffer (b,d). Mean values ± SD are indicated, n=3.

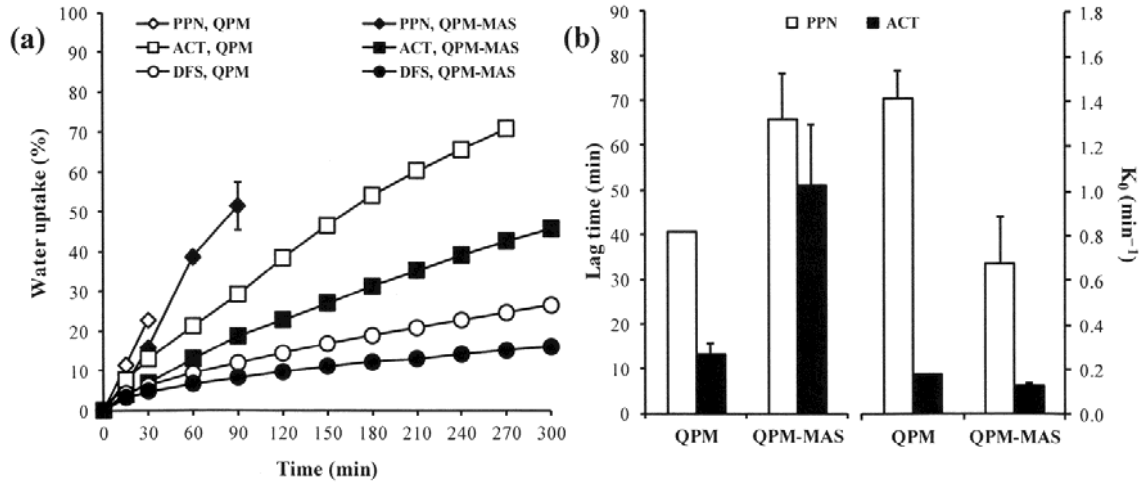


**Figure 22.** Effect of drug type on water uptake (a) and drug release parameters of QPM- and QPM-MAS (4:0.75) tablets in pH 6.8 phosphate buffer. Mean values ± SD are indicated, n=3.

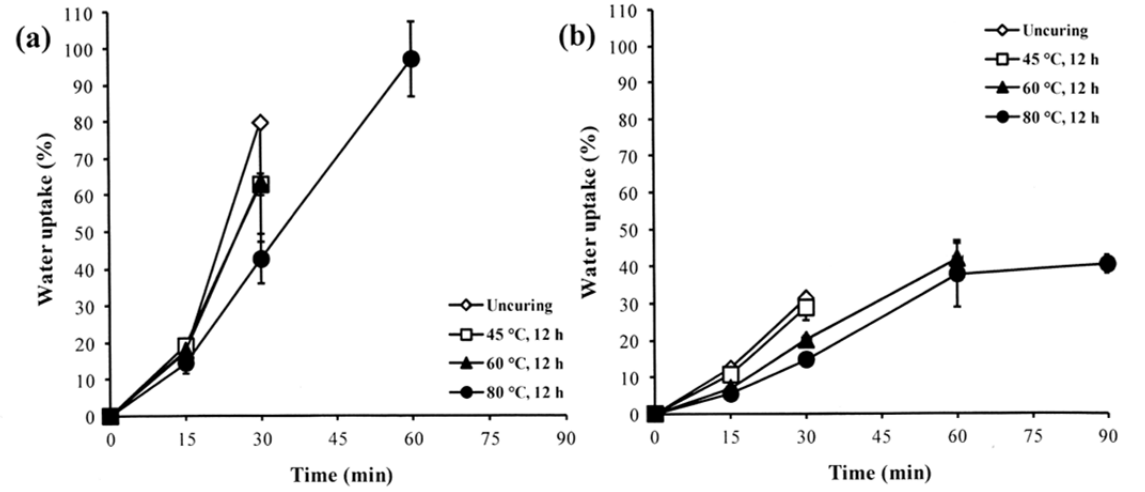


**Figure 23.** Effect of curing temperature on water uptake of PPN tablets coated with QPM (a) and QPM-MAS (4:0.75) films (b) in 0.1 M HCl. Mean values ± SD are indicated, n=3.

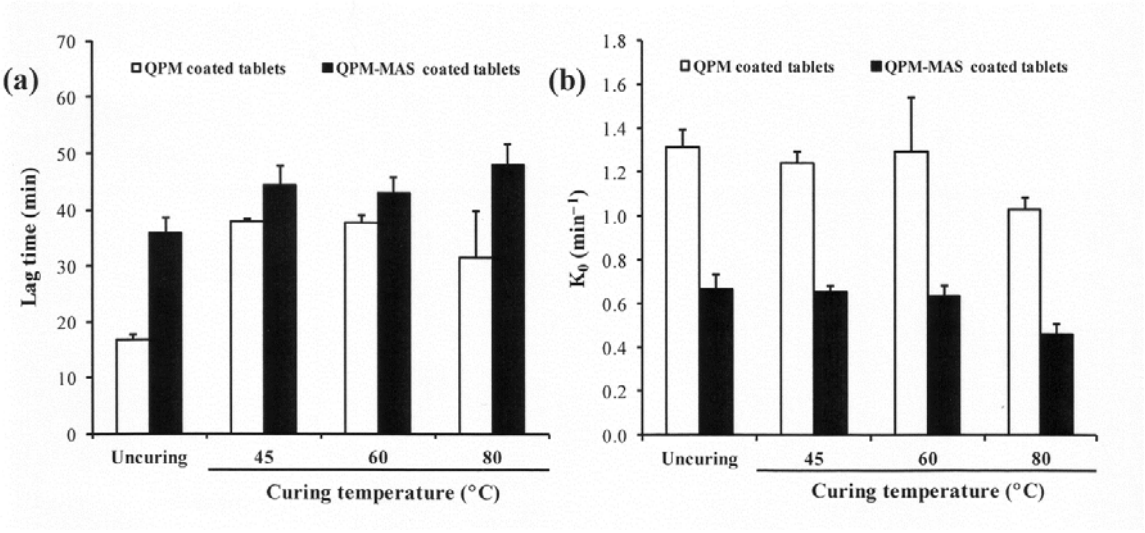


**Figure 24.** Effect of curing temperature on drug release parameters of PPN tablets coated with QPM and QPM-MAS (4:0.75) films in 0.1 M HCl. Mean values ± SD are indicated, n=3.

## Part II: QPM-SA films

### Particle size and zeta potential of QPM-SA dispersions

Aqueous QPM dispersion is a white milky liquid of the colloidal particles. The mean particle size of the QPM was 0.19 μm, and the QPM particles exhibited a positive charge with a zeta potential of 59.9 ± 0.72 mV (Fig. 25) because QPM contains quaternary ammonium groups in its structure. The zeta potential of the SA was -97.3 ± 0.83 mV (n=3). In the preparation of the QPM-SA dispersion, the SA dispersion was slowly added and mixed into the QPM dispersion; then, sedimentation of the dispersed phase of the QPM-SA dispersion was visually observed. The formation of QPM-SA flocculates was expected. It is likely to be caused by electrostatic interactions between the positively charged quaternary ammonium groups ($-N(CH_3)_3^+$) of QPM and the negatively charged carboxyl moiety of SA.

The particle size and zeta potential of the dispersed phase of the QPM-SA dispersions are shown in Fig. 25. The dispersed phase of the QPM-SA dispersions exhibited remarkably larger particle sizes than the QPM particles. This finding indicates that QPM-SA flocculates were formed after adding SA into the QPM dispersion. Furthermore, the particle size and zeta potential of the QPM-SA flocculates decreased as the amount of SA in the dispersions increased. The flocculates, which were positively charged for lower SA concentrations, were negatively charged instead for higher ratios of SA (4:0.5 and 4:1).

Because of the opposite charges of QPM and SA, the positively charged quaternary ammonium groups of QPM could electrostatically interact with the negatively charged carboxyl groups of SA. This interaction caused a decrease in the zeta potential of the QPM, leading to the flocculation of the QPM. In addition, QPM particles were able to form flocculates because of a bridging mechanism via a long side-chain molecule of SA. These phenomena caused the larger particle size of the QPM-SA flocculates in comparison to the QPM particle size. Increasing the SA amount changed the surface charge of the QPM-SA flocculates from positive to negative. This indicates that an excess of SA molecules could completely deposit onto or cover the flocculate surface. Such a change in the QPM-SA flocculates may affect the film characteristics and drug permeability.

**Appearance, thickness and morphology of the films**

QPM films without plasticizer are hard and brittle. Diethyl sebacate (15 %w/w of QPM) was used as a plasticizer in the QPM films to improve the flexibility and promote the particle coalescence that is the mechanism of film formation for aqueous colloidal dispersion polymers (Lehmann, 1997). Transparent QPM films were obtained in this study. The thickness of the films was in the range of 151.8-237.9 μm, as shown in Table 5. The incorporation of SA into the QPM films also resulted in transparent and continuous films for all investigated SA contents, although QPM particle flocculation was occurred when SA was added. Wong and Bodmeier (1996) have suggested that the flocculation of QPM particles may have important implications for film formation. This study demonstrated that the presence of SA did not affect the film formation of the QPM particles. The successful QPM-SA film formation may be attributed to the film-forming property of SA, which can form continuous films, coupled with the coalescence of the QPM particles.

Figure 26a shows the surface and matrix morphologies of the QPM films and the QPM-SA films at 4:0.5 ratio. The surface morphology of the QPM films was smoother than that of the QPM-SA (4:0.5) films. Moreover, the matrix structure of the QPM films was obviously changed with the incorporation of SA. The surface morphologies of the films that were treated with 0.1 M HCl (Fig. 26b) and the pH 6.8 phosphate buffer (Fig. 26c) for 1 h showed evidence of the erosion of the film surface; in particular, small pores appeared in the surface of the QPM-SA films that were treated with the pH 6.8 phosphate buffer. In addition, the matrix morphology of the films was also altered, and pore formation occurred in the QPM-SA film matrix in the pH 6.8 phosphate buffer (Fig. 26c). This result suggests that some ingredients leached out of the QPM films when they were exposed to both media and that the presence of SA had a significant effect on the erosion and pore formation of the QPM-SA films.

**Molecular interaction between QPM and SA**

The molecular interaction between QPM and SA in the films was investigated using ATR-FTIR spectroscopy. The ATR-FTIR spectra of the SA film, QPM films, and QPM-SA films are presented in Fig. 27. The SA film exhibited three outstanding peaks corresponding to a $COO^-$ (asymmetric) stretching at 1593 $cm^{-1}$, a $COO^-$ (symmetric) stretching peak at 1409 $cm^{-1}$, and a C–O–C stretching peak at 1026 $cm^{-1}$(Fig. 27a)

(Sartori et al., 1997). The spectrum of the QPM film exhibited a C–H stretching, a C=O stretching, a $CH_2$ symmetric bending, a $CH_3$ asymmetric bending, a C–CO–C stretching and a C–O–C stretching at approximately 2857-2983, 1727, 1447, 1382, 1146, and 1027 $cm^{-1}$, respectively (Fig. 27b).The QPM films with SA showed a shift in the $COO^-$ (asymmetric) stretching peak of SA from 1593 to a higher wavenumber, in the range of 1604-1622 $cm^{-1}$ (Fig. 27c-27f). Moreover, the QPM-SA films at 4:1 ratio also exhibited the $COO^-$ (symmetric) stretching peak of SA at 1414 $cm^{-1}$ (Fig. 27f), which was shifted from 1409 $cm^{-1}$ (Fig. 27a). These shifts strongly indicate an ionic interaction of the carboxyl groups of SA with positively charged molecules (Sartori et al., 1997; Lawrie et al., 2007). When higher SA contents were added to the films, the C–H stretching peaks of QPM were changed, and a new peak corresponding to C–N stretching at 1093-1095 $cm^{-1}$ was clearly observed (Fig. 27e and 27f).This result suggests that the quaternary ammonium groups of QPM electrostatically interacted with the carboxyl groups of SA. This interaction may cause a change in the film properties and drug permeability.

**Thermal behavior of the films**

The QPM films exhibited an endothermic peak at approximately 340 °C, followed by an exothermic degradation peak at 380.4 °C (Fig. 28a).The SA exhibited an exothermic peak at 215 °C, followed by an endothermic peak at approximately 220 °C (Fig. 28b), indicating that a recrystallization and a phase transition of the SA after heat induction may have occurred (Pongjanyakul et al., 2005). Then, the first and second exothermic degradation peaks of SA were observed at 257.8 and 362.8 °C, respectively. The thermal behavior of the QPM-SA films at the ratios of 4:0.1 and 4:0.25 showed a small shift of the QPM degradation peak toward lower temperatures (Fig. 28c and 28d), suggesting that the SA disturbed the film-structure formation of the QPM. In addition, the QPM-SA films with higher amounts of SA (4:0.5 and 4:1) showed both degradation peaks of SA without the degradation peak of the QPM films (Fig. 28e and 28d). It was possible to conclude that the degradation of SA could induce QPM degradation at a lower temperature. The appearance of the degradation peaks of SA suggests that a phase separation of SA in the microenvironment of the film might have occurred. It also suggests that the QPM-SA flocculates that formed for higher contents of SA were covered with SA molecules, as discussed in the zeta potential studies, and the SA molecules around the QPM-SA flocculates could undergo intermolecular interactions with adjacent flocculate particles.

This phenomenon could change the matrix structure and modify the characteristics of the QPM films.

**Water uptake and erosion of the films**

The water uptake and erosion of the QPM-SA films in 0.1 M HCl and pH 6.8 phosphate buffer after 30 and 60 min of the test are shown in Fig. 29. The water uptake of the QPM-SA films tended to decrease with increasing SA content in the acidic medium (Fig. 29a), whereas the erosion seemed to decrease with the addition of 6.3 %w/w SA, and an increase in film erosion was found for the QPM-SA films at 4:0.5 and 4:1 ratios (Fig. 29c). The decrease in the water uptake of the QPM-SA films was caused by the conversion of SA to a water-insoluble alginic acid in acidic conditions (Østberg et al., 1994), leading to a reduction of the film erosion. However, the QPM-SA films at 4:0.5 and 4:1 ratios showed higher erosion because the SA could leach out of the films before converting to alginic acid.

In neutral pH conditions, the QPM-SA films demonstrated a clear decrease in water uptake for SA contents in the ratios of 4:0.1 and 4:0.25, and the lowest water uptake was observed for 6.3 %w/w SA (Fig. 29b). The incorporation of 12.5 %w/w SA (4:0.5) into the films caused an increase in the water uptake, and the water uptake of the films with 25 %w/w SA (4:1) could not be determined because of a very high swelling of the films that could not be accommodated. In contrast, the erosion of the QPM-SA films gradually increased with increasing SA content (Fig. 29d). From these results, it could be understood that the SA in the films could rapidly swell and dissolve in the neutral medium (Pongjanyakul and Puttipipatkhachorn, 2007a), leading to an increase in the matrix erosion of the films. However, the decrease in the water uptake of the films at the ratios of 4:0.1 and 4:0.25 indicates a strong interaction between QPM and SA in the wet state because of a disentanglement of the SA molecules, especially in the case of the film at 4:0.25 ratio. This interaction resulted in the lower water uptake of the films. Furthermore, the QPM-SA (4:0.5) films demonstrated the influence of an excess of SA in the films, which caused higher water uptake and matrix erosion.

**Mechanical properties of the films**

The puncture strength and elongation of the QPM and QPM-SA films in the dry and wet states were investigated and are listed in Table 5. In the dry state, the addition of SA to the QPM films caused an increase in the puncture strength, but a decrease in the %elongation was observed. This result suggests that the interaction between QPM and SA could enhance the film strength. Because of the film-forming property of SA, SA in a region of phase separation coupled with the coalescence process of QPM particles could form a continuous matrix. This interaction resulted in the stronger film formation of the QPM-SA films for higher SA contents. However, the stronger matrix of the films was usually accompanied by lower flexibility of the films (Remuñán-López and Bodmeier, 1997), as can be seen from this study.

The wet QPM films in 0.1 M HCl and the pH 6.8 phosphate buffer exhibited lower puncture strength and higher %elongation than the dry QPM films (Table 5). This result suggests that water molecules could be absorbed and inserted into the polymeric matrix, which caused a reduction in the film strength. Moreover, water molecules could also act as a plasticizer, leading to higher flexibility of the films (Bodmeier and Paeratakul, 1993). In the case of the QPM-SA films at acidic pH, the puncture strength of the QPM-SA films increased with increasing SA content, whereas the %elongation of the films decreased. SA can be converted to an unionized form, a water-insoluble alginic acid, under acidic conditions. The alginic acid that was embedded in the film matrix enhanced the film strength but decreased the flexibility of the films.

On the other hand, in the pH 6.8 phosphate buffer, the puncture strength and %elongation of the QPM-SA films at the ratios of 4:0.1 and 4:0.25 were not decreased in comparison to the QPM films (Table 5). The addition of a larger amount of SA (4:0.5) resulted in a remarkable reduction in both these parameters of the QPM-SA films. Furthermore, the films with SA at 4:1 ratio could not be properly handled, so their puncture strength and %elongation could not be determined. As expected, SA could ionize and swell in the pH 6.8 phosphate buffer, resulting in considerable swelling of the films when used in higher amounts (4:0.5 and 4:1). This behavior could explain the clear decrease that was observed in both parameters and the inability to measure the films with the highest SA content used in this study. However, for lower SA contents, the swelling of the negatively charged SA still promoted the interaction between the QPM and the SA via electrostatic force. In addition, the disentanglement of the SA could enhance the

flexibility of the films at neutral pH. This finding indicates that the interaction of QPM with SA can strengthen the films in both the dry and wet states. This could be a major advantage for the use of such films as coating material for solid dosage forms intended to modify drug release in the gastrointestinal tract.

**Tackiness of the films**

QPM films normally present a tackiness that is the primary disadvantage of these films during the tablet-coating process and the storage of coated tablets. Therefore, an anti-tacking agent was used to prevent the agglomeration of the coating on the substrate. In this study, the tackiness of the QPM films was measured by determining the detachment force, as shown in Fig. 30. In the dry state, the incorporation of SA at the ratios of 4:0.25, 4:0.5 and 4:1 clearly reduced the detachment force of the QPM films, but the decrement of the detachment force appeared to be unrelated to the amount of SA that was added. Moreover, in the wet state, the QPM-SA films at 4:0.25 and 4:0.5 ratios exhibited lower detachment forces than the QPM films. The QPM-SA (4:1) films could not be measured because of the very high swelling of the films. These results suggest that the incorporation of SA could reduce the tackiness of QPM films by decreasing the contact area of the QPM on the film surface (Nimkulrat et al., 2004). Moreover, the interaction of QPM and SA hindered the interdiffusion of the QPM chains, and the QPM exhibited a lower attractive force.

**Drug permeability of the films**

The cumulative PPN permeation profiles across the films using 0.1 M HCl and a pH 6.8 phosphate buffer, as shown in Fig. 31, exhibited a good linearity ($R^2 > 0.98$) with a lag time. These permeation profiles indicate that the PPN permeation reached a steady state and could be described using the Fick's first law (Eq. 7 and 8). The PPN permeation parameters for 0.1 M HCl are listed in Table 6. A similar lag time was found for SA contents in the ratios of 4:0.1, 4:0.25 and 4:0.5, but a longer lag time was found in the QPM-SA (4:1) films. The permeation flux and P values of PPN decreased with increasing SA content in the films. To compare the drug diffusion through the films independent of the effect of the wet film thickness, which increased with increasing SA content (data not shown), the $D_C$ values were estimated using Eq. 8. The QPM-SA films exhibited higher $D_C$ values than the QPM films, but increasing the SA content did not significantly affect

the $D_C$ values of the QPM-SA films. This finding suggests that the incorporation of SA into the QPM films led to higher drug diffusion, despite the observed decrease in water uptake of the QPM-SA films (Fig. 29a). This result indicates that the QPM-SA films contained large water-filled channels with low tortuosity because of the conversion of SA to alginic acid in the acidic medium. The alginic acid that formed had weak intermolecular bonding (Aslani and Kennedy, 1996), which led to large aqueous pores in the films, resulting in the higher D values of the QPM-SA films in comparison to those of the QPM films.

In the pH 6.8 phosphate buffer, the PPN flux and $P_C$ values of the QPM-SA films also decreased with increasing SA content, and the films at 4:1 ratio could not be tested. The longest lag time was observed in the QPM-SA film at 4:0.25. The $D_C$ values of the films decreased with increasing SA contents in the ratios of 4:0.1 and 4:0.25, and then an increase in the $D_C$ value was observed for the QPM-SA (4:0.5) film. This is consistent with the fact that the QPM-SA films had lower water uptake than the QPM films (Fig. 29b). Moreover, the SA in the films could ionize and disentangle in this medium, which promoted electrostatic interaction with positively charged QPM. This phenomenon enhanced the strong matrix structure (shown in the mechanical properties of the films in Table 1) with small water-filled channels of high tortuosity, especially in the case of the QPM-SA (4:0.25) films, which exhibited the lowest water uptake. Moreover, the positive charge of drug, PPN in this case, may have interacted with the ionized SA (Pongjanyakul and Suksri, 2009), thereby causing longer lag times and slower drug diffusion across the films. For higher SA content (4:0.5), the excess SA in the films led to higher swelling and matrix erosion, resulting in larger water-filled channels and the formation of small pores on the film surface and matrix, which are shown in Fig. 26c. Therefore, a higher $D_C$ value was obtained. Furthermore, the $D_C$ values of the films in the neutral medium were lower than those in the acidic medium. This result suggests that the ionization of SA in the neutral medium had a crucial effect on the drug permeability of the QPM-SA films.

**Effect of SA block on film properties**

Generally, QPM films without plasticizers are hard and brittle, which led to the use of diethyl sebacate (15 %w/w of QPM) as a plasticizer in this study. Consequently, transparent QPM films were obtained. The incorporation of SA into the QPM films also resulted in transparent and continuous films for all investigated SA contents. Successful QPM-SA film formation may be attributed to the film-forming property of SA, both G-block SA (GSA) and M-block SA (MSA), which can form continuous films, coupled with QPM particle coalescence. The QPM-SA films had a similar appearance using GSA or MSA. Moreover, the thicknesses of the QPM-GSA and QPM-MSA films at various ratios were not different, as shown in Table 7. However, increasing SA content in the films caused an increase in film thickness due to higher solid content in the dispersions used for film casting (Pongjanyakul and Puttipipatkhachorn, 2008).

The water uptake and erosion of the QPM-SA films in 0.1 M HCl and pH 6.8 phosphate buffer after 30 min are shown in Fig. 32. In the acidic medium, the QPM-MSA films had remarkably higher water uptake than the QPM-GSA films (Fig. 32a). The water uptake of the QPM-GSA films decreased with increasing GSA amounts, whereas increasing MSA amounts did not affect QPM-MSA film water uptake(Fig. 32a).The matrix erosions of the QPM-MAS films were also greater than those of the QPM-GSA films (Fig. 32c). Additionally, higher SA amounts in the films increased matrix erosion. In fact, SA was changed to a water-insoluble alginic acid in acidic conditions (Østberg et al., 1994). In addition, GSA had a stronger gel structure of alginic acid than MSA (Draget et al., 1994; Pongjanyakul, 2009), leading to decreased water uptake in the QPM-GSA films when the GSA amount was increased. This result could explain why the matrix erosions in the QPM-GSA films were lower than those of the QPM-MSA films.

In pH 6.8 phosphate buffer, the QPM-SA films demonstrated a clear decrease in water uptake in films that had increased QPM-SA ratios; the lowest water uptake was observed for QPM-SA ratios of 4:0.25 (Fig. 32b). Then, increased QPM-SA ratios caused an increase in water uptake; the water uptake of films with an SA ratio of 4:1 could not be measured due to the very high swelling of the films, which could not be accommodated. The QPM-GSA films at the ratios of 4:0.1 and 4:0.5 had greater water uptake than the QPM-MSA films when compared at the same ratios. Apart from water uptake results, the erosion of the QPM-SA films gradually increased with increasing SA content (Fig. 32d). It can be observed that the matrix erosion of the QPM-GSA films was higher than that of

the QPM-MSA films (Fig. 32d). From these results, it could be hypothesized that the SA in the films could rapidly swell and dissolve in pH 6.8 phosphate buffer (Sriamornsak et al. 2007; Pongjanyakul and Puttipipatkhachorn, 2007), leading to an increase in the matrix erosion of the films. However, the decreased water uptake in the QPM-SA films at 4:0.1 and 4:0.25 ratios suggested a strong interaction between QPM and SA in the wet state because the SA molecules could fully disentangle in this medium, particularly in the films at a ratio of 4:0.25. This interaction resulted in the lower water uptake of the films. In addition, the QPM-SA (4:0.5) films demonstrated the influence of excess SA in the films, causing higher water uptake and matrix erosion. Furthermore, these results also suggest that GSA incorporation into the QPM films caused higher swelling than MSA, leading to greater water uptake and matrix erosion in the QPM-GSA films.

The puncture strength and elongation of the dry and wet QPM-SA films are listed in Table 7. The dry QPM-GSA films had an obviously higher puncture strength than the dry QPM-MSA films at increased SA ratios, whereas the % elongations were not different. Moreover, increased GSA ratios enhanced the puncture strength of the wet films when using 0.1 M HCl. This effect did not occur for MSA, which had comparable puncture strengths with increasing MSA amounts. However, the QPM-GSA and QPM-MSA films had decreased % elongation with increasing SA ratios in 0.1 M HCl. Using pH 6.8 phosphate buffer, the puncture strength of the QPM-GSA films remarkably decreased when using a QPM-GSA ratio of 4:0.5, whereas decreased puncture strength in the QPM-MSA films was observed for the 4:0.25 ratio. The % elongation of the QPM-SA films rapidly decreased when using the 4:0.5 ratio in neutral medium. Furthermore, the 4:1 ratio films could not be properly handled; therefore, their puncture strength and %elongation could not be determined. In addition, the % elongations of the films in neutral medium were higher than in acidic medium.

In addition to the coalescence process of the QPM particles, SA that was dispersed and interacted with the QPM particles was still able to form a continuous matrix. This is likely due to the film-forming property of SA. In the dry state, GSA enhanced the mechanical strength of the QPM films compared with MSA. This result suggests that GSA may have a stronger interaction with QPM than does MSA. However, the stronger matrix of the films was usually accompanied by lower film flexibility (Remuñán-López et al., 1997), which is evident in this study. For the QPM-SA films at acidic pH, the puncture strength of the QPM-GSA films was higher than the QPM-MSA films due to the

stronger alginic acid gel of GSA (Draget et al., 1994; Pongjanyakul, 2009). However, the alginic acid that was embedded in the film matrix enhanced the film strength but decreased the flexibility of the films.

As expected, SA was able to ionize and swell in the neutral pH medium, resulting in considerable swelling of the films when higher SA ratios were used (4:0.5 and 4:1). This behavior could explain the clear decrease that was observed in both parameters and the inability to measure the films with the highest SA content used in this study. However, for the QPM-GSA films, the strength was clearly decreased when using GSA at a 4:0.5 ratio, whereas the 4:0.25 ratio of MSA caused decreased film strength. This result also suggested that GSA may interact with QPM via a stronger electrostatic force when compared with MSA because the chain conformation of GSA may promote the interaction with QPM. In addition, disentanglement of the SA may enhance film flexibility at neutral pH. Collectively, this result indicated that the interaction between QPM and SA can strengthen the films in both the dry and wet states, particularly GSA. This could be a major advantage for the use of such films as a coating material for solid dosage forms that are intended to modify drug release in the gastrointestinal tract.

The cumulative PPN permeation profiles across the QPM-SA films using 0.1 M HCl and pH 6.8 phosphate buffer exhibited good linearity ($R^2$ higher than 0.98) with a lag time. The permeation parameters of PPN across the films were able to be computed using Eq. 7 and 8, as shown in Fig. 33. In 0.1 M HCl, the QPM-GSA films had a longer lag time at increasing GSA ratios. In contrast, a higher ratio of MSA in the films caused a shorter lag time (Fig. 33a). The QPM-GSA films had longer lag times than the QPM-MSA films at ratios higher than 4:0.25. The $P_C$ values of the QPM-MSA films were lower than those of QPM-GSA, and this value decreased with increasing SA ratios (Fig. 33c). The reduction of the $P_C$ values of the QPM-SA films may be resulted in the increase of film thickness, thus the $D_C$ values were calculated by using Eq. 8 for comparison of drug permeation. The $D_C$ values appeared to increase with increasing SA ratios (Fig. 33e). However, the QPM-GSA film had a remarkably smaller $D_C$ value than the QPM-MSA film at a ratio of 4:1. This result indicated that the incorporation of SA into the QPM films led to lower drug permeability but higher drug diffusion, particularly for the QPM-MSA films, which had the same water uptake with increasing MSA ratios. This result suggested that water-filled channels that have low tortuosity could possibly form when SA is converted to alginic acid in the acidic medium. The alginic acid that formed has

weak intermolecular bonding (Aslani and Kennedy, 1996), leading to low tortuosity of the aqueous channels in the films. However, the QPM-GSA (1:1) films had lower $D_C$ values than the MSA films due to the formation of the strong alginic gel in the GSA film. Additionally, there was a stronger interaction between GSA and QPM, which also caused smaller water-filled channels that have higher tortuosity for drug diffusion. Furthermore, this hypothesis is supported by the water uptake results.

In neutral pH medium, the longest lag time of PPN permeation was observed in the QPM-SA films at 4:0.25 ratio, and the QPM-MSA films had shorter lag times than the QPM-GSA films (Fig. 33b). The $P_C$ values decreased with increasing SA ratios (Fig. 33d), and MSA had higher $P_C$ values in the QPM films than GSA. However, the QPM-SA films prepared using GSA and MSA at various ratios had similar $D_C$ values; the lowest $D_C$ value was observed for the 4:0.25 ratio (Fig. 33f). This is consistent with the observation that the QPM-SA films at this ratio had the smallest water uptake. The overall results in the neutral pH buffer demonstrated that the QPM-MSA films had higher drug permeability than the QPM-GSA films. However, similar drug diffusivity for both films was obtained, but the QPM-GSA films had greater water uptake and matrix erosion. It is expected that the QPM-GSA films may also have high tortuosity in their matrix structure after hydration and erosion due to the possibly stronger interaction of GSA with QPM, which may cause the similar barrier properties for drug diffusion in the QPM-GSA and QPM-MSA films.

**Characteristics of the QPM-GSA coated tablets**

The QPM-GSA dispersions at various ratios were used as coating materials to modify PPN release. Moreover, PPN core tablets coated with the QPM-GSA (4:1) film at different coating levels were also prepared. An issue for tablet coating occurred when using the QPM-GSA dispersions at the ratios of 4:0.1 and 4:0.25. The incorporation of GSA into the QPM dispersions decreased the zeta potential of the positively charged QPM particles, which caused the formation of QPM-GSA flocculates. The flow of these dispersions in a small tube before spraying caused an induction of larger flocculates, leading to nozzle clogging. Therefore, these dispersions were only able to be coated onto the core tablets at the 4 % coating level. However, the 4:0.5 and 4:1 ratio QPM-GSA dispersions did not cause nozzle clogging because GSA was able to interact with QPM

causing the zeta potential of the flocculates to become negative. This phenomenon led to a strong repulsion force in the flocculates and the dispersion had good stability.

The surface and film matrix morphologies of the QPM-coated tablets are shown in Fig. 34a. A rougher surface of the coated tablets was observed when GSA was added into the films at ratios of 4:0.5 and 4:1 (Fig. 34b and 34c, respectively), but the coated films had similar matrix morphologies. Moreover, increased coating levels corresponded to increased film thickness on the coated tablets, as shown in Fig. 34c-34e.

**Effect of QPM-GSA ratios and coating levels on coated tablets**

The PPN release profiles of the QPM-GSA coated tablets (4 % coating level) at different QPM-GSA ratios in 0.1 M HCl and pH 6.8 phosphate buffer are presented in Fig. 35a and 35b, respectively. The dissolution of PPN from the core tablets in both media was completed within 30 min. The QPM or QPM-GSA coated tablets had slower PPN release rates than the core tablets. The parameters used for PPN release rate comparisons were lag time and zero-order release rate ($K_0$).The relationship between % PPN released and time had good linearity with an $R^2$ higher than 0.98 when drug release was less than 50%. Therefore, the lag times and $K_0$ values were calculated and are listed in Table 8.

The PPN tablets coated with the QPM-GSA films at ratios of 4:0.1 and 4:0.25 had similar drug release profiles in acidic medium, and the $K_0$ values appeared to decrease with increasing GSA ratios. However, the lag time of the QPM-GSA coated tablets at ratios of 4:0.1 and 4:0.25 could not be determined. It is expected that PPN would rapidly release from the coated tablets at the initial stage of the release process. Additionally, longer lag times and lower PPN release rates were observed in the QPM-GSA tablets at ratios of 4:0.5 and 4:1, which were related to the GSA ratio. These results suggest that the QPM-GSA films at ratios of 4:0.5 and 4:1 could sustain drug release from tablets in acidic medium because alginic formation may enhance film strength and create a stable film for controlling drug release.

In pH 6.8 phosphate buffer, the QPM-GSA coated tablets had shorter lag times and higher PPN release rates than the QPM coated tablets, except the QPM-GSA (4:0.5) coated tablets had a sustained-release of PPN (Fig. 35b and Table 8).The rapid release of PPN from the QPM-GSA coated tablets caused SA swelling and erosion in the films. However, the sustained release of the QPM-GSA (4:0.5) coated tablets could be occurred

because the coated films at this ratio may be strengthened in neutral pH medium. This phenomenon suggested that the strongest interaction between QPM and GSA may occur at this ratio during drug release testing. This effect is observed because SA ionized in pH 6.8 medium is able to interact with the positively charged QPM. Moreover, the 4:1 ratio QPM-GSA films may have excess SA, which promoted matrix erosion of the films. Therefore, a faster release rate in the QPM-GSA (4:1) coated tablets was obtained.

The QPM-GSA (4:1) coated tablets at 4, 8, and 12 % coating levels were prepared and the PPN release profiles in 0.1 M HCl and pH 6.8 phosphate buffer are illustrated in Fig. 35c and 35d, respectively. Increased coating levels resulted in longer lag times and lower PPN release rates in the coated tablets (Table 8). This was attributed to an increased drug diffusion path length through the coated films, which was stable in the films when they were in an acidic medium. Additionally, increased film coating levels caused lower water uptake into the core tablets, which affected drug dissolution and release (Pongjanyakul et al., 2005). Apart from the use of 0.1 M HCl, the PPN released from the coated tablets was not related to the coating levels. Increasing the coating level from 4 % to 8 % caused a longer lag time and a decreased PPN release rate (Table 8). However, similar PPN release rates were observed in the coated tablets with 8 and 12% coating levels. This was due to SA dissolution in neutral pH medium, where many aqueous pore channels could be created, leading to film erosion. This phenomenon may accelerate drug release when the coated tablets have higher coating levels.

**Effect of SA block structure on coated tablets**

The PPN core tablets coated with the QPM-GSA and QPM-MSA films using a 4:0.5 ratio at a 4 % coating level were prepared and the water uptake was tested in 0.1 M HCl and pH 6.8 phosphate buffer prior to the PPN release study. The QPM-GSA coated tablets had less water uptake than the QPM-MSA coated tablets in both media (Fig. 36). The QPM-MSA coated tablets had rapid water uptake in neutral medium. The PPN release profiles of the QPM-GSA and QPM-MSA coated tablets in 0.1 M HCl and pH 6.8 phosphate buffer are shown in Fig. 37a and 37b, respectively. The lag times and PPN release rates are also presented in Fig. 37c and 37d, respectively. The QPM-GSA coated tablets had an insignificant lag time and lower PPN release rate than the QPM-MSA coated tablets in acidic medium. This was due to the lower water uptake of the QPM-GSA coated tablets. Moreover, the lower drug permeability of the QPM-GSA films

adequately explains this result. Conversely, the QPM-GSA coated tablets had a longer lag time and lower drug release rate in pH 6.8 phosphate buffer. The higher water uptake of the QPM-MSA coated tablets may enhance PPN dissolution and diffusion, leading to faster PPN release than the QPM-GSA coated tablets. However, the PPN release rate of the coated tablets using pH 6.8 phosphate buffer was lower than when using 0.1 M HCl. This result suggests that SA swelling in neutral medium may induce a strong interaction with QPM, leading to higher tortuosity of the films. Specifically, a longer lag time and lower PPN release rate in the QPM-GSA coated tablets was obtained.

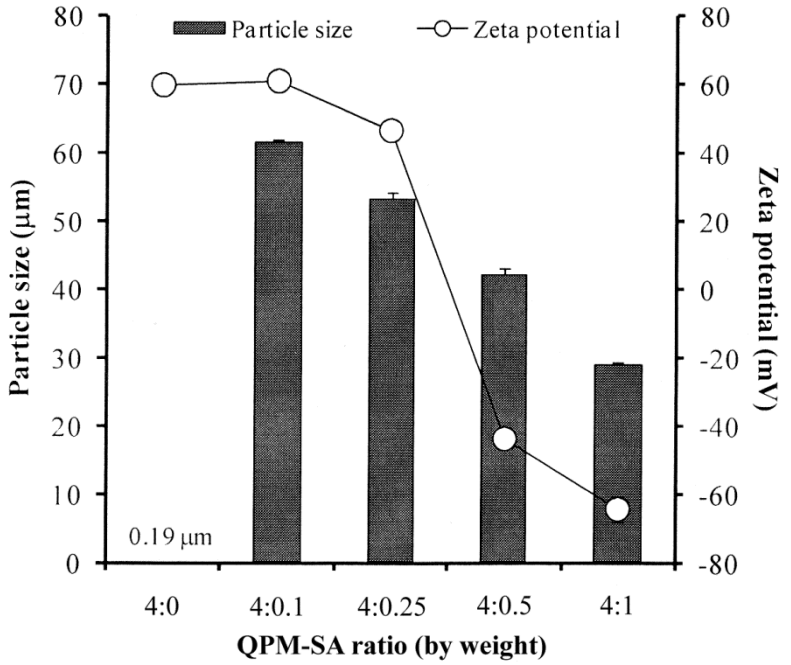


**Figure 25.** Particle size and zeta potential of QPM-SA flocculates in QPM dispersions containing various SA concentrations. Data are mean ± S.D., n=3.

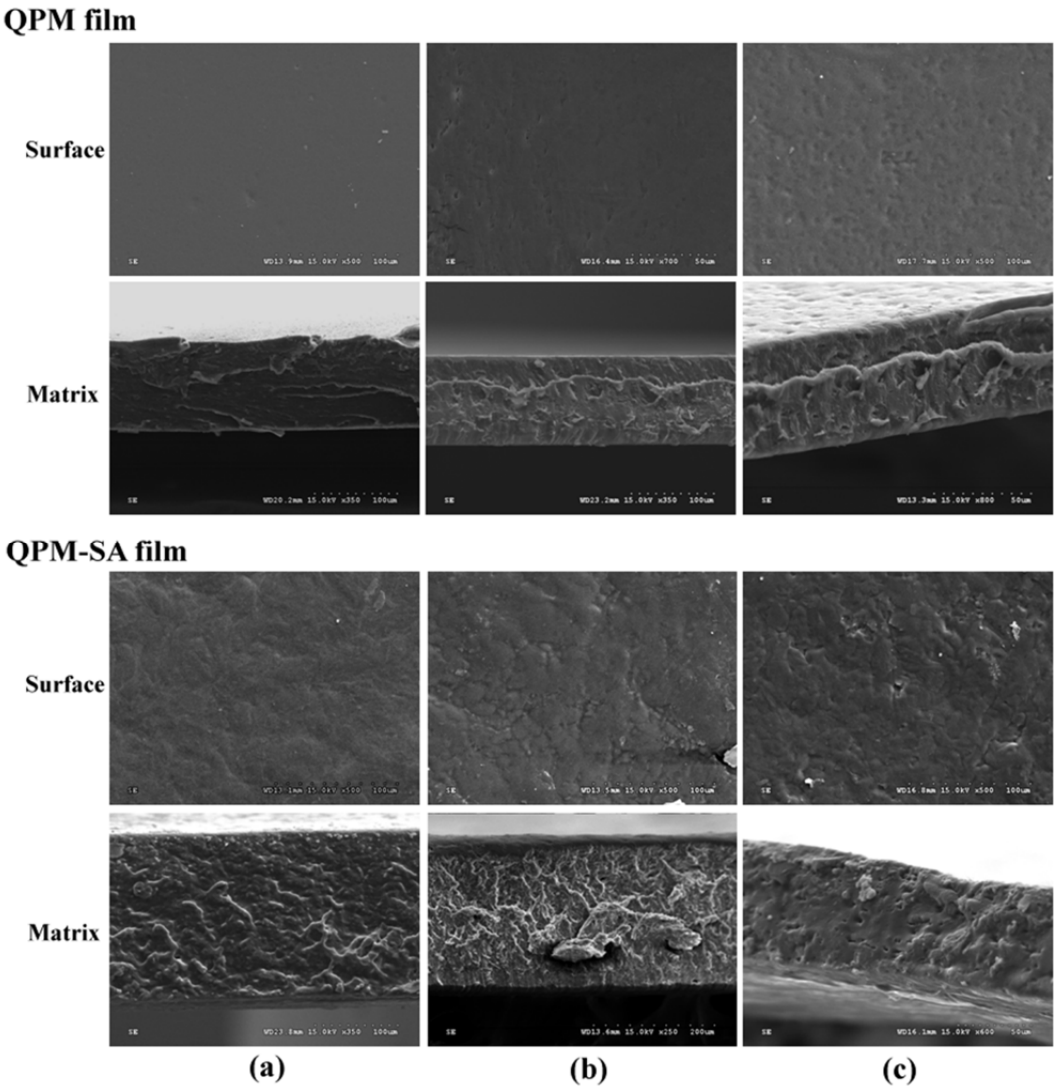


**Figure 26.**Surface and matrix morphology of QPM film and QPM-SA film with 12.5 %w/w SA (a), and the films treated with 0.1 M HCl (b) and pH 6.8 phosphate buffer (c) for 1 h.

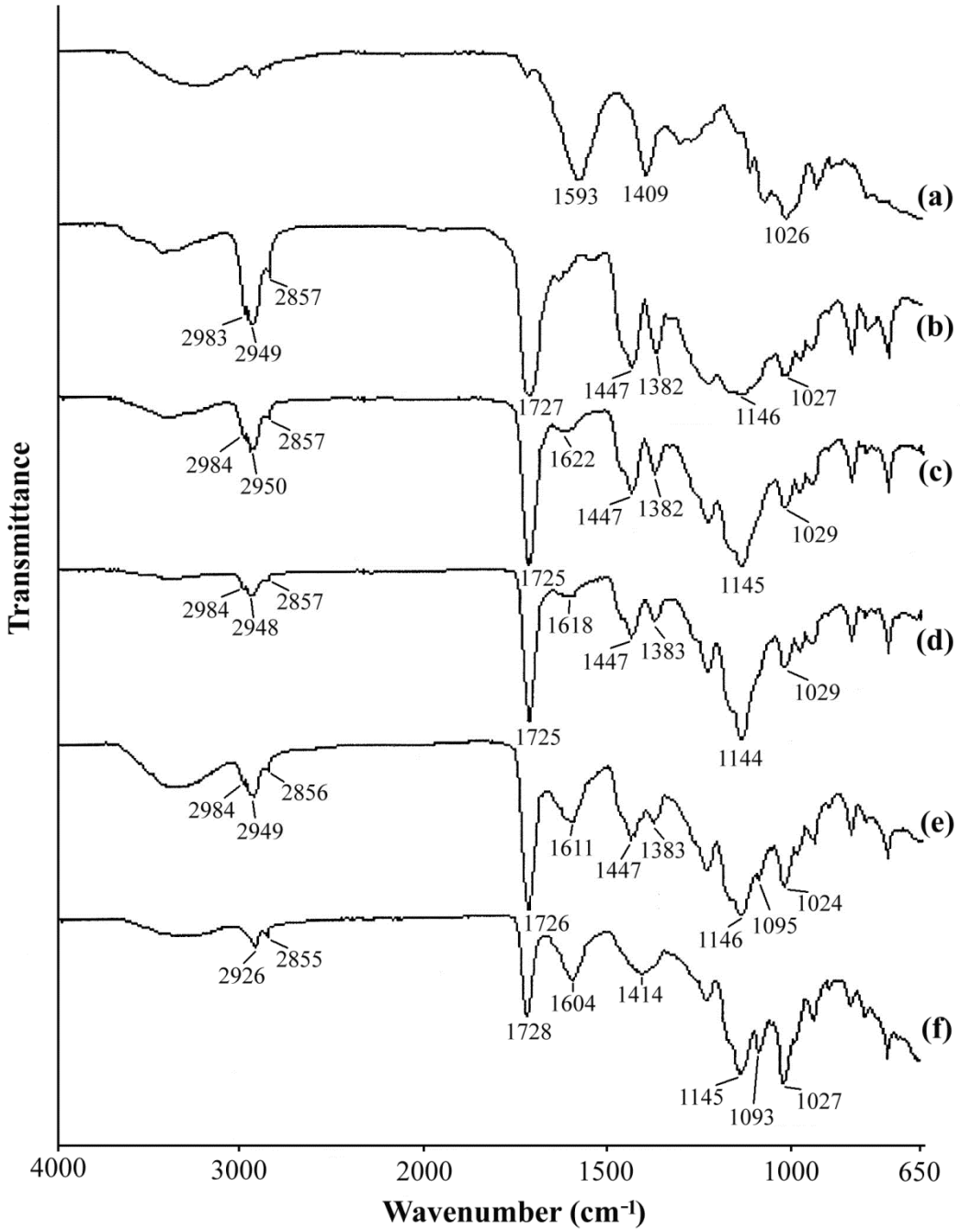


**Figure 27.** ATR-FTIR spectra of SA film (a), QPM film (b), and QPM-SA films at the ratios of 4:0.1 (c), 4:0.25 (d), 4:0.5 (e) and 4:1 (f).

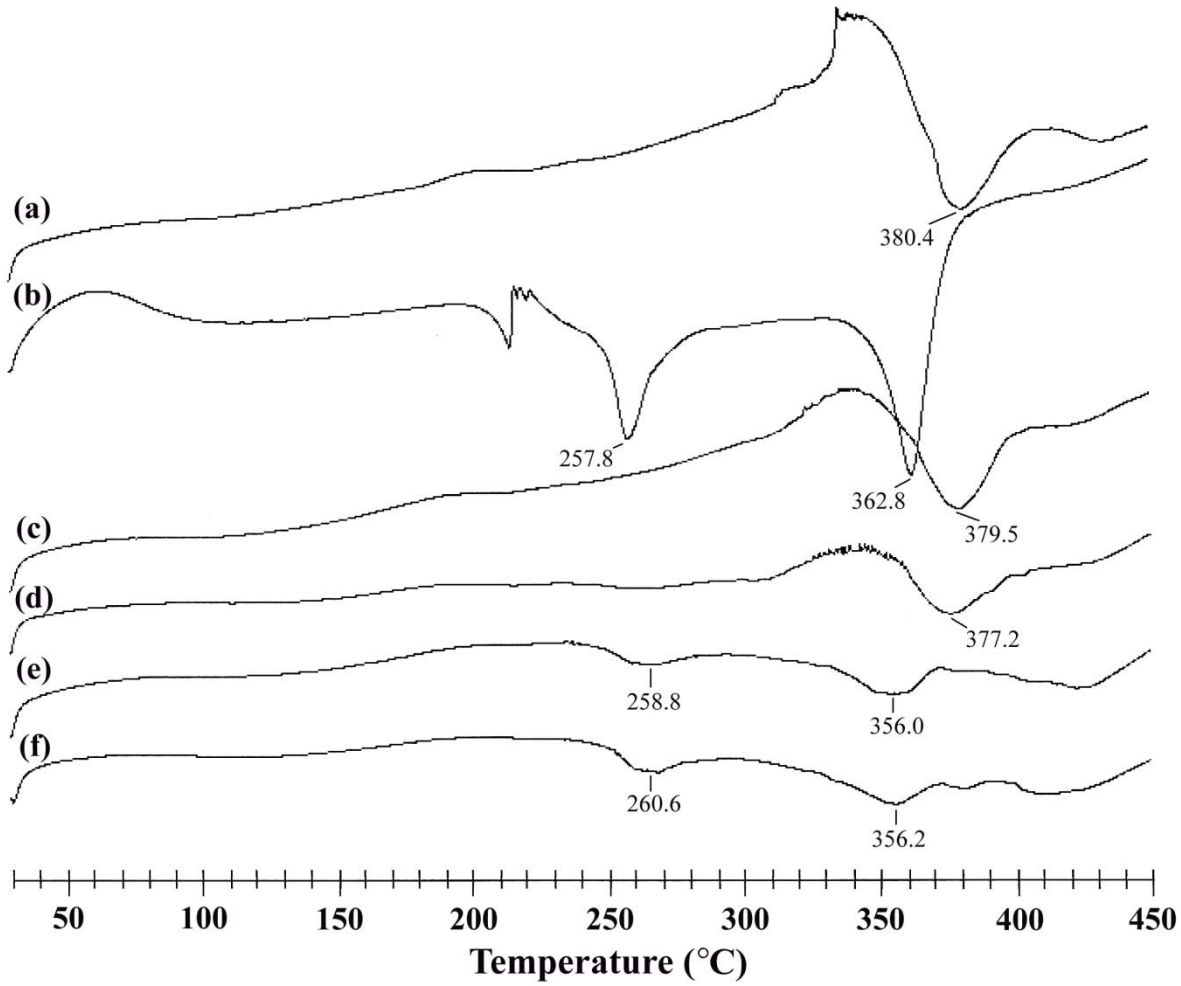


**Figure 28.** DSC thermogram of QPM film (a), SA film (b), and QPM-SA films at the ratios of 4:0.1 (c), 4:0.25 (d), 4:0.5 (e) and 4:1 (f).

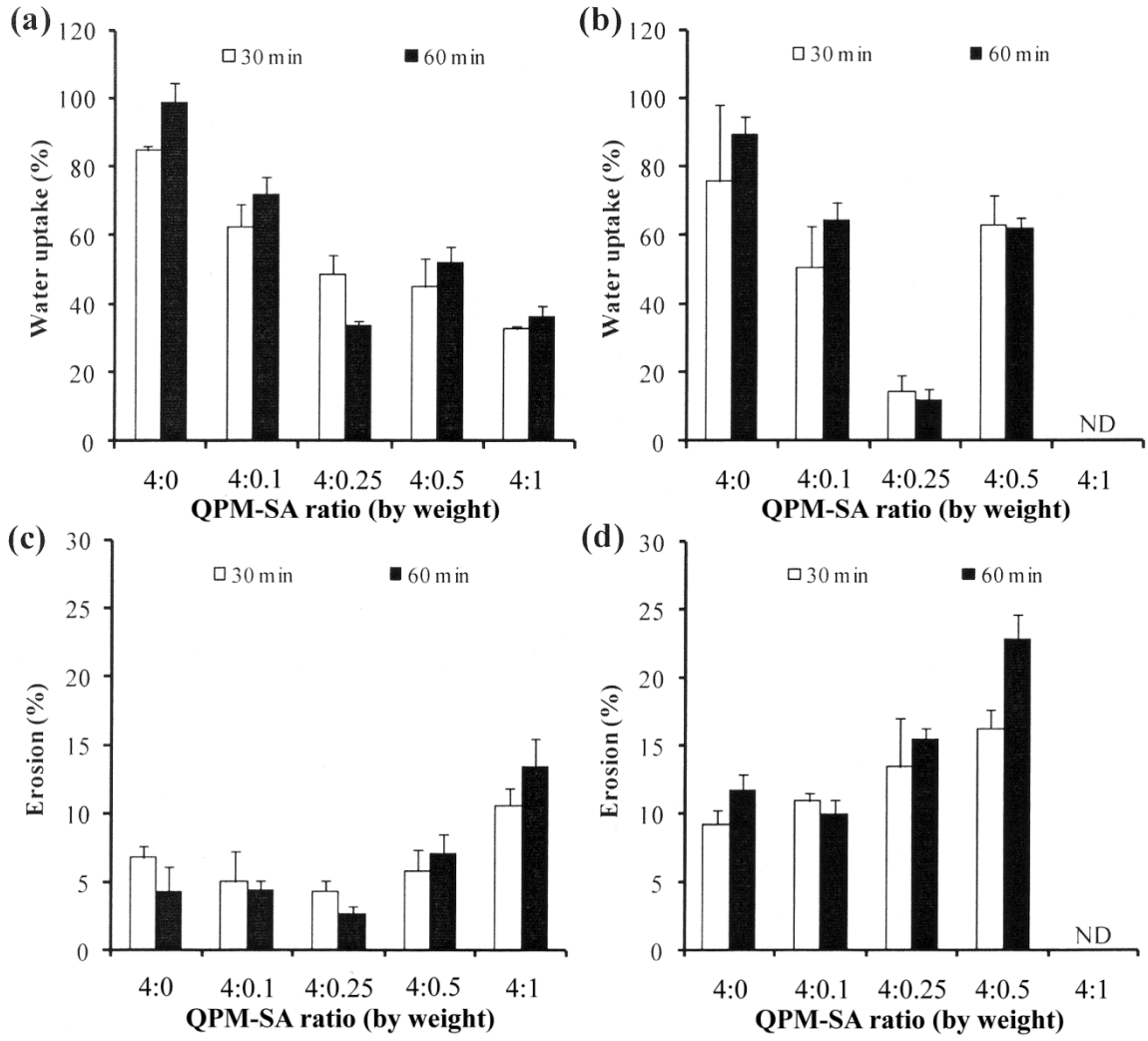


**Figure 29**. Water uptake (a,b) and erosion (c,d) of QPM-SA films in 0.1 M HCl (a,c) and pH 6.8 phosphate buffer (b,d). Data are mean ± S.D., n=5. ND = could not be determined.

**Table 5.** Thickness and mechanical properties of QPM and QPM-SA films.

| QPM-SA | Thickness[a] | Dry film | | Wet film using 0.1 M HCl | | Wet film using pH 6.8 PB | |
|---|---|---|---|---|---|---|---|
| | (μm) | Puncture strength[b] (MPa) | Elongation[b] (%) | Puncture strength[b] (MPa) | Elongation[b] (%) | Puncture strength[b] (MPa) | Elongation[b] (%) |
| 4:0 | 215.6 ± 29.83 | 7.97 ± 1.47 | 115.2 ± 7.85 | 0.95 ± 0.20 | 312.4 ± 26.69 | 1.28 ± 0.19 | 228.8 ± 17.17 |
| 4:0.1 | 151.8 ± 28.31 | 8.07 ± 1.53 | 78.02 ± 12.12 | 1.02 ± 0.11 | 87.31 ± 4.88 | 1.05 ± 0.06 | 213.9 ± 7.38 |
| 4:0.25 | 187.8 ± 11.40 | 10.06 ± 1.65 | 69.60 ± 39.72 | 1.34 ± 0.17 | 56.56 ± 3.95 | 1.55 ± 0.10 | 200.1 ± 3.87 |
| 4:0.5 | 219.7 ± 29.70 | 12.83 ± 2.57 | 46.73 ± 5.25 | 1.83 ± 0.32 | 44.06 ± 2.23 | 0.65 ± 0.10 | 56.81 ± 5.92 |
| 4:1 | 237.9 ± 25.65 | 12.43 ± 1.69 | 37.29 ± 8.66 | 1.54 ± 0.23 | 41.04 ± 17.48 | ND | ND |

[a]Data are mean ± S.D., n=15.
[b]Data are mean ± S.D., n=5.
ND = could not be determined.

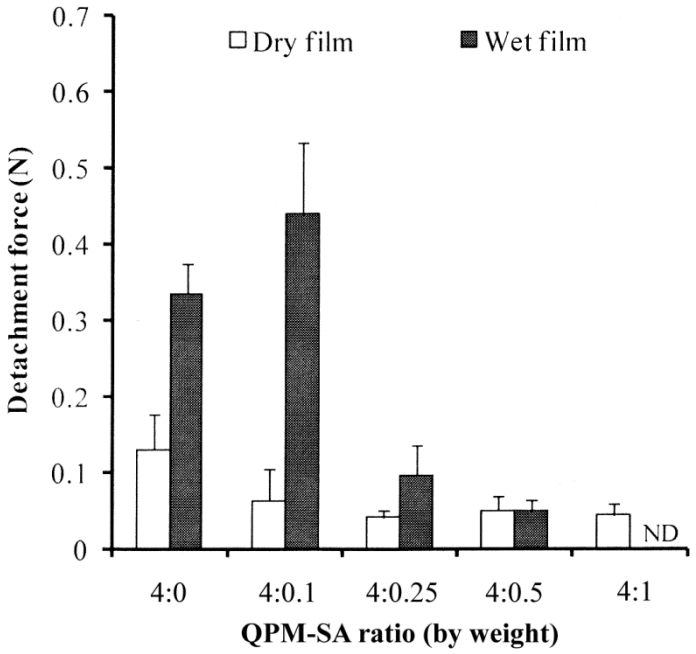


**Figure 30**. Detachment force of QPM and QPM-SA films in dry and wet state. Data are mean ± S.D., n=5. ND = could not be determined.

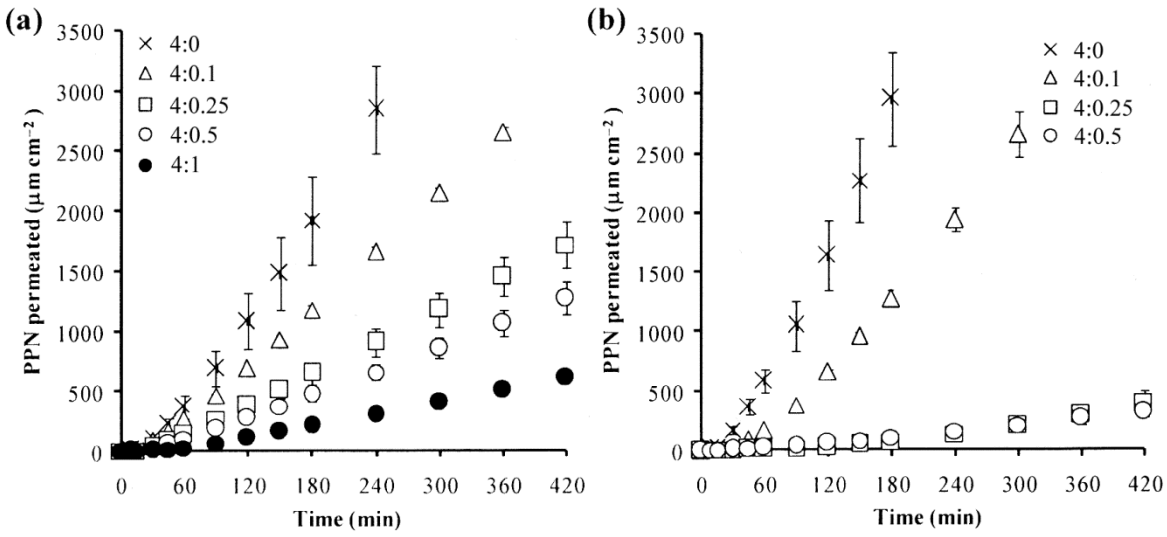


**Figure 31.** Permeation profiles of PPN across QPM and QPM-SA films in 0.1 M HCl (a) and pH 6.8 phosphate buffer (b). Each point is mean ± S.D., n=3.

**Table 6.** Permeation parameters of PPN across QPM and QPM-SA films.

| QPM-SA | 0.1 M HCl | | | | pH 6.8 phosphate buffer | | | |
|---|---|---|---|---|---|---|---|---|
| | Flux ($\mu m\ cm^{-2}\ min^{-1}$) | Lag time (min) | $P_C \times 10^5$ ($cm\ sec^{-1}$) | $D_C \times 10^8$ ($cm^2\ sec^{-1}$) | Flux ($\mu m\ cm^{-2}\ min^{-1}$) | Lag time (min) | $P_C \times 10^5$ ($cm\ sec^{-1}$) | $D_C \times 10^8$ ($cm^2\ sec^{-1}$) |
| 4:0 | 13.07 ± 1.60 | 31.72 ± 8.44 | 5.43 ± 0.66 | 1.90 ± 0.59 | 18.52 ± 2.53 | 26.87 ± 1.78 | 7.49 ± 1.02 | 2.71 ± 0.18 |
| 4:0.1 | 7.86 ± 0.14 | 25.29 ± 1.34 | 3.27 ± 0.06 | 5.89 ± 0.30 | 10.89 ± 0.93 | 55.84 ± 3.44 | 4.40 ± 0.38 | 1.58 ± 0.95 |
| 4:0.25 | 4.39 ± 0.46 | 29.86 ± 3.66 | 1.82 ± 0.19 | 6.03 ± 0.70 | 1.22 ± 0.38 | 114.7 ± 6.65 | 0.49 ± 0.15 | 0.75 ± 0.04 |
| 4:0.5 | 3.23 ± 0.34 | 29.42 ± 0.43 | 1.32 ± 0.14 | 7.70 ± 0.11 | 0.91 ± 0.06 | 65.11 ± 16.45 | 0.37 ± 0.02 | 2.29 ± 0.66 |
| 4:1 | 1.61 ± 0.09 | 43.58 ± 3.77 | 0.67 ± 0.04 | 5.72 ± 0.48 | ND | ND | ND | ND |

Data are mean ± S.D., n=3.
ND = could not be determined.

**Table 7.** Thickness and mechanical properties of QPM-SA films.

| Film | Thickness[a] | Puncture strength[b] (MPa) | | | Elongation[b] (%) | | |
|---|---|---|---|---|---|---|---|
| | (μm) | Dry film | Wet film (0.1 M HCl) | Wet film (pH 6.8 phosphate buffer) | Dry film | Wet film (0.1 M HCl) | Wet film (pH 6.8 phosphate buffer) |
| QPM-GSA | | | | | | | |
| 4:0 | 215.6 ± 29.8 | 7.97 ± 1.47 | 0.95 ± 0.20 | 1.28 ± 0.19 | 115.2 ± 7.85 | 312.4 ± 26.7 | 228.8 ± 17.2 |
| 4:0.1 | 151.8 ± 28.3 | 8.07 ± 1.53 | 1.02 ± 0.11 | 1.05 ± 0.06 | 78.02 ± 12.1 | 87.31 ± 4.88 | 213.9 ± 7.38 |
| 4:0.25 | 187.8 ± 11.4 | 10.06 ± 1.65 | 1.34 ± 0.17 | 1.56 ± 0.10 | 69.60 ± 39.7 | 56.56 ± 3.95 | 200.1 ± 3.87 |
| 4:0.5 | 219.7 ± 29.7 | 12.83 ± 2.57 | 1.83 ± 0.32 | 0.65 ± 0.10 | 46.74 ± 5.25 | 44.06 ± 2.23 | 56.81 ± 5.92 |
| 4:1 | 237.9 ± 25.7 | 12.43 ± 1.69 | 1.54 ± 0.23 | ND | 37.29 ± 8.66 | 41.04 ± 17.5 | ND |
| QPM-MSA | | | | | | | |
| 4:0 | 215.6 ± 29.8 | 7.97 ± 1.47 | 0.95 ± 0.20 | 1.28 ± 0.19 | 115.2 ± 7.85 | 312.4 ± 26.7 | 228.8 ± 17.2 |
| 4:0.1 | 184.8 ± 23.9 | 6.48 ± 0.77 | 0.73 ± 0.08 | 1.33 ± 0.12 | 95.18 ± 8.34 | 138.3 ± 17.1 | 202.9 ± 19.2 |
| 4:0.25 | 192.5 ± 19.1 | 6.27 ± 0.75 | 0.80 ± 0.11 | 0.71 ± 0.13 | 65.16 ± 15.0 | 73.22 ± 8.15 | 132.1 ± 7.85 |
| 4:0.5 | 196.3 ± 49.9 | 7.97 ± 1.25 | 1.05 ± 0.16 | 0.50 ± 0.02 | 58.47 ± 6.15 | 58.86 ± 9.09 | 81.97 ± 8.71 |
| 4:1 | 247.2 ± 59.2 | 7.46 ± 0.46 | 0.92 ± 0.22 | ND | 27.88 ± 2.00 | 35.37 ± 11.9 | ND |

[a]Data are mean ± S.D., n=15.

[b]Data are mean ± S.D., n=5.

ND = could not be determined.

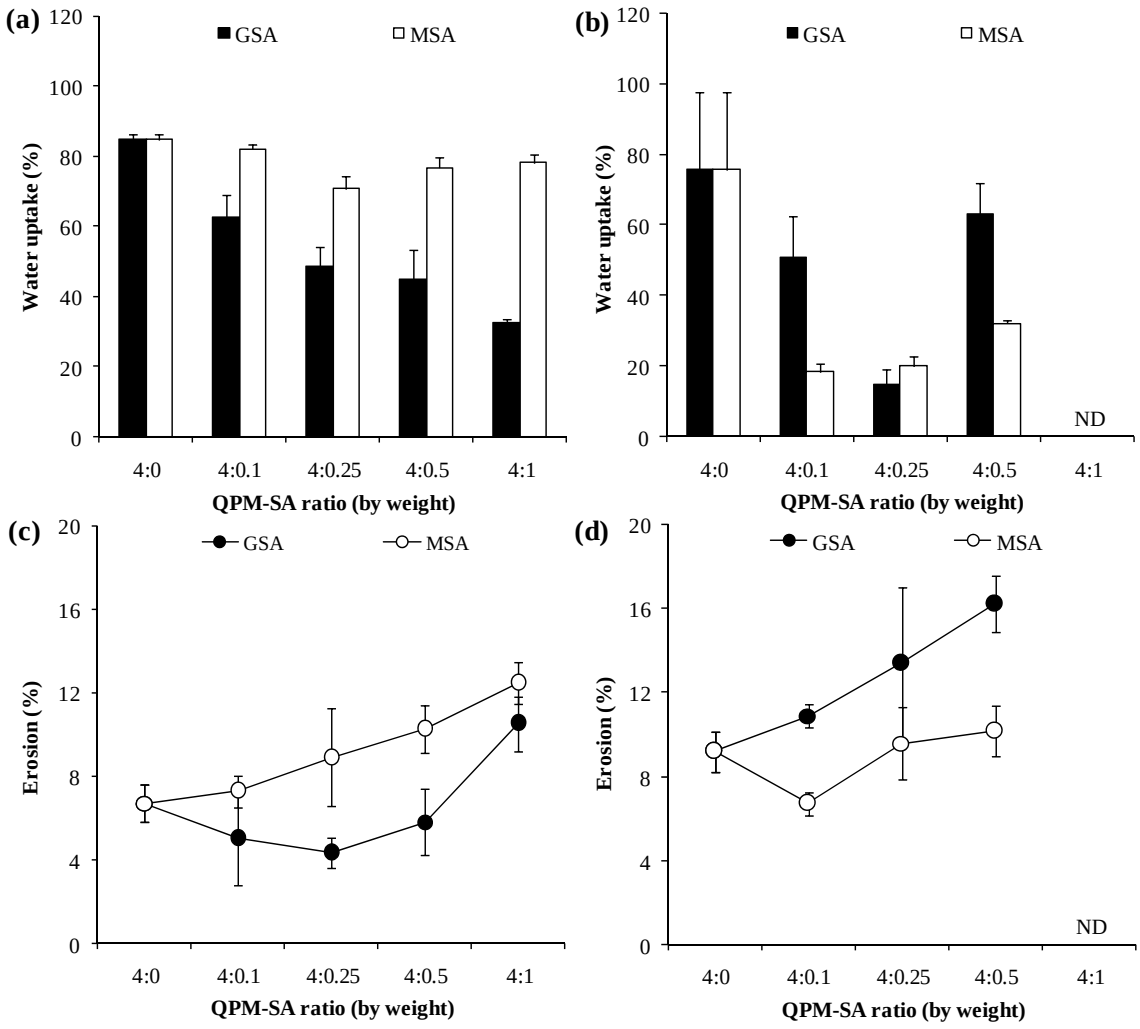


**Figure 32.** Water uptake and erosion of QPM-SA films using 0.1 M HCl (a,c) and pH 6.8 phosphate buffer (b,d) at 30 min. Each value is mean ± S.D., n=5.

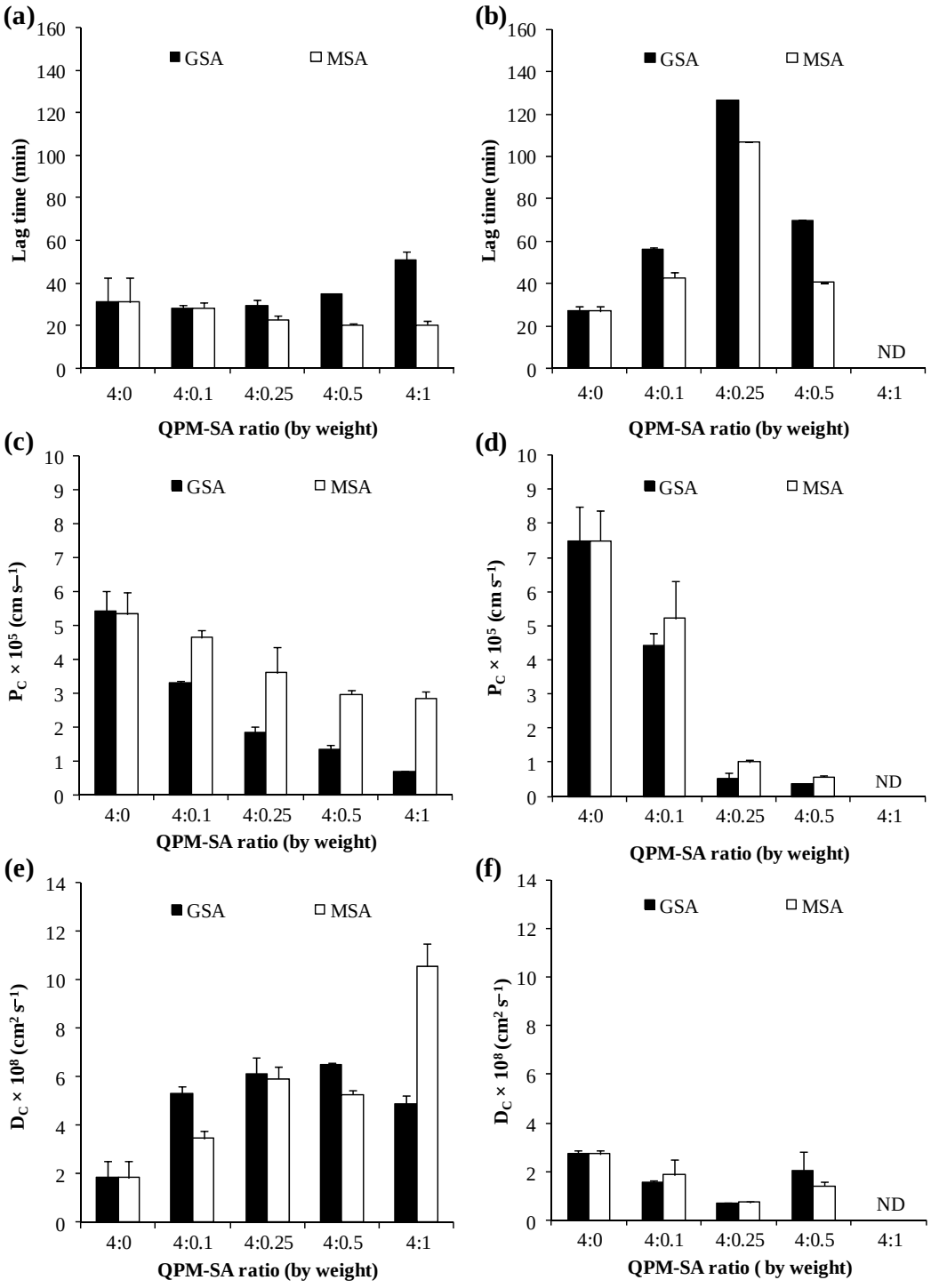


**Figure 33.** Lag time (a,b), permeability coefficient (c,d), and diffusion coefficient (e,f) of QPM-SA films using 0.1 M HCl (a,c,e) and pH 6.8 phosphate buffer (b,d,f). Each value is mean ± S.D., n=3.

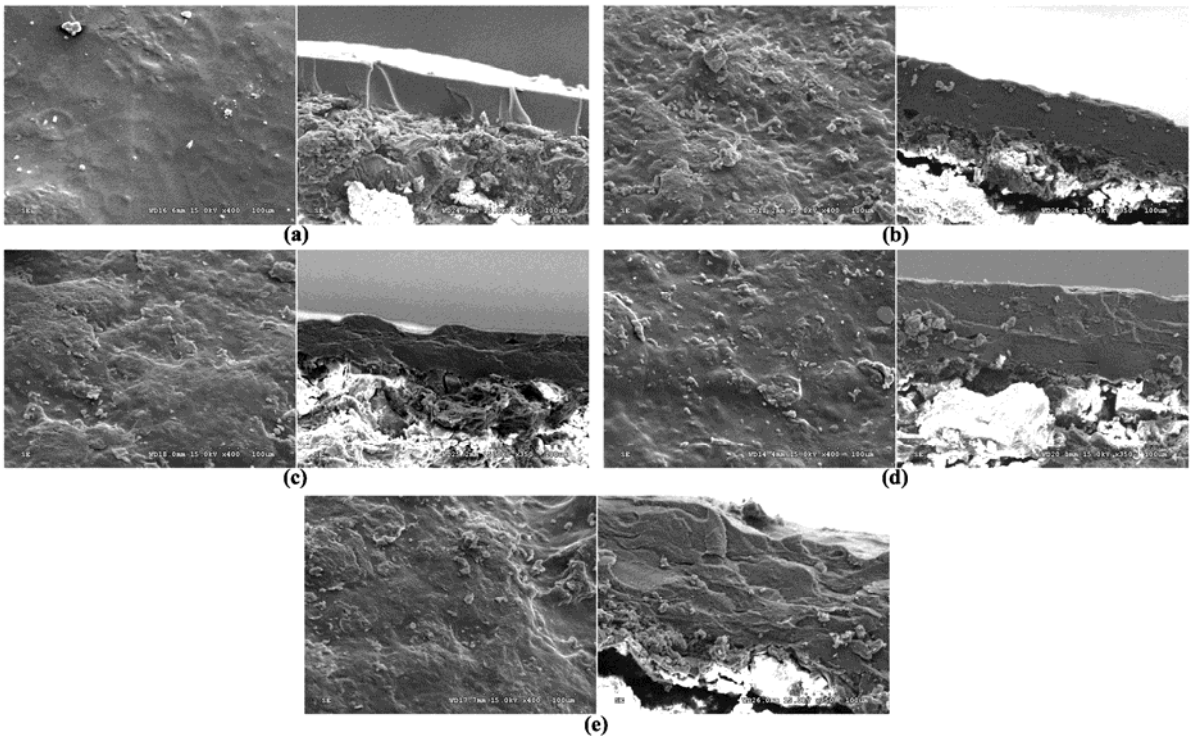


**Figure 34.** Surface and film matrix morphology of PPN tablets coated with QPM film (4 % coating level) (a), QPM-GSA (4:0.5) film (4 % coating level) (b), and QPM-GSA (4:1) films at 4 (c), 8 (d), and 12 (e) % coating levels.

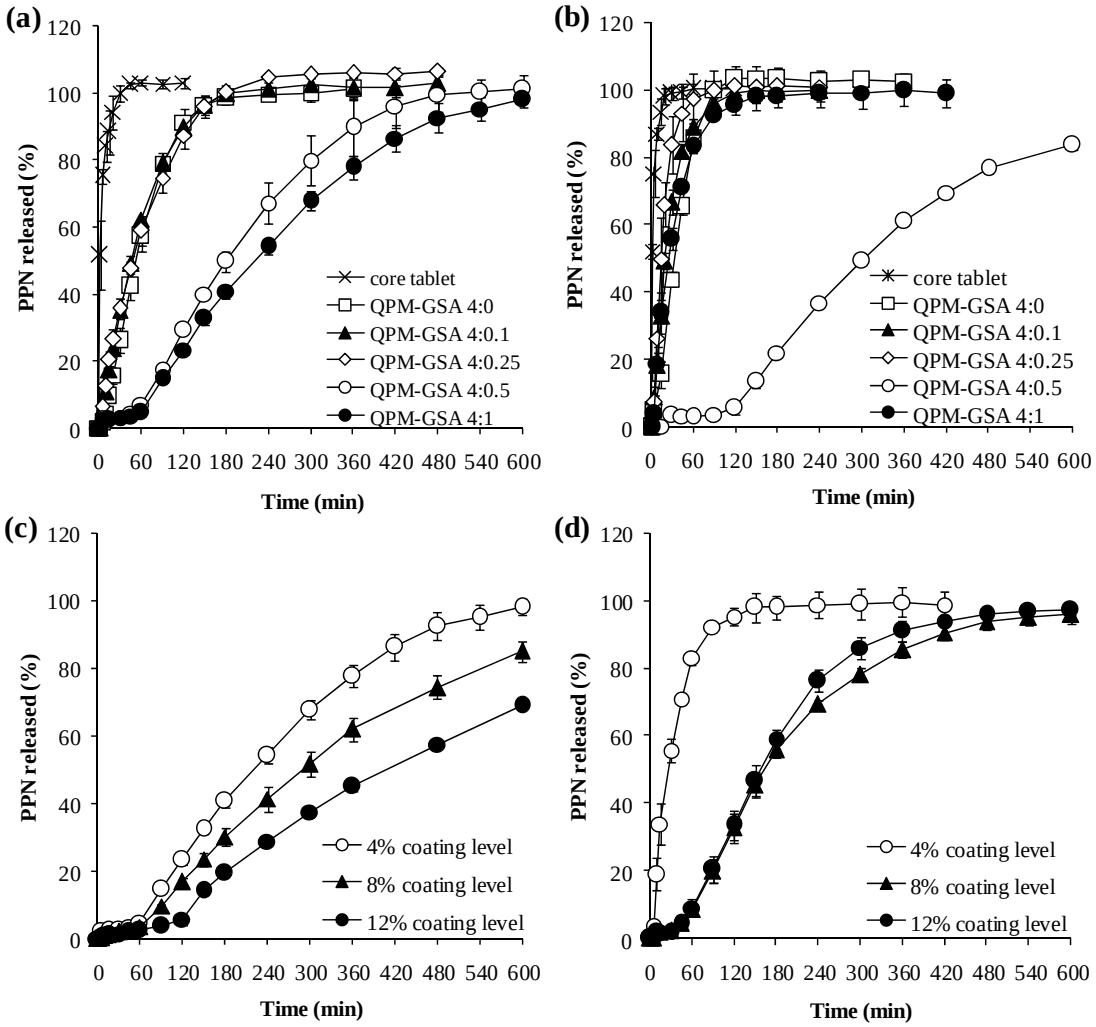


**Figure 35.** PPN release profiles of PPN tablets coated with different QPM-GSA ratios at 4 % coating level (a,b) and different coating levels of QPM-GSA at the ratio of 4:1 (c,d) in 0.1 M HCl (a,c) and pH 6.8 phosphate buffer (b,d). Each point is mean ± S.D., n=3.

**Table 8.** Lag time and PPN release rate of QPM-GSA coated tablets with different QPM-GSA ratios and film coating levels in 0.1 M HCl and pH 6.8 phosphate buffer.

| QPM-GSA film | Coating level (%) | 0.1 M HCl | | pH 6.8 phosphate buffer | |
|---|---|---|---|---|---|
| | | Lag time (min) | $K_0$ (% $min^{-1}$) | Lag time (min) | $K_0$ (% $min^{-1}$) |
| 4:0 | 4 | 5.64 ± 1.63 | 1.06 ± 0.08 ($R^2$=0.998) | 2.58 ± 0.21 | 1.54 ± 0.05 ($R^2$=0.994) |
| 4:0.1 | 4 | ND | 1.02 ± 0.05 ($R^2$=0.994) | ND | 2.67 ± 0.14 ($R^2$=0.986) |
| 4:0.25 | 4 | ND | 0.84 ± 0.09 ($R^2$=0.995) | ND | 3.88 ± 0.98 ($R^2$=0.985) |
| 4:0.5 | 4 | 39.93 ± 2.71 | 0.36 ± 0.02 ($R^2$=0.997) | 89.17 ± 8.97 | 0.23 ± 0.01 ($R^2$=0.995) |
| 4:1 | 4 | 42.49 ± 4.38 | 0.30 ± 0.02 ($R^2$=0.995) | 2.74 ± 0.35 | 2.69 ± 0.49 ($R^2$=0.981) |
| 4:1 | 8 | 45.22 ± 2.15 | 0.22 ± 0.02 ($R^2$=0.999) | 36.10 ± 5.55 | 0.39 ± 0.01 ($R^2$=0.996) |
| 4:1 | 12 | 50.07 ± 3.62 | 0.15 ± 0.01 ($R^2$=0.998) | 37.22 ± 6.22 | 0.41 ± 0.01 ($R^2$=0.997) |

Data are mean ± S.D., n=3.

ND = could not be determined.

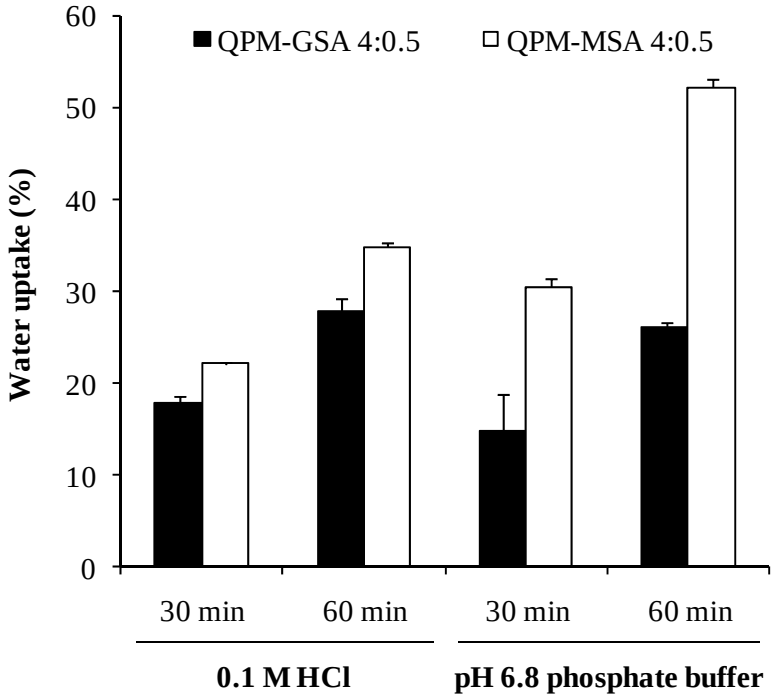


**Figure 36.** Water uptake of PPN tablets coated with QPM-GSA and QPM-MSA films at the ratio of 4:0.5 (4% coating level) in 0.1 M HCl and pH 6.8 phosphate buffer. Each value is mean ± S.D., n=3.

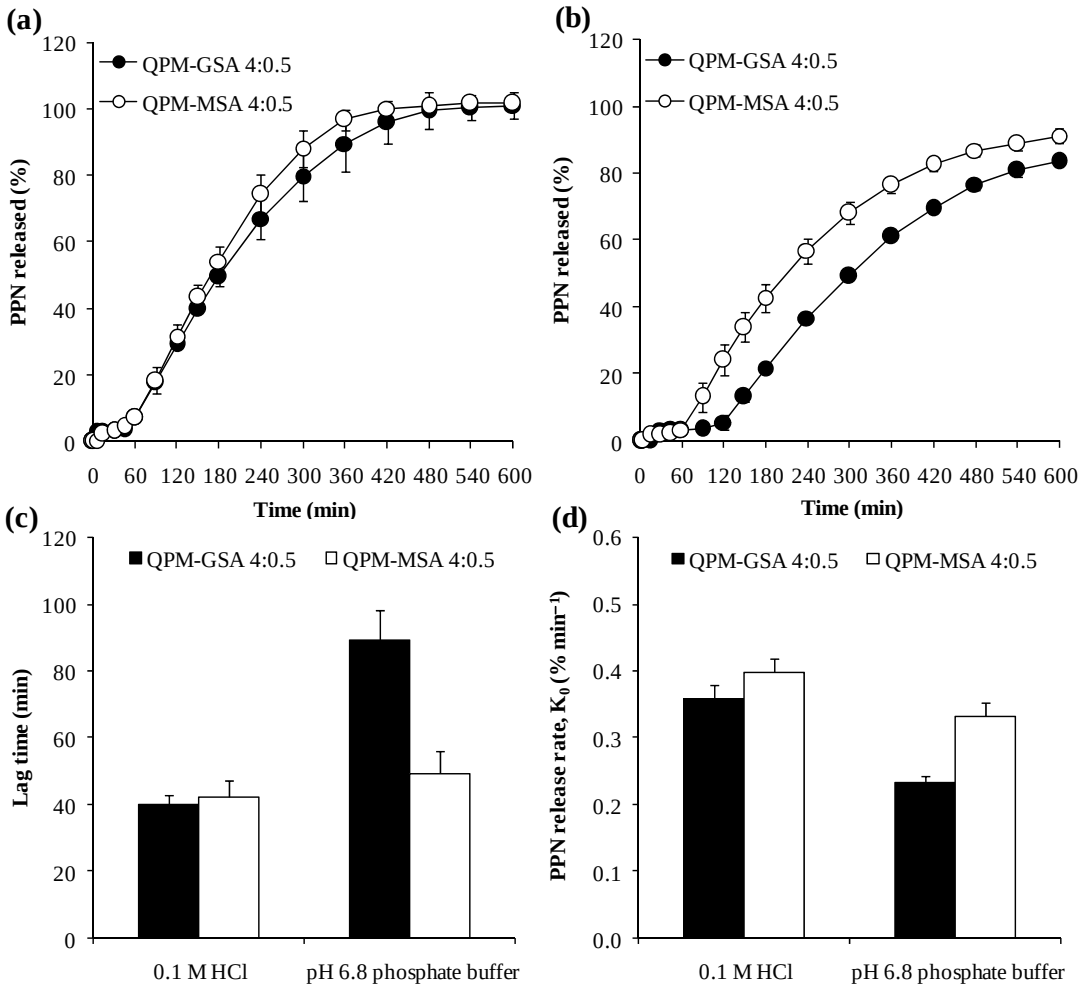


**Figure 37.** PPN release profiles (a,b), lag time (c), and PPN release rate (d) of PPN tablets coated with QPM-GSA and QPM-MSA films at the ratio of 4:0.5 (4 % coating level) in 0.1 M HCl (a) and pH 6.8 phosphate buffer (b). Each value is mean ± S.D., n=3.

## Conclusions

1. This study indicates that the QPM films can be modified by incorporating anionic substances that are MAS, clay particle, and SA, long chain polymer. The positively charged QPMs can interact with MAS or SA via electrostatic forces and hydrogen bonding. These interactions lead to the formation of QPM-MAS or QPM-SA flocculates due to reduction of zeta potential of QPM.

2. The QPM-MAS films present a continuous film when MAS is incorporated less than 18.8 % in the films. Interaction between QPM and MAS causes a formation of nanocomposites that can enhance thermal stability of the films. The puncture strength and elongation of the dry composite films decrease with increasing MAS ratio in the films. On the other hand, increasing MAS ratio results in an increase of puncture strength of the wet composite films in acidic and neutral media. Incorporation of MAS reduces a tackiness of the QPM films in both dry and wet states. The QPM-MAS films at higher ratio of MAS provide lower water uptake than the QPM films in both acidic and neutral media. Water vapor permeability of the dry QPM films decreased with increasing MAS ratio. Moreover, a longer lag time can be found when increasing MAS ratios. In contrast, the higher MAS ratios cause lower permeability and diffusion coefficients of the films, which is depended upon drug affinity on MAS embedded. Additionally, drug type and molecular weight (hydrocarbon side chain) of drug also influence permeation characteristic of the QPM-MAS films.

3. QPM-SA films can be successfully prepared using the casting/solvent evaporation method. The QPM-SA films are transparent and continuous films are obtained, even for an SA content of 25%w/w SA. Interaction between QPM and SA results in an increase in the film strength in the dry state and a decrease in the film tackiness in the dry and wet states. The puncture strength of the films in acidic media increases with increasing SA content, but the flexibility of the films decreases. The wet films still exhibit good strength and flexibility in neutral pH for lower content of SA because of their lower water uptake in such media, but a higher amount of SA leads to lower puncture strength and elongation. The incorporation of SA into QPM films can reduce drug permeability of the films in acidic medium. However, the drug diffusivity in this medium increases because of the creation of large water-filled channels with low tortuosity in the films when the SA converts into alginic acid. On the other hand, the drug diffusivity in neutral media

decreases with the addition of a small amount of SA because the SA can ionize and disentangle, creating small water-filled channels with high tortuosity. The QPM-GSA films have higher film strength and lower drug permeability than the QPM-MSA films.

4. The QPM-MAS and QPM-SA films can be successfully applied for tablet coatings that tackiness problem of the coated tablets is remarkably reduced. The QPM-MAS coated tablets have rougher surface than the QPM coated tablets. Increasing MAS ratio in the films causes lower water uptake of the coated tablets, resulting in longer lag time and lower drug release rate. The drug release of the QPM-MAS coated tablets can be modulated by varying film coating level. Furthermore, the drug characteristics, such as charge, molecular weight, and aqueous solubility, affect drug release of the QPM-MAS coated tablets. Curing process is also necessary to produce the homogeneous film formation after coating process. Higher temperature of curing provides slower drug release rate of the QPM-MAS coated tablets. Additionally, the PPN released from the QPM-GSA coated tablets is dependent on the film coating levels. The QPM-MSA coated tablets present higher PPN release rates than the QPM-GSA coated tablets in acidic and neutral media. The 4:0.5 ratio QPM-GSA and QPM-MSA films display stable films and are able to sustain PPN release in both media. This study suggests that the QPM-MAS or QPM-SA films can be used as a tablet film coating material for modifying drug release pattern of tablets.

## References

Aceves JM, Cruz R, Hernandez E. Preparation and characterization of furosemide-Eudragit controlled release systems. Int J Pharm 2000; 195: 45-53.

Alexandre M, Dubois P. Polymer-layered silicate nanocomposites: preparation, properties and uses of a new class of materials. Mater Sci Eng 2000; 28: 1-63.

Aslani P, Kennedy RA. Studies on diffusion in alginate gels. I. effect of crosslinking with calcium or zinc ions on diffusion of acetaminophen. J Control Release 1996; 42: 75–82.

Azarmi S, Farid J, Nokhodchi A, Bahari-Saravi SM, Valizadeh H. Thermal treating as a tool for sustained release of indomethacin from Eudragit RS and RL matrices. Int J Pharm 2002; 246: 171-177.

Bauer KH, Lehmann K, Osterwald HP, Rothgang G. Coated pharmaceutical dosage forms: fundamentals, manufacturing techniques, biopharmaceutical aspects, test methods, and raw materials. Stuttgart: Medpharm GmbH Scientific Publishers, 1998.

Bhattacharjya S, Wurster DE. Investigation of the drug release and surface morphological properties of film-coated pellets, and physical, thermal and mechanical properties of free films as a function of various curing conditions. AAPS PharmSciTech 2008; 9: 449-457.

Bley O, Siepmann J, Bodmeier R. Protection of moisture-sensitive drugs with aqueous polymer coatings: Importance of coating and curing conditions. Int J Pharm 2009; 378: 59-65.

Bodmeier R, Guo X, Sarabia RE, Skultety PF. The influence of buffer species and strength on diltiazem HCl release from beads coated with the aqueous cationic polymer dispersions, Eudragit RS, RL 30D. Pharm Res 1996; 13: 52-56.

Bodmeier R, Paeratakul O. Dry and wet strengths of polymeric films prepared from an aqueous colloidal polymer dispersion, Eudragit RS30D. Int J Pharm 1993; 96: 129-138.

Bodmeier R, Paeratakul O. Mechanical properties of dry and wet cellulosic and acrylic films prepared from aqueous colloidal polymer dispersions used in the coating of solid dosage forms. Pharm Res 1994; 11: 882-888.

Bodmeier R, Paeratakul O. Plasticizer uptake by aqueous colloidal polymer dispersions used for the coating of solid dosage forms. Int J Pharm 1997; 152: 17-26.

Bodmeier R, Paeratakul O. Propranolol HCl release from acrylic films prepared from aqueous latexes. Int J Pharm 1990; 59: 197-204.

Ciullo PA, Braun DB. Clay/carbomer mixtures enhance emulsion stability. Cosmet Toilet 1991; 106: 89-95

Ciullo PA. Rheological properties of magnesium aluminum silicate/xanthan gum dispersions. J Soc Cosmet Chem 1981; 32: 275-285

Dong Z, Wang Q, Du Y. Alginate/gelatin blend films and their properties for drug controlled release. J Membr Sci 2006; 280: 37-44.

Draget KI, Skjåak Bræk G, Smidsrød O. Alginic acid gels: the effect of alginate chemical composition and molecular weight. Carbohydr Polym 1994; 25: 31-38.

Fernández-Cervera M, Heinämäki J, Räsänen E, Antikainen O, Nieto OM, Iraizoz-Colarte A, Yliruusi J. Determination of tackiness of chitosan film-coated pellets exploiting minimum fluidization velocity. Int J Pharm 2004; 281: 119-127.

Flynn GL, Yalkowsky SH, Roseman TJ. Mass transport phenomena and models: theoretical concepts. J Pharm Sci 1974; 63: 479-510.

Ghaffari A, Navaee K, Oskoui M, Bayati K, Rafiee-Tehrani M. Preparation and characterization of free mixed-film of pectin/chitosan/Eudragit® RS intended for sigmoidal drug delivery. Eur J Pharm Biopharm 2007; 67: 175-186.

Ghebre-Sellassie I, Nesbitt RU, Wang J. Eudragit aqueous dispersions as pharmaceutical controlled release coatings. In: McGinity, J.W. (Ed), Aqueous Polymeric Coatings for Pharmaceutical Dosage Forms. Marcel Dekker, Inc., New York, 1997, pp. 267-286.

Gupta MK, Vanwert A, Bogner RH. Formation of physical stable amorphous drugs by milling with Neusilin. J Pharm Sci 2003; 92: 536–551.

Hasanzadeh D, Ghaffari S, Monajjemzadeh F, Al-Hallak MHDK, Soltani G, Azarmi S. Thermal treating of acrylic matrices as a tool for controlling drug release. Chem Pharm Bull 2009; 57: 1356-1362.

Heckötter UM, Larsson A, Sriamornsak P, Kumpugdee–Vollrath M. Effect of annealing time and addition of lactose on release of a model substance from Eudragit® RS coated pellets produced by a fluidized bed coater. Chem Eng Res Des 2011; 89: 697-705.

Khunawattanakul W, Puttipipatkhachorn S, Rades T, Pongjanyakul T. Novel chitosan-magnesium aluminum silicate nanocomposite film coatings for modified-release tablets. Int J Pharm 2011; 407: 132-141.

Khunawattanakul W, Puttipipatkhachorn S, Rades T, Pongjanyakul T. Chitosan-magnesium aluminum silicate nanocomposite films: Physicochemical characterization and drug permeability. Int J Pharm 2010; 393: 219-229.

Khunawattanakul W, Puttipipatkhachorn S, Rades T, Pongjanyakul T. Chitosan-magnesium aluminum silicate composite dispersions: Characterization of rheology, flocculate size and zeta potential. Int J Pharm 2008; 351: 227-235.

Kibbe HA. Handbook of pharmaceutical excipients, third ed. American Pharmaceutical Association, Washington, 2000, pp. 295–298.

Knop K. Influence of buffer solution composition on drug release from pellets coated with neutral and quaternary acrylic polymers and on swelling of free polymer films. Eur J Pharm Sci 1996; 4: 293-300.

Lawrie G, Keen I, Drew B, Chandler-Temple A, Rintoul L, Fredericks P, Grøndahl L. Interactions between alginate and chitosan biopolymers characterized using FTIR and XPS. Biomacromolecules 2007; 8: 2533-2541.

Lecomte F, Siepmann J, Walther M, Macrae RJ, Bodmeier R. Polymer blends used for the aqueous coating of solid dosage forms: importance of the type of plasticizer. J Control Release 2004; 99: 1-13.

Lee BJ, Min GH, Cui JH. Correlation of drug solubility with trapping efficiency and release characteristics of alginate beads. Pharm Pharmacol Commun 1999; 5: 85-89.

Lehmann KOR. Chemistry and application properties of polymethacrylate coating systems. In: McGinity, J.W. (Ed), Aqueous Polymeric Coatings for Pharmaceutical Dosage Forms. Marcel Dekker, Inc., New York, 1997, pp. 101-176.

Liew CV, Chan LW, Ching AL, Heng PWS. Evaluation of sodium alginate as drug release modifier in matrix tablets. Int J Pharm 2006; 309: 25-37.

Maejima T, McGinity JW. Influence of film additives on stabilizing drug release rates from pellets coated with acrylic polymers. Pharm Dev Technol 2001; 6: 211-221.

Mendoza-Romero L, Piñón-Segundo E, Nava-Arzaluz MG, Ganem-Quintanar A, Cordero-Sánchez S, Quintanar-Guerrero D. Comparison of pharmaceutical films prepared from aqueous polymeric dispersions using the cast method and the spraying technique. Colloid Surf A 2009; 337: 109-116.

Moustafine RI, Kemenova VA, Van den Mooter G. Characteristics of interpolyelectrolyte complexes of Eudragit E100 with sodium alginate. Int J Pharm 2005; 294: 113-120.

Moustafine RI, Salachova AR, Frolova ES, Kemenova VA, Mooter GV. Interpolyelectrolyte complexes of Eudragit E PO with sodium alginate as potential carriers for colonic drug delivery: monitoring of structural transformation and composition changes during swellability and release evaluating. Drug Dev Ind Pharm 2009; 35: 1439-1451.

Moustafine RI, Zakharov IM. Diffusion transport properties of polymeric complex matrix systems based on Eudragit E and sodium alginate. Pharm Chem J 2004; 38: 456-458.

Nagai T, Obara S, Kokubo H, Hoshi N. Application of HPMC and HPMCAS to aqueous film coating of pharmaceutical dosage forms. In: McGinity, J.W. (Ed), Aqueous Polymeric Coatings for Pharmaceutical Dosage Forms. Marcel Dekker, Inc., New York, 1997, pp. 177-226.

Narisawa S, Nagata M, Hirakawa Y, Kobayashi M, Yoshino H. An organic acid-induced sigmoidal release system for oral controlled-release preparations. 2. Permeability enhancement of eudragit RS coating led by the physicochemical interactions with organic acid. J Pharm Sci 1996; 85: 184-188.

Nimkulrat S, Suchiva K, Phinyocheep P, Puttipipatkhachorn S. Influence of selected surfactants on the tackiness of acrylic polymer films. Int J Pharm 2004; 287: 27-37.

Nyamweya N, Mehta KA, Hoag SW. Characterization of the interactions between polymethacrylate-based aqueous polymeric dispersions and aluminum lakes. J Pharm Sci 2001; 90: 1937-1947.

Østberg T, Lund EM, Graffner C. Calcium alginatematrices for oral multiple unit administration. IV. Release characteristics in different media. Int J Pharm 1994; 112: 241-248.

Pongjanyakul T, Khunawattanakul W, Puttipipatkhachorn S. Physicochemical characterizations and release studies of nicotine-magnesium aluminum silicate complexes. Appl Clay Sci 2009; 44: 242-250.

Pongjanyakul T, Priprem A, Puttipipatkhachorn S. Influence of magnesium aluminium silicate on rheological, release and permeation characteristics of diclofenac sodium aqueous gels in-vitro. J Pharm Pharmacol. 2005b; 57: 429-434.

Pongjanyakul T, Priprem A, Puttipipatkhachorn S. Investigation of novel alginate-magnesium aluminum silicate microcomposite films for modified-release tablets. J Control Release 2005a; 107: 343-356.

Pongjanyakul T, Puttipipatkhachorn S. Alginate-magnesium aluminum silicate composite films: Effect of film thickness on physical characteristics and permeability. Int J Pharm 2008; 346: 1-9.

Pongjanyakul T, Puttipipatkhachorn S. Modulating drug release and matrix erosion of alginate matrix capsules by microenvironmental interaction with calcium ion. Eur J Pharm Biopharm 2007a; 67: 187-195.

Pongjanyakul T, Puttipipatkhachorn S. Sodium alginate-magnesium aluminum silicate composite gels: Characterization of flow behavior, microviscosity and drug diffusivity. AAPS PharmSciTech 2007b; 8: Article 72.

Pongjanyakul T, Suksri H. Alginate-magnesium aluminum silicate films for buccal delivery of nicotine. Colloid and Surface B 2009; 74: 103–113.

Pongjanyakul T. Alginate–magnesium aluminum silicate films: Importance of alginate block structures. Int J Pharm 2009; 365: 100-108.

Remuñán-López C, Bodmeier R. Mechanical, water uptake and permeability properties of crosslinked chitosan glutamate and alginate films. J Control Release 1997; 44: 215-225.

Remuñán-López C, Bodmeier R. Mechanical, water uptake and permeability properties of crosslinked chitosan glutamate and alginate films. J Control Release 1997; 44: 215-225.

Ritthidej GC, Phaechamud T, Koizumi T. Moist heat treatment on physicochemical change of chitosan salt films. Int J Pharm 2002; 232: 11-22.

Rojtanatanya S, Pongjanyakul T. Propranolol-magnesium aluminum silicate complex dispersions and particles: Characterization and factors influencing drug release. Int J Pharm 2010; 383: 106-115.

Rowe RC, Sheskey PJ, Owen SC. Handbook of Pharmaceutical Excipients. 5th ed. Pharmaceutical Press and American Pharmaceutical Association, Washington, 2006.

Saettone MF, Perini G, Rijli P, Rodriguez L, Cini M. Effect of different polymer-plasticizer combinations on ‘in vitro’ release of theophylline from coated pellets. Int J Pharm 1995; 126: 83-88.

Sartori C, Finch DS, Ralph B. Determination of the cation content of alginate thin films by FTIR spectroscopy. Polymer 1997; 38: 43-51.

Semdé R, Amighi K, Devleeschouwer MJ, Moës AJ. Effect of pectinolytic enzymes on the theophylline release from pellets coated with water insoluble polymers containing pectin HM or calcium pectinate. Int J Pharm 2000; 197: 169-179.

Semdé R, Amighi K, Pierre D, Devleeschouwer MJ, Moës AJ. Leaching of pectin from mixed pectin/insoluble polymer films intended for colonic drug delivery. Int J Pharm 1998; 174: 233-241.

Siepmann J, Paeratakul O, Bodmeier R. Modeling plasticizer uptake in aqueous polymer dispersions. Int. J. Pharm. 1997; 165: 191-200.

Sipos P, Szücs M, Szabó A, Erös I, Szabó-Révész P. An assessment of the interactions between diclofenac sodium and ammonio methacrylate copolymer using thermal analysis and Raman spectroscopy. J Pharm Biomed Anal 2008; 46: 288-294.

Sriamornsak P, Kennedy RA. Development of polysaccharide gel-coated pellets for oral administration 2. Calcium alginate. Eur J Pharm Sci 2006; 29: 139-147.

Sriamornsak P, Thirawong N, Korkerd K. Swelling, erosion and release behavior of alginate-based matrix tablets. Eur J Pharm Biopharm 2007; 66: 435-450.

Suksri H, Pongjanyakul T. Interaction of nicotine with magnesium aluminum silicate at different pHs: characterization of flocculate size, zeta potential and nicotine adsorption behavior. Colloids Surf B 2008; 65: 54-60.

Vecchio C, Fabiani F, Gazzaniga A. 1995. Use of colloidal silica as a separating agent in film forming processed performed with aqueous dispersion of acrylic resin. Drug Dev Ind Pharm 1995; 21: 1781-1787.

Voyutskii SS. Some comments on the series of papers “interfactial contact and bonding in autohesion”. J. Adhesion 1971; 3: 69-76.

Wagner KG, Gruetzmann R. Anionic-induced water flux as drug release mechanism through cationic Eudragit RS 30D film coatings. AAPS J 2005; 67: E668-E677.

Wagner KG, McGinity JW. Influence of chloride ion exchange on the permeability and drug release of Eudragit RS 30 D films. J Control Release 2002; 82: 385-397.

Wang CC, Zhang G, Shah NH, Infeld MH, Malick AW, McGinity JW. Influence of plasticizer on the mechanical properties of pellets containing Eudragit® RS 30 D. Int J Pharm 1997; 152: 153-162.

Wen H, Morris KR, Park K. Hydrogen bonding interactions between adsorbed polymer molecules and crystal surface of acetaminophen. J Colloid Interf Sci 2005; 290: 325–35.

Wesseling M, Kuppler F, Bodmeier R. Tackiness of acrylic and cellulosic polymer films used in the coating of solid dosage forms. Eur J Pharm Biopharm 1999; 47: 73-78.

Wheatley TA, Steuernagel CR. Latex emulsions for controlled drug delivery. In: McGinity, J.W. (Ed), Aqueous Polymeric Coatings for Pharmaceutical Dosage Forms. Marcel Dekker, Inc., New York, 1997, pp. 1-54.

Williams III RO, Liu J. Influence of processing and curing conditions on beads coated with an aqueous dispersion of cellulose acetate phthalate. Eur J Pharm Biopharm 2000; 49: 243-252.

Wittaya-areekul S, Prahsarn C, Sungthongjeen S. Development and in vitro evaluation of chitosan-Eudragit RS 30D composite wound dressings. AAPS PharmSciTech 2006; 7: E1-E6.

Wong D, Bodmeier R. Flocculation of an aqueous colloidal ethyl cellulose dispersion (Aquacoat®) with a water-soluble polymer, hydroxypropyl methylcellulose. Eur J Pharm Biopharm 1996; 42: 12-15.

Wu C, McGinity JW. Influence of methylparaben as a solid-state plasticizer on the physicochemical properties of Eudragit RS PO hot-melt extrudates. Eur J Pharm Biopharm 2003; 56: 95-100.

Wu C, McGinity JW. Influence of relative humidity on the mechanical and drug release properties of theophylline pellets coated with an acrylic polymer containing methylparaben as a non-traditional plasticizer. Eur J Pharm Biopharm 2000; 50: 277-284.

Wu SHW, Wyatt DM, Adams MW. Chemistry and applications of cellulosic polymers for enteric coatings of solid dosage forms. In: McGinity, J.W. (Ed), Aqueous Polymeric Coatings for Pharmaceutical Dosage Forms. Marcel Dekker, Inc., New York, 1997, pp. 385-418.

Wurster DE, Bhattacharjya S, Flanagan DR. Effect of curing on water diffusivities in acrylate free films as measured via a sorption technique. AAPS PharmSciTech 2007; 8(3): E1-E6.

Yang QW, Flament MP, Siepmann F, Busignies V, Leclerc B, Herry C, et al. Curing of aqueous polymeric film coatings: Importance of the coating level and type of plasticizer. Eur J Pharm Biopharm 2010; 74: 362-370.

Zheng W, Sauer D, McGinity JW. Influence of hydroxyethylcellulose on the drug release properties of theophylline pellets coated with Eudragit® RS 30D. Eur J Pharm Biopharm 2005; 59: 147-154.

# Outputs

### International publications

1. Rongthong T, Sungthongjeen S, Siepmann J, **Pongjanyakul T**. Quaternary polymethacrylate-magnesium aluminum silicate films: Molecular interactions, mechanical properties and tackiness. International Journal of Pharmaceutics 2013; 458 (1): 57-64. (Impact factor 2014 = 3.650)
2. Khuathan N, **Pongjanyakul T**. Modification of quaternary polymethacrylate films using sodium alginate: Film characterization and drug permeability. International Journal of Pharmaceutics 2014; 460 (1-2): 63-72. (Impact factor 2014 = 3.650)
3. Rongthong T, Sungthongjeen S, Siepmann F, Siepmann J, **Pongjanyakul T**. Quaternary polymethacrylate–magnesium aluminum silicate films: Water uptake kinetics and film permeability. International Journal of Pharmaceutics 2015; 490(1–2): 165–172. (Impact factor 2014 = 3.650)
4. **Pongjanyakul T**, Khuathan N. Quaternary polymethacrylate-sodium alginate films: effect of alginate block structure and use for sustained release tablets. Pharmaceutical Development and Technology. (in press). (Impact factor 2014 = 1.202)
5. Quaternary polymethacrylate–magnesium aluminum silicate films for tablet coating (In preparation)

### Thai Patent

1. **Pongjanyakul T**, Rongthong T. Composite films for drug coating. Application no. 1301002021, Date filed 17 April 2013.

### Presentations

1. Rongthong T, Sungthongjeen S, **Pongjanyakul T**. Interaction of quaternary polymethacrylate with magnesium aluminum silicate in dispersions and films. The RGJ Seminar Series No. 86th: Research and Development in Pharmaceutical products, Khon Kaen, 19 April 2012.
2. Rongthong T, Sungthongjeen S, **Pongjanyakul T**. Characterization of ammonio-methacrylate copolymer-clay composite dispersions and films. Pharmacy Profession: Moving Forward to ASEAN Harmonization, Mahasarakham, 16-17 February 2013.

3. Rongthong T, Sungthongjeen S, Siepmann F, Siepmann J, **Pongjanyakul T**. Investigation of Eudragit RL-magnesium aluminum silicate composite dispersions and films. The 7th Annual PSSRC Symposium "Advanced Characterization Techniques for Solid Pharmaceutical Dosage Forms", Lille, 4-6 July 2013.
4. Rongthong T, Sungthongjeen S, Siepmann F, Siepmann J, **Pongjanyakul T**. Investigation of water uptake and drug release of Eudragit-magnesium aluminum silicate coated tablets. The 9th World Meeting on Pharmaceutics, Biopharmaceutics and Pharmaceutical Technology, Lisbon, 31 March-3 April 2014.
5. Khuathan K, T. Rongthong T, **Pongjanyakul T**. Quaternary polymethacrylate-alginate films: Effect of alginate block structure on water uptake and drug permeability. The 9th World Meeting on Pharmaceutics, Biopharmaceutics and Pharmaceutical Technology, Lisbon, 31 March-3 April 2014.
6. **Pongjanyakul T**, Sungthongjeen S, Siepmann J, Rongthong T. Quaternary polymethacrylate-magnesium aluminum silicate films: Tackiness and drug permeability. The 9th World Meeting on Pharmaceutics, Biopharmaceutics and Pharmaceutical Technology, Lisbon, 31 March-3 April 2014.
7. Rongthong T, Sungthongjeen S, Siepmann J, **Pongjanyakul T**. Quaternary polymethacrylaye--magnesium aluminum silicate films for modified-release tablets. In: Proceeding to the RGJ-PhD Congress XV, Chonburi, 28-30 May 2014, pp. 412.
8. **Pongjanyakul T**, Sungthongjeen S, Siepmann J, Rongthong T. Modification of quaternary polymethacrylate films using magnesium aluminum silicate for tablet film coatings. The 14th TRF meeting, Chonburi, 23-25 October 2014, pp. 8.
9. **Pongjanyakul T**, Khlibsuwan R, Khuathan N. Quaternary polymethacrylate-alginate coated tablets: Effect of alginate block structure and curing on drug release. The 1st European Conference on Pharmaceutics: Drug delivery, Reims, 13-14 April 2015.

**Connections with other experts within and outside Thailand**

1. Associate Professor Dr. Srisagul Sungthongjeen, Department of Pharmaceutical Technology, Naresuan University, Phitsanulok, Thailand.
2. Professor Dr. Juergen Siepmann, College of Pharmacy, INSERM U1008, University of Lille, Lille, France.
3. Dr. Florence Siepmann, College of Pharmacy, INSERM U1008, University of Lille, Lille, France.

# Appendix

## Thai Patent

**Pongjanyakul T**, Rongthong T. Composite films for drug coating. Application no. 1301002021, Date filed 17 April 2013.

**International publications**

Rongthong T, Sungthongjeen S, Siepmann J, **Pongjanyakul T**. Quaternary polymethacrylate-magnesium aluminum silicate films: Molecular interactions, mechanical properties and tackiness. Int J Pharm 2013; 458 (1): 57-64.

Khuathan N, **Pongjanyakul T**. Modification of quaternary polymethacrylate films using sodium alginate: Film characterization and drug permeability. Int J Pharm 2014; 460 (1-2): 63-72.

Rongthong T, Sungthongjeen S, Siepmann F, Siepmann J, **Pongjanyakul T**. Quaternary polymethacrylate–magnesium aluminum silicate films: Water uptake kinetics and film permeability. Int J Pharm 2015; 490(1–2): 165–172.

**Pongjanyakul T**, Khuathan N. Quaternary polymethacrylate-sodium alginate films: effect of alginate block structure and use for sustained release tablets. Pharm Dev Technol. (in press).

Quaternary polymethacrylate–magnesium aluminum silicate films for tablet coating (In preparation)

# Outputs

### International publications

1. Rongthong T, Sungthongjeen S, Siepmann J, **Pongjanyakul T**. Quaternary polymethacrylate-magnesium aluminum silicate films: Molecular interactions, mechanical properties and tackiness. International Journal of Pharmaceutics 2013; 458 (1): 57-64. (Impact factor 2014 = 3.650)
2. Khuathan N, **Pongjanyakul T**. Modification of quaternary polymethacrylate films using sodium alginate: Film characterization and drug permeability. International Journal of Pharmaceutics 2014; 460 (1-2): 63-72. (Impact factor 2014 = 3.650)
3. Rongthong T, Sungthongjeen S, Siepmann F, Siepmann J, **Pongjanyakul T**. Quaternary polymethacrylate–magnesium aluminum silicate films: Water uptake kinetics and film permeability. International Journal of Pharmaceutics 2015; 490(1–2): 165–172. (Impact factor 2014 = 3.650)
4. **Pongjanyakul T**, Khuathan N. Quaternary polymethacrylate-sodium alginate films: effect of alginate block structure and use for sustained release tablets. Pharmaceutical Development and Technology. (in press). (Impact factor 2014 = 1.202)
5. Quaternary polymethacrylate–magnesium aluminum silicate films for tablet coating (In preparation)

### Thai Patent

1. **Pongjanyakul T**, Rongthong T. Composite films for drug coating. Application no. 1301002021, Date filed 17 April 2013.

### Presentations

1. Rongthong T, Sungthongjeen S, **Pongjanyakul T**. Interaction of quaternary polymethacrylate with magnesium aluminum silicate in dispersions and films. The RGJ Seminar Series No. 86th: Research and Development in Pharmaceutical products, Khon Kaen, 19 April 2012.
2. Rongthong T, Sungthongjeen S, **Pongjanyakul T**. Characterization of ammonio-methacrylate copolymer-clay composite dispersions and films. Pharmacy Profession: Moving Forward to ASEAN Harmonization, Mahasarakham, 16-17 February 2013.

3. Rongthong T, Sungthongjeen S, Siepmann F, Siepmann J, **Pongjanyakul T**. Investigation of Eudragit RL-magnesium aluminum silicate composite dispersions and films. The 7th Annual PSSRC Symposium "Advanced Characterization Techniques for Solid Pharmaceutical Dosage Forms", Lille, 4-6 July 2013.
4. Rongthong T, Sungthongjeen S, Siepmann F, Siepmann J, **Pongjanyakul T**. Investigation of water uptake and drug release of Eudragit-magnesium aluminum silicate coated tablets. The 9th World Meeting on Pharmaceutics, Biopharmaceutics and Pharmaceutical Technology, Lisbon, 31 March-3 April 2014.
5. Khuathan K, T. Rongthong T, **Pongjanyakul T**. Quaternary polymethacrylate-alginate films: Effect of alginate block structure on water uptake and drug permeability. The 9th World Meeting on Pharmaceutics, Biopharmaceutics and Pharmaceutical Technology, Lisbon, 31 March-3 April 2014.
6. **Pongjanyakul T**, Sungthongjeen S, Siepmann J, Rongthong T. Quaternary polymethacrylate-magnesium aluminum silicate films: Tackiness and drug permeability. The 9th World Meeting on Pharmaceutics, Biopharmaceutics and Pharmaceutical Technology, Lisbon, 31 March-3 April 2014.
7. Rongthong T, Sungthongjeen S, Siepmann J, **Pongjanyakul T**. Quaternary polymethacrylaye--magnesium aluminum silicate films for modified-release tablets. In: Proceeding to the RGJ-PhD Congress XV, Chonburi, 28-30 May 2014, pp. 412.
8. **Pongjanyakul T**, Sungthongjeen S, Siepmann J, Rongthong T. Modification of quaternary polymethacrylate films using magnesium aluminum silicate for tablet film coatings. The 14th TRF meeting, Chonburi, 23-25 October 2014, pp. 8.
9. **Pongjanyakul T**, Khlibsuwan R, Khuathan N. Quaternary polymethacrylate-alginate coated tablets: Effect of alginate block structure and curing on drug release. The 1st European Conference on Pharmaceutics: Drug delivery, Reims, 13-14 April 2015.

**Connections with other experts within and outside Thailand**

1. Associate Professor Dr. Srisagul Sungthongjeen, Department of Pharmaceutical Technology, Naresuan University, Phitsanulok, Thailand.
2. Professor Dr. Juergen Siepmann, College of Pharmacy, INSERM U1008, University of Lille, Lille, France.
3. Dr. Florence Siepmann, College of Pharmacy, INSERM U1008, University of Lille, Lille, France.

# Appendix

## Thai Patent

**Pongjanyakul T**, Rongthong T. Composite films for drug coating. Application no. 1301002021, Date filed 17 April 2013.

ภาษา

**คำขอรับสิทธิบัตร/อนุสิทธิบัตร**

☒ การประดิษฐ์
☐ การออกแบบผลิตภัณฑ์
☐ อนุสิทธิบัตร

ข้าพเจ้าผู้ลงลายมือชื่อในคำขอรับสิทธิบัตร/อนุสิทธิบัตรนี้ ขอรับสิทธิบัตร/อนุสิทธิบัตร ตามพระราชบัญญัติสิทธิบัตร พ.ศ 2522 แก้ไขเพิ่มเติมโดยพระราชบัญญัติสิทธิบัตร (ฉบับที่ 2) พ.ศ 2535 และ พระราชบัญญัติสิทธิบัตร (ฉบับที่ 3) พ.ศ 2542

**สำหรับเจ้าหน้าที่**

| วันรับคำขอ 17 เม.ย. 2556 | เลขที่คำขอ 1301002021 |
|---|---|
| วันยื่นคำขอ - 3 [illegible] 2556 | |

สัญลักษณ์จำแนกการประดิษฐ์ระหว่างประเทศ

ใช้กับแบบผลิตภัณฑ์
ประเภทผลิตภัณฑ์

| วันประกาศโฆษณา | เลขที่ประกาศโฆษณา |
|---|---|
| วันออกสิทธิบัตร/อนุสิทธิบัตร | เลขที่สิทธิบัตร/อนุสิทธิบัตร |

ลายมือชื่อเจ้าหน้าท

1.ชื่อที่แสดงถึงการประดิษฐ์/การออกแบบผลิตภัณฑ์
ฟิล์มผสมสำหรับเคลือบยา

2.คำขอรับสิทธิบัตรการออกแบบผลิตภัณฑ์นี้เป็นคำขอสำหรับแบบผลิตภัณฑ์อย่างเดียวกันและเป็นคำขอลำดับที่
ในจำนวน คำขอ ที่ยื่นในคราวเดียวกัน

3.ผู้ขอรับสิทธิบัตร/อนุสิทธิบัตร และที่อยู่ (เลขที่ ถนน ประเทศ)
3.1 มหาวิทยาลัยขอนแก่น
123 ถนนมิตรภาพ ต.ในเมือง อ. เมือง จ.ขอนแก่น 40002
3.2 สำนักงานกองทุนสนับสนุนการวิจัย
979/17-21 อาคารเอส เอ็ม เพาเวอร์ ชั้น 14 ถ.พหลโยธิน แขวงสามเสนใน เขตพญาไท กรุงเทพฯ 10400

| | |
|---|---|
| 3.1 สัญชาติ | ไทย |
| 3.2 โทรศัพท์ | 0-4320-2222-41 |
| 3.3 โทรสาร | - |
| 3.4 อีเมล์ | - |

4.สิทธิในการขอรับสิทธิบัตร/อนุสิทธิบัตร
☐ ผู้ประดิษฐ์/ผู้ออกแบบ ☒ ผู้รับโอน ☐ ผู้ขอรับสิทธิโดยเหตุอื่น

5.ตัวแทน(ถ้ามี)/ที่อยู่ (เลขที่ ถนน จังหวัด รหัสไปรษณีย์)
นางจิราภรณ์ เหลืองไพรินทร์
สำนักงานบริหารจัดการทรัพย์สินทางปัญญา
123 มหาวิทยาลัยขอนแก่น ต.ในเมือง อ. เมือง จ.ขอนแก่น ประเทศไทย 40002

| | |
|---|---|
| 5.1 ตัวแทนเลขที่ | 2217 |
| 5.2 โทรศัพท์ | 0-4336-4409 |
| 5.3 โทรสาร | 0-4336-4409 |
| 5.4 อีเมล์ | ip@kku.ac.th |

6.ผู้ประดิษฐ์/ผู้ออกแบบผลิตภัณฑ์ และที่อยู่ ( เลขที่ ถนน ประเทศ )
6.1รองศ าสตราจารย์ธเนศ พงศ์จรรยากุล ที่อยู่ คณะเภสัชศาสตร์ มหาวิทยาลัยขอนแก่น ต.ในเมือง อ. เมือง จ. ขอนแก่น 40002
6.2 นางสาวฐิติพร รองทอง ที่อยู่ คณะเภสัชศาสตร์ มหาวิทยาลัยขอนแก่น ต.ในเมือง อ. เมือง จ. ขอนแก่น 40002

7. คำขอรับสิทธิบัตร/อนุสิทธิบัตรนี้แยกจากหรือเกี่ยวข้องกับคำขอเดิม
ผู้ขอรับสิทธิบัตร/อนุสิทธิบัตร ขอให้ถือว่าได้ยื่นคำขอรับสิทธิบัตร/อนุสิทธิบัตรนี้ ในวันเดียวกับคำขอรับสิทธิบัตร เลขที่ วันยื่น เพราะคำขอรับสิทธิบัตร/อนุสิทธิบัตรนี้แยกจากหรือเกี่ยวข้องกับคำขอเดิมเพราะ
☐ คำขอเดิมมีการประดิษฐ์หลายอย่าง ☐ ถูกคัดค้านเนื่องจากผู้ขอไม่มีสิทธิ ☐ ขอเปลี่ยนแปลงประเภทของสิทธิ

**หมายเหตุ** ในกรณีที่ไม่อาจระบุรายละเอียดได้ครบถ้วน ให้จัดทำเป็นเอกสารแนบท้ายแบบพิมพ์นี้โดยระบุหมายเลขกำกับข้อและหัวข้อที่แสดงรายละเอียดเพิ่มเติมดังกล่าวด้วย

8.การยื่นคำขอนอกราชอาณาจักร

| วันยื่นคำขอ | เลขที่คำขอ | ประเทศ | สัญลักษณ์จำแนกการประดิษฐ์ระหว่างประเทศ | สถานะคำขอ |
|---|---|---|---|---|
| 8.1 | | | | |
| 8.2 | | | | |
| 8.3 | | | | |

8.4 ☐ ผู้ขอรับสิทธิบัตร/อนุสิทธิบัตรขอสิทธิให้ถือว่าได้ยื่นคำขอนี้ในวันที่ได้ยื่นคำขอรับสิทธิบัตร/อนุสิทธิบัตรในต่างประเทศเป็นครั้งแรกโดย
☐ ได้ยื่นเอกสารหลักฐานพร้อมคำขอนี้ ☐ ขอยื่นเอกสารหลักฐานหลังจากวันยื่นคำขอนี้

9.การแสดงการประดิษฐ์ หรือการออกแบบผลิตภัณฑ์ ผู้ขอรับสิทธิบัตร/อนุสิทธิบัตรได้แสดงการประดิษฐ์ที่หน่วยงานของรัฐเป็นผู้จัด
วันแสดง วันเปิดงานแสดง ผู้จัด

10.การประดิษฐ์เกี่ยวกับจุลชีพ

| 10.1 เลขทะเบียนฝากเก็บ | 10.2 วันที่ฝากเก็บ | 10.3 สถาบันฝากเก็บ/ประเทศ |
|---|---|---|
| | | |

11.ผู้ขอรับสิทธิบัตร/อนุสิทธิบัตร ขอยื่นเอกสารภาษาต่างประเทศก่อนในวันยื่นคำขอนี้ และจะจัดยื่นคำขอรับสิทธิบัตร/อนุสิทธิบัตรนี้ที่จัดทำเป็นภาษาไทยภายใน 90 วัน นับจากวันยื่นคำขอนี้ โดยขอยื่นเป็นภาษา
☐ อังกฤษ ☐ ฝรั่งเศส ☐ เยอรมัน ☐ ญี่ปุ่น ☐ อื่นๆ

12.ผู้ขอรับสิทธิบัตร/อนุสิทธิบัตร ขอให้อธิบดีประกาศโฆษณาคำขอรับสิทธิบัตร หรือรับจดทะเบียน และประกาศโฆษณาอนุสิทธิบัตรนี้ หลังจากวันที่ เดือน พ.ศ
☐ ผู้ขอรับสิทธิบัตร/อนุสิทธิบัตรขอให้ใช้รูปเขียนหมายเลข ในการประกาศโฆษณา

13.คำขอรับสิทธิบัตร/อนุสิทธิบัตรนี้ประกอบด้วย
ก. แบบพิมพ์คำขอ 2 หน้า
ข. รายละเอียดการประดิษฐ์ หรือคำพรรณนาแบบผลิตภัณฑ์ 10 หน้า
ค. ข้อถือสิทธิ 1 หน้า
ง. รูปเขียน 33 รูป 19 หน้า
จ. ภาพแสดงแบบผลิตภัณฑ์
☐ รูปเขียน รูป หน้า
☐ ภาพถ่าย รูป หน้า
ฉ. บทสรุปการประดิษฐ์ 1 หน้า

14.เอกสารประกอบคำขอ
☐ เอกสารแสดงสิทธิในการขอรับสิทธิบัตร/อนุสิทธิบัตร
☐ หนังสือรับรองการแสดงการประดิษฐ์/การออกแบบผลิตภัณฑ์
☐ หนังสือมอบอำนาจ
☐ เอกสารรายละเอียดเกี่ยวกับจุลชีพ
☐ เอกสารการขอนับวันยื่นคำขอในต่างประเทศเป็นวันยื่นคำขอในประเทศไทย
☐ เอกสารขอเปลี่ยนแปลงประเภทของสิทธิ
☐ เอกสารอื่น ๆ

15. ข้าพเจ้าขอรับรองว่า
☒ การประดิษฐ์นี้ไม่เคยยื่นขอรับสิทธิบัตร/ อนุสิทธิบัตรมาก่อน
☐ การประดิษฐ์นี้ได้พัฒนาปรับปรุงมาจาก.....

16.ลายมือชื่อ ( ☐ ผู้ขอรับสิทธิบัตร / อนุสิทธิบัตร; ☒ ตัวแทน )
(นางจิราภรณ์ เหลืองไพรินทร์)

**หมายเหตุ** บุคคลใดยื่นขอรับสิทธิบัตรการประดิษฐ์หรือการออกแบบผลิตภัณฑ์ หรืออนุสิทธิบัตร โดยการแสดงข้อความอันเป็นเท็จแก่พนักงานเจ้าหน้าที่ เพื่อให้ได้ไปซึ่งสิทธิบัตรหรืออนุสิทธิบัตร ต้องระวางโทษจำคุกไม่เกินหกเดือน หรือปรับไม่เกินห้าพันบาท หรือทั้งจำทั้งปรับ

International Journal of Pharmaceutics 458 (2013) 57–64

Contents lists available at ScienceDirect

International Journal of Pharmaceutics

journal homepage: www.elsevier.com/locate/ijpharm

# Quaternary polymethacrylate–magnesium aluminum silicate films: Molecular interactions, mechanical properties and tackiness

Thitiphorn Rongthong[a], Srisagul Sungthongjeen[b], Juergen Siepmann[c], Thaned Pongjanyakul[a,*]

[a] Faculty of Pharmaceutical Sciences, Khon Kaen University, Khon Kaen 40002, Thailand
[b] Department of Pharmaceutical Technology, Faculty of Pharmaceutical Sciences, Naresuan University, Phitsanulok 65000, Thailand
[c] College of Pharmacy, INSERM U1008, University of Lille, 3 rue du Professeur Laguesse, 59006 Lille, France

ARTICLE INFO

*Article history:*
Received 21 June 2013
Received in revised form 2 August 2013
Accepted 3 October 2013
Available online 19 October 2013

*Keywords:*
Quaternary polymethacrylate
Magnesium aluminum silicate
Molecular interaction
Tackiness
Mechanical properties

ABSTRACT

The aim of this study was to investigate the impact of the addition of magnesium aluminum silicate (MAS), a natural clay, on the properties of polymeric films based on quaternary polymethacrylates (QPMs). Two commercially available aqueous QPM dispersions were studied: Eudragit® RS 30D and Eudragit® RL 30D (the dry copolymers containing 5 and 10% quaternary ammonium groups, respectively). The composite QPM-MAS films were prepared by casting. Importantly, QPM interacted with MAS and formed small flocculates prior to film formation. Continuous films were obtained up to MAS contents of 19% (referred to the QPM dry mass). ATR-FTIR and PXRD revealed that the positively charged quaternary ammonium groups of QPM interacted with negatively charged —$SiO^-$ groups of MAS, creating nanocomposite materials. This interaction led to improved thermal stability of the composite films. The puncture strength and elongation at break of dry systems decreased with increasing MAS content. In contrast, the puncture strength of the wet QPM-MAS films (upon exposure to acidic or neutral media) increased with increasing MAS content. Furthermore, incorporation of MAS into QPM films significantly decreased the latter's tackiness in the dry and wet state. These findings suggest that nanocomposite formation between QPM and MAS in the systems can enhance the strength of wet films and decrease their tackiness. Thus, MAS offers an interesting potential as novel anti-tacking agent for QPM coatings.



## 1. Introduction

Quaternary polymethacrylate (QPM), a synthetic polymer built of acrylic and methacrylic esters, is widely used as a film forming agent for pharmaceutical dosage forms (Skalsky and Petereit, 2008). QPMs containing 5 and 10% quaternary ammonium groups (abbreviated as "5QPM" and "10QPM" in this article) are for instance commercially available in the form of aqueous dispersions with a solids content of 30%, under the trade names "Eudragit® RS 30D" and "Eudragit® RL 30D". In these products the counter ions of the positively charged quaternary ammonium groups are chloride ions. Fig. 1a shows their chemical structure. Since 5QPM contains less quaternary ammonium groups than 10QPM, it swells less upon contact with aqueous fluids and is generally less permeable for water soluble drugs (Knop, 1996). 5QPM, 10QPM as well as blends thereof are frequently used as controlled release film coatings, e.g. for pellets (Bodmeier et al., 1996; Wu and McGinity, 2003; Heckötter et al., 2011) and tablets (Sungthongjeen et al., 2008). Moreover, they can also be used for odor and taste masking purposes (Douroumis et al., 2011). To provide appropriate film flexibility, often water soluble or water insoluble plasticizers are added.

One of the major challenges to be addressed when using QPM film coatings is their stickiness. This can be an important obstacle in practice, rendering the manufacturing procedure highly challenging. Different anti-tacking agents have been proposed to overcome this hurdle, such as talcum (Wesseling et al., 1999; Maejima and McGinity, 2001), glyceryl monostearate (Wesseling et al., 1999), and sorbitan monostearate (Nimkulrat et al., 2004). However, these anti-tacking agents also provide disadvantages. For example, talcum is generally required in high amounts. For instance, Wesseling et al. (1999) used 25–50% (w/w) talc (referred to the polymer contents) to reduce film tackiness. Such high amounts may cause nozzle clogging during the coating process. Interestingly, glyceryl monostearate (GMS) and sorbitan monostearate are effective at much lower concentrations (e.g., 5–10%, w/w), but their incorporation into the coating dispersion might not be straightforward. For these reasons it is interesting to seek for novel types of additives for QPM films, which can effectively reduce their tackiness and allow for an efficient film coating process.

* Corresponding author at: Faculty of Pharmaceutical Sciences, Khon Kaen University, Khon Kaen 40002, Thailand. Tel.: +66 43 362092; fax: +66 43 202379.
*E-mail address:* thaned@kku.ac.th (T. Pongjanyakul).

0378-5173/$ – see front matter © 2013 Elsevier B.V. All rights reserved.
http://dx.doi.org/10.1016/j.ijpharm.2013.10.016

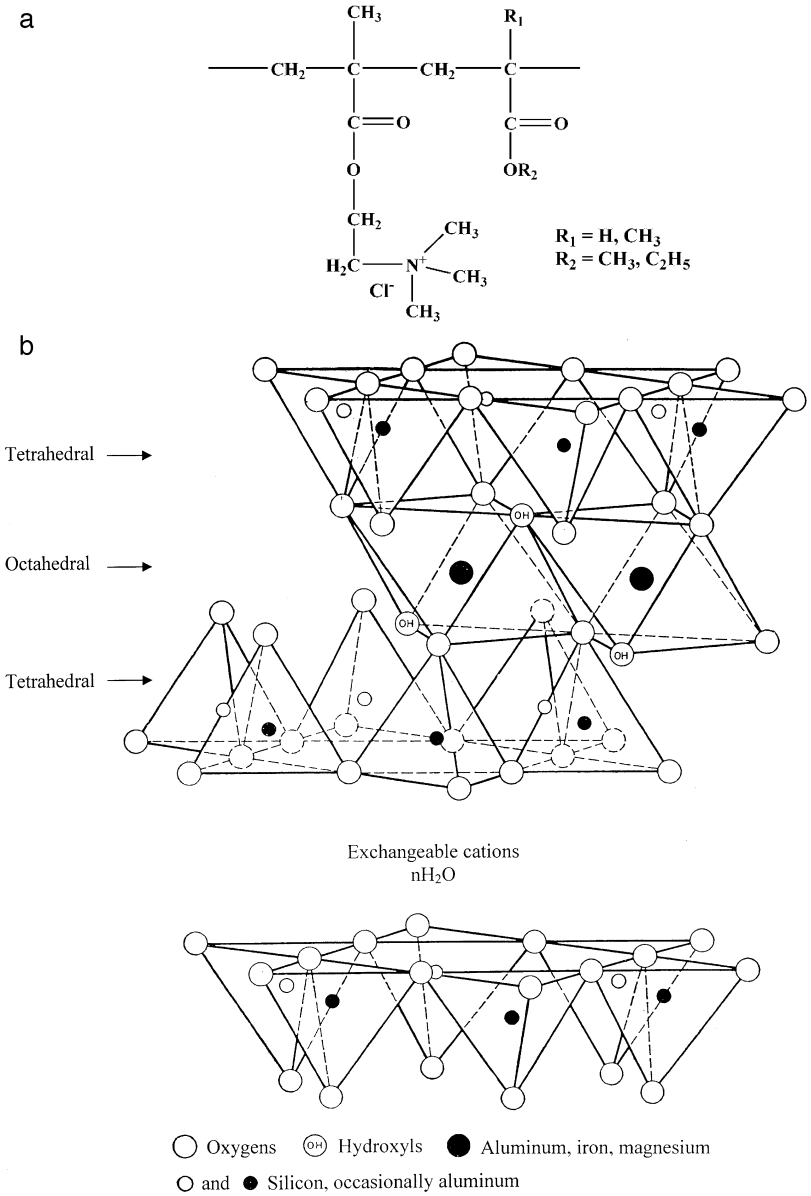


**Fig. 1.** Chemical structures of the investigated quaternary polymethacrylates (QPMs) (a), and magnesium aluminum silicate (MAS) (b).

Magnesium aluminum silicate (MAS) is a mixture of montmorillonite and saponite clays (Alexandre and Dubois, 2000; Kibbe, 2000). It is used as a pharmaceutical excipient, being non-toxic and non-irritant at levels commonly applied in drug products (Kibbe, 2000). It is composed of three-lattice layers, a central octahedral sheet of aluminum or magnesium and two external silica tetrahedron layers (Alexandre and Dubois, 2000). The structure of MAS is presented in Fig. 1b. The different layers can be separated upon hydration, and MAS can exhibit negative charges in the surface layer (—$SiO^-$ groups). For this reason MAS may interact with positively charged drugs, such as protonated nicotine (Suksri and Pongjanyakul, 2008) and propranolol (Rojtanatanya and Pongjanyakul, 2010), resulting in a more sustained drug release from such complexes. Furthermore, the negative charges of MAS silicate layers may also interact with positively charged polysaccharides, e.g. chitosan (Khunawattanakul et al., 2008) to form nanocomposite films that possess improved mechanical properties and drug permeability (Khunawattanakul et al., 2010). Such nanocomposite films can for instance be used for tablet coating (Khunawattanakul et al., 2011). For these reasons, MAS may potentially also interact with positively charged QPM colloidal particles, eventually leading to improved QPM film properties.

The objective of the present work was to study the impact of the addition of various amounts of MAS to aqueous QPM dispersions. Particular focus was placed on the key features of the: (i) aqueous dispersion blends themselves: particle size and zeta potential, and (ii) films prepared by casting such dispersions: thickness, inner and external morphology, thermal behavior, molecular interactions between QPM and MAS, mechanical properties and tackiness. Such QPM-MAS composite films may potentially be used for controlled release film coatings.

## 2. Materials and methods

### 2.1. Materials

Aqueous dispersions of 5QPM and 10QPM (Eudragit® RS 30D and Eudragit® RL 30D) were purchased from Röhm Pharma GmbH (Darmstadt, Germany). MAS in granular form (Veegum®HV) was

obtained from R.T. Vanderbilt Company Inc. (Norwalk, CT, USA). Diethyl sebacate was purchased from Aldrich Chemistry (Dorset, UK). All other reagents and solvents were of analytical grade and used as received.

### 2.2. Preparation of QPM–MAS composite dispersions

MAS dispersion (4%, w/v) was prepared with hot water and kept at room temperature overnight. Zero, 2.5, 6.25, 12.5, 18.75, or 25 mL of this dispersion was slowly poured into appropriate amounts of QPM dispersions (30%, w/w polymer solids content) containing 4 g copolymer. The resulting QPM:MAS (mass:mass) ratios were 4:0, 4:0.1, 4:0.25, 4:0.5, 4:0.75, or 4:1, respectively. The mixtures were stirred using a magnetic stirrer and distilled water was added to reach a final volume of 100 mL in each case. The QPM–MAS composite dispersions were further stirred at room temperature for 30 min and then shaken in a water bath at 75 oscillations $min^{-1}$ for 24 h at 37 °C.

### 2.3. Characterization of QPM–MAS composite dispersions

#### 2.3.1. Particle size measurements

The particle sizes of the QPM dispersions, MAS dispersions, and QPM-MAS composite dispersions were determined using a laser diffraction particle size analyzer (Mastersizer2000 Model Hydro2000SM, Malvern Instrument Ltd., UK). The samples were dispersed in 70 mL distilled water in a sample dispersion unit and stirred at 50 Hz for 30 s prior to the measurements. The volume weighted mean diameters are reported.

#### 2.3.2. Zeta potential measurements

The zeta potential was measured using a laser Doppler electrophoresis analyzer (Zetasizer Model ZEN 2600, Malvern Instrument Ltd., UK). The samples were kept at 25 °C. The dispersions of QPM, MAS, and QPM–MAS composites were diluted to obtain appropriate concentrations (count rates >20,000 counts $s^{-1}$) prior to the measurements.

### 2.4. Preparation of QPM–MAS composite films

QPM and QPM–MAS composite films were prepared by casting and subsequent water evaporation. Twenty grams QPM dispersions (30%, w/w polymer solids content) were mixed with 0.9 g diethyl sebacate (15%, w/w plasticizer referred to the QPM dry mass), and stirred for 30 min. Then, appropriate amounts of 4%, w/v MAS dispersion (prepared with hot water and kept at room temperature overnight) was added to obtain QPM:MAS ratios of 4:0, 4:0.1, 4:0.25, 4:0.5, 4:0.75, or 4:1, respectively. These QPM–MAS composite dispersions were stirred for 30 min, and then adjusted to a final volume of 150 mL with distilled water before shaking in a water bath at 75 oscillations $min^{-1}$ for 24 h at 37 °C. Subsequently, the dispersions were degassed, poured into Teflon® plates (17 cm × 18 cm) and dried at 50 °C for 48 h. The dry films were peeled off and kept in desiccators prior to characterization.

### 2.5. Characterization of QPM–MAS composite films

#### 2.5.1. Thickness measurement

The film thicknesses were measured at twenty different positions using a microprocessor coating thickness gauge (Minitest 600B, ElektroPhysik, Germany). The films were placed on a control plate. The probe was connected to the measurement gauze and calibrated using a reference film.

#### 2.5.2. Scanning electron microscopy (SEM)

The external and internal morphology of QPM and QPM-MAS composite films were studied using SEM. Cross-sections were obtained by cutting with a knife. The samples were mounted onto holders, coated with gold in a vacuum evaporator, and analyzed with a scanning electron microscope (Joel Model JSM-6480LV, Tokyo, Japan).

#### 2.5.3. ATR–FTIR spectroscopy

The spectra (4000 to 650 $cm^{-1}$ at a resolution of 4 $cm^{-1}$) of the samples were recorded using an ATR-FTIR spectrophotometer (Spectrum One, Perkin Elmer, Norwalk, CT). Each sample was cut and placed on a ZnSe prism of a sample holder.

#### 2.5.4. Powder X-ray diffractometry (PXRD)

PXRD patterns of the samples were recorded using a powder X-ray diffractometer (Philips PW3710 mpd control, The Netherlands). A Cu radiation with a wavelength of 1.54 Å was used (30 kV, 20 mA, $2\theta$ = 1–30°, step angle = 0.02° $2\theta$ $s^{-1}$). The thickness of the silicate MAS layers was calculated using Bragg's equation:

$$n\lambda = 2d \sin\theta \quad (1)$$

where $n$ is 1 (the first order reflection was used), $\lambda$ is the X-ray wavelength (1.54 Å), $\theta$ is the angle of the basal spacing peak of MAS, and d is the thickness of the MAS silicate layer.

#### 2.5.5. Differential scanning calorimetry (DSC)

DSC thermograms were recorded using a differential scanning calorimeter (DSC822, Mettler Toledo, Switzerland). The samples (2–3 mg) were accurately weighted into 40 μL open aluminum pans. The temperature was increased from 30 to 450 °C at 10 °C $min^{-1}$.

#### 2.5.6. Determination of the mechanical properties

The puncture strength and %elongation at break of the films in the dry and wet state were determined using a texture analyzer (TA-XT2, Stable Micro Systems, Ltd., UK), equipped with a 500 N load cell. Films were cut into 2 cm × 2 cm pieces and kept at 55% relative humidity and 25 °C for 3 d prior to testing. If measured in the wet state, films were exposed to 0.1 M HCl or pH 6.8 phosphate buffer (under occasional shaking) at 37 °C for 1 h prior to the measurements. Excess water was removed by blotting. Dry and wet film samples were fixed using a film holder between two mounting plates. A 5 mm diameter spherical stainless puncturing probe was fixed at the load cell and moved downwards at 0.1 mm $s^{-1}$. The applied force and displacement were recorded. The puncture strength and %elongation at break were calculated as follows:

$$\text{Puncture strength} = \frac{F}{A} \quad (2)$$

where $F$ is the maximum force and $A$ is the cross-sectional area of the edge of the film located in the path of the cylindrical opening of the film holder.

$$\%\,\text{Elongation at break} = \frac{\sqrt{r^2 + D^2} - r}{r} \times 100\% \quad (3)$$

where $r$ is the radius of the film exposed in the cylindrical hole of the film holder and $D$ is the displacement of the probe from the point of probe-film contact to the point of film puncture.

#### 2.5.7. Tackiness measurement

A modification of the method reported by Wesseling et al. (1999) was applied, using a texture analyzer (TA-XT2), equipped with a 50 N load cell. The films were cut into pieces of 2 cm × 7 cm. The samples were kept at 75% relative humidity and 25 °C for 3 d prior to testing. In case of wet films, the latter were exposed

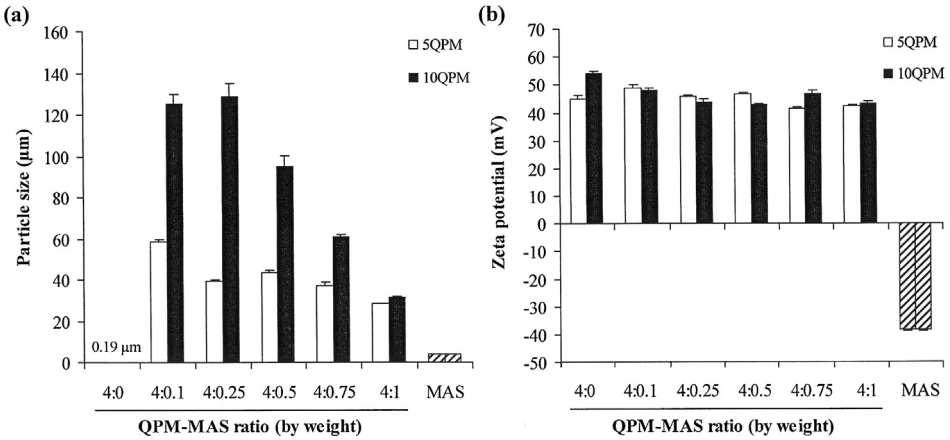


**Fig. 2.** Particle size (a) and zeta potential (b) of QPM dispersions, MAS dispersions, and QPM–MAS composite dispersions. Data are mean ± S.D., $n = 3$.

to distilled water for 10 min prior to the measurements. Excess water was removed by blotting. The films were tightly placed together and compressed with 500 g weights for 1 h. One end of each film was placed in the upper and lower clamps of tensile grips. The upper clamp was attached to the load cell, which was driven upwards at a cross-head speed of 15 mm $min^{-1}$; whereas the lower clamp was stationary. The detachment force needed to separate the films was recorded. The average detachment forces were obtained from twenty measurement points of the linear parts of the force–displacement curves.

### 2.6. Statistical analysis

The results of the particle size, zeta potential, puncture strength, %elongation at break and tackiness measurements were analyzed using one-way analysis of variance (ANOVA) with the least significant difference (LSD) test for multiple comparisons or the Student t-test. All statistical tests were performed using the software SPSS for MS Windows, release 11.5 (SPSS (Thailand) Co. Ltd., Bangkok, Thailand). The significance of the difference was determined with the 95% confident limit ($\alpha = 0.5$) and considered to be significant at a level of $P$ less than 0.05.

## 3. Results and discussion

### 3.1. Characteristics of QPM–MAS composite dispersions

Aqueous colloidal dispersions of 5QPM and 10QPM are white (milky) liquids, showing no signs for particle sedimentation. The mean particle sizes of 5QPM and 10QPM dispersions were found to be 0.187 and 0.194 μm, respectively (Fig. 2a). Moreover, the particles of 5QPM and 10 QPM presented positive charges, the zeta potentials being equal to 44.9 and 54.2 mV, respectively (Fig. 2b). The zeta potential of 10QPM was higher than that of 5QPM, because of the higher number of quaternary ammonium groups. The 4% MAS dispersion was opaque, the mean particle size was 3.92 ± 0.02 μm and the zeta potential −38.2 ± 0.6 mV. When the MAS dispersion was slowly added to the QPM dispersions, sedimentation was visible. This is likely due to the formation of QPM–MAS flocculates, resulting from attractive electrostatic interactions between the negatively charged $-SiO^-$ groups of the MAS and the positively charged quaternary ammonium groups ($-N(CH_3)_3^+$) of the QPMs.

The particle sizes and zeta potentials of the QPM–MAS dispersions are shown in Fig. 2. The dispersed phase of QPM–MAS dispersions exhibited significantly greater particle sizes ($P < 0.05$) than the QPM and MAS dispersions, indicating the formation of QPM-MAS flocculates. The particle sizes of the 5QPM–MAS flocculates were statistically smaller ($P < 0.05$) than those of the 10QPM–MAS flocculates. Moreover, the QPM–MAS flocculate sizes decreased with increasing MAS contents. The zeta potential of the QPM–MAS flocculates also decreased ($P < 0.05$) with increasing MAS contents, but remained positive in the investigated range.

### 3.2. Appearance, thickness and morphology of the films

QPM films free of plasticizer were hard and brittle. The addition of a plasticizer is important to improve film flexibility, and also to promote particle coalescence during film formation from the aqueous polymer dispersions (Lehmann, 1997). Insoluble plasticizers at a level of 10–40% (w/w) are often used for QPM films (Bodmeier and Paeratakul, 1997; Siepmann et al., 1997). In this study, diethyl sebacate was used as a plasticizer for QPM at a level of 15%. Plasticized QPM films were transparent. However, upon addition of MAS opaque films were obtained. Films formed at the QPM:MAS ratios 4:0.1, 4:0.25, 4:0.5 and 4:0.75. When further increasing the MAS content to QPM:MAS = 4:1, no continuous films were formed. This is a practical limitation when using MAS as an additive for QPM films and can be explained by the fact that the presence of so high MAS quantities effectively hinders the fusion of the QPM nanoparticles to form continuous, three-dimensional polymeric networks.

The thickness of the QPM–MAS composite films increased with increasing MAS content (Table 1), because the solids content of the cast formulations increased. SEM pictures of surfaces and cross-sections of 5QMP and 5QMP:MAS 4:0.75 composite films are shown in Fig. 3. The 5QPM films had a smooth surface, whereas composite films showed a rougher surface (due to the presence of micron-sized MAS particles). Moreover, the matrix morphology of the 5QPM films appeared to be denser structure than that of the 5QPM–MAS composite films. Similar results were obtained with the 10QPM and 10QPM–MAS composite films (data not shown).

### 3.3. Molecular interactions between QPM and MAS

Molecular interactions between QPM and MAS in the films were investigated using ATR–FTIR spectroscopy and powder X-ray diffraction. The ATR–FTIR spectra of MAS powder, QPM films, and QPM-MAS composite films are shown in Fig. 4. MAS showed an O—H bending of residual water at 1630 $cm^{-1}$, and a Si—O—Si stretching at 981 $cm^{-1}$ (Fig. 4a). The spectra of the 5QPM films presented a C—H stretching around 2857–2983 $cm^{-1}$, a C═O stretching at 1722 $cm^{-1}$, a $CH_2$ symmetric bending at 1446 $cm^{-1}$, a $CH_3$ asymmetric bending at 1380 $cm^{-1}$, a C—CO—C stretching at 1143 $cm^{-1}$, and a C—N stretching at 1095 $cm^{-1}$ (Fig. 4b). The 10QPM film spectra

**Table 1**
Thickness and mechanical properties of QPM films and QPM–MAS films.

| Film | Thickness[a] (μm) | Dry film | | Wet film using 0.1 M HCl | | Wet film using pH 6.8 phosphate buffer | |
|---|---|---|---|---|---|---|---|
| | | Puncture strength[b] (MPa) | Elongation[b] (%) | Puncture strength[b] (MPa) | Elongation[b] (%) | Puncture strength[b] (MPa) | Elongation[b] (%) |
| 5QPM–MAS | | | | | | | |
| 4:0 | 162.5 ± 24.1 | 7.10 ± 0.29 | 113.9 ± 9.12 | 1.69 ± 0.19 | 118.8 ± 7.93 | 1.36 ± 0.08 | 131.9 ± 16.4 |
| 4:0.1 | 187.4 ± 34.4 | 5.97 ± 0.45 | 48.31 ± 7.18 | 1.45 ± 0.14 | 59.96 ± 5.30 | 1.13 ± 0.08 | 65.74 ± 8.56 |
| 4:0.25 | 216.4 ± 27.7 | 5.67 ± 0.19 | 33.90 ± 6.24 | 1.97 ± 0.20 | 32.92 ± 1.81 | 1.72 ± 0.10 | 35.85 ± 3.39 |
| 4:0.5 | 202.4 ± 21.3 | 5.58 ± 0.23 | 21.27 ± 4.02 | 1.90 ± 0.07 | 22.09 ± 2.10 | 1.78 ± 0.11 | 23.77 ± 3.34 |
| 4:0.75 | 226.9 ± 22.7 | 4.36 ± 0.37 | 18.62 ± 3.15 | 2.73 ± 0.20 | 15.58 ± 1.38 | 2.54 ± 0.27 | 15.60 ± 2.06 |
| 10QPM–MAS | | | | | | | |
| 4:0 | 182.4 ± 25.7 | 13.63 ± 1.06 | 58.01 ± 10.5 | 0.41 ± 0.14 | 320.4 ± 78.9 | 0.35 ± 0.09 | 245.1 ± 44.0 |
| 4:0.1 | 186.4 ± 22.0 | 10.56 ± 0.54 | 45.62 ± 7.31 | 0.70 ± 0.04 | 88.81 ± 1.70 | 0.52 ± 0.03 | 69.17 ± 5.98 |
| 4:0.25 | 204.4 ± 25.1 | 8.79 ± 0.47 | 37.15 ± 7.73 | 0.49 ± 0.04 | 57.62 ± 5.82 | 0.48 ± 0.02 | 45.18 ± 5.23 |
| 4:0.5 | 199.8 ± 37.1 | 7.48 ± 0.59 | 23.14 ± 3.52 | 0.78 ± 0.05 | 23.62 ± 2.21 | 0.73 ± 0.08 | 20.65 ± 1.40 |
| 4:0.75 | 209.5 ± 8.32 | 6.77 ± 1.38 | 24.08 ± 5.00 | 1.36 ± 0.14 | 22.16 ± 1.16 | 1.50 ± 0.15 | 19.79 ± 1.50 |

[a] Data are mean ± S.D., $n = 20$.
[b] Data are mean ± S.D., $n = 5$.

(Fig. 4c) were similar to those of 5QPM films. Incorporation of MAS within the QPM films caused an obvious C—N stretching peak that shifted from 1095 $cm^{-1}$ to 1080 $cm^{-1}$ (Fig. 4d and e). Moreover, the Si—O—Si stretching of MAS moved to higher wavenumbers: 991–1006 $cm^{-1}$. These results suggest that the silanol groups of MAS and quaternary ammonium groups of QP interacted, probably via electrostatic forces. This interaction may cause the formation of a nanocomposite material, a phenomenon which should be detectable using PXRD.

The PXRD patterns of MAS, QPM films and QPM-MAS composite films are shown in Fig. 5. MAS showed a basal spacing peak at 7.0° (2$\theta$), indicating a thickness of 1.26 nm of the MAS silicate layers (according to Eq. (1)). The 5QPM and 10QPM films showed diffusive halos, suggesting an amorphous state of these copolymers (and/or crystals, which are not detectable under the given conditions). No basal spacing peak was visible in 5QPM:MAS 4:0.1 composite films, whereas this MAS peak was visible at 6.6° (2$\theta$) in 10QPM–MAS films at the same blend ratio. The disappearance of the basal MAS spacing peak in 5QPM–MAS films suggests that the MAS silicate layers might be completely separated in the 5QPM matrix. This is called an "exfoliated" nanocomposite (Alexandre and Dubois, 2000). This type of nanocomposite could be possibly occurred when lower MAS ratio was used. The fact that the 10QPM–MAS (4:0.1) films presented this peak, indicates that MAS could at least partially keep its layered structure in these systems. Incorporating higher amounts of MAS resulted in visible spacing peaks for both types of polymers. Interestingly, the basal spacing MAS peak was shifted to lower angles in both cases: 6.7–6.3° (2$\theta$), corresponding to MAS silicate layer thicknesses of 1.32–1.40 nm. These results suggest the formation of intercalated nanocomposites, in which QPM intercalates into the MAS silicate layers. Thus, according to the ATR–FTIR and X-ray diffraction patterns, QPM and MAS electrostatically interact, leading to the formation of "exfoliated" nanocomposite films at very low MAS contents, and to the formation of the intercalated nanocomposite films at higher MAS contents.

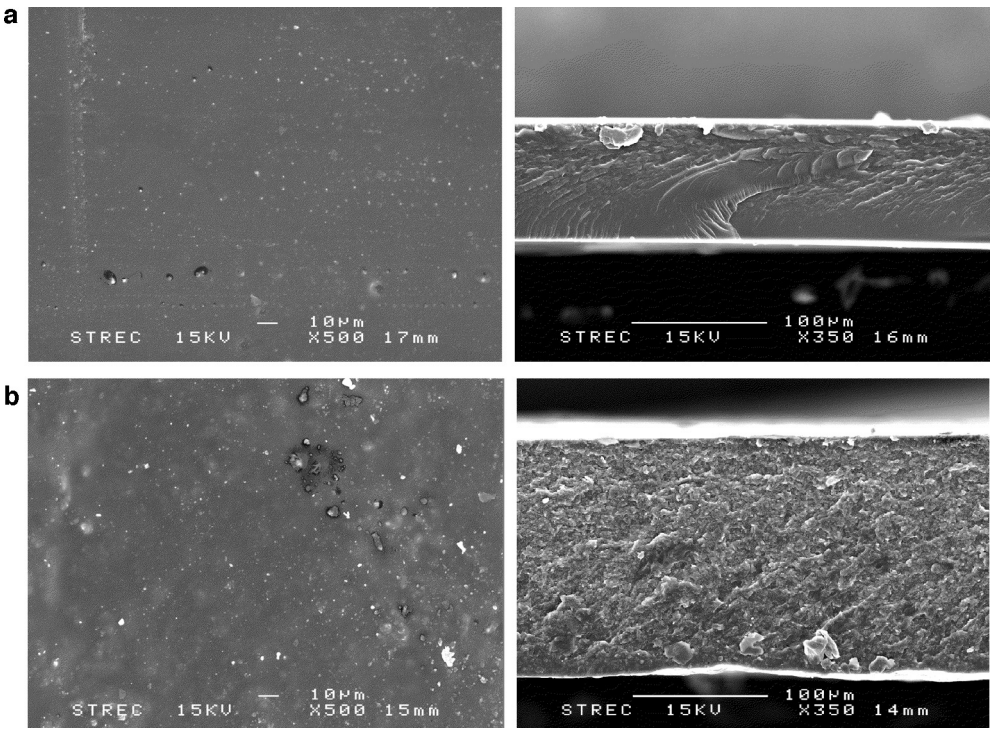


**Fig. 3.** SEM pictures of surfaces and cross-sections of 5QPM films (a), and 5QPM–MAS (4:0.75) films (b).

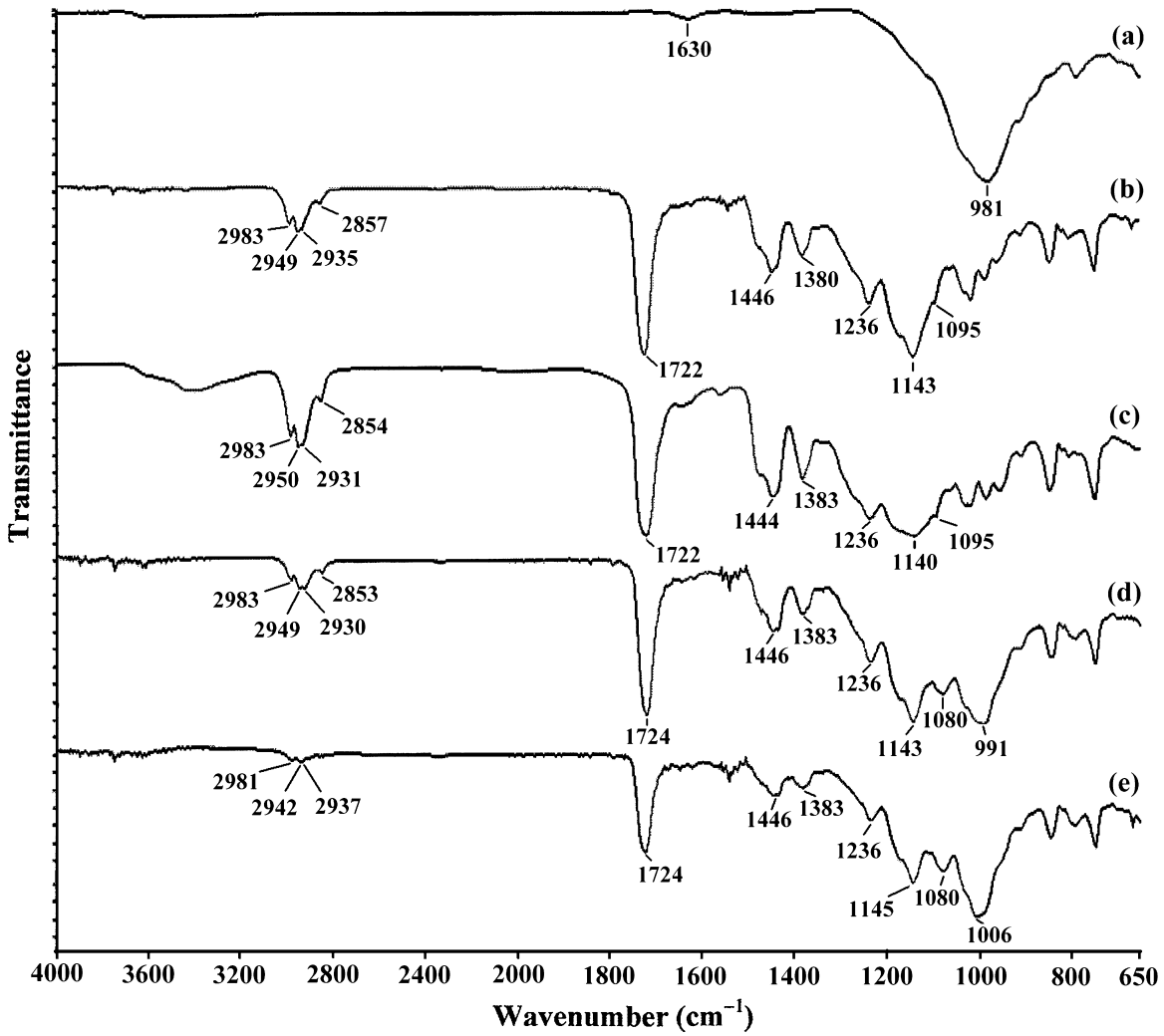


**Fig. 4.** ATR–FTIR spectra of MAS powder (a), 5QPM films (b), 10QPM films (c), 5QPM–MAS (4:0.75) films (d), and 10QPM–MAS (4:0.75) films (e).

### 3.4. Thermal behavior of the films

MAS presented an endothermic peak at 77.7 °C, corresponding to evaporation of water. At higher temperatures no further thermal event was visible in the investigated range (Fig. 6a). Thus, MAS is likely to be stable up to 450 °C. The 5QPM and 10QPM films showed exothermic degradation peaks at 386.5 and 383.4 °C, respectively (Fig. 6b). These exothermic degradation peaks were also visible in 5QPM–MAS and 10QPM–MAS composite films. The peak intensity increased with increasing MAS content. Importantly, the peaks

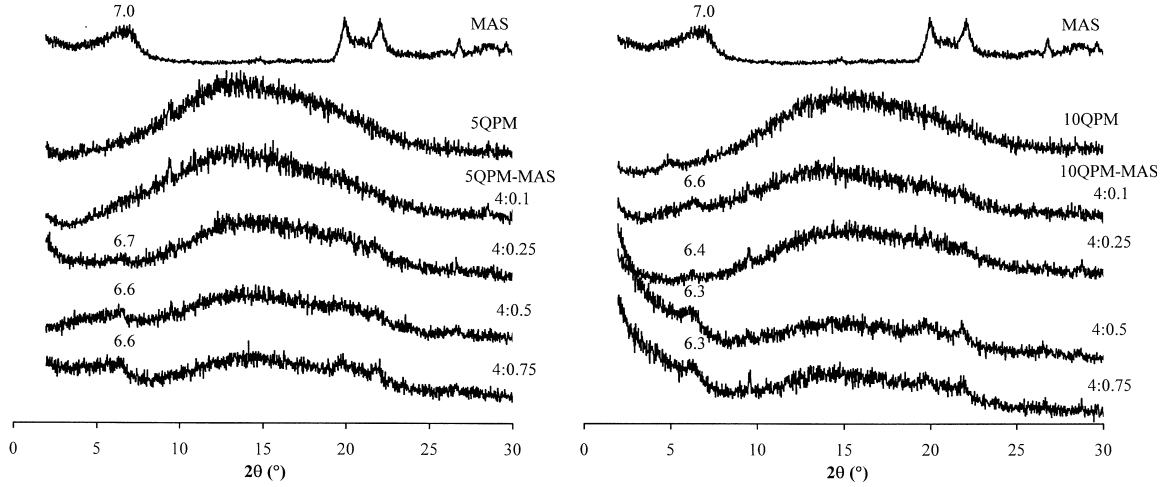


**Fig. 5.** PXRD patterns of MAS powder, QPM films, and QPM–MAS composite films.

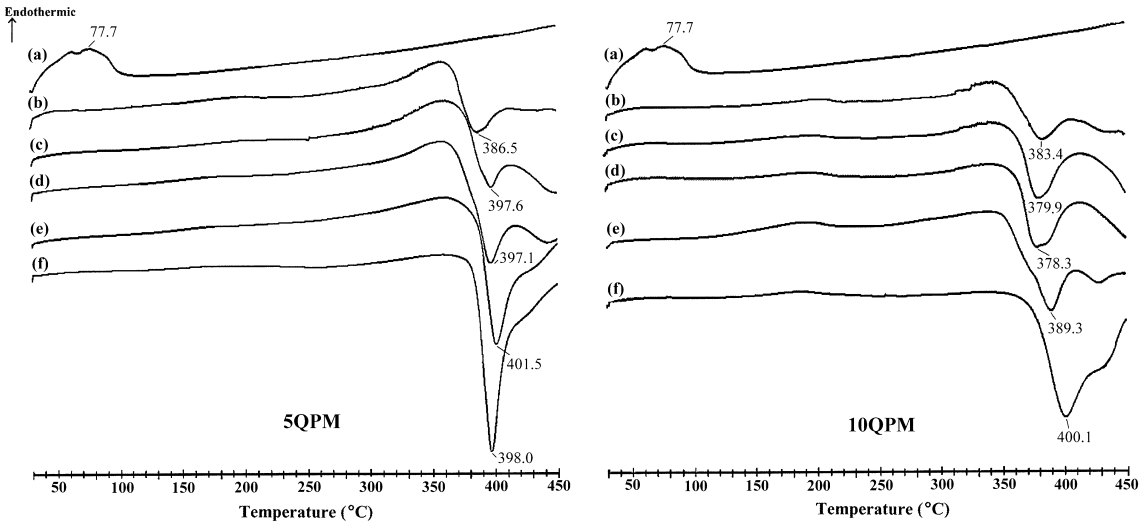


**Fig. 6.** DSC thermograms of MAS powder (a), QPM films (b), and QPM–MAS composite films at the ratios of 4:0.1 (c), 4:0.25 (d), 4:0.5 (e), and 4:0.75 (f).

were shifted to higher temperatures, especially in the case of films with the highest MAS contents. These results are in good agreement with reports on nanocomposite films composed of chitosan and MAS (Khunawattanakul et al., 2010), suggesting that the interaction of QPM with MAS can improve the thermal stability of the systems at elevated temperature, especially the QPM–MAS film at the ratio of 4:0.5 and 4:1.

### 3.5. Mechanical properties of the films

The mechanical properties of film coating for pharmaceutical dosage forms are crucial for the systems' performance. Hard and brittle films are not suitable, leading to a considerable risk of accidental film damage during processing, transport, storage and/or handling and subsequent dose dumping. The mechanical properties of QPM films are known to depend on the type of copolymer, as well as on the type and amounts of eventually added plasticizers (Bodmeier and Paeratakul, 1994). The puncture strength and %elongation of the investigated QPM and QPM–MAS composite films in the dry and wet state are listed in Table 1. In the dry state, the 10QPM films showed higher puncture strength than the 5QPM films, whereas the %elongation at break was smaller. These results were on the contrary with the previous study (Bodmeier and Paeratakul, 1994). This was likely to be due to different of plasticizer used. Incorporation of MAS into the QPM films caused a decrease of puncture strength and %elongation in dry films, irrespective of the contents of quaternary ammonium groups. This can probably be attributed to the fact that the presence of the MAS particles hinders the formation of a continuous, three-dimensional polymeric QPM network (Fig. 3).

In the wet state, the puncture strength of QPM films decreased compared to the dry state, whereas the %elongation at break increased (Table 1). This is in good agreement with reports in the literature and indicates that water acts as a plasticizer for these copolymers (Bodmeier and Paeratakul, 1993; Glaessl et al., 2010a, 2010b). Furthermore, the wet 10QPM films showed lower puncture strength and higher %elongation than the wet 5QPM films (Table 1). Since 10QPM contains more quaternary ammonium groups, more water penetrates into the films, leading to a more pronounced increase in the %elongation at break compared to 5QPM.

Incorporation of MAS into the QPM films led to an increase in the puncture strength in wet state when increasing MAS ratio (Table 1). The QPM–MAS films at the ratios of 4:0.5 and 4:0.75 gave statistically higher puncture strength ($P < 0.05$) than the QPM films in the wet state when using both 0.1 M HCl and pH 6.8 phosphate buffer. On the other hand, %elongation of the wet QPM–MAS films significantly decreased ($P < 0.05$) with increasing MAS ratio. Thus, the interaction of QPM with MAS can strengthen the films in the

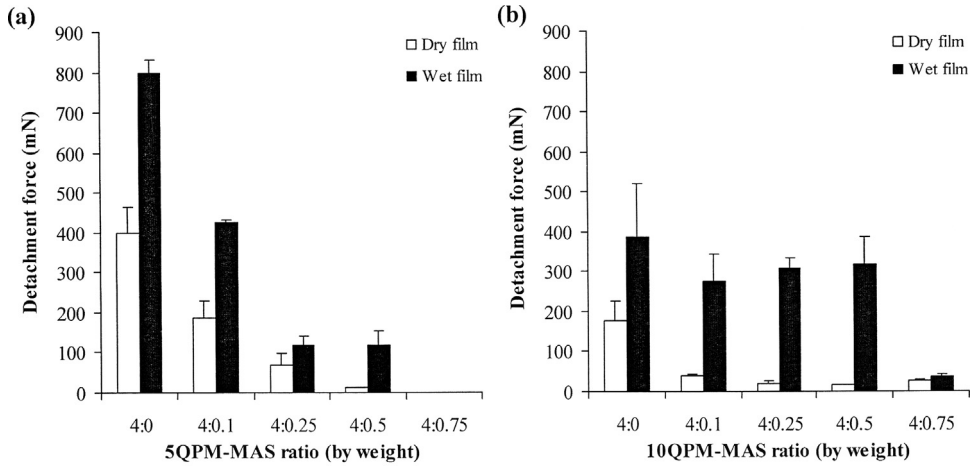


**Fig. 7.** Effects of the addition of MAS on the tackiness of 5QPM films (a), and 10QPM films (b) in the dry and wet state. Data are mean ± S.D., $n = 5$.

wet state. This can be a major advantage when used as controlled release film coatings surrounding for instance capsules, tablets or pellets. These films are exposed to mechanical stress within the gastro intestinal tract.

### 3.6. Tackiness of the films

One of the major challenges to be addressed when using QPM for film coatings is the tackiness of the polymer. In practice, often anti-tacking agents are added to facilitate the manufacturing process. In this study, the tackiness of the films was measured as the detachment force of two films, which were tightly pressed together. As it can be seen in Fig. 7, the detachment force of 5QPM films was significantly higher ($P < 0.05$) than that of 10QPM films, in the dry and wet state. This is in good agreement with reports in the literature, e.g. Wesseling et al. (1999). Also, wet films were stickier than dry films, irrespective of the quaternary ammonium group contents. This can at least partially be attributed to the facts that: (i) water acts as a plasticizer for these copolymers (as discussed above), and (ii) QPM polymer chains can more easily inter-diffuse in the presence of water.

Importantly, the detachment force of the QPM films decreased significantly when adding increasing amounts of MAS to the films (Fig. 7). This was true, irrespective of the amount of quaternary ammonium groups in the copolymer (5QPM and 10QPM). This anti-tacking activity of MAS can probably be attributed to the facts that: (i) the MAS particles occupy parts of the films' surfaces, hindering direct QPM–QPM contact between the films (Nimkulrat et al., 2004), and (ii) the presence of MAS is likely to decrease the water uptake of the films (interacting with the quaternary ammonium groups of the QPMs). Thus, the increase in polymer molecular mobility due to the presence of water is decreased, resulting in less macromolecular inter-diffusion.

## 4. Conclusions

The QPM–MAS composite films can be prepared using the casting/solvent evaporation method. The quaternary ammonium groups of QPM interact with the negatively charged silanol groups of MAS via electrostatic force in the dispersions and films. The QPM–MAS films present a continuous film when MAS is incorporated less than 18.8% in the films. Interaction between QPM and MAS causes a formation of nanocomposites that can enhance thermal stability of the films. The puncture strength and elongation of the dry composite films decrease with increasing MAS ratio in the films. On the other hand, increasing MAS ratio results in an increase of puncture strength of the wet composite films in acidic and neutral media. Incorporation of MAS reduces a tackiness of the QPM films in both dry and wet states. These findings suggest that nanocomposite formation between QPM and MAS in the composite films can enhance strength of the wet films, and also decrease film tackiness. MAS provides an interesting potential as novel anti-tacking agent for QPM film coatings. Future studies will evaluate the suitability of QPM–MAS composite film coatings for controlled drug delivery applications.

## Acknowledgements

The authors wish to thank the Thailand Research Fund (Bangkok, Thailand) for research funding (Grant no. BRG5580016) and the Faculty of Pharmaceutical Sciences, Khon Kaen University, Khon Kaen, Thailand for technical support. Financial support from the Thailand Research Fund through the Royal Golden Jubilee Ph.D. Program (Grant No. PHD/0136/2551) for T.R. and T.P. is gratefully acknowledged.

## References

Alexandre, M., Dubois, P., 2000. Polymer-layered silicate nanocomposites: preparation, properties and uses of a new class of materials. Mater. Sci. Eng. 28, 1–63.

Bodmeier, R., Guo, X., Sarabia, R.E., Skultety, P.F., 1996. The influence of buffer species and strength on diltiazem HCl release from beads coated with the aqueous cationic polymer dispersions, Eudragit RS, RL 30D. Pharm. Res. 13, 52–56.

Bodmeier, R., Paeratakul, O., 1993. Dry and wet strengths of polymeric films prepared from an aqueous colloidal polymer dispersion, Eudragit RS30D. Int. J. Pharm. 96, 129–138.

Bodmeier, R., Paeratakul, O., 1994. Mechanical properties of dry and wet cellulosic and acrylic films prepared from aqueous colloidal polymer dispersions used in the coating of solid dosage forms. Pharm. Res. 11, 882–888.

Bodmeier, R., Paeratakul, O., 1997. Plasticizer uptake by aqueous colloidal polymer dispersions used for the coating of solid dosage forms. Int. J. Pharm. 152, 17–26.

Douroumis, D.D., Gryczke, A., Schminke, S., 2011. Development and evaluation of cetirizine HCl taste-masked oral disintegrating tablets. AAPS Pharm. Sci. Technol. 12, 141–151.

Glaessl, B., Siepmann, F., Tucker, I., Rades, T., Siepmann, J., 2010a. Deeper insight into the drug release mechanisms in Eudragit RL-based delivery systems. Int. J. Pharm. 389, 139–146.

Glaessl, B., Siepmann, F., Tucker, I., Rades, T., Siepmann, J., 2010b. Mathematical modeling of drug release from Eudragit RS-based delivery systems. J. Drug Deliv. Sci. Technol. 20, 127–133.

Heckötter, U.M., Larsson, A., Sriamornsak, P., Kumpugdee-Vollrath, M., 2011. Effect of annealing time and addition of lactose on release of a model substance from Eudragit® RS coated pellets produced by a fluidized bed coater. Chem. Eng. Res. Des. 89, 697–705.

Khunawattanakul, W., Puttipipatkhachorn, S., Rades, T., Pongjanyakul, T., 2008. Chitosan–magnesium aluminum silicate composite dispersions: characterization of rheology, flocculate size and zeta potential. Int. J. Pharm. 351, 227–235.

Khunawattanakul, W., Puttipipatkhachorn, S., Rades, T., Pongjanyakul, T., 2010. Chitosan–magnesium aluminum silicate nanocomposite films: physicochemical characterization and drug permeability. Int. J. Pharm. 393, 219–229.

Khunawattanakul, W., Puttipipatkhachorn, S., Rades, T., Pongjanyakul, T., 2011. Novel chitosan–magnesium aluminum silicate nanocomposite film coatings for modified-release tablets. Int. J. Pharm. 407, 132–141.

Kibbe, H.A., 2000. Handbook of Pharmaceutical Excipients, 3rd ed. American Pharmaceutical Association, Washington, pp. 295–298.

Knop, K., 1996. Influence of buffer solution composition on drug release from pellets coated with neutral and quaternary acrylic polymers and on swelling of free polymer films. Eur. J. Pharm. Sci. 4, 293–300.

Lehmann, K.O.R., 1997. Chemistry and application properties of polymethacrylate coating systems. In: McGinity, J.W. (Ed.), Aqueous Polymeric Coatings for Pharmaceutical Dosage Forms. Marcel Dekker, New York, pp. 101–179.

Maejima, T., McGinity, J.W., 2001. Influence of film additives on stabilizing drug release rates from pellets coated with acrylic polymers. Pharm. Dev. Technol. 6, 211–221.

Nimkulrat, S., Suchiva, K., Phinyocheep, P., Puttipipatkhachorn, S., 2004. Influence of selected surfactants on the tackiness of acrylic polymer films. Int. J. Pharm. 287, 27–37.

Rojtanatanya, S., Pongjanyakul, T., 2010. Propranolol-magnesium aluminum silicate complex dispersions and particles: characterization and factors influencing drug release. Int. J. Pharm. 383, 106–115.

Siepmann, J., Paeratakul, O., Bodmeier, R., 1997. Modeling plasticizer uptake in aqueous polymer dispersions. Int. J. Pharm. 165, 191–200.

Skalsky, B., Petereit, H.U., 2008. Chemistry and application properties of polymethacrylate systems. In: McGinity, J.W., Felton, L.A. (Eds.), Aqueous Polymeric Coatings for Pharmaceutical Dosage Forms. , 3rd ed. Informa, New York, pp. 237–278.

Suksri, H., Pongjanyakul, T., 2008. Interaction of nicotine with magnesium aluminum silicate at different pHs: characterization of flocculate size, zeta potential, and nicotine absorption behavior. Colloids Surf. B 65, 54–60.

Sungthongjeen, S., Sriamornsak, P., Puttipipatkhachorn, S., 2008. Design and evaluation of floating multi-layer coated tablets based on gas formation. Eur. J. Pharm. Biopharm. 69, 255–263.

Wesseling, M., Kuppler, F., Bodmeier, R., 1999. Tackiness of acrylic and cellulosic polymer films used in the coating of solid dosage forms. Eur. J. Pharm. Biopharm. 47, 73–78.

Wu, C., McGinity, J.W., 2003. Influence of an enteric polymer on drug release rate of theophylline from pellets coated with Eudragit® RS 30D. Drug Dev. Ind. Pharm. 8, 103–110.

International Journal of Pharmaceutics 460 (2014) 63–72

Contents lists available at ScienceDirect

International Journal of Pharmaceutics

journal homepage: www.elsevier.com/locate/ijpharm

# Modification of quaternary polymethacrylate films using sodium alginate: Film characterization and drug permeability

Natnicha Khuathan, Thaned Pongjanyakul*

*Faculty of Pharmaceutical Sciences, Khon Kaen University, Khon Kaen 40002, Thailand*

ARTICLE INFO

*Article history:*
Received 1 September 2013
Received in revised form 18 October 2013
Accepted 29 October 2013
Available online 6 November 2013

*Keywords:*
Quaternary polymethacrylate
Sodium alginate
Molecular interaction
Film permeability
Mechanical properties

ABSTRACT

The aims of this study were to investigate the molecular interaction of quaternary polymethacrylate (QPM) in aqueous-dispersion form with sodium alginate (SA) and to characterize the physicochemical properties, mechanical properties, and drug permeability of the QPM–SA films. The results demonstrated that QPM can interact with SA via electrostatic force, leading to the formation of flocculate particles in the dispersions. Transparent QPM–SA films were prepared using a casting/solvent evaporation method. The positively charged quaternary ammonium groups of QPM can interact with the negatively charged carboxyl groups of SA, which was observed using ATR-FTIR spectroscopy. This interaction caused a change of thermal properties, an increase in film strength, and a decrease in film tackiness. The puncture strength of the wet films in acidic media increased as the amount of SA was increased, but the flexibility of the films decreased. The wet films still presented good strength and flexibility in neutral pH when using 2.5–6.3%w/w SA because of their lower water uptake in such media. The incorporation of SA into QPM films was able to reduce drug permeability but increase drug diffusivity in acidic media. In contrast, the drug diffusivity decreased with the addition of a small amount of SA into the films when using a neutral medium. This phenomenon can be attributed to the effect of pH on the water uptake of the film and the ionization of the SA in the microenvironment of the films. These findings suggest that SA can modify the characteristics of QPM films, and QPM–SA films present a strong potential for application as a film coating material for modified-release tablets.



## 1. Introduction

Preparation of thin polymeric films is very important for pharmaceutical manufacturing, particularly film coating for solid dosage forms such as tablets and pellets. The coated films on such dosage forms can mask the unpleasant taste and odor of drugs, and protect drugs from degradation caused by light and moisture (e.g. oxidation and hydrolysis) (Nagai et al., 1997). In addition, film coating can provide sustained drug release, and protect the drugs from acid degradation in the gastrointestinal tract (Wu et al., 1997). Materials that are commonly used for these purposes are synthetic polymers, such as hydroxypropyl methylcellulose (Cao et al., 2004; Sangalli et al., 2004), and polymethacrylates (Moustafine et al., 2012). In addition, natural polymers, such as chitosan (Koizumi et al., 2001; Nunthanid et al., 2002), and sodium alginate (SA) (Pongjanyakul et al., 2005; Lai et al., 2011) have been previously employed as tablet-coating materials for the modified release of drugs.

Quaternary polymethacrylate (QPM), a polymer that is synthesized from acrylic and methacrylic esters, has been widely employed as a film coating material in pharmaceutical dosage form (Lehmann, 1997). QPM is available in aqueous-dispersion form as the commercial products, Eudragit® RS30D and Eudragit® RL30D, which contain 5 and 10% quaternary ammonium groups (5QPM and 10QPM), respectively (Lehmann, 1997). These copolymers contain positively charged quaternary ammonium groups that have chloride ions as counter ions in their structures (Fig. 1a). The 5QPM films provide a lower swelling property and drug permeability than the 10QPM films (Knop, 1996). Mixing the 5QPM and 10QPM dispersions can modify the drug permeability of the resultant films, but the mixed films are still limited by a narrow range of film permeability (Bodmeier and Paeratakul, 1990). Furthermore, QPM films have poor mechanical properties. This can be increased by the incorporation of water-soluble or water-insoluble plasticizers to improve the flexibility of the films (Bodmeier and Paeratakul, 1993). Moreover, anionic hydrophilic polymers, such as pectin (Semdé et al., 2000), which interact with QPM via electrostatic force, can reduce the hydration and swelling of QPM films, resulting in the retardation of drug diffusion across the film.

SA, a negatively charged biopolysaccharide, is extracted from brown seaweed. It is composed of alternating blocks of 1–4 linked

* Corresponding author. Tel.: +66 43 362092; fax: +66 43 202379.
*E-mail address:* thaned@kku.ac.th (T. Pongjanyakul).

0378-5173/$ – see front matter © 2013 Elsevier B.V. All rights reserved.
http://dx.doi.org/10.1016/j.ijpharm.2013.10.050

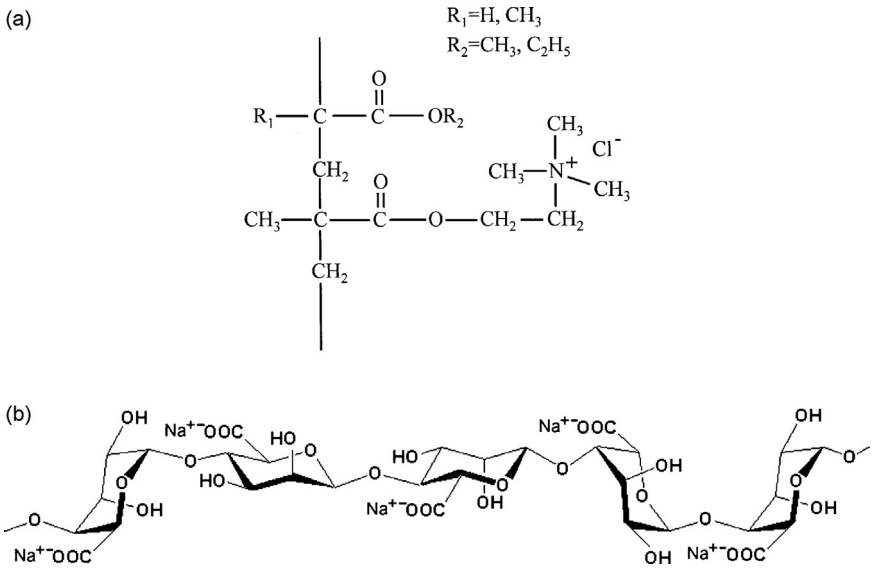


**Fig. 1.** Molecular structures of QPM (a) and SA (b).

α-L-guluronic and β-D-mannuronic acid residues, as shown in Fig. 1b. SA is regarded as an excellent polysaccharide for use in drug-delivery systems because of its unique biocompatibility, biodegradability, and non-toxicity. For these reasons, it has been widely used as an excipient in pharmaceutical dosage forms (Rowe et al., 2006) and can be used to fabricate drug delivery systems such as matrix dosage forms (Liew et al., 2006; Sriamornsak et al., 2007), film-coated dosage forms (Sriamornsak and Kennedy, 2006), beads (Lee et al., 1999), and controlled-release capsules (Pongjanyakul and Puttipipatkhachorn, 2007). In addition, SA can interact with positively charged chitosan to form polyelectrolyte complexes (Takahashi et al., 1990; Lawrie et al., 2007). Recently, a report has been published concerning the interaction between SA and cationic polymers with dimethylamino groups (Moustafine et al., 2005). The complexes obtained were used to prepare a matrix tablet for colon drug delivery (Moustafine et al., 2009). For these reasons, SA is an interesting material and has potential for modifying the characteristics and drug permeability of QPM films.

Therefore, the aim of this work was to study the effect of SA on the characteristics of QPM dispersions and films. The particle size and zeta potential of the QPM–SA dispersions with various SA contents were examined before film casting. The QPM–SA films were prepared using a casting/solvent evaporation method. The characteristics of the films such as thickness, surface and matrix morphology, thermal behavior, molecular interaction between QPM and SA, mechanical properties, tackiness, and drug permeability, were investigated. Propranolol HCl (PPN) was used as a model drug in this study. QPM–SA films could potentially be used in tablet film coatings intended to modify drug release.

## 2. Materials and methods

### 2.1. Materials

QPM in aqueous-dispersion form (Eudragit® RL 30D) was purchased from Röhm Pharma GmbH (Darmstadt, Germany). SA (Manugel® DMB) was obtained from ISP Thailand Ltd. (Bangkok, Thailand). Diethyl sebacate and PPN were purchased from Aldrich Chemistry (Dorset, UK) and Changzhou Yabang Pharmaceutical Co., Ltd. (Jiangsu, China), respectively. All other reagents and solvents were of analytical grade and used as received.

### 2.2. Preparation of QPM–SA dispersions

SA dispersion (2%w/v) was prepared by dispersing SA powder (2 g) in deionized water. The volume of the dispersion was adjusted to 100 ml, and the obtained SA dispersion was stored at room temperature overnight for full hydration. The QPM dispersion (30%w/w polymer solid content) was weighed to obtain a QPM amount of 4 g. After that, 2%w/v SA dispersion in a volume of 0, 5, 12.5, 25.0, or 50.0 ml was measured and mixed with the QPM dispersion to achieve a SA content of 0, 2.5, 6.3, 12.5, or 25.0%w/w based on the QPM content, respectively. The SA dispersion was slowly poured into the QPM dispersion, and the mixture was stirred using a magnetic stirrer. The 100-ml final volume was adjusted using deionized water. The obtained QPM–SA dispersions were stirred at room temperature for 30 min and then incubated in a water bath at 37 °C with shaking at 75 oscillations $min^{-1}$ for 24 h.

### 2.3. Characterization of QPM–SA dispersions

#### 2.3.1. Particle size determination

The particle size of dispersed phase of the QPM and QPM–SA dispersions was determined using a laser-diffraction particle-size analyzer (Mastersizer2000 Model Hydro2000SM, Malvern Instruments Ltd., UK). The samples were mixed in 70 ml of deionized water in a sample dispersion unit and stirred at a rate of 50 Hz for 30 s before the determination. The volume-weighted mean diameter was recorded.

#### 2.3.2. Zeta potential measurement

The zeta potential of the QPM, SA and QPM–SA dispersions was measured using a laser Doppler electrophoresis analyzer (Zetasizer Model ZEN 2600, Malvern Instruments Ltd., UK) at a temperature of 25 °C. The samples were diluted to obtain appropriate concentrations (count rates >20,000 counts $s^{-1}$) prior to the measurement.

#### 2.3.3. Viscosity determination

The viscosity of the QPM and QPM–SA dispersions was measured using a small sample adapter of Brookfield digital rheometer (Model DV-III, Brookfield Engineering Labs Inc., Stoughton, MA) at 37 ± 1 °C. Average and standard deviation of three data of the single point viscosity at a shear rate of 27.2 $s^{-1}$ were reported.

### 2.4. Preparation of QPM–SA films

QPM and QPM–SA composite films were prepared by a casting/solvent evaporation method that was modified from the report of Wesseling et al. (1999). Twenty grams of the QPM dispersions (30%w/w polymer solid content) were weighed and then mixed with diethyl sebacate (0.9 g, 15%w/w of QPM), which was used as a plasticizer. The mixed dispersion was stirred for 30 min. Then, the 2%w/v SA dispersion was mixed with the QPM dispersion to obtain a SA content of 0, 2.5, 6.3, 12.5, or 25.0%w/w based on the QPM content. The QPM–SA dispersions were stirred for 30 min and then adjusted to a final volume of 150 ml using deionized water before being incubated in a water bath at 37 °C with shaking at 75 oscillations $min^{-1}$ for 24 h. Afterward, the QPM–SA dispersions (150 ml) were degassed, poured into Teflon® plates (17 cm × 18 cm) and dried at 50 °C for 48 h. The dry films were peeled off and stored in desiccators prior to use.

### 2.5. Characterization of QPM–SA films

#### 2.5.1. Film thickness determination

The film thicknesses were measured at 15 different locations using a microprocessor coating-thickness gauge (Minitest 600B, ElektroPhysik, Germany). The films were placed on a control plate. The probe was calibrated using a standard film before the measurement. Then, the probe was slowly moved downward to contact the film surface, and the film thickness was recorded.

#### 2.5.2. Scanning electron microscopy (SEM)

The surface and matrix morphology of the QPM and QPM–SA films were observed using SEM. The samples were mounted on dummies, coated with gold in a vacuum evaporator, and then viewed using a scanning electron microscope (Hitachi S-3000N, Tokyo, Japan).

#### 2.5.3. ATR-FTIR spectroscopy

The spectra of the QPM, SA and QPM–SA films were recorded using an ATR-FTIR spectrophotometer (Spectrum One, Perkin Elmer, Norwalk, CT, USA). Each sample was cut and placed on a ZnSe prism as a sample holder and run from 4000 to 650 $cm^{-1}$ at a resolution of 4 $cm^{-1}$.

#### 2.5.4. Differential scanning calorimetry (DSC)

DSC thermograms of the films were recorded using a differential scanning calorimeter (DSC822, Mettler Toledo, Switzerland). Accurately weighted samples (2–3 mg) were placed in a 40-μl aluminium pan without an aluminium cover. The measurement was performed using a heating rate of 10 °C $min^{-1}$ in the temperature range of 30–450 °C.

#### 2.5.5. Water uptake and erosion of films

The water uptake and erosion of the films were determined using a gravimetric method. The films (1 cm × 1 cm) were weighed ($W_0$) and then soaked in 0.1 M HCl or a pH 6.8 phosphate buffer that had been incubated at 37 °C and shaken occasionally. After a predetermined time interval, each film was withdrawn, blotted to remove excess water, immediately weighed ($W_t$), and then dried in a hot air oven at 50 °C for 3 days to reach a constant weight ($W_d$). The water uptake and erosion of the films were calculated from the following equations:

$$\text{Water uptake}(\%) = \left(\frac{W_t - W_d}{W_d}\right) \times 100 \quad (1)$$

$$\text{Erosion}(\%) = \left(\frac{W_0 - W_d}{W_0}\right) \times 100 \quad (2)$$

where $W_0$, $W_t$ and $W_d$ are the original, wet and dry weights of the films, respectively.

#### 2.5.6. Study of mechanical properties

The puncture strength and elongation of the films in the dry and wet states were determined using a texture analyzer (TA-XT2, Stable Micro Systems, Ltd., UK) equipped with a 500-N load cell. In the dry state, the films were cut to dimensions of 2 cm × 2 cm and kept in a humidity-controlled chamber at 55% RH and 25 °C for 3 days prior to the test. In the case of the wet films, the films were soaked in 0.1 M HCl or a pH 6.8 phosphate buffer and shaken occasionally at 37 °C for 1 h. The wet films were blotted to remove excess water before testing. The dry or wet films were placed in the film holder between two mounting plates, following which the holding screws were tightened to prevent slippage of the films. A 6-mm-diameter spherical stainless puncturing probe was fixed to the load cell. Then, the probe was slowly moved through the film with a cross-head speed of 0.1 mm $s^{-1}$. The maximum force at film puncture and the maximum displacement were recorded and then converted to puncture strength and elongation. The parameters were calculated using the following equations:

$$\text{Puncture strength} = \frac{F}{A} \quad (3)$$

where $F$ is the maximum force for film puncture, and $A$ is the cross-sectional area of the edge of the film located in the path of the cylindrical opening of the film holder.

$$\text{Elongation}(\%) = \frac{\sqrt{r^2 + D^2} - r}{r} \times 100 \quad (4)$$

where $r$ is the radius of the film exposed in the cylindrical hole of the film holder, and $D$ is the displacement of the probe from the point of contact to the point of film puncture.

#### 2.5.7. Tackiness study

The method used to determine the tackiness of the films was modified from that reported by Wesseling et al. (1999). The tackiness of the dry and wet films was measured using a texture analyzer (TA-XT2, Stable Micro Systems, Ltd., UK) equipped with a 50 N load cell. The films were cut to 2 cm × 7 cm strips. The films were stored in a humidity-controlled chamber (75% RH, 25 °C) for 3 days prior to the test at dry conditions. For the test at wet conditions, the films were immersed in distilled water for 10 min. Then, the wet films were blotted to remove excess water prior to the test. The films were congruously placed on the top of one another and compressed with 500-g weights for 1 h prior to the test. Tensile grips were used in this study. The end of each film was placed between the upper and lower clamp of a tensile grip. The upper clamp, which was attached to the load cell, was driven upward at a cross-head speed of 15 mm $min^{-1}$, whereas the lower clamp was fixed at the original position during testing. The detachment force required to separate the films was recorded. The average detachment force was obtained from twenty points within the constant-force portion of the force–displacement curve.

#### 2.5.8. Drug permeability studies

Drug-permeability studies were performed using a side-by-side diffusion cell (Crown Glass Co. Inc., Somerville, NJ, USA) at 37 °C. A phosphate buffer at a pH of 6.8 or 0.1 M HCl was used as the receptor phase in this study. The films (2 cm × 2 cm) were hydrated in the medium for 30 min and then clamped between the donor and receptor compartments, which had a 3-ml volume and a diffusion area of 0.66 $cm^2$. PPN solution at a concentration of 4 mg $ml^{-1}$ was placed in the donor compartment, while the receptor compartment contained 3 ml of medium. Both compartments were continuously stirred throughout the tests. At predetermined intervals, 2.6 ml of

medium in the receptor compartment was collected and replaced with an equal volume of fresh medium. The PPN concentration in the collected samples was measured via UV spectroscopy (Shimadzu UV1201, Japan) at a wavelength of 289 nm.

Drug permeation through the films was determined under steady-state conditions using Fick's first law (Flynn et al., 1974; Sinko, 2006), which can be expressed as follows:

$$\frac{dQ}{Adt} = PC_0 \quad (5)$$

where $dQ/Adt$ is the permeation flux (the slope calculated using linear regression analysis of the relation between the amount of drug permeated per surface area of the films ($A$) and time). $C_0$ is the concentration of drug in the donor compartment, and $P$ is the permeability coefficient. The apparent diffusion coefficient ($D$) was estimated from the following equation:

$$t_L = \frac{h^2}{6D} \quad (6)$$

where $t_L$ is the lag time that was obtained from the $x$ intercept of the permeation profiles, and $h$ is the mean thickness of the wet films.

## 3. Results and discussion

### 3.1. Particle size and zeta potential of QPM–SA dispersions

Aqueous QPM dispersion is a white milky liquid of the colloidal particles. The mean particle size of the QPM was 0.19 μm, and the QPM particles exhibited a positive charge with a zeta potential of 59.9 ± 0.72 mV (Fig. 2a) because QPM contains quaternary ammonium groups in its structure. The zeta potential of the SA was −97.3 ± 0.83 mV ($n$ = 3). In the preparation of the QPM–SA dispersion, the SA dispersion was slowly added and mixed into the QPM dispersion; then, sedimentation of the dispersed phase of the QPM–SA dispersion was visually observed. The possible formation of QPM–SA flocculates was expected. It is likely to be caused by electrostatic interactions between the positively charged quaternary ammonium groups ($-N(CH_3)_3^+$) of QPM and the negatively charged carboxyl moiety of SA.

The particle size and zeta potential of the dispersed phase of the QPM–SA dispersions are shown in Fig. 2a. The dispersed phase of the QPM–SA dispersions exhibited remarkably larger particle sizes than the QPM particles. This finding indicates that QPM–SA flocculates were formed after adding SA into the QPM dispersion. Furthermore, the particle size and zeta potential of the QPM–SA flocculates decreased as the amount of SA in the dispersions increased. The flocculates, which were positively charged for lower SA concentrations, were negatively charged instead for SA concentrations of 12.5 and 25.0%w/w. Furthermore, the QPM dispersion gave a very low viscosity, and the viscosity of the QPM–SA dispersions obviously increased with adding 12.5 and 25.0%w/w SA (Fig. 2b).

Because of the opposite charges of QPM and SA, the positively charged quaternary ammonium groups of QPM could electrostatically interact with the negatively charged carboxyl groups of SA. This interaction caused a decrease in the zeta potential of the QPM, leading to the flocculation of the QPM. In addition, QPM particles were able to form flocculates because of a bridging mechanism via a long side-chain molecule of SA. These phenomena caused the larger particle size of the QPM–SA flocculates in comparison to the QPM particle size. Increasing the SA amount changed the surface charge of the QPM–SA flocculates from positive to negative. This indicates that an excess of SA molecules could completely deposit onto or cover the flocculate surface. Furthermore, the excess of SA also caused an increase in viscosity of the QPM–SA dispersion. Such a change in the QPM–SA flocculates may affect the film characteristics and drug permeability.

### 3.2. Appearance, thickness and morphology of the films

QPM films without plasticizer are hard and brittle. Diethyl sebacate (15%w/w of QPM) was used as a plasticizer in the QPM films to improve the flexibility and promote the particle coalescence that is the mechanism of film formation for aqueous colloidal dispersion polymers (Lehmann, 1997). Transparent QPM films were obtained in this study. The thickness of the films was in the range of 151.8–237.9 μm, as shown in Table 1. The incorporation of SA into the QPM films also resulted in transparent and continuous films for all investigated SA contents, although QPM particle flocculation was occurred when SA was added. Wong and Bodmeier (1996) have suggested that the flocculation of QPM particles may have important implications for film formation. This study demonstrated that the presence of SA did not affect the film formation of the QPM particles. The successful QPM–SA film formation may be attributed to the film-forming property of SA, which can form continuous films, coupled with the coalescence of the QPM particles.

Fig. 3a shows the surface and matrix morphologies of the QPM films and the QPM–SA films with 12.5%w/w SA. The surface morphology of the QPM films was smoother than that of the QPM films with 12.5%w/w SA. Moreover, the matrix structure of the QPM films

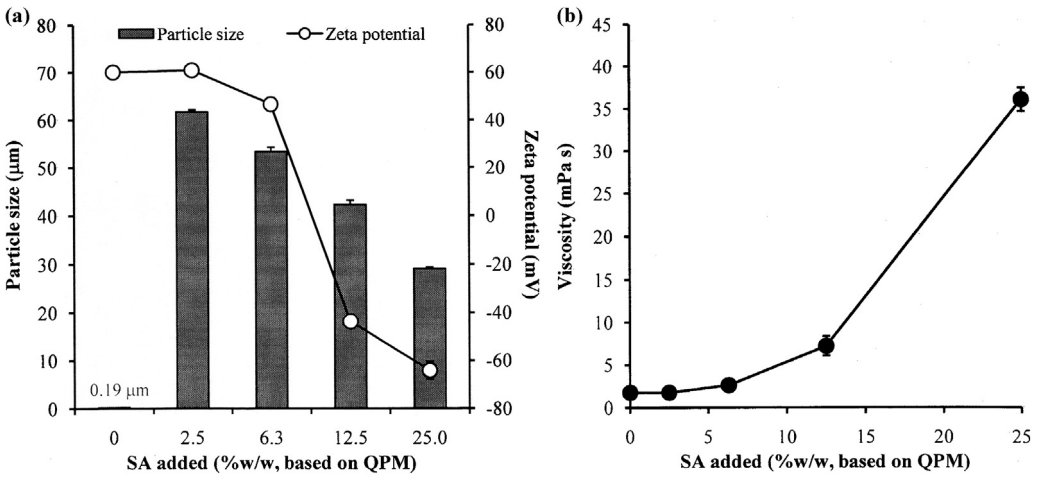


**Fig. 2.** Particle size and zeta potential of QPM–SA flocculates (a) and viscosity (b) of the QPM dispersions containing various SA concentrations. The data are presented as the mean ± S.D., $n$ = 3.

**Table 1**
Thickness and mechanical properties of QPM and QPM–SA films.

| SA added (%) | Thickness[a] (μm) | Dry film | | Wet film using 0.1 M HCl | | Wet film using pH 6.8 PB | |
|---|---|---|---|---|---|---|---|
| | | Puncture strength[b] (MPa) | Elongation[b] (%) | Puncture strength[b] (MPa) | Elongation[b] (%) | Puncture strength[b] (MPa) | Elongation[b] (%) |
| 0 | 215.6 ± 29.83 | 7.97 ± 1.47 | 115.2 ± 7.85 | 0.95 ± 0.20 | 312.4 ± 26.69 | 1.28 ± 0.19 | 228.8 ± 17.17 |
| 2.5 | 151.8 ± 28.31 | 8.07 ± 1.53 | 78.02 ± 12.12 | 1.02 ± 0.11 | 87.31 ± 4.88 | 1.05 ± 0.06 | 213.9 ± 7.38 |
| 6.3 | 187.8 ± 11.40 | 10.06 ± 1.65 | 69.60 ± 39.72 | 1.34 ± 0.17 | 56.56 ± 3.95 | 1.55 ± 0.10 | 200.1 ± 3.87 |
| 12.5 | 219.7 ± 29.70 | 12.83 ± 2.57 | 46.73 ± 5.25 | 1.83 ± 0.32 | 44.06 ± 2.23 | 0.65 ± 0.10 | 56.81 ± 5.92 |
| 25.0 | 237.9 ± 25.65 | 12.43 ± 1.69 | 37.29 ± 8.66 | 1.54 ± 0.23 | 41.04 ± 17.48 | ND | ND |

ND indicates that the value could not be determined.
[a] Data are mean ± S.D., $n = 15$.
[b] Data are mean ± S.D., $n = 5$.

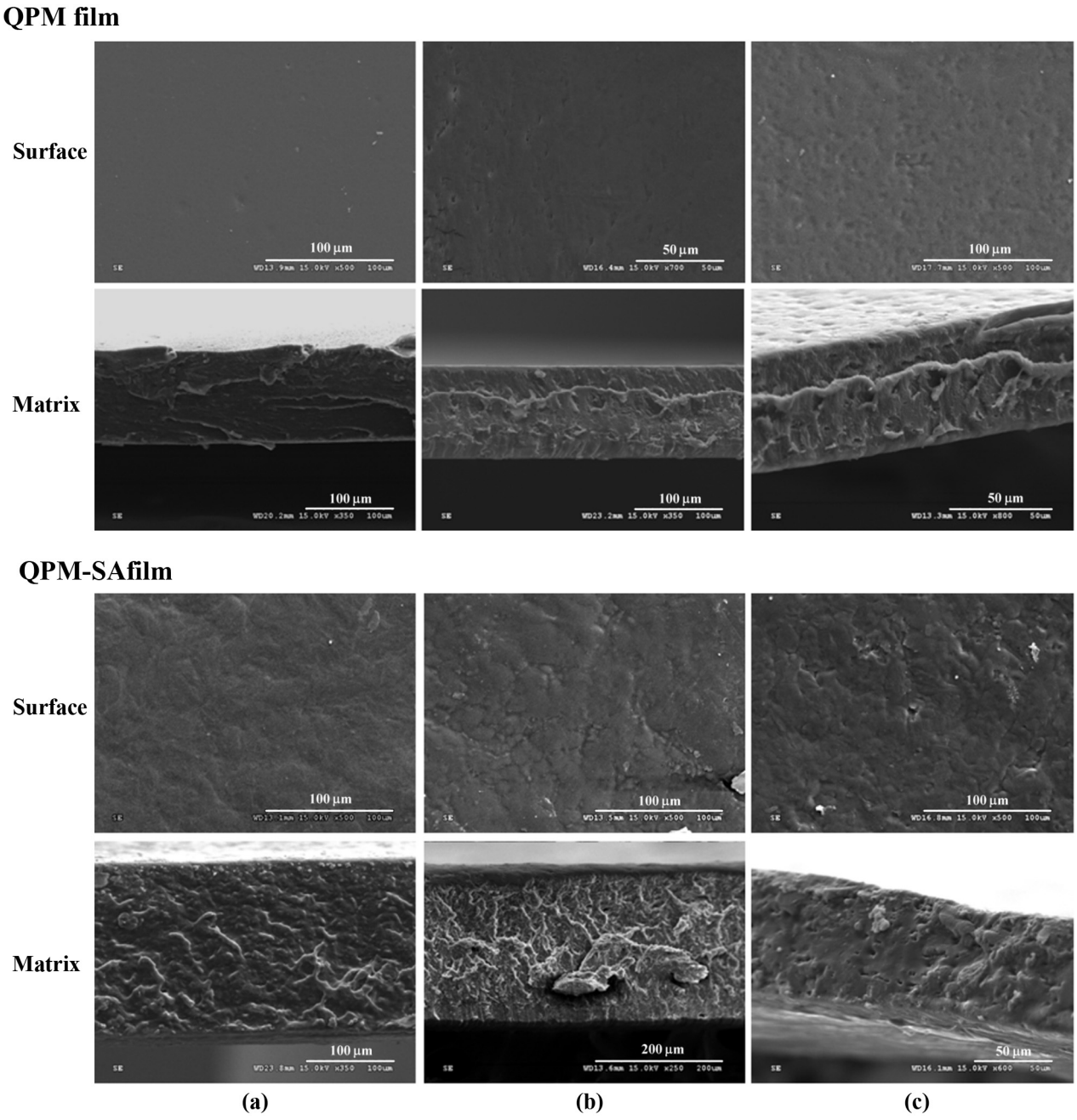


**Fig. 3.** Surface and matrix morphologies of QPM film and QPM–SA film with 12.5%w/w SA (a) and of the QPM–SA film treated with 0.1 M HCl (b) and pH 6.8 phosphate buffer (c) for 1 h.

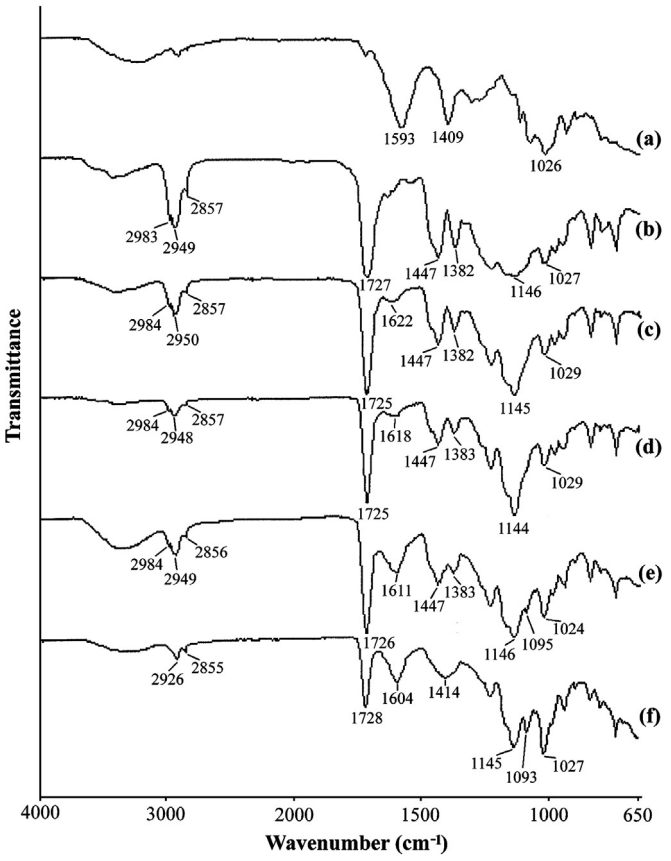


**Fig. 4.** ATR-FTIR spectra of the SA film (a), QPM film (b), and QPM–SA films containing SA in concentrations of 2.5 (c), 6.3 (d), 12.5 (e), and 25.0 (f) %w/w.

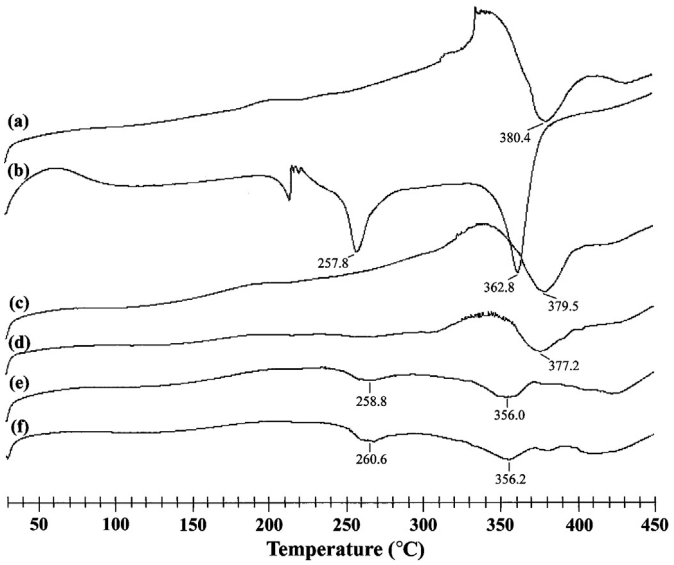


**Fig. 5.** DSC thermograms of the QPM film (a), SA film (b), and QPM–SA films containing SA in concentrations of 2.5 (c), 6.3 (d), 12.5 (e), and 25.0 (f) %w/w.

was obviously changed with the incorporation of SA. The surface morphologies of the films that were treated with 0.1 M HCl (Fig. 3b) and the pH 6.8 phosphate buffer (Fig. 3c) for 1 h showed evidence of the erosion of the film surface; in particular, small pores appeared in the surface of the QPM–SA films that were treated with the pH 6.8 phosphate buffer. In addition, the matrix morphology of the films was also altered, and pore formation occurred in the QPM–SA film matrix in the pH 6.8 phosphate buffer (Fig. 3c). This result suggests that some ingredients leached out of the QPM films when they were exposed to both media and that the presence of SA had a significant effect on the erosion and pore formation of the QPM–SA films.

### 3.3. Molecular interaction between QPM and SA

The molecular interaction between QPM and SA in the films was investigated using ATR-FTIR spectroscopy. The ATR-FTIR spectra of the SA film, QPM films, and QPM–SA films are presented in Fig. 4. The SA film exhibited three outstanding peaks corresponding to a $COO^-$ (asymmetric) stretching at 1593 $cm^{-1}$, a $COO^-$ (symmetric) stretching peak at 1409 $cm^{-1}$, and a C—O—C stretching peak at 1026 $cm^{-1}$(Fig. 4a) (Sartori et al., 1997). The spectrum of the QPM film exhibited a C—H stretching, a C=O stretching, a $CH_2$ symmetric bending, a $CH_3$ asymmetric bending, a C—CO—C stretching and a C—O—C stretching at approximately 2857–2983, 1727, 1447, 1382, 1146, and 1027 $cm^{-1}$, respectively (Fig. 4b). The QPM films with SA showed a shift in the $COO^-$ (asymmetric) stretching peak of SA from 1593 to a higher wavenumber, in the range of 1604–1622 $cm^{-1}$ (Fig. 4c–f). Moreover, the QPM–SA films with 25%w/w SA also exhibited the $COO^-$ (symmetric) stretching peak of SA at 1414 $cm^{-1}$ (Fig. 4f), which was shifted from 1409 $cm^{-1}$ (Fig. 4a). These shifts strongly indicate an ionic interaction of the carboxyl groups of SA with positively charged molecules (Sartori et al., 1997; Lawrie et al., 2007). When SA contents of 12.5 and 25%w/w were added to the films, the C—H stretching peaks of QPM were changed, and a new peak corresponding to C—N stretching at 1093–1095 $cm^{-1}$ was clearly observed (Fig. 4e and f).This result suggests that the quaternary ammonium groups of QPM electrostatically interacted with the carboxyl groups of SA. This interaction may cause a change in the film properties and drug permeability.

### 3.4. Thermal behavior of the films

The QPM films exhibited an endothermic peak at approximately 340 °C, followed by an exothermic degradation peak at 380.4 °C (Fig. 5a). The SA exhibited an exothermic peak at 215 °C, followed by an endothermic peak at approximately 220 °C (Fig. 5b), indicating that a recrystallization and a phase transition of the SA after heat induction may have occurred (Pongjanyakul et al., 2005). Then, the first and second exothermic degradation peaks of SA were observed at 257.8 and 362.8 °C, respectively. The thermal behavior of the QPM films with 2.5 and 6.3%w/w SA showed a small shift of the QPM degradation peak toward lower temperatures (Fig. 5c and d), suggesting that the SA disturbed the film-structure formation of the QPM. In addition, the QPM–SA films with higher amounts of SA (12.5 and 25%w/w) showed both degradation peaks of SA without the degradation peak of the QPM films (Fig. 5e and d). It was possible to conclude that the degradation of SA could induce QPM degradation at a lower temperature. The appearance of the degradation peaks of SA suggests that a phase separation of SA in the microenvironment of the film might have occurred. It also suggests that the QPM–SA flocculates that formed for SA concentrations of 12.5 and 25%w/w were covered with SA molecules, as discussed in the zeta potential studies, and the SA molecules around the QPM–SA flocculates could undergo intermolecular interactions with adjacent flocculate particles. This phenomenon could change the matrix structure and modify the characteristics of the QPM films.

### 3.5. Water uptake and erosion of the films

The water uptake and erosion of the QPM–SA films in 0.1 M HCl and pH 6.8 phosphate buffer after 30 and 60 min of the test are shown in Fig. 6. The water uptake of the QPM–SA films tended to decrease with increasing SA content in the acidic medium (Fig. 6a),

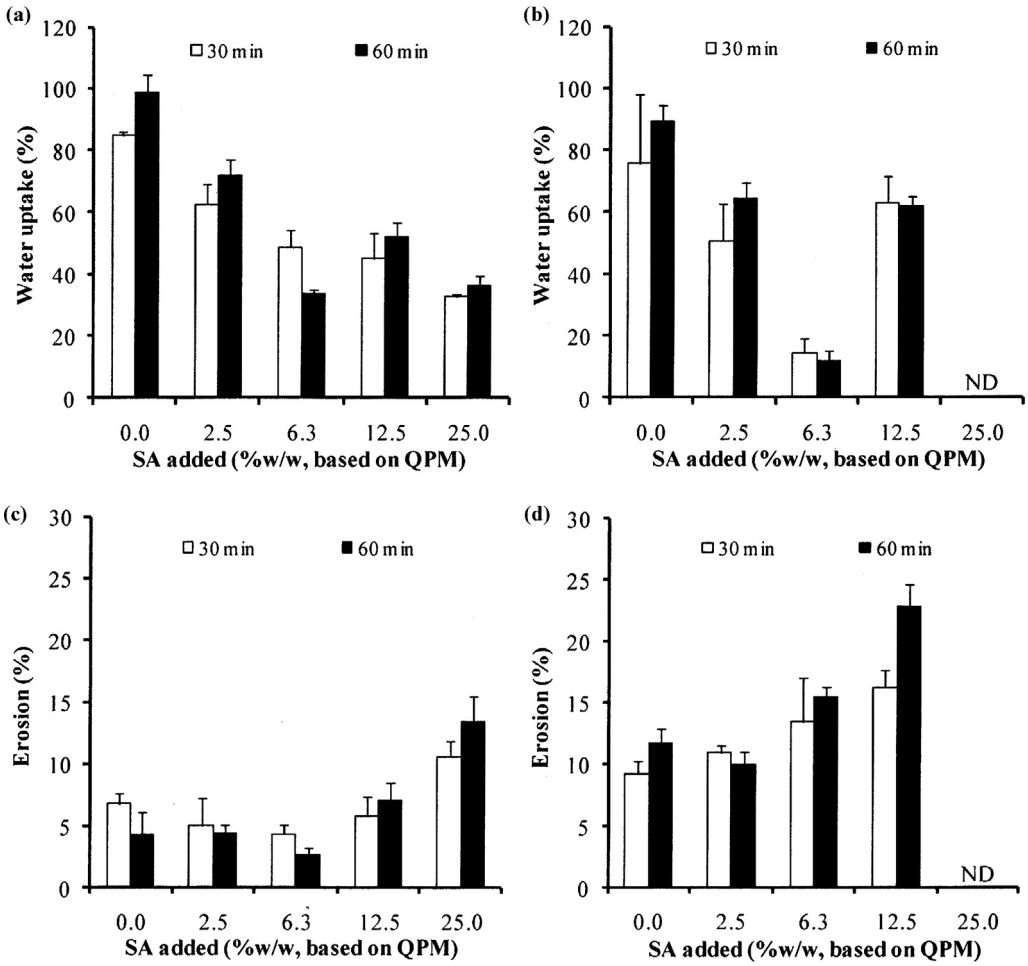


**Fig. 6.** Water uptake (a, b) and erosion (c, d) of the QPM–SA films in 0.1 M HCl (a, c) and pH 6.8 phosphate buffer (b, d). The data are presented as the mean ± S.D., $n = 5$. ND indicates that the value could not be determined.

whereas the erosion seemed to decrease with the addition of 6.3%w/w SA, and an increase in film erosion was found for 12.5 and 25%w/w SA (Fig. 6c). The decrease in the water uptake of the QPM–SA films was caused by the conversion of SA to a water-insoluble alginic acid in acidic conditions (Østberg et al., 1994), leading to a reduction of the film erosion. However, the films with 12.5 and 25%w/w SA showed higher erosion because the SA could leach out of the films before converting to alginic acid.

In neutral pH conditions, the QPM–SA films demonstrated a clear decrease in water uptake for SA contents in the range of 2.5–6.3%w/w, and the lowest water uptake was observed for 6.3%w/w SA (Fig. 6b). The incorporation of 12.5%w/w SA into the films caused an increase in the water uptake, and the water uptake of the films with 25%w/w SA could not be determined because of a very high swelling of the films that could not be accommodated. In contrast, the erosion of the QPM–SA films gradually increased with increasing SA content (Fig. 6d). From these results, it could be understood that the SA in the films could rapidly swell and dissolve in the neutral medium (Pongjanyakul and Puttipipatkhachorn, 2007), leading to an increase in the matrix erosion of the films. However, the decrease in the water uptake of the films with 2.5 and 6.3%w/w SA indicates a strong interaction between QPM and SA in the wet state because of a disentanglement of the SA molecules, especially in the case of 6.3%w/w SA. This interaction resulted in the lower water uptake of the films. Furthermore, the QPM–SA films with 12.5%w/w SA demonstrated the influence of an excess of SA in the films, which caused higher water uptake and matrix erosion.

### 3.6. Mechanical properties of the films

The puncture strength and elongation of the QPM and QPM–SA films in the dry and wet states were investigated and are listed in Table 1. In the dry state, the addition of SA to the QPM films caused an increase in the puncture strength, but a decrease in the %elongation was observed. This result suggests that the interaction between QPM and SA could enhance the film strength. Because of the film-forming property of SA, SA in a region of phase separation coupled with the coalescence process of QPM particles could form a continuous matrix. This interaction resulted in the stronger film formation of the QPM–SA films for higher SA contents. However, the stronger matrix of the films was usually accompanied by lower flexibility of the films (Remuñán-López and Bodmeier, 1997), as can be seen from this study.

The wet QPM films in 0.1 M HCl and the pH 6.8 phosphate buffer exhibited lower puncture strength and higher %elongation than the dry QPM films (Table 1). This result suggests that water molecules could be absorbed and inserted into the polymeric matrix, which caused a reduction in the film strength. Moreover, water molecules could also act as a plasticizer, leading to higher flexibility of the films (Bodmeier and Paeratakul, 1993). In the case of the QPM–SA films at acidic pH, the puncture strength of the QPM–SA films increased with increasing SA content, whereas the %elongation of the films decreased. SA can be converted to an unionized form, a water-insoluble alginic acid, under acidic conditions. The alginic acid that was embedded in the film matrix

enhanced the film strength but decreased the flexibility of the films.

On the other hand, in the pH 6.8 phosphate buffer, the puncture strength and %elongation of the QPM–SA films with 2.5 and 6.3%w/w SA were not decreased in comparison to the QPM films (Table 1). The addition of a larger amount of SA (12.5%w/w) resulted in a remarkable reduction in both these parameters of the QPM–SA films. Furthermore, the films with 25%w/w SA could not be properly handled, so their puncture strength and %elongation could not be determined. As expected, SA could ionize and swell in the pH 6.8 phosphate buffer, resulting in considerable swelling of the films when used in higher amounts (12.5 and 25%w/w). This behavior could explain the clear decrease that was observed in both parameters and the inability to measure the films with the highest SA content used in this study. However, for lower SA contents, the swelling of the negatively charged SA still promoted the interaction between the QPM and the SA via electrostatic force. In addition, the disentanglement of the SA could enhance the flexibility of the films at neutral pH. This finding indicates that the interaction of QPM with SA can strengthen the films in both the dry and wet states. This could be a major advantage for the use of such films as coating material for solid dosage forms intended to modify drug release in the gastrointestinal tract.

### 3.7. Tackiness of the films

QPM films normally present a tackiness that is the primary disadvantage of these films during the tablet-coating process and the storage of coated tablets. Therefore, an anti-tacking agent was used to prevent the agglomeration of the coating on the substrate. In this study, the tackiness of the QPM films was measured by determining the detachment force, as shown in Fig. 7. In the dry state, the incorporation of SA contents of 6.3, 12.5, and 25%w/w clearly reduced the detachment force of the QPM films, but the decrement of the detachment force appeared to be unrelated to the amount of SA that was added. Moreover, in the wet state, the QPM–SA films with 6.3 and 12.5%w/w SA exhibited lower detachment forces than the QPM films. The QPM–SA films with 25%w/w SA could not be measured because of the very high swelling of the films. These results suggest that the incorporation of SA could reduce the tackiness of QPM films by decreasing the contact area of the QPM on the film surface (Nimkulrat et al., 2004). Moreover, the interaction of QPM and SA hindered the interdiffusion of the QPM chains, and the QPM exhibited a lower attractive force.

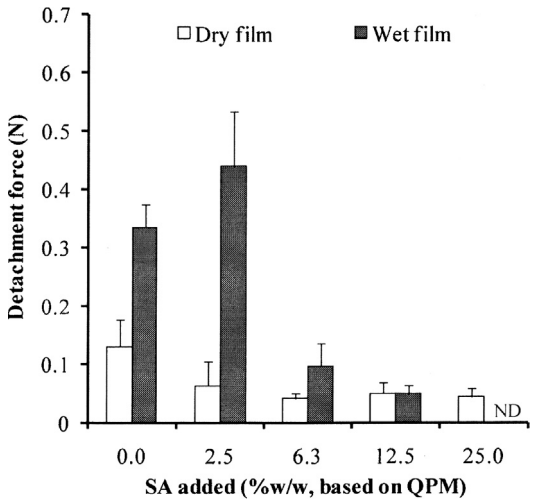


**Fig. 7.** Detachment force of the QPM and QPM–SA films in the dry and wet states. The data are presented as the mean ± S.D., $n = 5$. ND indicates that the value could not be determined.

### 3.8. Drug permeability of the films

The cumulative PPN permeation profiles across the films using 0.1 M HCl and a pH 6.8 phosphate buffer, as shown in Fig. 8, exhibited a good linearity ($R^2 > 0.98$) with a lag time. These permeation profiles indicate that the PPN permeation reached a steady state and could be described using the Fick's first law (Eqs. (5) and (6)). The PPN permeation parameters for 0.1 M HCl are listed in Table 2. A similar lag time was found for SA contents in the range of 6.3–12.5%w/w, but a longer lag time was found in the films with 25%w/w SA. The permeation flux and $P$ values of PPN decreased with increasing SA content in the films. To compare the drug diffusion through the films independent of the effect of the wet film thickness, which increased with increasing SA content (data not shown), the $D$ values were estimated using Eq. (6). The QPM–SA films exhibited higher $D$ values than the QPM films, but increasing the SA content did not significantly affect the $D$ values of the QPM–SA films. This finding suggests that the incorporation of SA into the QPM films led to higher drug diffusion, despite the observed decrease in water uptake of the QPM–SA films (Fig. 6a). This result indicates that the QPM–SA films contained large water-filled channels with low tortuosity because of the conversion of SA to alginic

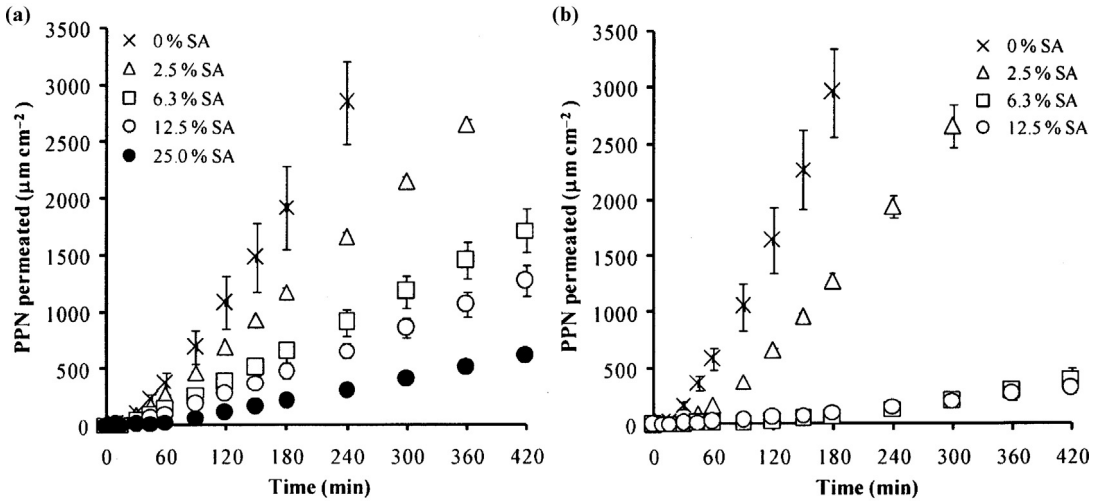


**Fig. 8.** The permeation profiles of PPN across the QPM and QPM–SA films in 0.1 M HCl (a) and pH 6.8 phosphate buffer (b). Each point corresponds to mean ± S.D., $n = 3$.

**Table 2**
Permeation parameters of PPN across QPM and QPM–SA films.

| SA added (%) | 0.1 M HCl | | | | pH 6.8 phosphate buffer | | | |
|---|---|---|---|---|---|---|---|---|
| | Flux ($\mu g\,cm^{-2}\,min^{-1}$) | Lag time (min) | $P \times 10^5$ ($cm\,s^{-1}$) | $D \times 10^8$ ($cm^2\,s^{-1}$) | Flux ($\mu g\,cm^{-2}\,min^{-1}$) | Lag time (min) | $P \times 10^5$ ($cm\,s^{-1}$) | $D \times 10^8$ ($cm^2\,s^{-1}$) |
| 0 | 13.07 ± 1.60 | 31.72 ± 8.44 | 5.43 ± 0.66 | 1.90 ± 0.59 | 18.52 ± 2.53 | 26.87 ± 1.78 | 7.49 ± 1.02 | 2.71 ± 0.18 |
| 2.5 | 7.86 ± 0.14 | 25.29 ± 1.34 | 3.27 ± 0.06 | 5.89 ± 0.30 | 10.89 ± 0.93 | 55.84 ± 3.44 | 4.40 ± 0.38 | 1.58 ± 0.95 |
| 6.3 | 4.39 ± 0.46 | 29.86 ± 3.66 | 1.82 ± 0.19 | 6.03 ± 0.70 | 1.22 ± 0.38 | 114.7 ± 6.65 | 0.49 ± 0.15 | 0.75 ± 0.04 |
| 12.5 | 3.23 ± 0.34 | 29.42 ± 0.43 | 1.32 ± 0.14 | 7.70 ± 0.11 | 0.91 ± 0.06 | 65.11 ± 16.45 | 0.37 ± 0.02 | 2.29 ± 0.66 |
| 25.0 | 1.61 ± 0.09 | 43.58 ± 3.77 | 0.67 ± 0.04 | 5.72 ± 0.48 | ND | ND | ND | ND |

Data are mean ± S.D., $n = 3$.
ND indicates that the value could not be determined.

acid in the acidic medium. The alginic acid that formed had weak intermolecular bonding (Aslani and Kennedy, 1996), which led to large aqueous pores in the films, resulting in the higher $D$ values of the QPM–SA films in comparison to those of the QPM films.

In the pH 6.8 phosphate buffer, the PPN flux and $P$ values of the QPM–SA films also decreased with increasing SA content, and the films with 25%w/w SA could not be tested. The longest lag time was observed in the QPM–SA film with 6.3%w/w SA. The $D$ values of the films decreased with increasing SA contents in the range of 2.5–6.3%w/w, and then an increase in the $D$ value was observed for 12.5%w/w SA. This is consistent with the fact that the QPM–SA films had lower water uptake than the QPM films (Fig. 6b). Moreover, the SA in the films could ionize and disentangle in this medium, which promoted electrostatic interaction with positively charged QPM. This phenomenon enhanced the strong matrix structure (shown in the mechanical properties of the films in Table 1) with small water-filled channels of high tortuosity, especially in the case of the QPM–SA films with 6.3%w/w SA, which exhibited the lowest water uptake. Moreover, the positive charge of drug, PPN in this case, may have interacted with the ionized SA (Pongjanyakul and Suksri, 2009), thereby causing longer lag times and slower drug diffusion across the films. For higher SA content (12.5%w/w), the excess SA in the films led to higher swelling and matrix erosion, resulting in larger water-filled channels and the formation of small pores on the film surface and matrix, which are shown in Fig. 3c. Therefore, a higher $D$ value was obtained. Furthermore, the $D$ values of the films in the neutral medium were lower than those in the acidic medium. This result suggests that the ionization of SA in the neutral medium had a crucial effect on the drug permeability of the QPM–SA films.

## 4. Conclusions

QPM can electrostatically interact with SA to form flocculate particles in dispersions. QPM–SA films can be successfully prepared using the casting/solvent evaporation method. The QPM–SA films are transparent and continuous films are obtained, even for an SA content of 25%w/w SA. The positively charged quaternary ammonium groups of QPM can interact with the negatively charged carboxyl groups of SA, leading to a change in the thermal properties of the films. Moreover, this interaction results in an increase in the film strength in the dry state and a decrease in the film tackiness in the dry and wet states. The puncture strength of the films in acidic media increases with increasing SA content, but the flexibility of the films decreases. The wet films still exhibit good strength and flexibility in neutral pH for 2.5–6.3%w/w SA because of their lower water uptake in such media, but a higher amount of SA leads to lower puncture strength and elongation. The incorporation of SA into QPM films can reduce drug permeability of the films in acidic medium. However, the drug diffusivity in this medium increases because of the creation of large water-filled channels with low tortuosity in the films when the SA converts into alginic acid. On the other hand, the drug diffusivity in neutral media decreases with the addition of a small amount of SA because the SA can ionize and disentangle, creating small water-filled channels with high tortuosity. These findings suggest that QPM–SA films can potentially be developed for use as tablet-coating film material intended to modify drug release.

## Acknowledgments

The authors would like to acknowledge the Thailand Research Fund (Bangkok, Thailand) for research funding (Grant no. BRG5580016) and the Faculty of Pharmaceutical Sciences, Khon Kaen University (Khon Kaen, Thailand) for technical support. We wish to thank the Graduate School, Khon Kaen University (Khon Kaen, Thailand) for a scholarship for Natnicha Khuathan.

## References

Aslani, P., Kennedy, R.A., 1996. Studies on diffusion in alginate gels. I. Effect of crosslinking with calcium or zinc ions on diffusion of acetaminophen. J. Control. Release 42, 75–82.
Bodmeier, R., Paeratakul, O., 1990. Propranolol HCl release from acrylic films prepared from aqueous latexes. Int. J. Pharm. 59, 197–204.
Bodmeier, R., Paeratakul, O., 1993. Dry and wet strengths of polymeric films prepared from an aqueous colloidal polymer dispersion, Eudragit RS30D. Int. J. Pharm. 96, 129–138.
Cao, Q.R., Choi, H.G., Kim, D.C., Lee, B.J., 2004. Release behavior and photo-image of nifedipine tablet coated with high viscosity grade hydroxypropylmethylcellulose: effect of coating conditions. Int. J. Pharm. 274, 107–117.
Flynn, G.L., Yalkowsky, S.H., Roseman, T.J., 1974. Mass transport phenomena and models: theoretical concepts. J. Pharm. Sci. 63, 479–510.
Knop, K., 1996. Influence of buffer solution composition on drug release from pellets coated with neutral and quaternary acrylic polymers and on swelling of free polymer films. Eur. J. Pharm. Sci. 4, 293–300.
Koizumi, T., Ritthidej, G.C., Phaechamud, T., 2001. Mechanistic modeling of drug release from chitosan coated tablets. J. Control. Release 70, 277–284.
Lai, H., Zhu, F., Yuan, W., He, N., Zhang, Z., Zhang, X., He, Q., 2011. Development of multiple-unit colon-targeted drug delivery system by using alginate: in vitro and in vivo evaluation. Drug Dev. Ind. Pharm. 37, 1347–1356.
Lawrie, G., Keen, I., Drew, B., Chandler-Temple, A., Rintoul, L., Fredericks, P., Grøndahl, L., 2007. Interactions between alginate and chitosan biopolymers characterized using FTIR and XPS. Biomacromolecules 8, 2533–2541.
Lee, B.J., Min, G.H., Cui, J.H., 1999. Correlation of drug solubility with trapping efficiency and release characteristics of alginate beads. Pharm. Pharmacol. Commun. 5, 85–89.
Lehmann, K.O.R., 1997. Chemistry and application properties of polymethacrylate coating systems. In: McGinity, J.W. (Ed.), Aqueous Polymeric Coatings for Pharmaceutical Dosage Forms. Marcel Dekker, New York, pp. 101–179.
Liew, C.V., Chan, L.W., Ching, A.L., Heng, P.W.S., 2006. Evaluation of sodium alginate as drug release modifier in matrix tablets. Int. J. Pharm. 309, 25–37.
Moustafine, R.I., Salachova, A.R., Frolova, E.S., Kemenova, V.A., Mooter, G.V., 2009. Interpolyelectrolyte complexes of Eudragit E PO with sodium alginate as potential carriers for colonic drug delivery: monitoring of structural transformation and composition changes during swellability and release evaluating. Drug Dev. Ind. Pharm. 35, 1439–1451.
Moustafine, R.I., Bodrov, A.V., Kemenova, V.A., Rombaut, P., Van Den Mooter, G., 2012. Drug release modification by interpolymer interaction between countercharged types of Eudragit® RL 30D and FS 30D in double-layer films. Int. J. Pharm. 439, 17–21.
Moustafine, R.I., Kemenova, V.A., Van den Mooter, G., 2005. Characteristics of interpolyelectrolyte complexes of Eudragit E100 with sodium alginate. Int. J. Pharm. 294, 113–120.

Nagai, T., Obara, S., Kokubo, H., Hoshi, N., 1997. Application of HPMC and HPMCAS to aqueous film coating of pharmaceutical dosage forms. In: McGinity, J.W. (Ed.), Aqueous Polymeric Coatings for Pharmaceutical Dosage Forms. Marcel Dekker Inc., New York, pp. 177–226.

Nimkulrat, S., Suchiva, K., Phinyocheep, P., Puttipipatkhachorn, S., 2004. Influence of selected surfactants on the tackiness of acrylic polymer films. Int. J. Pharm. 287, 27–37.

Nunthanid, J., Wanchana, S., Sriamornsak, P., Limmatavapirat, S., Luangtana-anan, M., Puttipipatkhachorn, S., 2002. Effect of heat on characteristics of chitosan film coated on theophylline tablets. Drug Dev. Ind. Pharm. 28, 919–930.

Østberg, T., Lund, E.M., Graffner, C., 1994. Calcium alginate matrices for oral multiple unit administration. IV. Release characteristics in different media. Int. J. Pharm. 112, 241–248.

Pongjanyakul, T., Puttipipatkhachorn, S., 2007. Modulating drug release and matrix erosion of alginate matrix capsules by microenvironmental interaction with calcium ion. Eur. J. Pharm. Biopharm. 67, 187–195.

Pongjanyakul, T., Priprem, A., Puttipipatkhachorn, S., 2005. Investigation of novel alginate-magnesium aluminum silicate microcomposite films for modified-release tablets. J. Control. Release 107, 343–356.

Pongjanyakul, T., Suksri, H., 2009. Alginate-magnesium aluminum silicate films for buccal delivery of nicotine. Colloid Surf. B 74, 103–113.

Remuñán-López, C., Bodmeier, R., 1997. Mechanical, water uptake and permeability properties of crosslinked chitosan glutamate and alginate films. J. Control. Release 44, 215–225.

Rowe, R.C., Sheskey, P.J., Owen, S.C., 2006. Handbook of Pharmaceutical Excipients, 5th ed. Pharmaceutical Press and American Pharmaceutical Association, Washington.

Sangalli, M.E., Maroni, A., Foppoli, A., Zema, L., Giordano, F., Gazzaniga, A., 2004. Different HPMC viscosity grades as coating agents for an oral time and/or site-controlled delivery system: a study on process parameters and in vitro performances. Eur. J. Pharm. Sci. 22, 469–476.

Sartori, C., Finch, D.S., Ralph, B., 1997. Determination of the cation content of alginate thin films by FTIR spectroscopy. Polymer 38, 43–51.

Semdé, R., Amighi, K., Devleeschouwer, M.J., Moës, A.J., 2000. Effect of pectinolytic enzymes on the theophylline release from pellets coated with water insoluble polymers containing pectin HM or calcium pectinate. Int. J. Pharm. 197, 169–179.

Sinko, P.J., 2006. Matin's Physical Pharmacy and Pharmaceutical Sciences, 5th ed. Lippincott Williams & Wilkins, Philadelphia.

Sriamornsak, P., Kennedy, R.A., 2006. Development of polysaccharide gel-coated pellets for oral administration 2. Calcium alginate. Eur. J. Pharm. Sci. 29, 139–147.

Sriamornsak, P., Thirawong, N., Korkerd, K., 2007. Swelling, erosion and release behavior of alginate-based matrix tablets. Eur. J. Pharm. Biopharm. 66, 435–450.

Takahashi, T., Takayama, K., Machida, Y., Nagai, T., 1990. Characteristics of polyion complexes of chitosan with sodium alginate and sodium polyacrylate. Int. J. Pharm. 61, 35–41.

Wesseling, M., Kuppler, F., Bodmeier, R., 1999. Tackiness of acrylic and cellulosic polymer films used in the coating of solid dosage forms. Eur. J. Pharm. Biopharm. 47, 73–78.

Wong, D., Bodmeier, R., 1996. Flocculation of an aqueous colloidal ethyl cellulose dispersion (Aquacoat®) with a water-soluble polymer, hydroxypropyl methylcellulose. Eur. J. Pharm. Biopharm. 42, 12–15.

Wu, S.H.W., Wyatt, D.M., Adams, M.W., 1997. Chemistry and applications of cellulosic polymers for enteric coatings of solid dosage forms. In: McGinity, J.W. (Ed.), Aqueous Polymeric Coatings for Pharmaceutical Dosage Forms. Marcel Dekker Inc., New York, pp. 385–418.

International Journal of Pharmaceutics 490 (2015) 165–172

Contents lists available at ScienceDirect

International Journal of Pharmaceutics

journal homepage: www.elsevier.com/locate/ijpharm

# Quaternary polymethacrylate–magnesium aluminum silicate films: Water uptake kinetics and film permeability

Thitiphorn Rongthong [a], Srisagul Sungthongjeen [b], Florence Siepmann [c,d], Juergen Siepmann [c,d,**], Thaned Pongjanyakul [a,*]

[a] Faculty of Pharmaceutical Sciences, Khon Kaen University, Khon Kaen 40002, Thailand
[b] Department of Pharmaceutical Technology, Faculty of Pharmaceutical Sciences, Naresuan University, Phitsanulok 65000, Thailand
[c] University of Lille, College of Pharmacy, 3 rue du Professeur Laguesse, 59006 Lille, France
[d] INSERM U1008, Controlled Drug Delivery Systems and Biomaterials, 3 rue du Professeur Laguesse, 59006 Lille, France

ARTICLE INFO

*Article history:*
Received 15 January 2015
Received in revised form 21 April 2015
Accepted 17 May 2015
Available online 21 May 2015

*Keywords:*
Quaternary polymethacrylate
Eudragit RS/RL
Magnesium aluminum silicate
Film permeability
Water uptake
Diffusion coefficient

ABSTRACT

The aim of this study was to investigate the impact of the addition of different amounts of magnesium aluminum silicate (MAS) to polymeric films based on quaternary polymethacrylates (QPMs, here Eudragit RS and RL). MAS contains negatively charged —$SiO^-$ groups, while QPM contains positively charged quaternary ammonium groups. The basic idea is to be able to provide desired water and drug permeability by simply varying the amount of added MAS. Thin, free films of varying composition were prepared by casting and exposed to 0.1 M HCl and pH 6.8 phosphate buffer. The water uptake kinetics and water vapor permeability of the systems were determined gravimetrically. The transport of propranolol HCl, acetaminophen, methyl-, ethyl- and propylparaben across thin films was studied using side-by-side diffusion cells. A numerical solution of Fick's second law of diffusion was applied to determine the apparent compound diffusion coefficients, partition coefficients between the bulk fluids and the films as well as the apparent film permeability for these compounds. The addition of MAS resulted in denser inner film structures, at least partially due to ionic interactions between the positively charged quaternary ammonium groups and the negatively charged —$SiO^-$ groups. This resulted in lower water uptake, reduced water vapor permeability and decreasing apparent compound diffusivities. In contrast, the affinity of the investigated drugs and parabens to the films substantially increased upon MAS addition. The obtained new knowledge can be helpful for the development of novel coating materials (based on QPM–MAS blends) for controlled-release dosage forms.



## 1. Introduction

Polymeric films offer a great potential as coating materials for pharmaceutical dosage forms for controlled drug delivery (Maroni et al., 2013; Siepmann and Siepmann, 2013) or aiming at taste masking or moisture protection (Joshi and Petereit, 2013). Various parameters, including the polymer properties and the type of preparation method can affect the resulting system performance, e.g., drug release patterns in the gastro-intestinal tract. However, in practice it can be difficult to identify the required film coating composition and preparation procedure to provide desired system characteristics. An interesting strategy to overcome this hurdle is to use blends of two types of polymers: by simply varying the polymer: polymer blend ratio broad spectra of film coating properties can be provided (Siepmann et al., 2008). Alternatively, a polymer can be blended with a clay to achieve this goal (Pongjanyakul et al., 2005; Khunawattanakul et al., 2010). Importantly, molecular interactions of the polymer chains with the clay compounds can occur, which can effectively alter the physicochemical properties of the composite films (Khunawattanakul et al., 2010; Caridade et al., 2013).

Quaternary polymethacrylate (QPM) is a positively charged polymer that is widely used as coating material for pharmaceutical dosage forms. Eudragit RS 30D and Eudragit RL 30D are examples for two commercial QPM products. These are aqueous polymer dispersions (solids content = 30%). In Eudragit RS 30D and Eudragit RL 30D, the QPM contains 5 and 10% w/w quaternary ammonium groups (here abbreviated 5 QPM and 10 QPM). QPM is an insoluble,

* Corresponding author at: Faculty of Pharmaceutical Sciences, Khon Kaen University, Khon Kaen 40002, Thailand. Tel.: +66 43 362092 fax: +66 43 202379.
** Corresponding author at: University of Lille, College of Pharmacy, INSERMU1008, 3rue du Professeur Laguesse, 59006 Lille, France. Tel.: +33 320 964708; fax: +33 320964942.
*E-mail addresses:* juergen.siepmann@univ-lille2.fr (J. Siepmann), thaned@kku.ac.th (T. Pongjanyakul).

http://dx.doi.org/10.1016/j.ijpharm.2015.05.048
0378-5173/

but swellable polymer. The quaternary ammonium groups play an important role for its hydration, attracting water into the system: thus, the swelling of 10 QPM is more pronounced than the swelling of 5 QPM (Akhgaria et al., 2006), resulting in a higher permeability for many drugs and consequently faster release. The swelling of QPM is a priori independent of the pH of the release medium, but can strongly depend on the type and concentration of ions in the bulk fluid (Bodmeier et al., 1996; Sun et al., 2001). Limitations for the use of QPMs as film formers include their considerable sticking tendency encountered during the coating process (Wesseling et al., 1999) and potentially unsuitable drug permeability (Lehmann, 1997). To adjust desired drug release rates, blends of 5 QPM and 10 QPM can be used. For instance, Amighi and Moës (1995) successfully applied this strategy, but the high sticking tendency during the coating process remains. Alternatively, a naturally occurring anionic polymer can be added to QPM, such as pectin or sodium alginate. The positively charged QPM can interact with the anionic polymer via electrostatic interactions. The complexation of QPM with pectin was for example shown to reduce the swelling of the films and retard pectin leaching out of the systems (Semdé et al., 1998). Incorporation of sodium alginate into QPM films resulted in increased film strength, decreased film tackiness, and retardation of drug transport across thin films (Khuathan and Pongjanyakul, 2014).

Magnesium aluminum silicate (MAS), a natural smectite clay, is composed of a central octahedral sheet of aluminum or magnesium and double external silica tetrahedron layers (Alexandre and Dubois, 2000), also called silicate layers. Importantly, the surfaces of the silicate layers exhibit negative charges (containing numerous $-SiO^-$ groups). MAS is water-insoluble, but can hydrate in water. It is widely used in pharmaceutics, for example as a diluent, suspending agent or stabilizing agent (Kibbe, 2000). Negatively charged MAS can interact with positively charged polymers, such as chitosan. This offers the possibility to effectively alter the physicochemical properties, mechanical properties and drug permeability of composite films (Khunawattanakul et al., 2010). Moreover, MAS can form complexes with positively charged drugs, e.g., nicotine (Suksri and Pongjanyakul, 2008) and propranolol HCl (Rojtanatanya and Pongjanyakul, 2010). Such drug–MAS complexes have been reported to provide improved thermal properties and to result in more sustained drug release.

In a previous study, the impact of adding MAS to QPM films on the resulting mechanical properties and tackiness of the composite films was studied (Rongthong et al., 2013). The electrostatic interactions between QPM and MAS were shown to lead to the formation of exfoliated and intercalated nanocomposite films, resulting in improved thermal stability and reduced tackiness of the films. Also, wet QPM–MAS films exhibited higher mechanical strength in acidic and neutral media. However, yet it is unknown how the addition of MAS to QPM films affects the water uptake and drug permeability of these systems, which are two key properties for their use as advanced coating materials. Therefore, the objective of the present study was to investigate the water uptake kinetics of QPM–MAS films of various compositions upon exposure to 0.1 M HCl and pH 6.8 phosphate buffer and to monitor changes in the systems' permeability for different types of drugs and parabens.

## 2. Materials and methods

### 2.1. Materials

Aqueous dispersions of 10 QPM (Eudragit RL 30D) and 5 QPM (Eudragit RS 30D) were purchased from Roehm Pharma (Darmstadt, Germany). Magnesium aluminum silicate (MAS) (Veegum HV) was obtained from R.T. Vanderbilt Company (Norwalk, CT, USA). Diethyl sebacate was purchased from Aldrich Chemistry (Dorset, England). Propranolol HCl and acetaminophen were purchased from Changzhou Yabang Pharmaceutical (Jiangsu, China) and Praporn Dasut (Bangkok, Thailand), respectively. Methylparaben and ethylparaben were purchased from Sigma–Aldrich (Tokyo, Japan). Propylparaben was obtained from Fluka (Dorset, England). All other reagents and solvents were of analytical grade.

### 2.2. Preparation of thin, free films

QPM and QPM–MAS films were prepared using a casting method. MAS aqueous dispersion (4% w/v) was prepared with hot water and kept at room temperature overnight. Twenty grams aqueous QPM dispersion (30%, w/w polymer solids content) were mixed with 0.9 g diethyl sebacate (acting as a plasticizer) and stirred for 30 min. Appropriate amounts of the MAS aqueous dispersion were added to these aqueous, plasticized QPM dispersions to achieve the following QPM–MAS ratios: 4:0, 4:0.1, 4:0.25, 4:0.5, and 4:0.75 (w:w). These QPM–MAS dispersions were further stirred for 30 min, then adjusted to 150 mL with distilled water and shaken in a water bath at 75 oscillations $min^{-1}$ for 24 h at 37 °C. The dispersions were subsequently cast onto Teflon plates (17 × 18 cm) and dried at 50 °C for 48 h in an oven. Afterwards, the films were peeled off the plates and kept in a desiccator at room temperature prior to the measurements. The thickness of the films was measured with a thickness gauge.

### 2.3. Water uptake studies

Dynamic changes in the water contents of thin, free films upon exposure to 0.1 M HCl and pH 6.8 phosphate buffer were monitored gravimetrically. QPM and QPM–MAS films were cut into pieces of approximately 1 × 1 cm, which were exposed to the media in a horizontal shaker, kept at 37 °C. At pre-determined time points, film samples were withdrawn and weighed after careful removal of excess surface water by blotting with a filter paper (wet weight = $W_{wet}$). The film pieces were subsequently dried at 50 °C to constant weight ($W_{dry}$) in an oven. The water contents of the films at each time point were calculated as follows:

$$\text{water content}(\%) = \left(\frac{W_{wet} - W_{dry}}{W_{wet}}\right) \times 100\% \quad (1)$$

### 2.4. Determination of the water vapor permeability

Circular films pieces (1 cm in diameter) were placed onto (open) 5 mL glass vials, containing 3.5 g silica gel beads. The films were fixed with screw lids, the surface area available for water permeation per film was 0.58 $cm^2$. The vials were placed in a desiccator containing a saturated aqueous sodium chloride solution (providing 75% relative humidity). The desiccator was kept in a room at 26 °C, 55 ± 3% relative humidity (Pongjanyakul et al., 2005). The weight changes of the vials were monitored gravimetrically during 120 h. The water vapor permeability coefficient (WVP coefficient) was determined from the slope of the straight line obtained when plotting the cumulative amount of water vapor permeated through a film as a function of time, using the following equation (Pongjanyakul et al., 2005):

$$\text{WVP coefficient} = \frac{\text{rate} \times d}{A \times \Delta P_v} \quad (2)$$

where rate is the water permeation rate (=cumulative amount of water permeated through the film per time); $d$ is the mean thickness of the film; $A$ is the surface area available for water vapor

transport, and $rP_v$ is the difference in water vapor pressure (inside versus outside the vials).

### 2.5. Drug permeability studies

The permeability of acetaminophen, propranolol HCl and different parabens through thin films were measured using horizontal side-by-side diffusion cells (Crown Glass, Someville, NJ, USA). The donor and acceptor compartments had a volume of 3 mL each, the film surface area available for diffusion was 0.66 $cm^2$. The bulk fluid was 0.1 M HCl or pH 6.8 phosphate buffer, as indicated. The systems were kept at 37 °C. The films were cut into circular pieces and immersed into the respective medium for 30 min prior to testing. Pre-wetted film samples were clamped between a drug solution or paraben suspension (in 0.1 M HCl or pH 6.8 phosphate buffer) in the donor compartment and the (initially compound-free) bulk fluid (0.1 M HCl or pH 6.8 phosphate buffer) in the acceptor compartment. Both compartments were stirred at 600 revolution $min^{-1}$ using magnetic stirrers. At predetermined time points, 2.6 mL samples were withdrawn from the acceptor compartment and replaced with fresh medium. In the case of acetaminophen and propranolol HCl, the initial drug concentration in the donor compartment was 4 mg/mL (being well below the drugs' solubility). The amount of drug in the samples was analyzed using a UV–vis spectrophotometer (Shimadzu UV1201, Japan) at the wavelength of 265 and 289 nm, respectively. In the case of parabens, excess amounts of these compounds were exposed to 20 mL 0.1 M HCl in Erlenmeyer flasks, which were shaken at 37 °C for 3 d. The obtained suspensions were filled into the donor compartments of the side-by-side diffusion cells. The concentration of the parabens in the saturated solutions as well as in the samples withdrawn from the acceptor compartments were analyzed using a UV-visible spectrophotometer (Shimadzu UV1201, Japan) at the wavelength of 256 nm. The apparent compound diffusion coefficients ($D$) and their apparent partition coefficients (between the bulk fluids and the films, $K$) were determined by fitting an appropriate solution of Fick's second law of diffusion to the experimentally determined drug/paraben transport rates. The model is considers one dimensional diffusion through the films (Crank, 1975):

$$\frac{\partial c}{\partial t} = D \times \frac{\partial^2 c}{\partial x^2} \tag{3}$$

where $c$ is the concentration of the diffusing compound (drug or paraben); $t$ represents time; $D$ is the apparent compound diffusion coefficient and $x$ the film thickness (which was measured after

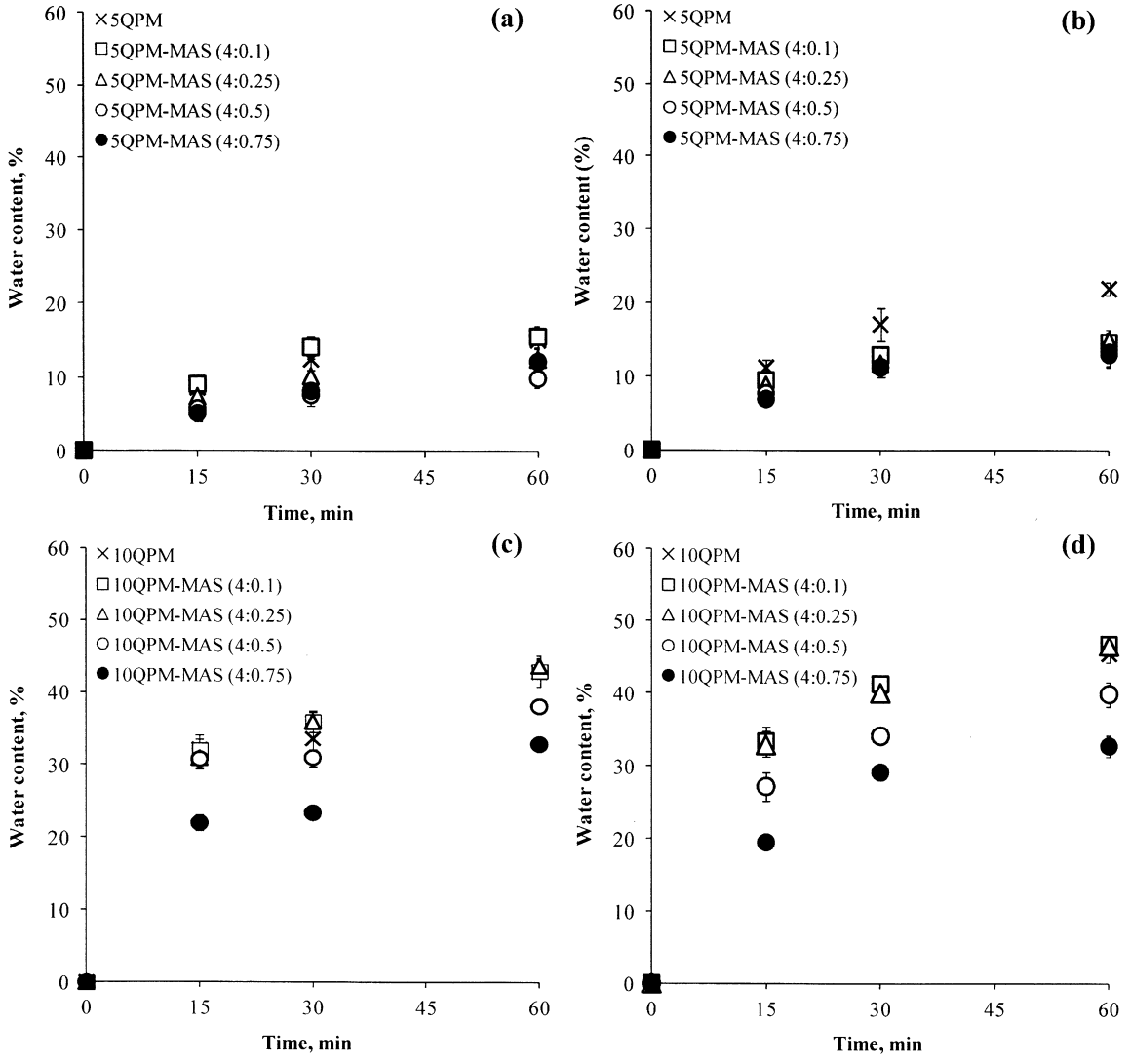


**Fig. 1.** Water content of thin films based on 5 QPM–MAS (a,b), or 10 QPM–MAS (c,d), containing different amounts of MAS, upon exposure to 0.1 M HCl (a,c), or pH 6.8 phosphate buffer (b,d). Mean values ± SD are indicated ($n = 5$).

30 min exposure to the respective bulk fluid). Constant film thickness and sink conditions in the acceptor compartment are assumed. In the case of acetaminophen and propranolol HCl, the drug solution in the donor compartment is considered to be non-saturated and the concentration to decrease with time. In the case of parabens, a saturated compound solution is considered in the donor compartment throughout the observation period. The mathematical model was solved numerically, using finite differences (Siepmann and Siepmann, 2008).

## 3. Results and discussion

### 3.1. Water uptake of thin, free films

The dynamic changes in the water contents of the thin, free films upon exposure to 0.1 M HCl and pH 6.8 phosphate buffer are illustrated in Fig. 1. As expected, the water uptake of 10 QPM-based films (Fig. 1c,d) was higher than that of 5 QPM-based films (Fig. 1a, b), irrespective of the type of medium. This is due to the high hydrophilicity of the quaternary ammonium groups in QPM, attracting water. Interestingly, the addition of increasing amounts of MAS led to an overall decrease in the water uptake of the films, irrespective of the QPM type. This might be explained by ionic interactions between the positively charged quaternary ammonium groups of QPM with the negatively charged —$SiO^-$ groups of MAS (Rongthong et al., 2013). The attractive forces between these oppositely charged ions can be expected to result in a denser network, offering more resistance for water transport. The formation of a denser network is also in good agreement with the reported increase in the strength of wet QPM films upon MAS addition (Rongthong et al., 2013). Importantly, these differences in the water contents of the systems might significantly affect the mobility of various types of drugs in the films (Lecomte et al., 2003).

### 3.2. Water vapor permeability

In addition to the water uptake kinetics upon exposure of thin films to the investigated media, also the water vapor permeability coefficients (WVP coefficients) of QPM–MAS films were determined. Briefly, the films were fixed on the openings of vials containing dry silica beads. The vials were exposed to a controlled environment exhibiting 75% relative humidity and dynamic changes in the vial mass were monitored gravimetrically. The WVP coefficients were determined from the slopes of the straight lines obtained when plotting the cumulative mass increase as a function of time. Fig. 2 shows the results observed with the investigated 5 QPM- and 10 QPM-based films, optionally containing different amounts of MAS. As it can be seen, the water vapor permeability was generally higher for 10 QPM containing films compared to 5 QPM containing films. This can probably be attributed to the higher water uptake of these films (due to the higher contents in highly hydrophilic quaternary ammonium groups), resulting in less dense inner film structures. In addition, water acts as a plasticizer for QPM (Glaessl et al., 2009, 2010a,b), increasing the mobility of the polymer chains. Furthermore, the water vapor permeability clearly decreased with increasing MAS content, irrespective of the type of QPM (Fig. 2). This is in good agreement with the above discussed water uptake kinetics of the composite films and likely reflects the denser film structure with increasing MAS content. This is also consistent with the reported interaction of the positively charged quaternary ammonium groups of QPM with the negatively charged $SiO^-$ groups of MAS, creating nanocomposite materials, as evidenced by ATR-FTIR and PXRD analysis (Rongthong et al., 2013).

### 3.3. Drug and paraben transport through thin films

The above described changes in the inner structure of QPM films upon MAS addition can be expected to affect also the permeability of various types of drugs through these films. Fig. 3 shows for example the transport of propranolol through 10 QPM-based films containing different amounts of MAS. For reasons of comparison, also drug permeation through 5 QPM-based films free of MAS is illustrated (filled diamonds). These results were obtained with side-by-side diffusion cells: the donor compartment contained initially a 4 mg/mL propranolol HCl solution in 0.1 M HCl, the acceptor compartment contained 0.1 M HCl. Clearly, two major observations can be made:

(1) Drug transport through the 5 QPM-based films was much slower than through the 10 QPM-based films (filled diamonds versus crosses). This can be explained by the lower water uptake rates and extents of these films (Fig. 1), resulting in less mobile polymeric chains and reduced drug mobility within the films. In addition, the partitioning of the freely water-soluble drug propranolol $H^+$ ions (most of the drug is likely to be ionized under

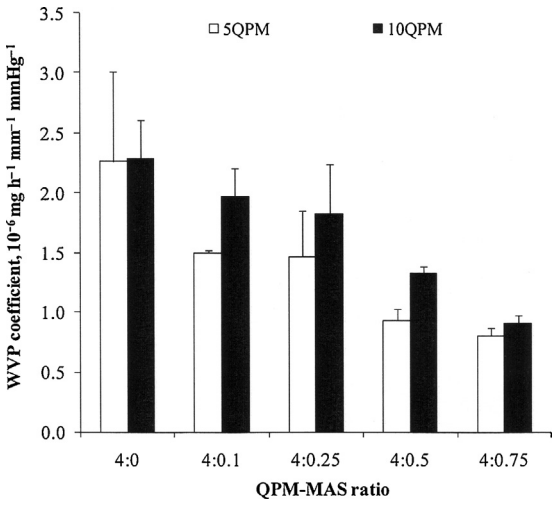


**Fig. 2.** Water vapor permeability (WVP) coefficient of QPM-MAS films. Mean values ± SD ($n = 3$) are indicated.

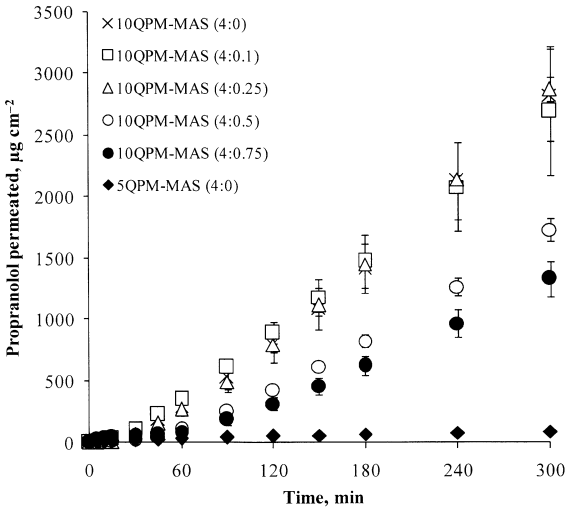


**Fig. 3.** Permeation of propranolol through QPM–MAS films exposed to 0.1 M HCl. Mean values ± SD ($n = 3$) are indicated.

the given conditions: $pK_a = 9.5$) into the film can be expected to be lower in films containing less water.

(2) The addition of increasing amounts of MAS to the films led to a decrease in the drug permeation rate. This can probably be explained by the attractive forces between the positively charged quaternary ammonium groups in QPM and the negatively charged —$SiO^-$ groups in MAS, resulting in denser inner film structures and, thus, reduced drug mobility. In addition, the reduced water uptake of the films with higher MAS contents (Fig. 1) can be expected to lower the partitioning of freely water-soluble propranolol $H^+$ ions into the films, and water acts as a plasticizer for QPM. Furthermore, since most of the drug is protonated and positively charged, it can interact with the negatively charged —$SiO^-$ groups of MAS (Rojtanatanya and Ponjanyakul, 2010), resulting in hindered drug transport across the films.

It has to be pointed out that the transport rate of a compound (e.g., drug) through a polymeric film is often governed by two processes: (i) compound partitioning into the film, and (ii) compound diffusion through the film. The first step can be characterized by the partition coefficient of the compound between the film and the bulk fluid (=concentration in the film/concentration in the bulk fluid), the second process by the diffusion coefficient of the compound within the film. The partition coefficient is a measure for the compound's affinity to the film, the diffusion coefficient is a measure for the compound's mobility within the film. In the present study, a numerical solution of Fick's second law of diffusion was used to determine both parameters for the various composite films/bulk fluid combinations. The model does not require a steady state compound transport to be reached in the side-by-side diffusion cells, neither the donor compartment to be saturated with the compound. Fitting the model to experimental data sets allowed determining the apparent partition coefficients and the apparent diffusion coefficients of the investigated compounds in the QPM–MAS films upon exposure to drug solutions in 0.1 M HCl and pH 6.8 phosphate buffer. Since the thicknesses of the films were not constant and the theory assumes constant diffusion pathway lengths, the determined values are no absolute values, but "apparent" ones. Note that the films were pre-exposed to the media for 30 min prior to the measurements. In addition, the apparent permeability ($P$) of the respective compound through the investigated films was calculated. In this study, $P$ is defined as the product "$D \times K$".

Fig. 4 shows the apparent diffusion coefficients ($D$), partition coefficients ($K$) and permeability ($P$) of propranolol in 10 QPM-based films, optionally containing different amounts of MAS. The bulk fluid was pH 6.8 phosphate buffer. Clearly, the drug diffusivity substantially decreased, while the partition coefficient increased when increasing the MAS content. The decrease in the diffusion coefficient (and, thus, the mobility) of the drug within the film with increasing MAS content might at least partially be attributable to: (i) the denser inner film structure, resulting from the ionic interactions between the quaternary ammonium groups of QPM with the —$SiO^-$ groups of MAS (as discussed above); (ii) the reduced water content of the films (Fig. 1), water acting as a plasticizer for this polymer (Glaessl et al., 2009, 2010a,b); and (iii) ionic interactions between positively charged propranolol $H^+$ ions ($pK_a = 9.5$) and negatively charged —$SiO^-$ groups of MAS. The increase in the apparent partition coefficient of propranolol between the films and the bulk fluid with increasing MAS content might at least partially be explained by the attractive forces between positively charged propranolol $H^+$ ions and negatively charged —$SiO^-$ groups of MAS.

When the ionic drug propranolol HCl was replaced by the neutral drug acetaminophen, the apparent diffusion coefficients, partition coefficients and permeability shown in Fig. 5 were obtained. Again, the drug diffusivity substantially decreased with

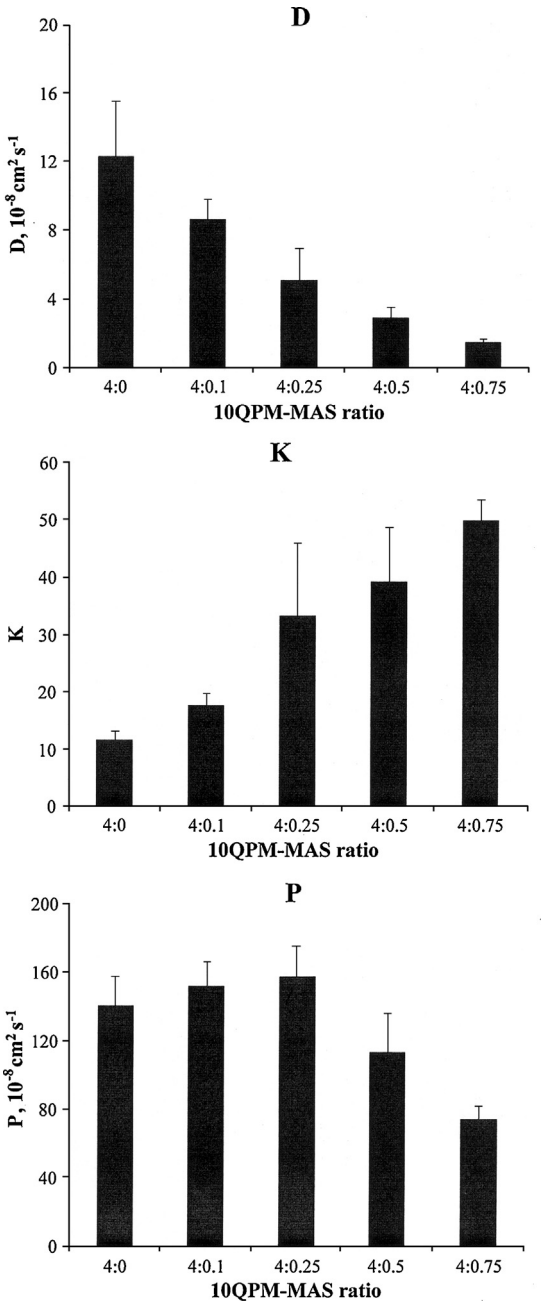


**Fig. 4.** Apparent diffusion coefficient ($D$), apparent partition coefficient ($K$) and apparent permeability ($P$) of propranolol in 10 QPM-based films containing different amounts of MAS. The results were obtained using side-by-side diffusion cells, filled with pH 6.8 phosphate buffer. Mean values ± SD ($n = 3$) are indicated.

increasing MAS content, whereas, the partition coefficient increased. The decrease in drug mobility is likely due to the denser inner film structure and reduced water content, water acting as a plasticizer for QPM. The increasing partition coefficient might at least partially also be attributable to the reduced water content of these films and the relatively higher affinity toward the polymer and/or MAS compared to the bulk fluid. Comparing the $D$ and $K$ values of acetaminophen with those of propranolol (Fig. 5 versus Fig. 4), it can be seen that the mobility of acetaminophen within the films is much higher, whereas the affinity to the films is much lower. The higher diffusivity can at least partially be explained by the lower molecular weight of acetaminophen compared to propranolol $H^+$ (151 Da versus 260 Da), and the absence of attractive ionic interactions between

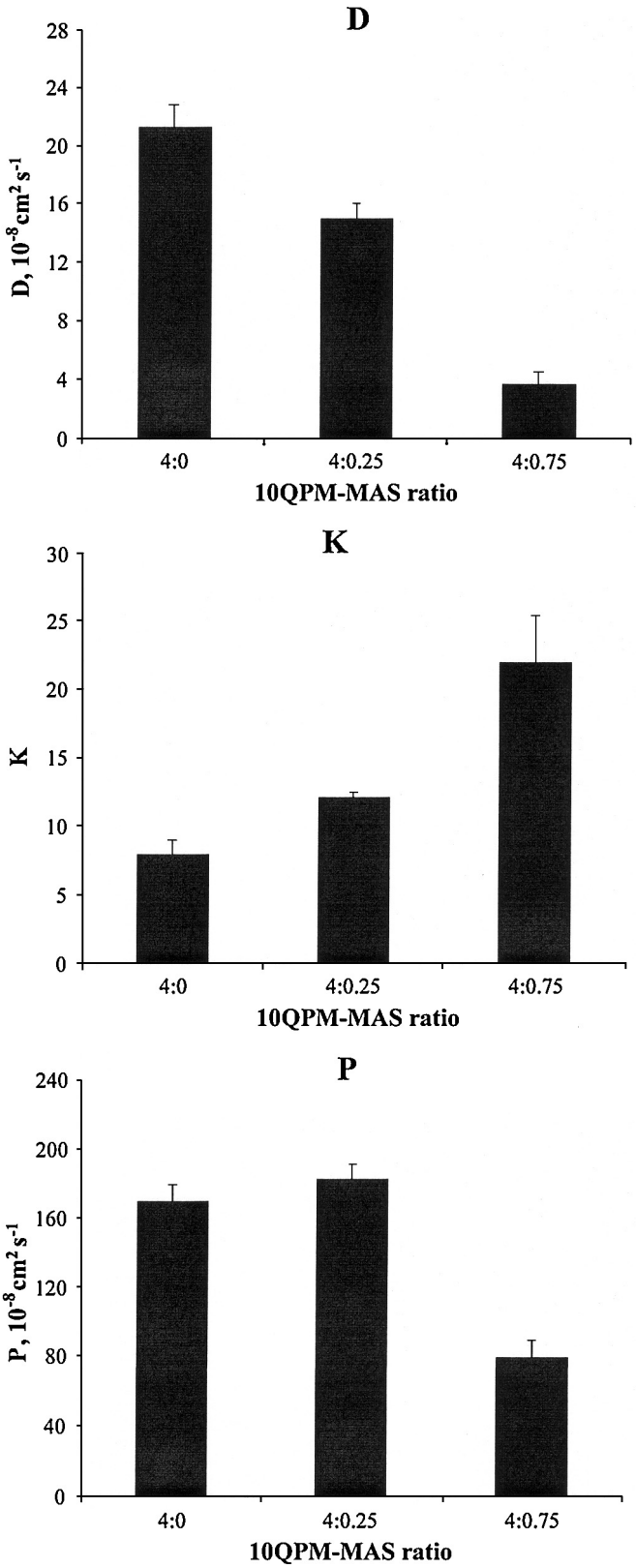


**Fig. 5.** Apparent diffusion coefficient ($D$), apparent partition coefficient ($K$) and apparent permeability ($P$) of acetaminophen in 10 QPM-based films containing different amounts of MAS. The results were obtained using side-by-side diffusion cells, filled with 0.1 M HCl. Mean values ± SD ($n = 3$) are indicated.

the drug and the MAS. The higher apparent partition coefficient of propranolol compared to acetaminophen can probably at least partially be attributed to the electrostatic interactions between the positively charged drug ions and negatively charged —$SiO^-$ groups of MAS and potentially more pronounced interactions of the drug with the QPM polymer backbone (Glaessl et al., 2009, 2010a,b).

Fig. 6 shows the apparent diffusion coefficients, partition coefficients and permeability of methyl-, ethyl- and propylparaben

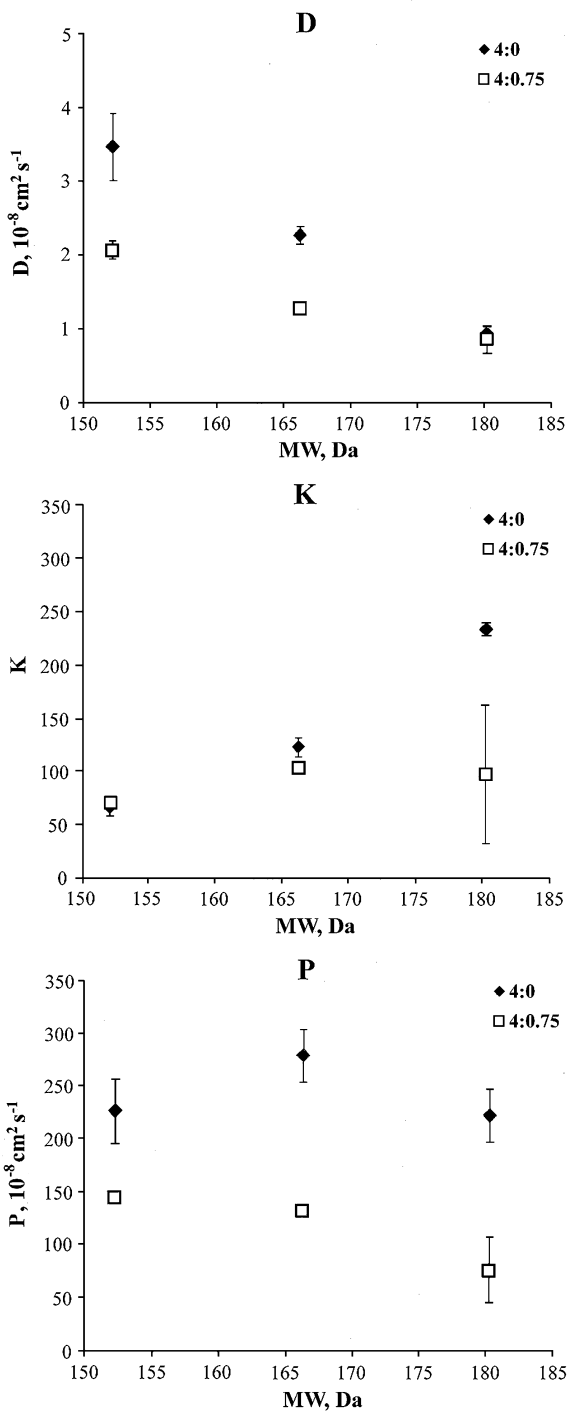


**Fig. 6.** Impact of the molecular weight of the investigated parabens (methyl-, ethyl- and propylparaben) on the apparent diffusion coefficient ($D$), apparent partition coefficient ($K$) and apparent permeability ($P$) of these compounds in 10 QPM–based films, optionally containing MAS. The 10 QPM–MAS ratio is indicated in the diagrams. The results were obtained using side-by-side diffusion cells, filled with 0.1 M HCl. Mean values ± SD ($n = 3$) are indicated.

in 10 QPM-based films, optionally containing different amounts of MAS. The bulk fluid was 0.1 M HCl in all cases. In contrast to the above described drug permeation studies, the donor compartment contained a paraben *suspension*: the bulk fluid was saturated with the respective compound and contained a large excess of it. Table 1 lists the experimentally determined solubility of the investigated parabens in this medium at 37 °C and shows the chemical structures of these compounds, together with their molecular

**Table 1**
Key characteristics of the investigated parabens.

| Paraben | Molecular weight and chemical structure | Solubility in 0.1 M HCl at 37 °C (mg mL$^{-1}$) |
|---|---|---|
| Methylparaben | 152.15 Da 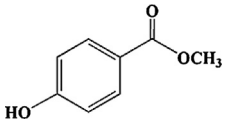 | 3.54 ± 0.05 |
| Ethylparaben | 166.18 Da 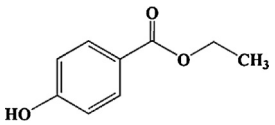 | 1.53 ± 0.04 |
| Propylparaben | 180.20 Da 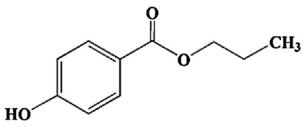 | 0.59 ± 0.02 |

weights. As it can be seen in Fig. 6, the mobility of the parabens within the films were much lower than those of the investigated drugs (much lower $D$ values compared to those in Figs. 4 and 5). Furthermore, the affinity of the parabens to the films was substantially higher than that of acetaminophen or propranolol (much higher $K$ values). The smaller apparent diffusion coefficients compared to the investigated drugs cannot be explained by the molecular weights of the diffusing compounds (e.g., 152–180 Da for the parabens compared 260 Da for propranolol $H^+$). The reason is probably the very high affinity of these parabens to the QPM: for example, methylparaben has been reported to be a very efficient plasticizer for QPM (Wu and McGinity, 2003). NMR spectroscopy revealed interactions between the hydroxyl group of the paraben with ester groups of the polymer. This particularly high affinity between the parabens and the QPM also explains the much higher $K$ values compared to the investigated drugs. When increasing the molecular weight of the paraben, the diffusion coefficient of the compound within the film decreased, irrespective of the presence/absence of MAS (Fig. 6, top diagram). This is in good agreement with reports in the literature (Pongjanyakul, 2009) and might at least partially be explained by the higher inertia of the molecules and/or altered interactions with the films' compounds. When adding MAS to the films, the paraben mobility generally decreased, probably due to the denser inner film structure. Furthermore, with increasing molecular weight the affinity of the paraben to MAS-free films monotonically increased (Fig. 6, middle diagram, filled symbols). This might be explained by more pronounced interactions between the longer alkyl chain of the paraben and the hydrophobic QPM polymer backbone. When adding MAS to the films, the $K$ value of propylparaben substantially decreased. This is in contrast to the presented acetaminophen and propranolol results, which all showed a systematic increase in the compound's affinity to the film upon MAS addition (Figs. 4 and 5). This phenomenon might be explained by the exceptionally high affinity of this paraben to QPM, which is likely to be reduced in the presence of MAS (due to hindered interactions). The apparent permeability values of the investigated parabens were generally higher than those of acetaminophen and propranolol, again

probably due to the exceptionally high affinity of these compounds to QPM.

## 4. Conclusion

The incorporation of MAS remarkably affects the transport of water, drugs and other compounds in QPM-based films, which can be attributed to altered inner film structures and compound–polymer or compound–MAS interactions. The obtained new knowledge can be very helpful for the development of innovative coating materials (based on polymer–clay blends) for controlled release dosage forms: the addition of varying amounts of MAS to QPM-based films might be used to effectively adjust desired water and drug permeability. This is at least partially due to the ionic interactions between positively charged quaternary ammonium groups of QPM and negatively charged $—SiO^-$ groups of MAS.

## Acknowledgements

The authors would like to thank the Thailand Research Fund (Bangkok, Thailand) for research funding (Grant no. BRG5580016), and the Faculty of Pharmaceutical Sciences, Khon Kaen University, Khon Kaen, Thailand for technical support. Financial support from the Thailand Research Fund through the Royal Golden Jubilee Ph.D. Program (Grant No. PHD/0136/2551) for T.R. and T.P. is gratefully acknowledged.

## References

Akhgaria, A., Farahmanda, F., Afrasiabi Garekania, H., Sadeghia, F., Vandammeb, T.F., 2006. Permeability and swelling studies on free films containing inulin in combination with different polymethacrylates aimed for colonic drug delivery. Eur. J. Pharm. Sci. 28, 307–314.

Alexandre, M., Dubois, P., 2000. Polymer-layered silicate nanocomposites: preparation, properties and uses of a new class of materials. Mater. Sci. Eng. 28, 1–63.

Amighi, K., Moës, A.J., 1995. Evaluation of thermal and film forming properties of acrylic aqueous polymer dispersion blends: application to the formulation of sustained-release film coated theophylline pellets. Drug Dev. Ind. Pharm. 21, 2355–2369.

Bodmeier, R., Guo, X., Sarabia, R.E., Skultety, P.F., 1996. The influence of buffer species and strength on diltiazem HCl release from beads coated with the aqueous cationic polymer dispersions Eudragit RS, RL 30D. Pharm. Res. 13, 52–56.

Caridade, S.G., Monge, C., Gilde, F., Boudou, T., Mano, J.F., Picart, C., 2013. Free-standing polyelectrolyte membranes made of chitosan and alginate. Biomacromolecules 14, 1653–1660.

The Mathematics of Diffusion. In: Crank, J. (Ed.), Clarendon Press, Oxford.

Glaessl, B., Siepmann, F., Tucker, I., Siepmann, J., Rades, T., 2009. Characterisation of quaternary polymethacrylate films containing tartaric acid, metoprolol free base or metoprolol tartrate. Eur. J. Pharm. Biopharm. 73, 366–372.

Glaessl, B., Siepmann, F., Tucker, I., Rades, T., Siepmann, J., 2010a. Deeper insight into the drug release mechanisms in Eudragit RL-based delivery systems. Int. J. Pharm. 389, 139–146.

Glaessl, B., Siepmann, F., Tucker, I., Rades, T., Siepmann, J., 2010b. Mathematical modeling of drug release from Eudragit RS-based delivery systems. J. Drug Del. Sci. Technol. 20, 127–133.

Joshi, S., Petereit, H.U., 2013. Film coatings for taste masking and moisture protection. Int. J. Pharm. 457, 395–406.

Khuathan, N., Pongjanyakul, T., 2014. Modification of quaternary polymethacrylate films using sodium alginate: film characterization and drug permeability. Int. J. Pharm. 460, 63–72.

Khunawattanakul, W., Puttipipatkhachorn, S., Rades, T., Pongjanyakul, T., 2010. Chitosan–magnesium aluminum silicate nanocomposite films: physicochemical characterization and drug permeability. Int. J. Pharm. 393, 219–229.

Kibbe, H.A., 2000. Handbook of pharmaceutical excipients, 3rd ed. American Pharmaceutical Association, Washington, pp. 295–298.

Lecomte, F., Siepmann, J., Walther, M., MacRae, R.J., Bodmeier, R., 2003. B lends of enteric and GIT-insoluble polymers used for film coating: physicochemical characterization and drug release patterns. J. Control. Release 89, 457–471.

Lehmann, K.O.R., 1997. Chemistry and application properties of polymethacrylate coating systems. In: McGinity, J.W. (Ed.), Aqueous Polymeric Coatings for Pharmaceutical Dosage Forms. Marcel Dekker, New York, pp. 101–176.

Maroni, A., Zema, L., Loreti, G., Palugan, L., Gazzaniga, A., 2013. Film coatings for oral pulsatile release. Int. J. Pharm. 457, 362–371.

Pongjanyakul, T., Priprem, A., Puttipipatkhachorn, S., 2005. Investigation of novel alginate–magnesium aluminum silicate microcomposite films for modified-release tablets. J. Control. Release 107, 343–356.

Pongjanyakul, T., 2009. Alginate–magnesium aluminum silicate films: importance of alginate block structures. Int. J. Pharm. 365, 100–108.

Rojtanatanya, S., Ponjanyakul, T., 2010. Propranolol–magnesium aluminum silicate complex dispersions and particles: characterization and factors influencing drug release. Int. J. Pharm. 383, 106–115.

Rongthong, T., Sungthongjeen, S., Siepmann, J., Pongjanyakul, T., 2013. Quaternary polymethacrylate–magnesium aluminum silicate films: molecular interactions, mechanical properties and tackiness. Int. J. Pharm. 458, 57–64.

Semdé, R., Amighi, K., Pierre, D., Devleeschouwer, M.J., Moës, A.J., 1998. Leaching of pectin from mixed pectin/insoluble polymer films intended for colonic drug delivery. Int. J. Pharm. 174, 233–241.

Siepmann, F., Siepmann, J., Walther, M., MacRae, R.J., Bodmeier, R., 2008. Polymer blends for controlled release coatings. J. Control. Release 125, 1–15.

Siepmann, J., Siepmann, F., 2008. Mathematical modeling of drug delivery. Int. J. Pharm. 364, 328–343.

Siepmann, J., Siepmann, F., 2013. Stability of aqueous polymeric controlled release film coatings. Int. J. Pharm. 457, 437–445.

Suksri, H., Pongjanyakul, T., 2008. Interaction of nicotine with magnesium aluminum silicate at different pHs: characterization of flocculate size, zeta potential and nicotine adsorption behavior. Colloid Surf. B 65, 54–60.

Sun, Y.M., Hsu, S.C., Lai, J.Y., 2001. Transport properties of ionic drugs in the ammonio methacrylate copolymer membranes. Pharm. Res. 18, 304–310.

Wesseling, M., Kuppler, F., Bodmeier, R., 1999. Tackiness of acrylic and cellulosic polymer films used in the coating of solid dosage forms. Eur. J. Pharm. Biopharm. 47, 73–78.

Wu, C., McGinity, J.W., 2003. Influence of methylparaben as a solid-state plasticizer on the physicochemical properties of Eudragit RS PO hot-melt extrudates. Eur. J. Pharm. Biopharm. 56, 95–100.

Pharmaceutical Development and Technology

http://informahealthcare.com/phd
ISSN: 1083-7450 (print), 1097-9867 (electronic)

Pharm Dev Technol, Early Online: 1–12
 DOI: 10.3109/10837450.2015.1022787

informa healthcare

RESEARCH ARTICLE

# Quaternary polymethacrylate–sodium alginate films: effect of alginate block structures and use for sustained release tablets

Thaned Pongjanyakul and Natnicha Khuathan

*Faculty of Pharmaceutical Sciences, Khon Kaen University, Khon Kaen, Thailand*

**Abstract**

The objectives in this study were to characterize quaternary polymethacrylate–sodium alginate (QPM–SA) films prepared using high G block or high M block SA (GSA or MSA, respectively), and to investigate the effects of QPM–SA ratios, film-coating levels and SA block structures on propranolol HCl (PPN) released from coated tablets. The results demonstrated that GSA and MSA shared a similar interaction mechanism with QPM. The QPM–GSA films had higher puncture strength than the QPM–MSA films in dry and wet states, whereas the % elongations were not different. The drug permeability of the QPM–GSA films was lower than that of the QPM–MSA films in both acidic and neutral media, but higher water uptake of the QPM–GSA films was found at neutral pH. Moreover, the QPM–MSA-coated tablets had a greater PPN release rate than the QPM–GSA-coated tablets, and drug release was dependent on the film-coating levels. In addition, the QPM–SA films at a ratio of 4:0.5 produced a stronger film and could sustain PPN release. These results indicate that the QPM–GSA films had greater film strength and lower drug permeability than the QPM–MSA films. Additionally, the QPM–SA films have a strong potential for use in sustained-release tablets.

**Keywords**

Block structure, drug release, film coating, quaternary polymethacrylate, sodium alginate

**History**

Received 2 December 2014
Revised 12 January 2015
Accepted 18 February 2015
Published online 11 March 2015



## Introduction

Tablet polymeric film coatings have been widely used in pharmaceutics because they can enhance drug stability from moisture, light and oxidation reactions and decrease unpleasant taste and odor of drugs[1]. Furthermore, the coated films on the tablets can control drug release and protect the drug from gastric fluid in the gastrointestinal tract[2]. Film coating materials can be obtained from both natural and synthetic polymers. Quaternary polymethacrylate (QPM) is a synthetic polymer that has been widely employed as a film coating material in pharmaceutical dosage forms[3]. QPM is available as an aqueous-dispersion form as a commercial product. QPM contains positively charged quaternary ammonium groups that have chloride ions as the counter ions in their structures. This structure brings about a pH-independent swelling of QPM. Unfortunately, the disadvantages of QPM films are poor mechanical properties and limited film permeability. The mechanical properties of QPM films can be improved by incorporating water-soluble or water-insoluble plasticizers, which enhance the flexibility of the films[4]. Moreover, the drug permeability of the QPM films can be modified by adding certain anionic hydrophilic polymers, such as pectin[5] and sodium alginate[6] (SA), which interact with QPM via electrostatic forces. These compounds can reduce the hydration and swelling of QPM films, resulting in decreased drug diffusion across the film.

SA, a negatively charged biopolysaccharide, is extracted from brown seaweed. It is composed of alternating blocks of $1 \rightarrow 4$ linked α-L-guluronic acid (G block) and β-D-mannuronic acid (M block). SA can be used to fabricate drug delivery systems, such as matrix dosage forms[7–9], beads[10] and controlled-release capsules[11], and can also be applied as a film-forming agent[12]. In a previous study, SA was able to incorporate into the QPM dispersion, and the molecular interactions between them caused QPM–SA flocculates. The composite dispersions were cast and dried, resulting in a continuous film. SA incorporation into the QPM films caused a change of thermal properties, an increase in film strength, a decrease in film tackiness and an alteration of drug permeability[6].

However, SA has a unique molecular structure characteristic between the G block and M block. The block structure of SA strongly influences the characteristics of drug delivery systems, such as films[13], beads[14], matrix tablets[8,15] and microparticles[16]. Consequently, the objective of this study was to investigate the effect of SA block structures, high G block and high M block SA (GSA and MSA, respectively) on the physicochemical properties, mechanical properties, water uptake and erosion, and drug permeability of QPM–SA films. In addition, QPM–SA dispersions were used as film coating materials to modify drug release from tablets using propranolol HCl (PPN) as a model drug. The effects of the QPM–SA ratio, film-coating level and SA block structure on PPN release from the coated tablets were characterized.

## Materials and methods

### Materials

QPM in an aqueous-dispersion form (Eudragit® RL 30D) was purchased from RöhmPharma GmbH (Darmstadt, Germany). GSA (ratio of M/G = 0.59) and MSA (ratio of M/G = 1.50) were

Address for correspondence: Thaned Pongjanyakul, Faculty of Pharmaceutical Sciences, Khon Kaen University, Khon Kaen, Thailand. E-mail: thaned@kku.ac.th

obtained from ISP Thailand Ltd. (Bangkok, Thailand). Diethyl sebacate and PPN were purchased from Aldrich Chemistry (Dorset, UK) and Changzhou Yabang Pharmaceutical Co., Ltd. (Jiangsu, China), respectively. Microcrystalline cellulose (Ceolus® PH102, Siam Chem-Pharm (1997) Co., Ltd., Bangkok, Thailand), spray-dried lactose (FlowLac® 100, Thai Meochems Co., Ltd., Bangkok, Thailand), magnesium stearate (Mallinckrodt Inc., St. Louis, MO) and colloidal silicon dioxide (Aerosil® 200, Degussa Japan Co., Ltd., Japan) were used as tablet excipients. All other reagents used were of analytical grade and used as received.

### Preparation of QPM–SA films

The QPM and QPM–SA films were prepared using a casting/solvent evaporation method. Twenty grams of the QPM dispersions (30%w/w polymer solid content) were weighed and then mixed with diethyl sebacate (0.9 g, 15%w/w QPM), which was used as a plasticizer. The mixed dispersion was stirred for 30 min. Then, a different volume of 2%w/v SA dispersion was mixed with the QPM dispersion to obtain QPM–SA ratios of 4:0, 4:0.1, 4:0.25, 4:0.5 and 4:1 by weight. The QPM–SA dispersions were stirred for 30 min and then adjusted to a final volume of 150 ml using deionized water before being incubated in a water bath at 37 °C with shaking at 75 oscillations $min^{-1}$ for 24 h. Afterward, the QPM–SA dispersions (150 ml) were degassed, poured into Teflon® plates (17 cm × 18 cm) and dried at 50 °C for 48 h. The dry films were peeled off and stored in desiccators until further use.

### QPM–SA film characterization

*Film thickness determination*

The film thicknesses were measured at 15 different locations using a microprocessor coating-thickness gauge (Minitest 600B, ElektroPhysik, Germany). The films were placed on a control plate. The probe was calibrated using a standard film prior to the measurement. Then, the probe was slowly moved downward to contact the film surface and the film thickness was recorded.

### ATR-FTIR spectroscopy

The spectra of the QPM, SA and QPM–SA films were recorded using an ATR-FTIR spectrophotometer (Spectrum One, Perkin Elmer, Norwalk, CT). Each sample was cut and placed on a ZnSe prism as a sample holder and run from 4000 to 650 $cm^{-1}$ at a resolution of 4 $cm^{-1}$.

### Differential scanning calorimetry

The differential scanning calorimetry (DSC) thermograms of the films were recorded using a differential scanning calorimeter (DSC822, Mettler Toledo, Switzerland). Accurately weighed samples (2–3 mg) were placed in a 40-µl aluminum pan without an aluminum cover. The measurement was performed using a heating rate of 10 °C $min^{-1}$ in the temperature range of 30–450 °C.

### Study of mechanical properties

The puncture strength and elongation of the dry and wet films were measured using a texture analyzer (TA-XT2, Stable Micro Systems, Ltd., UK) equipped with a 500-N standard load cell. The dry films were cut to 2 cm × 2 cm and stored in a humidity-controlled chamber at 55% RH and 25 °C for 3 days prior to the test. For the wet films, the films were immersed in a pH 6.8 phosphate buffer or 0.1 M HCl and were occasionally shaken at 37 °C for 30 min. The wet films were blotted to remove excess water prior to the measurements. The dry or wet films were placed in the film holder between two mounting plates and the holding screws were subsequently tightened to prevent slippage of the films. A 6-mm diameter spherical stainless puncturing probe was fixed to the load cell. Then, the probe was gently moved through the film with a cross-head speed of 0.1 mm $s^{-1}$. The maximum force at film puncture and the maximum displacement were recorded and then converted to puncture strength and % elongation. The parameters were calculated using the following equations:

$$\text{Puncture strength} = \frac{F}{A} \tag{1}$$

where $F$ is the maximum force for film puncture and $A$ is the cross-sectional area of the edge of the film located in the path of the cylindrical opening of the film holder.

$$\text{Elongation } (\%) = \frac{\sqrt{r^2 + D^2} - r}{r} \times 100 \tag{2}$$

where $r$ is the radius of the film exposed in the cylindrical hole of the film holder and $D$ is the displacement of the probe from the point of contact to the point of film puncture.

### Water uptake and erosion of films

The water uptake and erosion of the films were determined using a gravimetric method. The films (1 cm × 1 cm) were weighed ($W_0$) and then soaked in 0.1 M HCl or pH 6.8 phosphate buffer and were then incubated at 37 °C and occasionally shaken. After a predetermined time interval, each film was withdrawn, blotted to remove excess water, immediately weighed ($W_t$) and then dried in a hot air oven at 50 °C for 3 days to reach a constant weight ($W_d$). The water uptake and erosion of the films were calculated from the following equations[17]:

$$\text{Water uptake } (\%) = \left(\frac{W_t - W_d}{W_d}\right) \times 100 \tag{3}$$

$$\text{Erosion } (\%) = \left(\frac{W_0 - W_d}{W_0}\right) \times 100 \tag{4}$$

where $W_0$, $W_t$ and $W_d$ are the original, wet and dry weights of the films, respectively.

### Drug permeability studies

Drug permeability studies were performed using a side-by-side diffusion cell (Crown Glass Co., Inc., Somerville, NJ) at 37 °C. Phosphate buffer at pH 6.8 or 0.1 M HCl was used as the receptor phase in this study. The films (2 cm × 2 cm) were hydrated in the medium for 30 min and then clamped between the donor and receptor compartments, which had a 3-ml volume and a diffusion area of 0.66 $cm^2$. PPN solution (4 mg $ml^{-1}$) was placed in the donor compartment, and the receptor compartment contained 3 ml of medium. Both compartments were continuously stirred throughout the tests. At predetermined intervals, 2.6 ml of medium in the receptor compartment was collected and replaced with an equal volume of fresh medium. The PPN concentration in the collected samples was measured via UV spectroscopy (Shimadzu UV1201, Kyoto, Japan) at a wavelength of 289 nm.

Drug permeation through the films was determined under steady-state conditions using Fick's first law, which can be expressed as follows[18]:

$$\frac{dQ}{Adt} = PC_0 \tag{5}$$

where $dQ/Adt$ is the permeation flux (the slope calculated using linear regression analysis of the relation between the amount of

drug permeated per surface area of the films ($A$) and time). $C_0$ is the concentration of drug in the donor compartment and $P$ is the permeability coefficient. The apparent diffusion coefficient ($D$) was estimated from the following equation:

$$t_L = \frac{h^2}{6D} \quad (6)$$

where $t_L$ is the lag time that was obtained from the $x$ intercept of the permeation profiles and $h$ is the mean thickness of the wet films.

### Preparation and evaluation of core tablets

PPN core tablets were prepared using a direct compression method. The tablets consisted of PPN (20.0%), microcrystalline cellulose (28.0%), spray-dried lactose (49.7%), colloidal silicon dioxide (0.3%) and magnesium stearate (2.0%, all percentages are by weight). The drug powder, microcrystalline cellulose, spray-dried lactose and colloidal silicon dioxide were mixed using a Y-shape mixer for 30 min. Then, magnesium stearate was incorporated into the mixture for 5 min before tablet formation. A 10-mm biconvex punch and die were used. Core tablets were compressed using a single punch machine (Yeo Heng Co., Ltd, Bangkok, Thailand). The tablet hardness of the core tablets was $89.4 \pm 4.9$ N ($n = 10$). The average weight PPN core tablets obtained were $399.8 \pm 0.31$ mg/tablet ($n = 20$). The friability of both core tablets was less than 1.0%. The PPN content in the core tablets was extracted using 0.1 M HCl and measured via UV spectrophotometry (Shimadzu UV1201, Kyoto, Japan) at a wavelength of 289 nm. The core tablets contained $80.5 \pm 1.56$ mg/tablet ($n = 3$) PPN.

### Core tablet coating

The QPM–SA dispersions that were prepared using various QPM–MAS ratios were used as coating materials. The QPM–SA dispersions were prepared using the method previously mentioned in Section ''Preparation of QPM–SA films''. The core tablets obtained were coated using a side-vented pan coating machine (Thai Coater Model FC15, Pharmaceuticals and Medical Supply, Bangkok, Thailand). The core tablets (1000 g) were warmed in the coating pan under an inlet temperature of 57–60 °C and the coating pan was rotated at a rate of 6–7 revolutions $min^{-1}$. The spray rate of the coating dispersions was 8 ml $min^{-1}$ under 0.38 mPa spray pressure. After the coating process, the coated tablets were stored in a desiccator prior to further examination.

The effect of the QPM–GSA ratio on the coated tablet characteristics was investigated. The core tablets were coated with QPM–GSA films at ratios of 4:0, 4:0.1, 4:0.25, 4:0.5 and 4:1 at a mean coating level of 4% weight gain. To investigate the effect of film-coating level, the core tablets were coated with QPM–GSA (4:1) films at the mean coating levels of 4%, 8% and 12% weight gain. Moreover, a comparative study of the QPM–GSA- and QPM–MSA-coated tablets was performed using a QPM–SA ratio of 4:0.5 and a film-coating level of 4% weight gain.

### Evaluation of coated tablets

*Scanning electron microscopy*

The surface and film matrix morphology of the coated tablets was observed using scanning electron microscopy (SEM). The coated tablets and cross-sections of tablets were mounted onto stubs, coated with gold in a vacuum evaporator and investigated using a scanning electron microscope (Hitachi S-3000N, Tokyo, Japan).

*In vitro release studies*

Drug release from the coated tablets was characterized using a USP dissolution apparatus I (basket method). The dissolution media were 900 ml 0.1 M HCl or pH 6.8 phosphate buffer at $37.0 \pm 1.0$ °C. The baskets were rotated at a rate of 50 revolutions $min^{-1}$. At predetermined intervals, samples were collected and replaced with an equal volume of fresh medium. The concentration of PPN released was assayed using a UV–visible spectrophotometer (Shimadzu UV1201, Kyoto, Japan) at a wavelength of 289 nm.

The PPN release data of the coated tablets were evaluated using zero-order release kinetics because the drug release of the coated tablets could be mainly controlled via the coated films[19], as shown in Equation (7):

$$Q = K_0 t + B \quad (7)$$

where $Q$ is the amount of PPN released (%), $t$ is the time and $K_0$ is the zero-order release rate. $B$ is a constant value. The lag time of PPN released from the coated tablets can be calculated using Equation (7) when $Q$ equals zero. This equation was used to calculate the release parameters when the PPN released was less than 50% of the PPN content. Additionally, this release model can provide both parameters, drug release rate and lag time, for comparison in this study.

*Water uptake of coated tablets*

The water uptake of the coated tablets in both 0.1 M HCl and pH 6.8 phosphate buffer was determined using a USP dissolution apparatus I (basket) and the test conditions were the same as in the drug release study. The coated tablets were weighed ($W_i$), placed into baskets and immersed into the medium. At predetermined intervals, the wet coated tablets were collected, carefully blotted with tissue paper to remove surface water and weighed ($W_c$). The water uptake of the coated tablets can be calculated as follows[19]:

$$\text{Water uptake } (\%) = \left(\frac{W_c - W_i}{W_i}\right) \times 100 \quad (8)$$

## Results and discussion

### Film appearance and molecular interaction of QPM and SA

Generally, QPM films without plasticizers are hard and brittle, which led to the use of diethyl sebacate (15% w/w of QPM) as a plasticizer in this study. Consequently, transparent QPM films were obtained. The incorporation of SA into the QPM films also resulted in transparent and continuous films for all investigated SA contents. Successful QPM–SA film formation may be attributed to the film-forming property of SA (both GSA and MSA), which can form continuous films, coupled with QPM particle coalescence. The QPM–SA films had a similar appearance using GSA or MSA. Moreover, the thicknesses of the QPM–GSA and QPM–MSA films at various ratios were not different, as shown in Table 1. However, increasing SA content in the films caused an increase in film thickness due to higher solid content in the dispersions used for film casting[20].

The molecular interaction between QPM and GSA or MSA in the films was investigated using ATR-FTIR spectroscopy. The spectrum of the QPM film exhibited C=O stretching, $CH_2$ symmetric bending, $CH_3$ asymmetric bending, C–CO–C stretching and C–O–C stretching at approximately 1725, 1447, 1381, 1148 and 1023 $cm^{-1}$, respectively (Figure 1a).

Table 1. Thickness and mechanical properties of QPM–SA films.

| Film | Thickness[a] (μm) | Puncture strength[b] (MPa) | | | Elongation[b] (%) | | |
|---|---|---|---|---|---|---|---|
| | | Dry film | Wet film (0.1 M HCl) | Wet film (pH 6.8 phosphate buffer) | Dry film | Wet film (0.1 M HCl) | Wet film (pH 6.8 phosphate buffer) |
| QPM–GSA | | | | | | | |
| 4:0 | 215.6 ± 29.8 | 7.97 ± 1.47 | 0.95 ± 0.20 | 1.28 ± 0.19 | 115.2 ± 7.85 | 312.4 ± 26.7 | 228.8 ± 17.2 |
| 4:0.1 | 151.8 ± 28.3 | 8.07 ± 1.53 | 1.02 ± 0.11 | 1.05 ± 0.06 | 78.02 ± 12.1 | 87.31 ± 4.88 | 213.9 ± 7.38 |
| 4:0.25 | 187.8 ± 11.4 | 10.06 ± 1.65 | 1.34 ± 0.17 | 1.56 ± 0.10 | 69.60 ± 39.7 | 56.56 ± 3.95 | 200.1 ± 3.87 |
| 4:0.5 | 219.7 ± 29.7 | 12.83 ± 2.57 | 1.83 ± 0.32 | 0.65 ± 0.10 | 46.74 ± 5.25 | 44.06 ± 2.23 | 56.81 ± 5.92 |
| 4:1 | 237.9 ± 25.7 | 12.43 ± 1.69 | 1.54 ± 0.23 | ND | 37.29 ± 8.66 | 41.04 ± 17.5 | ND |
| QPM–MSA | | | | | | | |
| 4:0 | 215.6 ± 29.8 | 7.97 ± 1.47 | 0.95 ± 0.20 | 1.28 ± 0.19 | 115.2 ± 7.85 | 312.4 ± 26.7 | 228.8 ± 17.2 |
| 4:0.1 | 184.8 ± 23.9 | 6.48 ± 0.77 | 0.73 ± 0.08 | 1.33 ± 0.12 | 95.18 ± 8.34 | 138.3 ± 17.1 | 202.9 ± 19.2 |
| 4:0.25 | 192.5 ± 19.1 | 6.27 ± 0.75 | 0.80 ± 0.11 | 0.71 ± 0.13 | 65.16 ± 15.0 | 73.22 ± 8.15 | 132.1 ± 7.85 |
| 4:0.5 | 196.3 ± 49.9 | 7.97 ± 1.25 | 1.05 ± 0.16 | 0.50 ± 0.02 | 58.47 ± 6.15 | 58.86 ± 9.09 | 81.97 ± 8.71 |
| 4:1 | 247.2 ± 59.2 | 7.46 ± 0.46 | 0.92 ± 0.22 | ND | 27.88 ± 2.00 | 35.37 ± 11.9 | ND |

ND = could not be determined.
[a]Data are mean ± S.D., $n = 15$.
[b]Data are mean ± S.D., $n = 5$.



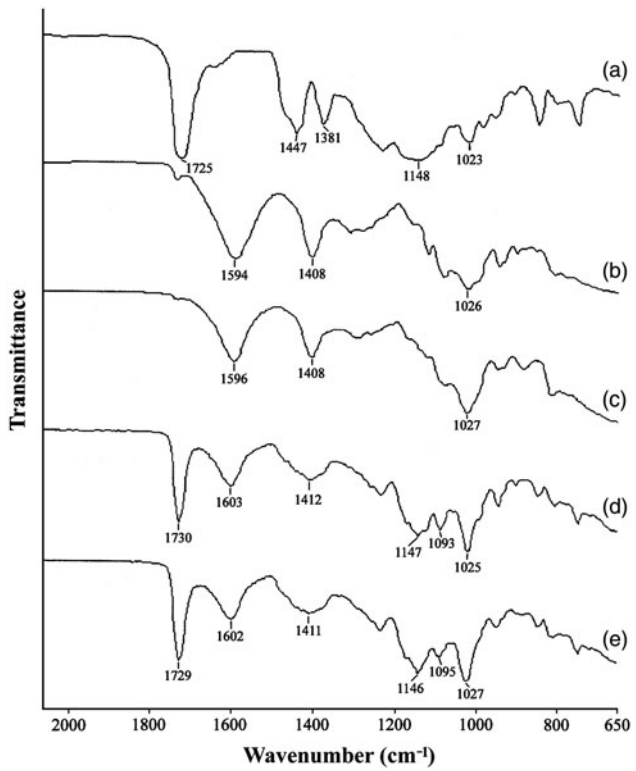


Figure 1. ATR-FTIR spectra of QPM film (a), GSA film (b), MSA film (c), QPM–GSA (1:1) film (d) and QPM-MSA (1:1) film (e).

The ATR-FTIR spectra of the GSA and MSA films had similar stretching peaks, i.e. $COO^-$ (symmetric), $COO^-$ (asymmetric) and C–O–C at approximately 1594–1596, 1408 and 1026–1027 $cm^{-1}$, respectively (Figure 1b and c). The QPM films with SA (GSA and MSA) showed a shift in the $COO^-$ (asymmetric) stretching peak of SA to a higher wavenumber, which was in the range of 1602–1603 $cm^{-1}$ (Figure 1d and e). The QPM–SA films also exhibited the $COO^-$ (symmetric) stretching peak of SA at 1411–1412 $cm^{-1}$ (Figure 1d and e), which was shifted from 1408 $cm^{-1}$ (Figure 1b and c). These shifts indicated that the SA carboxyl groups interacted with positively charged molecules via an electrostatic interaction[21,22]. Remarkably, a new peak, corresponding to C–N stretching at 1093–1095 $cm^{-1}$, was observed, and the C=O stretching (1725 $cm^{-1}$) of QPM shifted to a higher wavenumber at 1729–1730 $cm^{-1}$ (Figure 1d and e), suggesting an electrostatic and hydrogen bonding formation between QPM and SA, respectively. These results suggest that the quaternary ammonium groups of QPM electrostatically interact with the carboxyl groups of SA. Additionally, the carbonyl groups of QPM and hydroxyl groups of SA also could form intermolecular hydrogen bonds. Furthermore, GSA and MSA could interact with QPM via the same mechanism.

## Thermal behavior of the films

The first exothermic peak of the GSA and MSA films were approximately 258 and 250 °C, respectively (Figure 2), indicative of the first degradation of SA. Then, the second degradation peak of both films occurred at approximately 362–363 °C. The QPM films exhibited an endothermic peak at approximately 340 °C, followed by an exothermic degradation peak at 380 °C. The thermal behavior of the QPM–SA films at ratios of 4:0.1 and 4:0.25 displayed a shift of the QPM degradation peak toward lower temperatures, suggesting that the SA disturbed the film-structure formation of the QPM. In addition, the QPM–SA films that had higher amounts of SA (4:0.5 and 4:1) obviously showed both degradation peaks of SA, without the degradation peak of the QPM films. The GSA and MSA added to the QPM films exhibited similar effects on the thermal behavior of the QPM–SA films. These results suggested that SA at lower amounts was able to induce QPM degradation. When using higher amounts of SA, the appearance of the SA degradation peaks indicated that phase separation of the SA in the microenvironment of the film may have occurred. This phenomenon could change the matrix structure and modify the characteristics of the QPM films.

## Film water uptake and erosion

The water uptake and erosion of the QPM–SA films in 0.1 M HCl and pH 6.8 phosphate buffer after 30 min are shown in Figure 3. In the acidic medium, the QPM–MSA films had remarkably higher water uptake than the QPM–GSA films (Figure 3a). The water uptake of the QPM–GSA films decreased with increasing GSA amounts, whereas increasing MSA amounts did not affect QPM–MSA film water uptake (Figure 3a). The matrix erosions of the QPM–MAS films were also greater than those of the QPM–GSA films (Figure 3c). Additionally, higher SA amounts in the

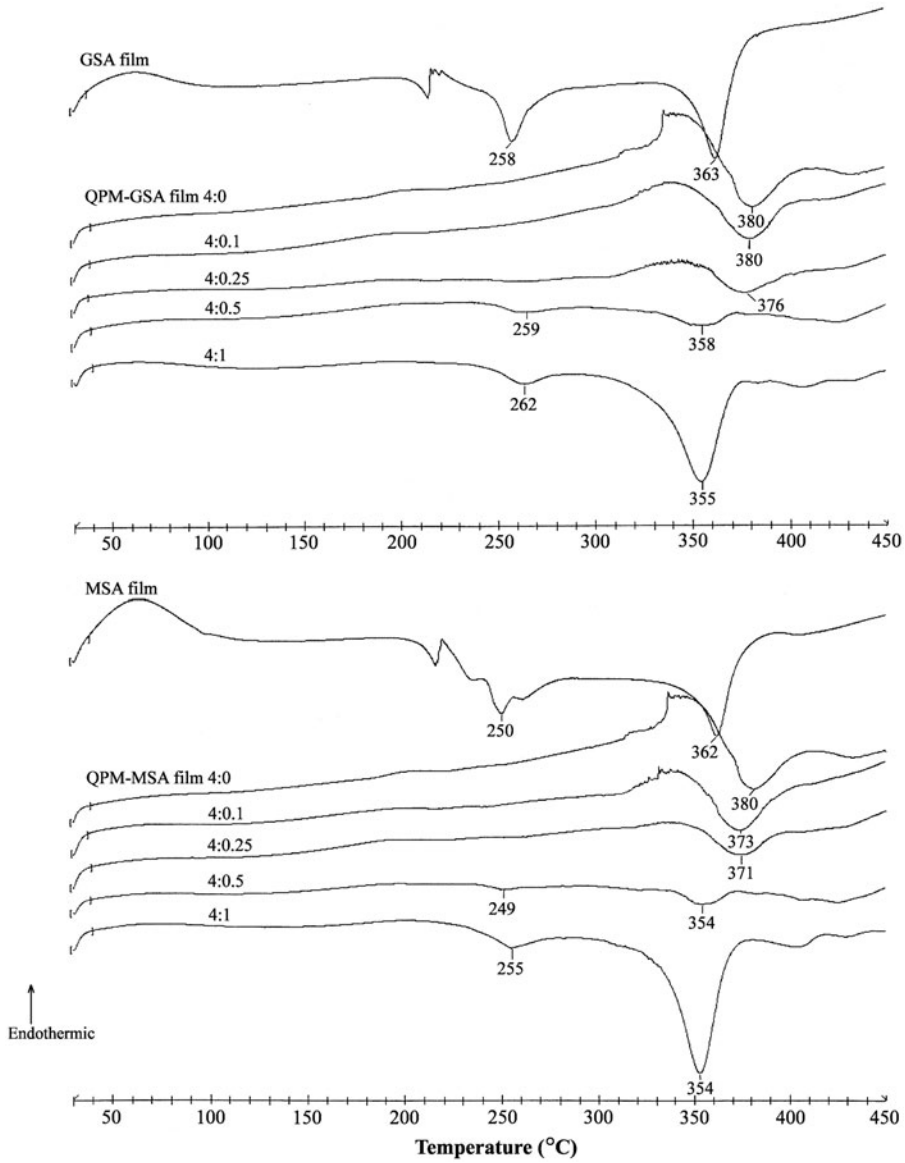


Figure 2. DSC thermograms of SA films, and QPM–SA films at different ratios of QPM and SA.

films increased matrix erosion. In fact, SA was changed to a water-insoluble alginic acid in acidic conditions[23]. In addition, GSA had a stronger gel structure of alginic acid than MSA[13,24], leading to decreased water uptake in the QPM–GSA films when the GSA amount was increased. This result could explain why the matrix erosions in the QPM–GSA films were lower than those of the QPM–MSA films.

In pH 6.8 phosphate buffer, the QPM–SA films demonstrated a clear decrease in water uptake in films that had increased QPM–SA ratios; the lowest water uptake was observed for QPM–SA ratios of 4:0.25 (Figure 3b). Then, increased QPM–SA ratios caused an increase in water uptake; the water uptake of films with an SA ratio of 4:1 could not be measured due to the very high swelling of the films, which could not be accommodated. The QPM–GSA films at the ratios of 4:0.1 and 4:0.5 had greater water uptake than the QPM–MSA films when compared at the same ratios. Apart from water uptake results, the erosion of the QPM–SA films gradually increased with increasing SA content (Figure 3d). It can be observed that the matrix erosion of the QPM–GSA films was higher than that of the QPM–MSA films (Figure 3d). From these results, it could be hypothesized that the SA in the films could rapidly swell and dissolve in pH 6.8 phosphate buffer[8,11], leading to an increase in the matrix erosion of the films. However, the decreased water uptake in the QPM–SA films at 4:0.1 and 4:0.25 ratios suggested a strong interaction between QPM and SA in the wet state because the SA molecules could fully disentangle in this medium, particularly in the films at a ratio of 4:0.25. This interaction resulted in the lower water uptake of the films. In addition, the QPM–SA (4:0.5) films demonstrated the influence of excess SA in the films, causing higher water uptake and matrix erosion. Furthermore, these results also suggest that GSA incorporation into the QPM films caused higher swelling than MSA, leading to greater water uptake and matrix erosion in the QPM–GSA films.

## Mechanical properties of the films

The puncture strength and elongation of the dry and wet QPM–SA films are listed in Table 1. The dry QPM–GSA films had an obviously higher puncture strength than the dry QPM–MSA films at increased SA ratios, whereas the % elongations were not different. Moreover, increased GSA ratios enhanced the puncture strength of the wet films when using 0.1 M HCl. This effect did not occur for MSA, which had comparable puncture strengths with increasing MSA amounts. However, the QPM–GSA and QPM–MSA films had decreased % elongation with increasing SA

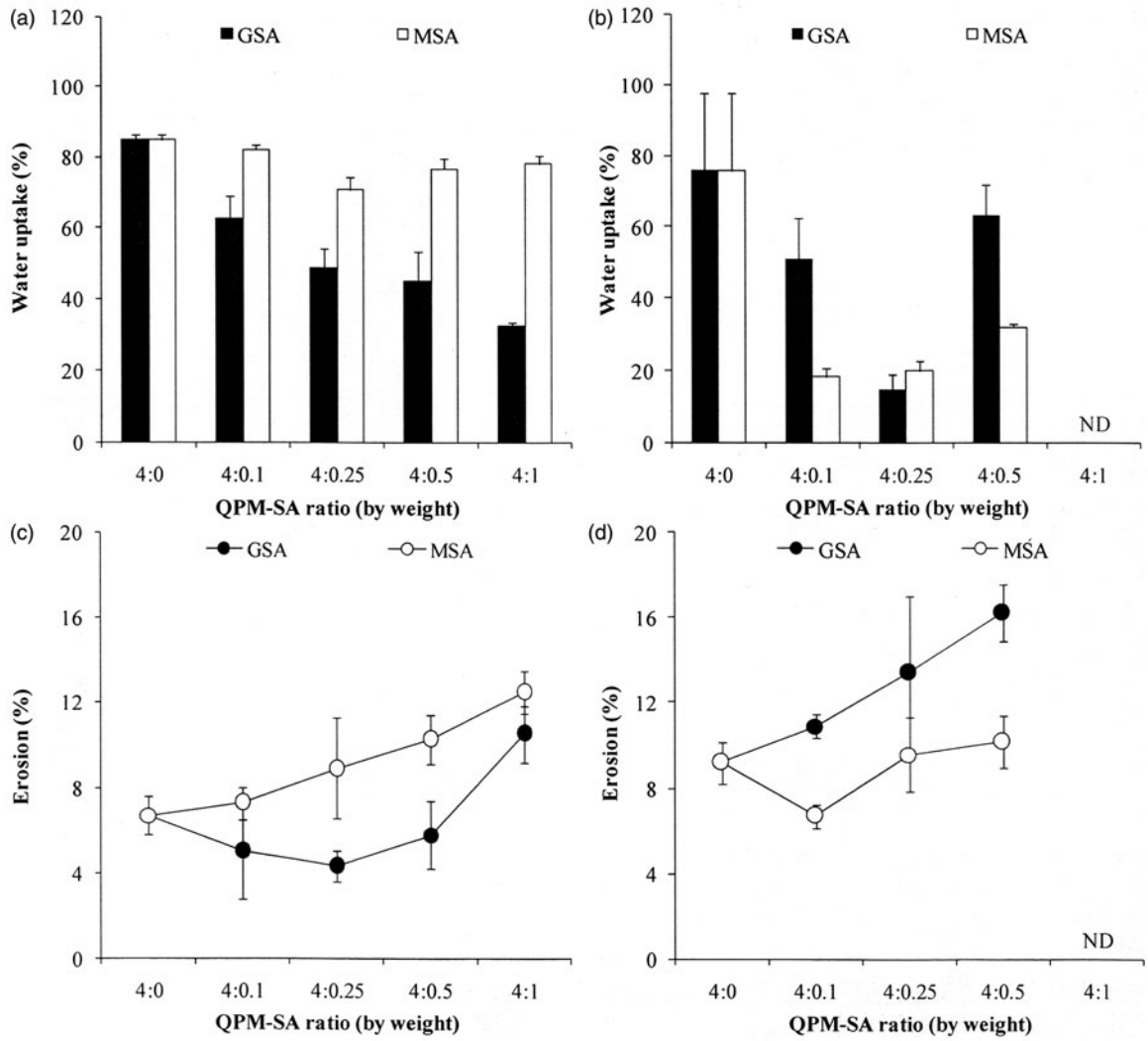


Figure 3. Water uptake and erosion of QPM–SA films using 0.1 M HCl (a, c) and pH 6.8 phosphate buffer (b, d) at 30 min. Each value is mean ± S.D., $n = 5$.

ratios in 0.1 M HCl. Using pH 6.8 phosphate buffer, the puncture strength of the QPM–GSA films remarkably decreased when using a QPM–GSA ratio of 4:0.5, whereas decreased puncture strength in the QPM–MSA films was observed for the 4:0.25 ratio. The % elongation of the QPM–SA films rapidly decreased when using the 4:0.5 ratio in neutral medium. Furthermore, the 4:1 ratio films could not be properly handled; therefore, their puncture strength and % elongation could not be determined. In addition, the % elongations of the films in neutral medium were higher than in acidic medium.

In addition to the coalescence process of the QPM particles, SA that was dispersed and interacted with the QPM particles was still able to form a continuous matrix. This is likely due to the film-forming property of SA. In the dry state, GSA enhanced the mechanical strength of the QPM films compared with MSA. This result suggests that GSA may have a stronger interaction with QPM than does MSA. However, the stronger matrix of the films was usually accompanied by lower film flexibility[25], which is evident in this study. For the QPM–SA films at acidic pH, the puncture strength of the QPM–GSA films was higher than the QPM–MSA films due to the stronger alginic acid gel of GSA[13,24]. However, the alginic acid that was embedded in the film matrix enhanced the film strength but decreased the flexibility of the films.

As expected, SA was able to ionize and swell in the neutral pH medium, resulting in considerable swelling of the films when higher SA ratios were used (4:0.5 and 4:1). This behavior could explain the clear decrease that was observed in both parameters and the inability to measure the films with the highest SA content used in this study. However, for the QPM–GSA films, the strength was clearly decreased when using GSA at a 4:0.5 ratio, whereas the 4:0.25 ratio of MSA caused decreased film strength. This result also suggested that GSA may interact with QPM via a stronger electrostatic force when compared with MSA because the chain conformation of GSA may promote the interaction with QPM. In addition, disentanglement of the SA may enhance film flexibility at neutral pH. Collectively, this result indicated that the interaction between QPM and SA can strengthen the films in both the dry and wet states, particularly GSA. This could be a major advantage for the use of such films as a coating material for solid dosage forms that are intended to modify drug release in the gastrointestinal tract.

## Drug permeability of the films

The cumulative PPN permeation profiles across the QPM–SA films using 0.1 M HCl and pH 6.8 phosphate buffer exhibited good linearity ($R^2$ higher than 0.98) with a lag time. The permeation parameters of PPN across the films were able to be computed using Equations (5) and (6), as shown in Figure 4. In 0.1 M HCl, the QPM–GSA films had a longer lag time at increasing GSA ratios. In contrast, a higher ratio of MSA in the

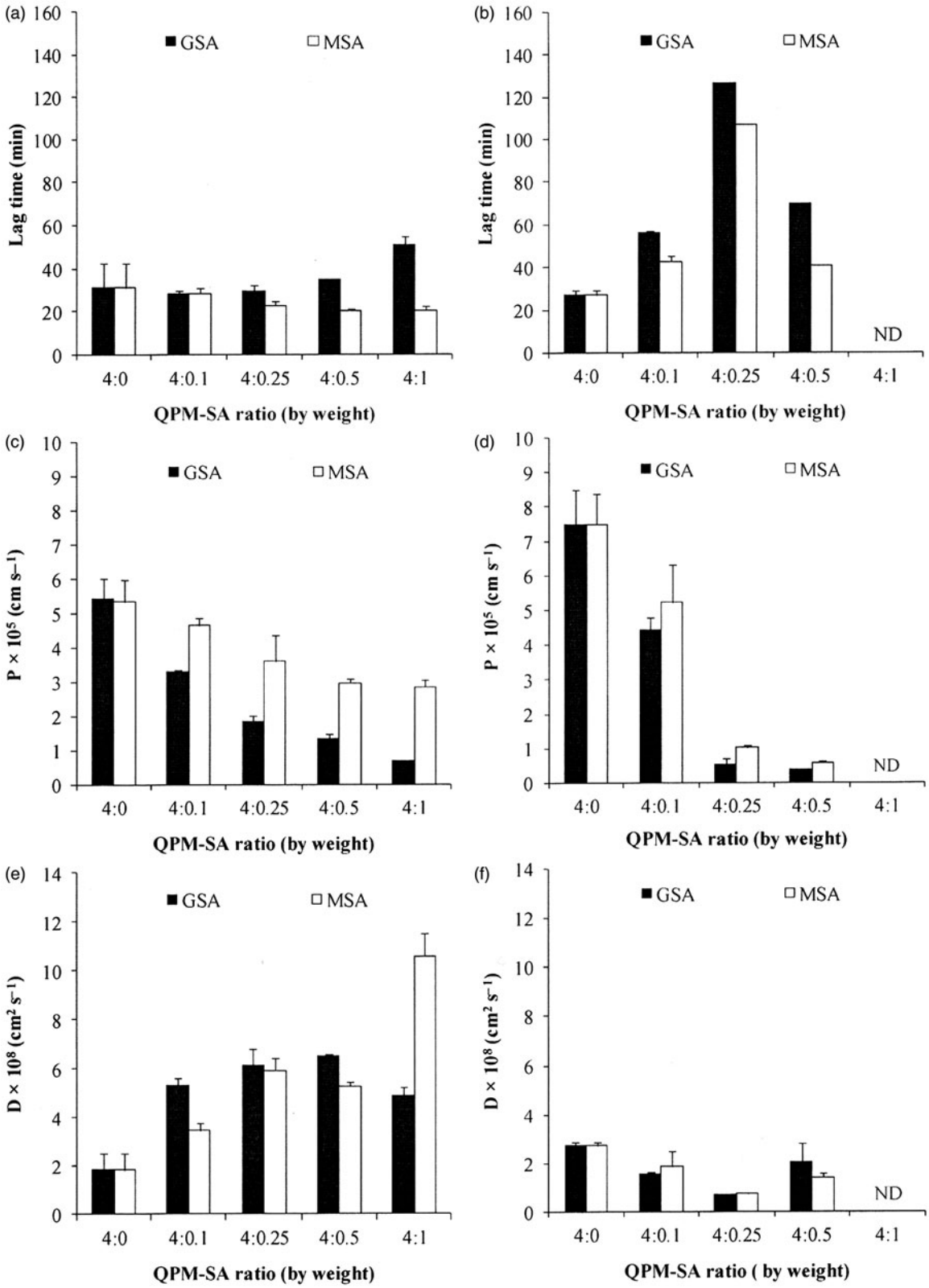


Figure 4. Lag time (a, b), permeability coefficient (c, d) and diffusion coefficient (e, f) of QPM–SA films using 0.1 M HCl (a, c, e) and pH 6.8 phosphate buffer (b, d, f). Each value is mean ± S.D., $n = 3$.

films caused a shorter lag time (Figure 4a). The QPM–GSA films had longer lag times than the QPM–MSA films at ratios higher than 4:0.25. The *P* values of the QPM–MSA films were lower than those of QPM–GSA, and this value decreased with increasing SA ratios (Figure 4c). The reduction of the *P* values of the QPM–SA films may be resulted in the increase of film thickness, thus the *D* values were calculated by using Equation (6) for comparison of drug permeation. The *D* values appeared to increase with increasing SA ratios (Figure 4e). However, the QPM–GSA film had a remarkably smaller *D* value than the QPM–MSA film at a ratio of 4:1. This result indicated that the incorporation of SA into the QPM films led to lower drug

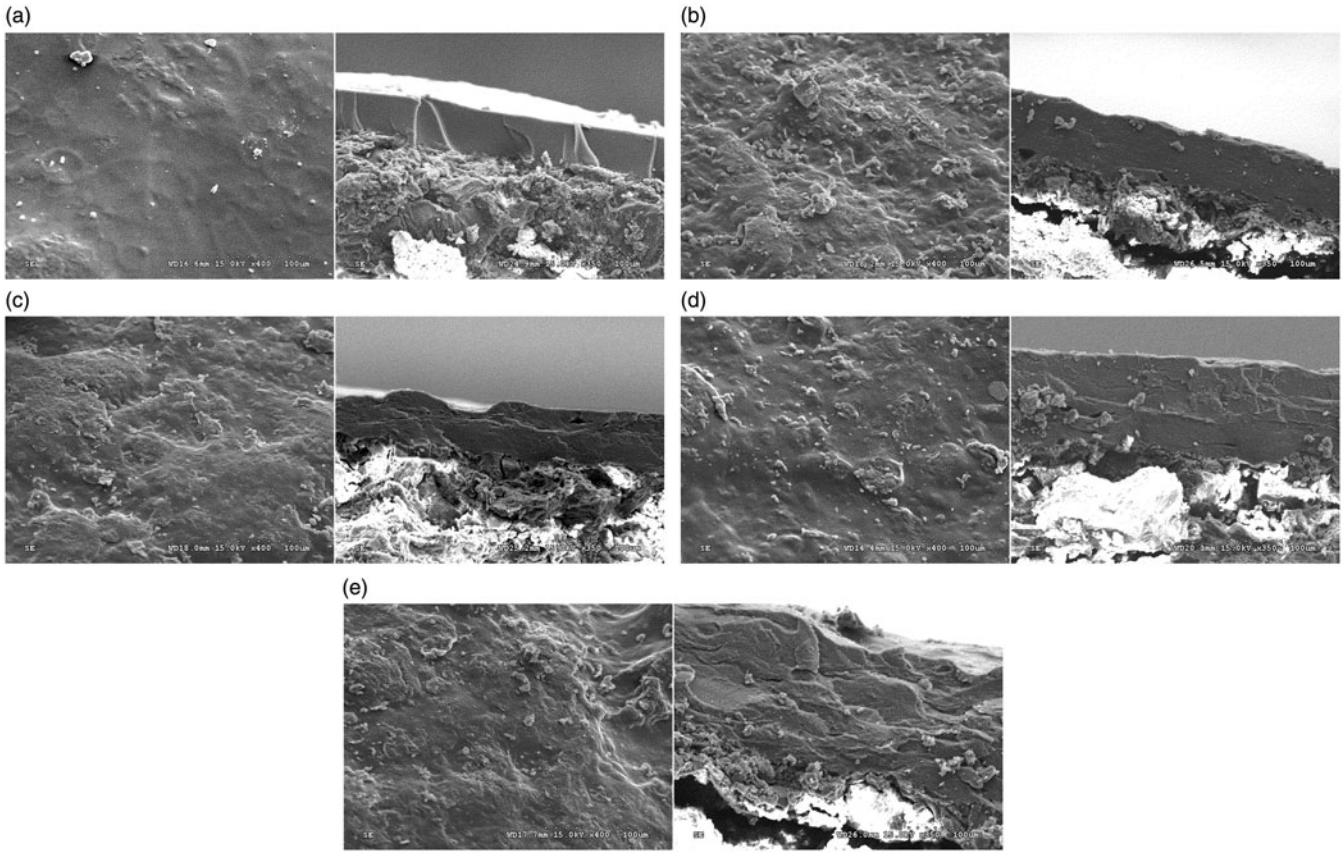


Figure 5. Surface and film matrix morphology of PPN tablets coated with QPM film (4% coating level) (a), QPM–GSA (4:0.5) film (4% coating level) (b) and QPM–GSA (4:1) films at 4% (c), 8% (d) and 12% (e) coating levels.

permeability but higher drug diffusion, particularly for the QPM–MSA films, which had the same water uptake with increasing MSA ratios. This result suggested that water-filled channels that have low tortuosity could possibly form when SA is converted to alginic acid in the acidic medium. The alginic acid that formed has weak intermolecular bonding[26], leading to low tortuosity of the aqueous channels in the films. However, the QPM–GSA (1:1) films had lower *D* values than the MSA films due to the formation of the strong alginic gel in the GSA film. Additionally, there was a stronger interaction between GSA and QPM, which also caused smaller water-filled channels that have higher tortuosity for drug diffusion. Furthermore, this hypothesis is supported by the water uptake results.

In neutral pH medium, the longest lag time of PPN permeation was observed in the QPM–SA films at a 4:0.25 ratio, and the QPM–MSA films had shorter lag times than the QPM–GSA films (Figure 4b). The *P* values decreased with increasing SA ratios (Figure 4d), and MSA had higher *P* values in the QPM films than GSA. However, the QPM–SA films prepared using GSA and MSA at various ratios had similar *D* values; the lowest *D* value was observed for the 4:0.25 ratio (Figure 4f). This is consistent with the observation that the QPM–SA films at this ratio had the smallest water uptake. The overall results in the neutral pH buffer demonstrated that the QPM–MSA films had higher drug permeability than the QPM–GSA films. However, similar drug diffusivity for both films was obtained, but the QPM–GSA films had greater water uptake and matrix erosion. It is expected that the QPM–GSA films may also have high tortuosity in their matrix structure after hydration and erosion due to the possibly stronger interaction of GSA with QPM, which may cause the similar barrier properties for drug diffusion in the QPM–GSA and QPM–MSA films.

## Characteristics of the QPM–GSA-coated tablets

The QPM–GSA dispersions at various ratios were used as coating materials to modify PPN release. Moreover, PPN core tablets coated with the QPM–GSA (4:1) film at different coating levels were also prepared. An issue for tablet coating occurred when using the QPM–GSA dispersions at the ratios of 4:0.1 and 4:0.25. The incorporation of GSA into the QPM dispersions decreased the zeta potential of the positively charged QPM particles, which caused the formation of QPM–GSA flocculates[6]. The flow of these dispersions in a small tube before spraying caused an induction of larger flocculates, leading to nozzle clogging. Therefore, these dispersions were only able to be coated onto the core tablets at the 4% coating level. However, the 4:0.5 and 4:1 ratio QPM–GSA dispersions did not cause nozzle clogging because GSA was able to interact with QPM causing the zeta potential of the flocculates to become negative. This phenomenon led to a strong repulsion force in the flocculates and the dispersion had good stability.

The surface and film matrix morphologies of the QPM-coated tablets are shown in Figure 5(a). A rougher surface of the coated tablets was observed when GSA was added into the films at ratios of 4:0.5 and 4:1 (Figure 5b and c, respectively), but the coated films had similar matrix morphologies. Moreover, increased coating levels corresponded to increased film thickness on the coated tablets, as shown in Figure 5(c–e).

## Effect of QPM–GSA ratios and coating levels on PPN released from the coated tablets

The PPN release profiles of the QPM–GSA-coated tablets (4% coating level) at different QPM–GSA ratios in 0.1 M HCl and pH 6.8 phosphate buffer are presented in Figure 6(a) and (b),

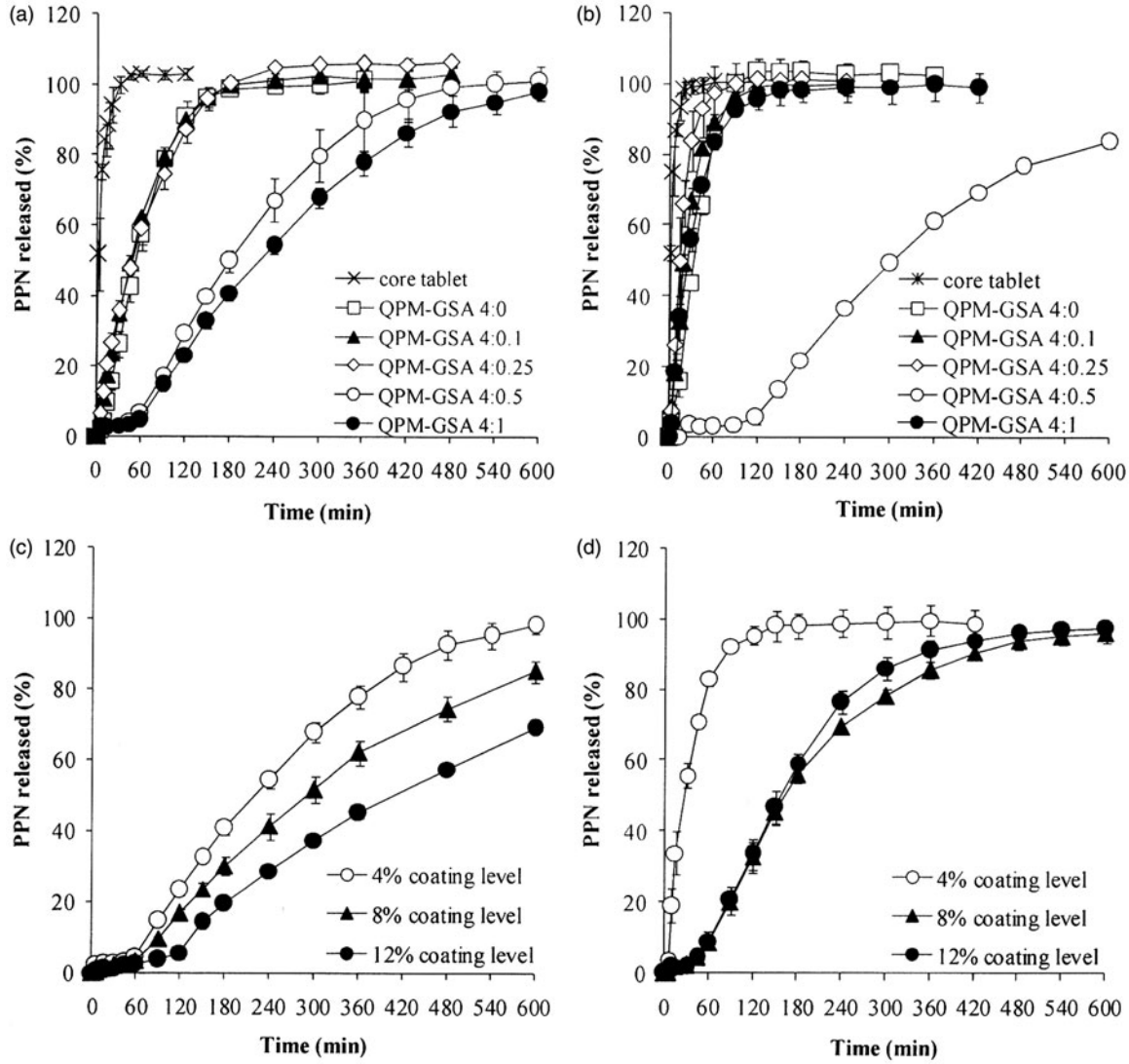


Figure 6. PPN release profiles of PPN tablets coated with different QPM–GSA ratios at 4% coating level (a, b) and different coating levels of QPM–GSA at the ratio of 4:1 (c, d) in 0.1 M HCl (a, c) and pH 6.8 phosphate buffer (b, d). Each point is mean ± S.D., $n = 3$.

Table 2. Lag time and PPN release rate of QPM–GSA-coated tablets with different QPM–GSA ratios and film-coating levels in 0.1 M HCl and pH 6.8 phosphate buffer.

| | | 0.1 M HCl | | pH 6.8 phosphate buffer | |
|---|---|---|---|---|---|
| QPM–GSA film | Coating level (%) | Lag time (min) | $K_0$ (% min$^{-1}$) | Lag time (min) | $K_0$ (% min$^{-1}$) |
| 4:0 | 4 | 5.64 ± 1.63 | 1.06 ± 0.08 ($R^2 = 0.998$) | 2.58 ± 0.21 | 1.54 ± 0.05 ($R^2 = 0.994$) |
| 4:0.1 | 4 | ND | 1.02 ± 0.05 ($R^2 = 0.994$) | ND | 2.67 ± 0.14 ($R^2 = 0.986$) |
| 4:0.25 | 4 | ND | 0.84 ± 0.09 ($R^2 = 0.995$) | ND | 3.88 ± 0.98 ($R^2 = 0.985$) |
| 4:0.5 | 4 | 39.93 ± 2.71 | 0.36 ± 0.02 ($R^2 = 0.997$) | 89.17 ± 8.97 | 0.23 ± 0.01 ($R^2 = 0.995$) |
| 4:1 | 4 | 42.49 ± 4.38 | 0.30 ± 0.02 ($R^2 = 0.995$) | 2.74 ± 0.35 | 2.69 ± 0.49 ($R^2 = 0.981$) |
| 4:1 | 8 | 45.22 ± 2.15 | 0.22 ± 0.02 ($R^2 = 0.999$) | 36.10 ± 5.55 | 0.39 ± 0.01 ($R^2 = 0.996$) |
| 4:1 | 12 | 50.07 ± 3.62 | 0.15 ± 0.01 ($R^2 = 0.998$) | 37.22 ± 6.22 | 0.41 ± 0.01 ($R^2 = 0.997$) |

Data are mean ± S.D., $n = 3$. ND = could not be determined.

respectively. The dissolution of PPN from the core tablets in both media was completed within 30 min. The QPM- or QPM–GSA-coated tablets had slower PPN release rates than the core tablets. The parameters used for PPN release rate comparisons were lag time and zero-order release rate ($K_0$). The relationship between % PPN released and time had good linearity with an $R^2$ higher than 0.98 when drug release was less than 50%. Therefore, the lag times and $K_0$ values were calculated and are listed in Table 2.

The PPN tablets coated with the QPM–GSA films at ratios of 4:0.1 and 4:0.25 had similar drug release profiles in acidic medium, and the $K_0$ values appeared to decrease with increasing GSA ratios. However, the lag time of the QPM–GSA-coated

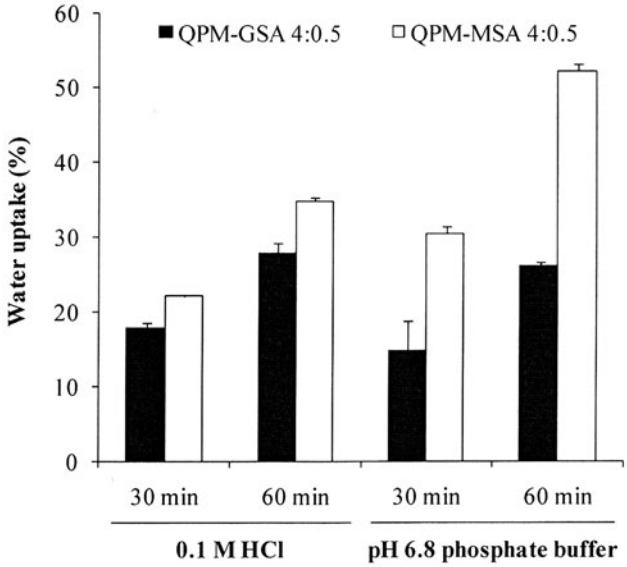


Figure 7. Water uptake of PPN tablets coated with QPM–GSA and QPM–MSA films at the ratio of 4:0.5 (4% coating level) in 0.1 M HCl and pH 6.8 phosphate buffer. Each value is mean ± S.D., $n = 3$.

tablets at ratios of 4:0.1 and 4:0.25 could not be determined. It is expected that PPN would rapidly release from the coated tablets at the initial stage of the release process. Additionally, longer lag times and lower PPN release rates were observed in the QPM–GSA tablets at ratios of 4:0.5 and 4:1, which were related to the GSA ratio. These results suggest that the QPM–GSA films at ratios of 4:0.5 and 4:1 could sustain drug release from tablets in acidic medium because alginic formation may enhance film strength and create a stable film for controlling drug release.

In pH 6.8 phosphate buffer, the QPM–GSA-coated tablets had shorter lag times and higher PPN release rates than the QPM-coated tablets, except the QPM–GSA (4:0.5)-coated tablets had a sustained-release of PPN (Figure 6b and Table 2). The rapid release of PPN from the QPM–GSA-coated tablets caused SA swelling and erosion in the films. However, the sustained release of the QPM–GSA (4:0.5)-coated tablets could be occurred because the coated films at this ratio may be strengthened in neutral pH medium. This phenomenon suggested that the strongest interaction between QPM and GSA may occur at this ratio during drug release testing. This effect is observed because SA ionized in pH 6.8 medium is able to interact with the positively charged QPM. Moreover, the 4:1 ratio QPM–GSA films may have excess SA, which promoted matrix erosion of the films.

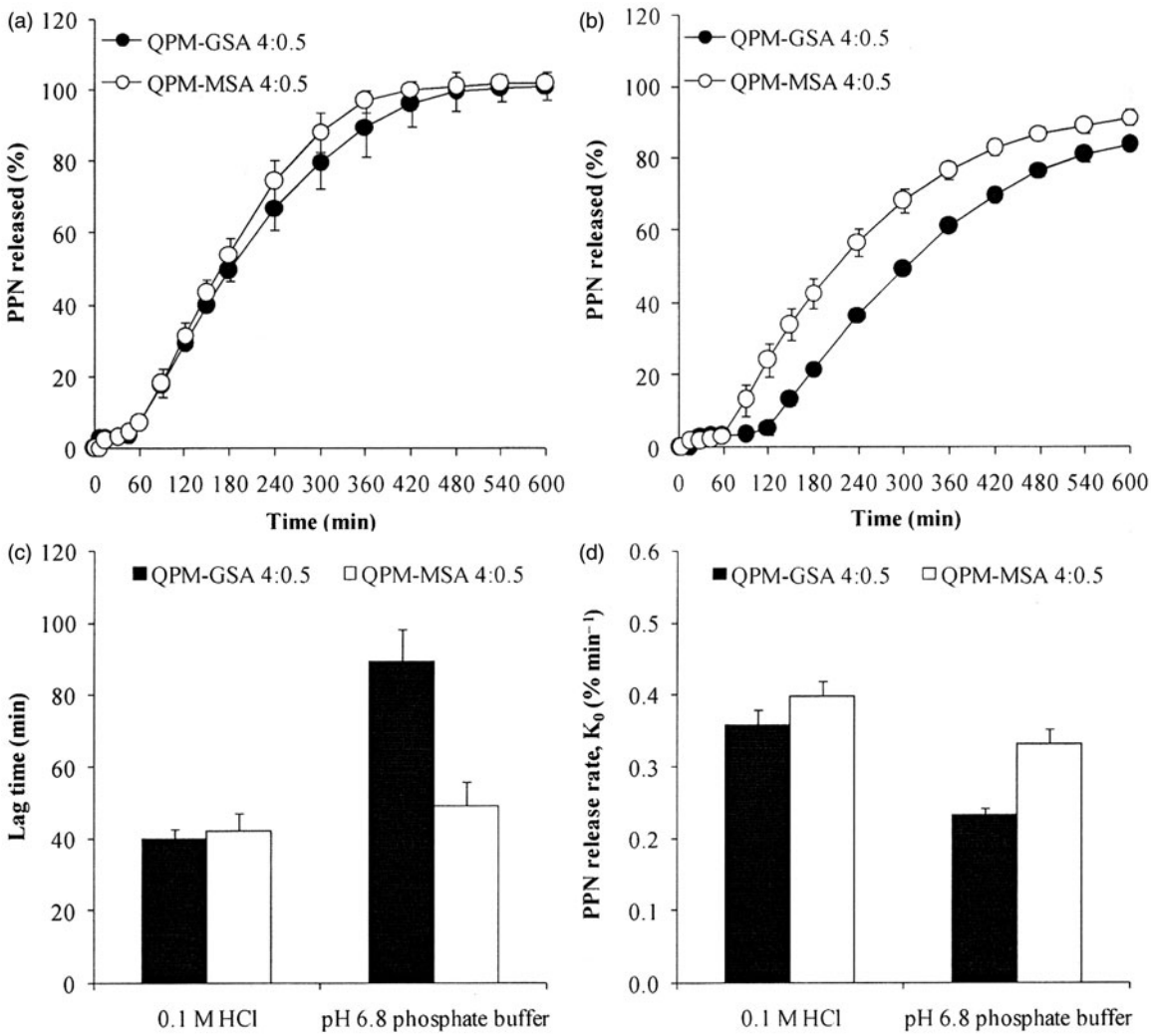


Figure 8. PPN release profiles (a, b), lag time (c) and PPN release rate (d) of PPN tablets coated with QPM–GSA and QPM–MSA films at the ratio of 4:0.5 (4% coating level) in 0.1 M HCl (a) and pH 6.8 phosphate buffer (b). Each value is mean ± S.D., $n = 3$.

Therefore, a faster release rate in the QPM–GSA (4:1)-coated tablets was obtained.

The QPM–GSA (4:1)-coated tablets at 4%, 8% and 12% coating levels were prepared and the PPN release profiles in 0.1 M HCl and pH 6.8 phosphate buffer are illustrated in Figure 6(c) and (d), respectively. Increased coating levels resulted in longer lag times and lower PPN release rates in the coated tablets (Table 2). This was attributed to an increased drug diffusion path length through the coated films, which was stable in the films when they were in an acidic medium. Additionally, increased film-coating levels caused lower water uptake into the core tablets, which affected drug dissolution and release[27]. Apart from the use of 0.1 M HCl, the PPN released from the coated tablets was not related to the coating levels. Increasing the coating level from 4% to 8% caused a longer lag time and a decreased PPN release rate (Table 2). However, similar PPN release rates were observed in the coated tablets with 8% and 12% coating levels. This was due to SA dissolution in neutral pH medium, where many aqueous pore channels could be created, leading to film erosion. This phenomenon may accelerate drug release when the coated tablets have higher coating levels.

### Effect of SA block structure on PPN released from the coated tablets

The PPN core tablets coated with the QPM–GSA and QPM–MSA films using a 4:0.5 ratio at a 4% coating level were prepared and the water uptake was tested in 0.1 M HCl and pH 6.8 phosphate buffer prior to the PPN release study. The QPM–GSA-coated tablets had less water uptake than the QPM–MSA-coated tablets in both media (Figure 7). The QPM–MSA-coated tablets had rapid water uptake in neutral medium. The PPN release profiles of the QPM–GSA and QPM–MSA-coated tablets in 0.1 M HCl and pH 6.8 phosphate buffer are shown in Figure 8(a) and (b), respectively. The lag times and PPN release rates are also presented in Figure 8(c) and (d), respectively. The QPM–GSA-coated tablets had an insignificant lag time and lower PPN release rate than the QPM–MSA-coated tablets in acidic medium. This was due to the lower water uptake of the QPM–GSA-coated tablets. Moreover, the lower drug permeability of the QPM–GSA films adequately explains this result. Conversely, the QPM–GSA-coated tablets had a longer lag time and lower drug release rate in pH 6.8 phosphate buffer. The higher water uptake of the QPM–MSA-coated tablets may enhance PPN dissolution and diffusion, leading to faster PPN release than the QPM–GSA-coated tablets. However, the PPN release rate of the coated tablets using pH 6.8 phosphate buffer was lower than when using 0.1 M HCl. This result suggests that SA swelling in neutral medium may induce a strong interaction with QPM, leading to higher tortuosity of the films. Specifically, a longer lag time and lower PPN release rate in the QPM–GSA-coated tablets was obtained.

## Conclusions

This study demonstrates that GSA and MSA have similar interaction mechanisms with QPM. The QPM–GSA and QPM–MSA films have indistinguishable thermal properties. However, the QPM–GSA films have higher puncture strengths than the QPM–MSA films at increasing SA ratios in dry and wet states, whereas the % elongations were not different. The QPM–GSA film drug permeabilities were lower than the QPM–MSA films in both 0.1 M HCl and pH 6.8 phosphate buffer, but the QPM–GSA films had higher water uptakes at neutral pH. The QPM–GSA dispersions can be applied as film coating materials. The PPN released from the QPM–GSA-coated tablets was dependent on the film-coating levels. The QPM–MSA-coated tablets had higher PPN release rates than the QPM–GSA-coated tablets in acidic and neutral media. The 4:0.5 ratio QPM–GSA and QPM–MSA films were stable films and were able to sustain PPN release in both media. These findings suggest that the QPM–GSA films have higher film strength and lower drug permeability than the QPM–MSA films. Additionally, the QPM–SA films have a potential use as tablet film coating materials for sustained drug release formulations.

## Declaration of interest

The authors wished to thank the Thailand Research Fund (Bangkok, Thailand) for research funding (Grant no. BRG5580016), and the Faculty of Pharmaceutical Sciences, Khon Kaen University (Khon Kaen, Thailand) for technical support. The authors report no conflicts of interest. The authors alone are responsible for the content and writing of this article.

## References

1. Nagai T, Obara S, Kokubo H, Hoshi N. Application of HPMC and HPMCAS to aqueous film coating of pharmaceutical dosage forms. In: McGinity JW, ed. Aqueous polymeric coatings for pharmaceutical dosage forms. New York: Marcel Dekker; 1997:177–226.
2. Wu SHW, Wyatt DM, Adams MW. Chemistry and applications of cellulosic polymers for enteric coatings of solid dosage forms. In: McGinity JW, ed. Aqueous polymeric coatings for pharmaceutical dosage forms. New York: Marcel Dekker; 1997:385–418.
3. Lehmann KOR. Chemistry and application properties of polymethacrylate coating systems. In: McGinity JW, ed. Aqueous polymeric coatings for pharmaceutical dosage forms. New York: Marcel Dekker; 1997:101–179.
4. Bodmeier R, Paeratakul O. Dry and wet strengths of polymeric films prepared from an aqueous colloidal polymer dispersion, Eudragit RS30D. Int J Pharm 1993;96:129–138.
5. Semdé R, Amighi K, Devleeschouwer MJ, Moës AJ. Effect of pectinolytic enzymes on the theophylline release from pellets coated with water insoluble polymers containing pectin HM or calcium pectinate. Int J Pharm 2000;197:169–179.
6. Khuathan N, Pongjanyakul T. Modification of quaternary polymethacrylate films using sodium alginate: film characterization and drug permeability. Int J Pharm 2014;460:63–72.
7. Liew CV, Chan LW, Ching AL, Heng PWS. Evaluation of sodium alginate as drug release modifier in matrix tablets. Int J Pharm 2006; 309:25–37.
8. Sriamornsak P, Thirawong N, Korkerd K. Swelling, erosion and release behavior of alginate-based matrix tablets. Eur J Pharm Biopharm 2007;66:435–450.
9. Nie S, Wu J, Liu H, et al. Influence of admixed citric acid and physiological variables on the vinpocetine release from sodium alginate compressed matrix tablets. Drug Dev Ind Pharm 2011;37: 954–962.
10. Tønnesen HH, Karlsen J. Alginate in drug delivery systems. Drug Dev Ind Pharm 2002;28:621–630.
11. Pongjanyakul T, Puttipipatkhachorn S. Modulating drug release and matrix erosion of alginate matrix capsules by microenvironmental interaction with calcium ion. Eur J Pharm Biopharm 2007;67: 187–195.
12. Sriamornsak P, Kennedy RA. Development of polysaccharide gel-coated pellets for oral administration. 2: calcium alginate. Eur J Pharm Sci 2006;29:139–147.
13. Pongjanyakul T. Alginate–magnesium aluminum silicate films: importance of alginate block structures. Int J Pharm 2009;365: 100–108.
14. Sugawara S, Imai T, Otagiri M. The controlled release of prednisolone using alginate gel. Pharm Res 1994;11:272–277.
15. Schmid W, Picker-Freyer KM. Tableting and tablet properties of alginates: characterisation and potential for Soft Tableting. Eur J Pharm Biopharm 2009;72:165–172.
16. Lee HY, Chan LW, Dolzhenko AV, Heng PWS. Influence of viscosity and uronic acid composition of alginates on the properties of alginate films and microparticles produced by emulsification. J Microencapsul 2006;23:912–927.
17. Ritthidej GC, Phaechamud T, Koizumi T. Moist heat treatment on physicochemical change of chitosan salt films. Int J Pharm 2002; 232:11–22.

18. Flynn GL, Yalkowsky SH, Roseman TJ. Mass transport phenomena and models: theoretical concepts. J Pharm Sci 1974;63:479–510.
19. Khunawattanakul W, Puttipipatkhachorn S, Rades T, Pongjanyakul T. Novel chitosan–magnesium aluminum silicate nanocomposite film coatings for modified-release tablets. Int J Pharm 2011;407: 132–141.
20. Pongjanyakul T, Puttipipatkhachorn S. Alginate–magnesium aluminum silicate composite films: effect of film thickness on physical characteristics and permeability. Int J Pharm 2008;346:1–9.
21. Sartori C, Finch DS, Ralph B. Determination of the cation content of alginate thin films by FTIR spectroscopy. Polymer 1997;38: 43–51.
22. Lawrie G, Keen I, Drew B, et al. Interactions between alginate and chitosan biopolymers characterized using FTIR and XPS. Biomacromolecules 2007;8:2533–2541.
23. Østberg T, Lund EM, Graffner C. Calcium alginatematrices for oral multiple unit administration. IV. Release characteristics in different media. Int J Pharm 1994;112:241–248.
24. Draget KI, Skjåak Bræk G, Smidsrød O. Alginic acid gels: the effect of alginate chemical composition and molecular weight. Carbohydr Polym 1994;25:31–38.
25. Remuñán-López C, Bodmeier R. Mechanical, water uptake and permeability properties of crosslinked chitosan glutamate and alginate films. J Control Release 1997;44:215–225.
26. Aslani P, Kennedy RA. Studies on diffusion in alginate gels. I. Effect of crosslinking with calcium or zinc ions on diffusion of acetaminophen. J Control Release 1996;42:75–82.
27. Pongjanyakul T, Priprem A, Puttipipatkhachorn S. Investigation of novel alginate-magnesium aluminum silicate microcomposite films for modified-release tablets. J Control Release 2005;107:343–356.

# Quaternary polymethacrylate-magnesium aluminum silicate nanocomposite films for tablet coating

**Thitiphorn Rongthong[a], Srisagul Sungthongjeen[b], Florence Siepmann[c,d], Juergen Siepmann[c,d], Thaned Pongjanyakul[a,*]**

[a]Faculty of Pharmaceutical Sciences, Khon Kaen University, Khon Kaen 40002, Thailand

[b]Department of Pharmaceutical Technology, Faculty of Pharmaceutical Sciences, Naresuan University, Phitsanulok 65000, Thailand

[c]University of Lille, College of Pharmacy, 3 rue du Professeur Laguesse, 59006 Lille, France

[d]INSERM U1008, Controlled Drug Delivery Systems and Biomaterials, 3 rue du Professeur Laguesse, 59006 Lille, France

[*]Corresponding author

**Abstract**

A positively charged quaternary polymethacrylate (QPM) could electrostatically interact with a negatively charged magnesium aluminum silicate (MAS) to form nanocomposite films. The use of this film for tablet coating was evaluated in this study. Surface and matrix morphology, water uptake, and drug release of the QPM and QPM-MAS coated tablets were examined. The results showed that tackiness problem of the QPM coated tablets was remarkably reduced by adding MAS. The QPM-MAS coated tablets had rougher surface than the QPM coated tablets. The water uptake of the coated tablets decreased with increasing MAS in the coated films, leading to longer lag time and lower drug release rate of the QPM-MAS coated tablets with higher ratio of MAS. The drug release of the QPM-MAS coated tablets could also be modulated by varying film coating level. Moreover, the drug characteristics, such as charge, molecular weight, and aqueous solubility, influenced drug release from the QPM-MAS coated tablets. Additionally, curing process could produce a homogeneous and denser film formation after coating process, resulting in longer lag time and lower drug release rate of the QPM-MAS coated tablets cured at higher temperature (80 °C). These findings suggest that the QPM-MAS films can be used as a tablet film coating material for modifying drug release pattern of tablets.

**Keywords**: Quaternary polymethacrylate; magnesium aluminum silicate; tablet coating; drug release; curing

## 1. Introduction

Quaternary polymethacrylate (QPM), a synthetic water insoluble polymer, has been widely used in pharmaceutical technology for using in drug delivery systems (Lehmann, 1997). This polymer has several forms to use, such as powders, granules, dispersions, and solutions. Aqueous dispersion form of this polymer has been widely used in pharmaceutical industry for film coating over an organic solution due to environmental protection and reducing hazard of organic solvent. Eudragit® RL 30D is the QPM commercial product in the dispersion form which contain 10% of quaternary ammonium groups. It is a positively charged polymer which can swell in the medium due to ionization of quaternary ammonium groups. This functional group plays a role of hydration of this polymer (Akhgaria et al, 2006). The swelling of this polymer was independent on pH of the medium, whereas it depended on type and ionic strength of anion in the medium (Bodmeier et al., 1996; Sun et al., 2001). The characteristics of QPM films were brittle film formations (Bodmeier and Paeratakul, 1994), high drug permeability (Lehmann, 1997), and tacking problem (Wesseling et al., 1999). Thus, the use of QPM films for developing drug delivery systems was necessary to modify the film properties.

Incorporation of some substances, such as plasticizers and anionic materials, could improve physical properties of QPM films. QPM films with plasticizers usually provided lower strength, but higher flexibility (Bodmeier and Paeratakul, 1994). QPM could electrostatically interact with sodium alginate, anionic polymer, which caused an increase in film strength, decrease film tackiness, and reduce drug permeability (Khuathan and Pongjanyakul, 2014). This led to slower drug release rate from tablets coated with sodium alginate-QPM films (Pongjanyakul and Khuathan, 2015). The complexation of QPM and pectin could reduce swelling and erosion of pectin during transit from mouth to caecum for colon drug delivery

(Semdé et al., 2000). Moreover, synthetic polymers could be used in this purpose, which incorporation of methacrylic acid copolymer (Eudragit® L), enteric polymer, into the QPM films could modify drug release in small intestine condition (Wulff and Leopold, 2014). QPM could also interact with Eudragit® FS 30D, anionic polymer, via electrostatic interaction, and the blended films was used as a film coating material (Moustafine et al., 2012).

Magnesium aluminum silicate (MAS) is a natural smectite clay with silicate layer structure, which composed of tetrahedrally coordinated silica atoms fused with octahedral plane of either aluminum hydroxide or magnesium hydroxide in a layer structure (Alexandre and Dubois, 2000; Kibbe, 2000). The surface of MAS silicate layers had negative charge, whereas the slightly positive charge was presented at the edge of layer structure. MAS has been widely used in pharmaceutical development as diluents, suspending agent, and stabilizing agent (Kibbe, 2000). MAS could enhance viscosity of chitosan dispersion (Khunawattanakul et al., 2008) because of molecular interaction of positively charged chitosan and MAS. Furthermore, the chitosan-MAS films showed better mechanical properties and lower drug permeability when compared with the chitosan films (Khunawattanakul et al., 2010). The chitosan-MAS films could use in tablet film coating for sustaining drug release (Khunawattanakul et al., 2011).

Incorporation of MAS into QPM film produced the exfoliated and intercalated nanocomposite films due to electrostatic interaction of both substances, leading to an increase in the thermal stability and strength of the film. Moreover, the tackiness of the QPM films reduced by adding MAS (Rongthong et al., 2013). Recently, water uptake and drug permeation characteristics of the QPM-MAS films were investigated (Rongthong et al.,

2015). Increasing MAS content in the QPM films gave lower water uptake and drug permeability. Moreover, the permeability of the QPM-MAS films was dependent on charge and molecular weight of permeants. Thus, it is interesting to use the QPM-MAS films for tablet coating intended for sustaining drug release and the drug release study of the QPM-MAS coated films is important for better understanding to the characteristics of the QPM-clay based films. This lead to the objective of the present study which was to prepare and evaluate the characteristics of the tablets coated with the QPM-MAS films. Effect of QPM-MAS ratio, coating level, drug type, and curing on water uptake and drug release of the QPM-MAS coated tablets were examined.

## 2.Materials and methods

### 2.1. Materials

QPM (Eudragit® RL 30D) was purchased from Röhm Pharma GmbH (Darmstadt, Germany). Magnesium aluminum silicate (MAS) (Veegum®HV) was obtained from R.T. Vanderbilt Company Inc. (Norwalk, CT, USA). Diethyl sebacate was purchased from Aldrich chemistry (UK). Propranolol HCl (PPN), acetaminophen (ACT), and diclofenac sodium (DFS) were purchased from Changzhou Yabang Pharmaceutical Co., Ltd. (Jiangsu, China), Praporn Dasut, Ltd. (Bangkok, Thailand), and Bang Trading 1992 Co., Ltd. (Bangkok, Thailand), respectively. Microcrystalline cellulose (Ceolus® PH102, SiamChem-Pharm (1997) Co., Ltd., Bangkok, Thailand), spray-dried lactose (Flowlac®100, Thai Meochems Co., Ltd., Bangkok, Thailand), magnesium stearate (Mallinckrodt Inc., USA), and colloidal silicon dioxide (Aerosil® 200, Degussa, Japan) were used as tablet excipients. All other reagents and solvents were of analytical grade.

2.2. Preparation and evaluation of core tablets

Core tablets (400 mg each), which were prepared using a direct compression method, consisted of 20 % active ingredient (PPN, ACT, or DFS), 49.7 % spray-dried lactose monohydrate, 28.0 % microcrystalline cellulose, 0.3 % colloidal silicon dioxide, and 2 % magnesium stearate. Drug powder, spray-dried lactose monohydrate, microcrystalline cellulose, and colloidal silicon dioxide were mixed using a Y-shape mixer for 45 min. Then, the mixtures were blended with magnesium stearate, lubricant, for 5 min before tabletting. The core tablets were prepared using a single punch machine with a 10-mm diameter biconvex punch. The mean surface area of the core tablets was approximately 2.55 $cm^2$/tablet. The average weight of the core tablets were over the range of 401.2-404.9 mg. The tablet hardnesses were found to be 104.3 ± 9.8, 117.8 ± 9.0, and 122.9 ± 8.3 N in the case of PPN, ACT, and DFS, respectively. The friability of the core tablets was less than 0.2 %. The core tablets could be completely disintegrated within 4 min in deionized water, 0.1 M HCl, or pH 6.8 phosphate buffer. The drug content of the PPN core tablets was extracted in 0.1 M HCl, whereas the ACT and DFS core tablets were extracted in pH 6.8 phosphate buffer. The amount of drug content was analyzed using a UV-spectrophotometer (Shimadzu UV1201, Japan) at the wavelength of 289, 265, and 260 nm, respectively. The drug content of the PPN, ACT, and DFS core tablets were 79.46 ± 0.70, 81.61 ± 2.19, and 78.99 ± 1.17 mg/tablet (n=3).

2.3. Film coating of core tablets

QPM dispersion and QPM-MAS dispersions with various ratios were prepared and used as a film coating material. Diethyl sebacate (15 %w/w of QPM content) was added into the QPM dispersion and the mixed dispersion was stirred for 30 min. After mixing, the dispersion was adjusted to the final volume with distilled water. For the QPM-MAS dispersions, accurate

amount of MAS, which had been prehydrated with hot water, was slowly added into the plasticized QPM dispersion and adjusted to the final volume using distilled water. The composite dispersion was continuously mixed with a propeller stirrer (Wisestir®, Daihan Scientific Co., Ltd, Korea) for overnight.

The film coating of the core tablets was conducted by using a side-vented coating pan (Thai Coater Model FC15, Pharmaceuticals and Medical Supply Ltd., Thailand). PPN, ACT, or DFS core tablets (1000 g) were warmed in a coating pan with an inlet temperature at 55-60 °C for 30 min before coating. The QPM dispersion or QPM-MAS dispersions was continuously stirred during coating process. The rotation rate of coating pan was 6-7 revolutions $min^{-1}$. The spray rate and spray pressure of the dispersion was controlled at 6 ml $min^{-1}$ and 0.38 MPa, respectively. The coating level was calculated from weight gained of coating films by total surface area of the core tablet (Bauer et al., 1998). After the coating process, the obtained coated tablets were further dried in the coating pan for 30 min before storing in desiccators at ambient condition.

Effect of QPM-MAS ratio on characteristics of the PPN coated tablets was investigated at the same coating level (13.1 mg $cm^{-2}$). The ratios of QPM-MAS films used were 4:0, 4:0.1, 4:0.25, 4:0.5, and 4:0.75 by weight. Coating level effect was investigated using the QPM and QPM-MAS (4:0.75) coated tablets. The PPN core tablets were coated to achieve the coating levels of 13.1 ± 0.94, 19.8 ± 1.03, and 25.3 ± 1.05 mg $cm^{-2}$. Moreover, PPN, ACT, and DFS was used as cationic, nonionic, and anionic drugs, respectively for investigating the effect of drug types on water uptake and drug release. Finally, influence of curing temperature (45, 60, and 80 °C for 12 h) on water uptake and drug release of PPN coated tablets was also investigated.

2.4. Evaluation of coated tablets

2.4.1. Surface and matrix morphology of coated tablets

Surface morphology and cross-sectional morphology of coated tablets was observed by using scanning electron microscope (Joel Model JSM-6480LV, Tokyo, Japan). The coated tablets and the cross-sectional coated tablets were mounted on the stubs and coated with gold in a vacuum evaporator. The surface and cross-sectional morphology of coated tablets were observed with different magnification.

2.4.2. Water uptake of coated tablets

Water uptake of the coated tablets was performed using a USP dissolution apparatus I (basket method) (Vankel VK7000, North Carolina, USA). The media used were 0.1 M HCl or pH 6.8 phosphate buffer at 37 °C. The coated tablet was weighted before placing in the basket and immersing in the medium. The rotation rate of the baskets was controlled at 50 revolutions $min^{-1}$. At the predetermined intervals times, the sample was collected and carefully blotted to remove an excess water at the surface of coated tablet and immediately weighed. After weighing, the sample was placed back in the basket and tested up to the time. The % water uptake of the coated tablets at different time points was calculated as follows:

$$\text{Water uptake (\%)} = \left( \frac{W_t - W_i}{W_i} \right) \times 100 \qquad \text{Eq. 1}$$

where $W_i$, and $W_t$ are the initial and wet weight at time point of the coated tablet, respectively.

2.4.3. Drug release study

*In vitro* drug release studies were performed using the USP dissolution apparatus I (basket method) (Vankel VK7000, North Carolina, USA). The dissolution media (900 ml) were 0.1

M HCl or pH 6.8 phosphate buffer at 37 °C. The coated tablet was placed into the basket which was rotated at a rate of 50 revolutions $min^{-1}$. At predetermined interval time, samples (7 ml) were collected and an equal volume of fresh medium was replaced into the vessel. The concentration of drug in the medium was analyzed using a UV-visible spectrophotometer (Shimadzu UV1201, Japan) at the wavelength of 289, 265, or 260 nm for PPN, ACT, or DFS, respectively. The release mechanism of the coated tablets was defined by fitting the obtained release data with the zero order kinetics (Eq. 2).

$$F = K_0 t + B \qquad \text{Eq. 2}$$

where $F$ is fraction of drug released, $t$ is time, $K_0$ is the zero-order rate constant and $B$ is a constant value.

## 3. Results and discussion

### 3.1. Appearance and morphology of coated tablets

The appearance of the PPN tablets coated with QPM and QPM-MAS films are shown in Fig. 1. The obtained QPM-MAS coated tablets had yellowish color when compared with the QPM coated tablets. The microscopic surface and matrix morphologies of the coated tablets (uncuring) using SEM are also presented in Fig. 1. The QPM coated tablets had smoother surface than the QPM-MAS coated tablets, whereas matrix morphology of the QPM-MAS films appeared to be looser structure than that of the QPM films. These morphologies were similar to the free QPM and QPM-MAS films that were prepared using a casting/solvent evaporation method (Rongthong et al., 2013).

All coated tablets did not have a sticking problem during coating process. After 3-months storage, the sticking of the QPM coated tablets occurred because the QPM films had a tackiness in nature. The QPM-MAS coated tablets at the ratios of 4:0.1 and 4:0.25 gave a few

sticking of the coated tablets. However, incorporation of MAS into the QPM films in the ratios of 4:0.5 and 4:0.75 brought about a lack of the sticking problem of the coated tablets. These results were in agreement with the previous study (Rongthong et al., 2013) that the tackiness of the QPM-MAS films decreased with increasing MAS content when tested using a texture analyzer.

### 3.2. Effect of QPM-MAS ratio

The water uptake of the PPN tablets coated with QPM-MAS films with different ratios (13.1 mg $cm^{-2}$ coating level) were investigated in 0.1 M HCl and pH 6.8 phosphate buffer as shown in Fig. 2a and 2b, respectively. The results showed that the water uptake of the QPM-MAS coated tablets tended to decrease with increasing MAS content in the films. It was suggested that electrostatic interaction between the silanol groups of MAS and the quaternary ammonium groups of QPM, which resulted in the nanocomposite formation (Rongthong et al., 2013), caused a denser network matrix with higher tortuosity. This led to a reduction of film hydration and retardation of water transport through the coated films (Rongthong et al., 2015). Additionally, the water uptakes of the coated tablets in acidic medium were greater than those in pH 6.8 phosphate buffer at the same time points. For observation, the QPM-MAS coated tablets in neutral medium displayed higher film strength and could be handled for longer immersing time when compared to the test in 0.1 M HCl.

Drug release profiles of the PPN tablets coated with QPM and QPM-MAS films in 0.1 M HCl and pH 6.8 phosphate buffer are shown in Fig. 2c and 2d, respectively. The PPN core tablets showed a fast release in both media. The pattern of PPN release from the coated tablets was similar in acidic and neutral media. The zero-order release model could be used to analyze and calculate drug release rate constant ($K_0$) and lag time. It was found that drug

release data could be fitted to the zero-order release model with $R^2$ higher than 0.99 when drug released was less than 60 %. Increase of MAS into the QPM film caused longer lag time and lower $K_0$ value that are shown in Table 1. This was due to slower water uptake of the QPM-MAS coated tablets that may cause a lower PPN dissolution rate in the core tablets before PPN permeation across the films. In addition, PPN, a positively charged molecule, could electrostatically interact with a negatively charged MAS (Rojtanatanya and Pongjanyakul, 2010), resulting in a lower diffusivity of PPN across the QPM-MAS films (Rongthong et al., 2015). This reason could be explained why the longer lag time was found in the QPM-MAS coated tablets using higher ratios of MAS.

The release medium used in this study also influenced the PPN release from the coated tablets. The lag time of the QPM coated tablets in pH 6.8 phosphate buffer was longer than that in 0.1 M HCl (Table 1), This is likely to be due to lower water uptake of the QPM coated tablets in neutral medium (Fig. 2b). However, the PPN release rate constant in neutral medium tended to higher than that in acidic medium (Table 1). It can be explained that PPN had higher solubility in neutral medium when compared with in acidic medium (Khunawattanakul et al., 2011). This led to higher concentration gradient of PPN in the core tablets, which caused a faster PPN release in neutral medium. This phenomenon also found in the QPM-MAS coated tablets in the ratios of 4:0.1 and 4:0.25. At higher ratio of MAS, the longer lag time was observed in neutral medium because the slower water uptake occurred when increasing MAS in the films. However, the PPN release rate constant was quite similar in both media (Table 1). The result suggested that the lower permeability of the QPM-MAS films at higher MAS ratios was observed, irrespective of type of medium that resulted in denser network matrix of the swollen films and higher PPN affinity onto the films. It was

indicated that the QPM-MAS coated tablets gave zero-order release kinetic with lag time and good efficiency for controlling drug release were obtained when using higher ratios of MAS.

### 3.3. Effect of coating level

The water uptake of the PPN tablets coated with QPM and QPM-MAS (4:0.75) films at various coating levels is shown in Fig. 3. The results showed that the water uptake of the coated tablets continuously increased with testing time. The water uptake of the QPM coated tablets at the lowest coating level (13.1 mg $cm^{-2}$) in acid condition was rapidly increased within 30 min, and the coated tablets could not be handled thereafter. The coated tablets at coating levels of 19.8 and 25.3 mg $cm^{-2}$ were not difference, but they had slower uptake of the water at the same time points comparing with the coated tablets with coating level of 13.1 mg $cm^{-2}$. Using neutral medium, the similar pattern of water uptake profile was found in the QPM coated tablets with different coating levels. However, the coated tablets with higher coating level could be handled at longer time of the test when compared to those with lower coating level. The water uptake of the QPM-MAS (4:0.75) coated tablets increased with increasing coating level in both media. The water uptake of the coated tablets in neutral medium was lower than that in acidic medium. Apart from water uptake studies, the PPN release profiles of the QPM and QPM-MAS coated tablets are presented in Fig. 4. The QPM-MAS coated tablets provided significantly longer lag time and lower drug release rate constant with increasing coating level (Table 1). On the other hand, the lag time and PPN release rate constant of the QPM coated tablets had no relation to the coating level. This was due to the similar of water uptake in some coating levels.

These results indicated that increasing coating level of the coated tablets could modify the drug release pattern from the QPM-MAS coated tablets. Increasing the coated film thickness

caused longer path length of water penetration into the core tablets and drug diffusion across the film, resulting in longer lag time and slower rate of drug release (Khunawattanakul et al., 2011). This study also showed that the QPM-MAS films were superior to the QPM films. The first was the higher strength and denser matrix of the QPM-MAS film, which could retard water uptake, sustain drug release and offer stable films during the tests. Secondly, the release parameters of the QPN-MAS coated tablets could be possibly predicted by varying coated level of the coated tablets.

### 3.4. Effect of drug types

Effect of drug types on water uptake of the QPM and QPM-MAS (4:0.75) coated tablets in pH 6.8 phosphate buffer are shown in Fig. 5a. PPN, ACT, and DFS were selected to use as cationic, nonionic, and anionic drugs, respectively. The coated tablets were prepared at the same coating level of 13.1 mg $cm^{-2}$. The water uptake of the PPN coated tablets was greater than that of the ACT coated tablets, and the lowest water uptake of the DFS coated tablets was found. The similar results were obtained in the case of the QPM and QPM-MAS coated tablets. The drug release of the coated tablets was tested in pH 6.8 phosphate buffer because of water insoluble of DFS in acidic medium. However, the DFS coated tablets showed very small amount of drug released (less than 10%) that could not calculate lag time and release rate constant. It could be described that this coated tablets had very low water uptake and the negative charge of DFS could possibly interact with QPM, leading to remarkable retardation of DFS release. Thus, the lag time and release rate constant of the PPN and ACT coated tablets could be compared in Fig. 5b. The lag time of the PPN coated tablets was longer than that of the ACT coated tablets. Moreover, the PPN coated tablets had higher $K_0$ values than the ACT coated tablets.

This study suggested that drug characteristics, such as molecular weight, charge, and water solubility, affected the release pattern of drug from the QPM and QPM-MAS coated tablets. The PPN coated tablets showed higher water uptake than the ACT coated tablets because PPN could induce water penetration into the core tablets due to greater water solubility of PPN when compared with ACT (Khunawattanakul et al., 2011). However, the longer lag time of the PPN tablets coated with QPM films was observed. This resulted from bigger molecule of PPN that also showed lower diffusivity across the coated films. In the case of the QPM-MAS coated films, incorporation of MAS caused longer lag time when compared with the QPM films. However, the PPN coated tablets gave insignificantly longer lag time than the ACT coated tablets. It could be possibly explained that PPN and ACT could interact with MAS in the films with different mechanisms, namely electrostatic force and hydrogen bonding, respectively. The higher affinity of PPN with MAS via electrostatic interaction may cause longer lag time of the coated tablets. Additionally, the $K_0$ value of the PPN coated tablets was higher than that of the ACT coated tablets. The greater water uptake of the PPN coated tablets was sufficient for dissolving the drug particles in the core tablets, leading to a rapidly high PPN concentration gradient for drug diffusion when compared to ACT. Thus, faster PPN release was obtained.

### 3.5. Curing effect

The surface and matrix morphologies of the QPM and QPM-MAS (4:0.75) coated tablets (13.1 mg $cm^{-2}$ coating level) cured at 45, 60, and 80 °C for 12 hr are shown in Fig. 1. The smoother surface of the QPM-cured tablets could be observed at higher temperature when compared to the QPM-uncured tablets (Fig. 1). In contrast, the surface of the QPM-MAS-cured tablets did not different with the uncured tablets (Fig. 1). Moreover, the curing temperature did not affect the internal structure morphology of the QPM and QPM-MAS

tablets when observing using SEM. However, some of the QPM coated tablets were swollen at an edge of the coated tablets when curing at 80 °C. This phenomenon was slightly found in the case of the QPM-MAS coated tablets. This may be due to a vapor pressure inside the core tablets that occurred from evaporation of remaining water at high temperature (Bley et al., 2009).

The water uptake of the QPM and QPM-MAS coated tablets decreased with increasing curing temperature and the lower water uptake could be found in the QPM-MAS coated tablets (Fig. 6a and 6b). For the PPN release, the curing process brought about a remarkable increase of lag time of the QPM coated tablets when compared to the uncured tablets, but was not dependent on curing temperature (Fig. 7a). The slightly longer lag time of the QPM-MAS coated tablets was found after curing. The PPN release rate constant of both coated tablets was unchanged when curing at 45 and 60 °C (Fig. 7b). However, the coated tablets cured at 80 °C provided lower PPN release rate than those cured at lower temperatures.

The curing process could induce the further fusion of QPM particles in the QPM coated tablets at investigation temperatures, even though the temperature of 45 °C was lower than glass transition temperature ($T_g$) of QPM, approximately 55 °C (Hasanzadeh et al., 2009). This temperature (45 °C) was higher than the minimum film formation temperature of QPM that was reported to be 38.3 ± 0.4 °C (Mendoza-Romero et al., 2009), leading to a continue deformation of QPM particles in the coated films during curing period and partial homogeneous matrix of the films may be formed. This may lead to lower film permeability. Thus, a longer lag time of PPN release was obtained. At 60 and 80 °C, these curing temperatures were greater than $T_g$ of QPM and caused the further fusions of QPM particles. Furthermore, polymer chain flexibility usually increased with increasing curing temperature.

For these reasons, the homogeneous matrix of the coated films could be occurred (Azarmi et al., 2002; Heckötter et al., 2011; Yang et al., 2010), resulting in lower film permeability at higher curing temperature. This led to restriction of water absorption and slower drug release with longer lag time (Wurster et al., 2007; Williams III and Liu, 2000).

For the QPM-MAS coated tablets, the curing process did not change the appearance of surface and matrix morphology when compared with the QPM coated tablets. This result suggested that MAS interacted electrostatically with QPM could obstruct deformation and fusion of QPM particles during curing. However, the water uptake of the QPM-MAS coated tablets cured at 60 and 80 °C was slower than that of the uncured and cured tablets at 45 °C. This suggested that some of QPM particles still had a deformation and denser matrix formation may be occurred, leading to the slowest PPN release of the QPM-MAS coated tablets cured at 80 °C.

## 4. Conclusion

The QPM-MAS films can be successfully applied for tablet coatings that tackiness problem of the coated tablets is remarkably reduced. The QPM-MAS coated tablets had rougher surface than the QPM coated tablets. Increasing MAS ratio in the films caused lower water uptake of the coated tablets, resulting in longer lag time and lower drug release rate. The drug release of the QPM-MAS coated tablets can be modulated by varying film coating level. Furthermore, the drug characteristics, such as charge, molecular weight, and aqueous solubility, affected drug release of the QPM-MAS coated tablets. Curing process is also necessary to produce the homogeneous film formation after coating process. Higher temperature of curing provides slower drug release rate of the QPM-MAS coated tablets. This

study suggests that the QPM-MAS films can be used as a tablet film coating material for modifying drug release pattern of tablets.

**Acknowledgements**

The authors wish to thank the Thailand Research Fund (Bangkok, Thailand) for research funding (Grant no. BRG5580016), and the Faculty of Pharmaceutical Sciences, Khon Kaen University, Khon Kaen, Thailand for technical support. Financial support from the Thailand Research Fund through the Royal Golden Jubilee Ph.D. Program (Grant No. PHD/0136/2551) for T.R. and T.P. is gratefully acknowledged.

**Reference**

Akhgaria A, Farahmanda F, Afrasiabi Garekania H, Sadeghia F, Vandammeb TF. Permeability and swelling studies on free films containing inulin in combination with different polymethacrylates aimed for colonic drug delivery. Eur J Pharm Sci 2006; 28: 307-314.

Alexandre M, Dubois P. Polymer-layered silicate nanocomposites: Preparation, properties and uses of a new class of materials. Mater Sci Eng 2000; 28: 1-63.

Azarmi S, Farid J, Nokhodchi A, Bahari-Saravi SM, Valizadeh H. Thermal treating as a tool for sustained release of indomethacin from Eudragit RS and RL matrices. Int J Pharm 2002; 246: 171-177.

Bauer KH, Lehmann K, Osterwald HP, Rothgang G. Coated pharmaceutical dosage forms: fundamentals, manufacturing techniques, biopharmaceutical aspects, test methods, and raw materials. Stuttgart: Medpharm GmbH Scientific Publishers, 1998.

Bley O, Siepmann J, Bodmeier R. Protection of moisture-sensitive drugs with aqueous polymer coatings: Importance of coating and curing conditions. Int J Pharm 2009; 378: 59-65.

Bodmeier R, Guo X, Sarabia RE, Skultety PF. The influence of buffer species and strength on diltiazem HCl release from beads coated with the aqueous cationic polymer dispersions, Eudragit RS, RL 30D. Pharm Res 1996; 13: 52-56.

Bodmeier R, Paeratakul O. Mechanical properties of dry and wet cellulosic and acrylic films prepared from aqueous colloidal polymer dispersions used in the coating of solid dosage forms. Pharm Res 1994; 11: 882-888.

Hasanzadeh, D., Ghaffari, S., Monajjemzadeh, F., Al-Hallak, M.H.D.K., Soltani, G., Azarmi, S., 2009. Thermal treating of acrylic matrices as a tool for controlling drug release. Chem Pharm Bull 57 (12), 1356-1362.

Heckötter UM, Larsson A, Sriamornsak P, Kumpugdee–Vollrath M. Effect of annealing time and addition of lactose on release of a model substance from Eudragit® RS coated pellets produced by a fluidized bed coater. Chem Eng Res Des 2011; 89: 697-705.

Khuathan N, Pongjanyakul T. Modification of quaternary polymethacrylate films using sodium alginate: Film characterization and drug permeability. Int J Pharm 2014; 460: 63-72.

Khunawattanakul W, Puttipipatkhachorn S, Rades T, Pongjanyakul T. Chitosan-magnesium aluminum silicate composite dispersions: Characterization of rheology, flocculate size and zeta potential. Int J Pharm 2008; 351: 227-235.

Khunawattanakul W, Puttipipatkhachorn S, Rades T, Pongjanyakul T. Chitosan-magnesium aluminum silicate nanocomposite films: Physicochemical characterization and drug permeability. Int J Pharm 2010; 393: 219-229.

Khunawattanakul W, Puttipipatkhachorn S, Rades T, Pongjanyakul T. Novel chitosan-magnesium aluminum silicate nanocomposite film coatings for modified-release tablets. Int J Pharm 2011; 407: 132-141.

Kibbe, H,A., 2000. Handbook of pharmaceutical excipients, third ed. American Pharmaceutical Association, Washington, pp. 295–298.

Lehmann KOR. Chemistry and application properties of polymethacrylate coating systems. In: McGinity JW, editor. Aqueous polymeric coatings for pharmaceutical dosage forms. 2nd ed. New York: Marcel Dekker; 1997. p. 101-176.

Mendoza-Romero, L., Piñón-Segundo, E., Nava-Arzaluz, M.G., Ganeum-Quintanar, A., Cordero-Sánchez, S., Quintanar-Guerrero, D., 2009. Comparison of pharmaceutical films prepared from aqueous polymeric dispersions using the cast method and the spraying technique. Colloid Surface A 337 (1-3), pp. 109-116.

Moustafine IR, Bodrov AV, Kemenova VA. Drug release modification by interpolymer interaction between countercharged types of Eudragit® RL 30D and FS 30D in double-layer films. Int J Pharm 2012; 439: 17-21.

Pongjanyakul T, Khuathan N. Quaternary polymethacrylate–sodium alginate films: effect of alginate block structures and use for sustained release tablets. Pharm Dev Technol. 2015 (DOI: 10.3109/10837450.2015.1022787).

Rojtanatanya S, Pongjanyakul T. Propranolol-magnesium aluminum silicate complex dispersions and particles: Characterization and factors influencing drug release. Int J Pharm 2010; 383: 106-115.

Rongthong T, Sungthongjeen S, Siepmann J, Pongjanyakul T. Quaternary polymethacrylate–magnesium aluminum silicate films: Molecular interactions, mechanical properties and tackiness. Int J Pharm 2013; 458: 57-64.

Rongthong, T., Sungthongjeen, S., Siepmann, F., Siepmann, J., Pongjanyakul, T., 2015. Quaternary polymethacrylate-magnesium aluminum silicate films: Water uptake kinetics and film permeability. International Journal of Pharmaceutics 490 (1-2), 14918, pp. 165-172.

Semdé R, Amighi K, Devleeschouwer MJ, Moës AJ. Studies of pectin HM/Eudragit® RL/Eudragit® NE film-coating formulations intended for colonic drug delivery. Int J Pharm 2000; 197: 181-192.

Sun YM, Hsu SC, Lai JY. Transport properties of ionic drugs in the ammonio methacrylate copolymer membranes. Pharm Res 2001; 18(3): 304-310.

Wesseling M, Kuppler F, Bodmeier R. Tackiness of acrylic and cellulosic polymer films used in the coating of solid dosage forms. Eur J Pharm Biopharm 1999; 47: 73-78.

Williams III RO, Liu J. Influence of processing and curing conditions on beads coated with an aqueous dispersion of cellulose acetate phthalate. Eur J Pharm Biopharm 2000; 49: 243-252.

Wulff R, Leopold CS. Coatings from blends of Eudragit® RL and L55: A novel approach in pH-controlled drug release. Int J Pharm 2014; 476: 78-87.

Wurster DE, Bhattacharjya S, Flanagan DR. Effect of curing on water diffusivities in acrylate free films as measured via a sorption technique. AAPS PharmSciTech 2007; 8(3): E1-E6.

Yang QW, Flament MP, Siepmann F, Busignies V, Leclerc B, Herry C, et al. Curing of aqueous polymeric film coatings: Importance of the coating level and type of plasticizer. Eur J Pharm Biopharm 2010; 74: 362-370.

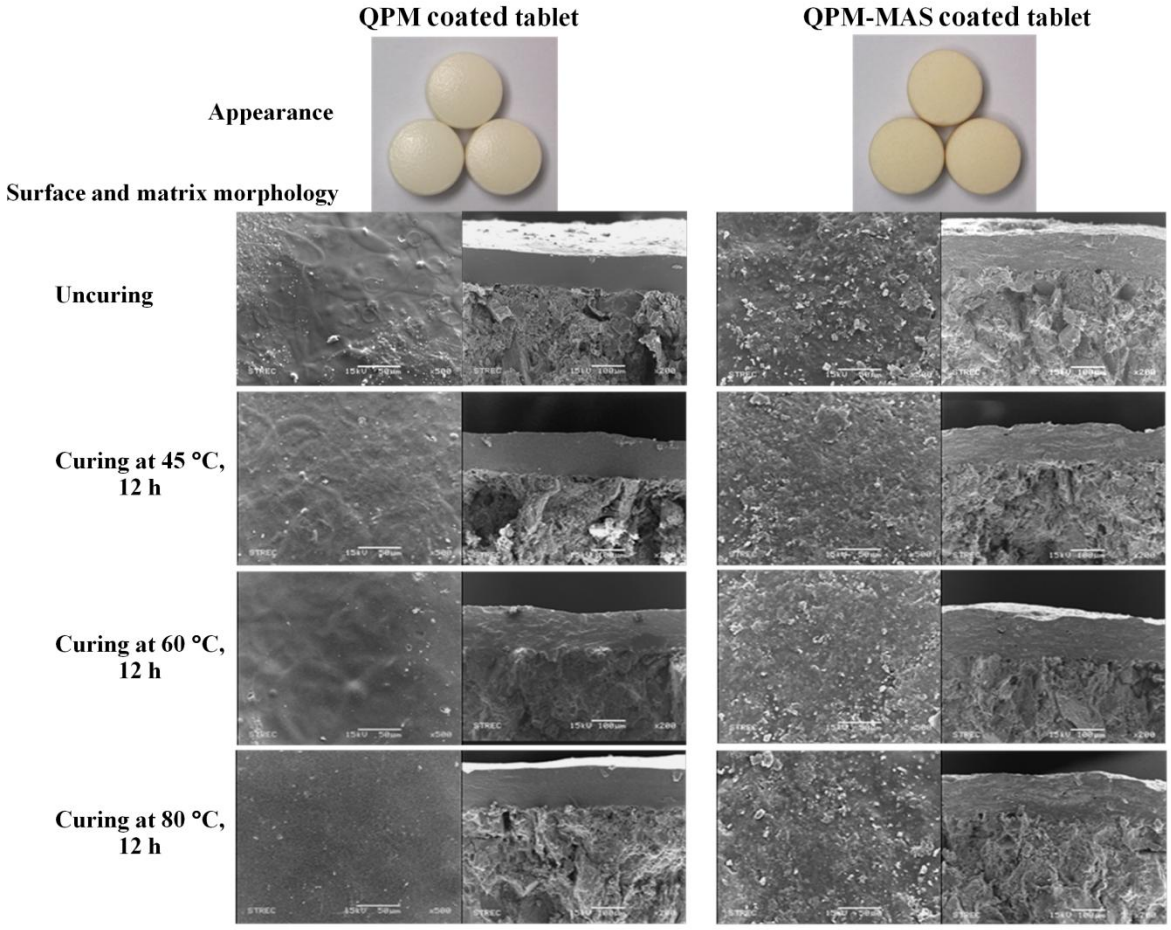


**Figure 1.** Appearance, and surface and matrix morphology of the PPN tablets coated with QPM and QPM-MAS (4:0.75) films with uncuring or curing at different temperatures.

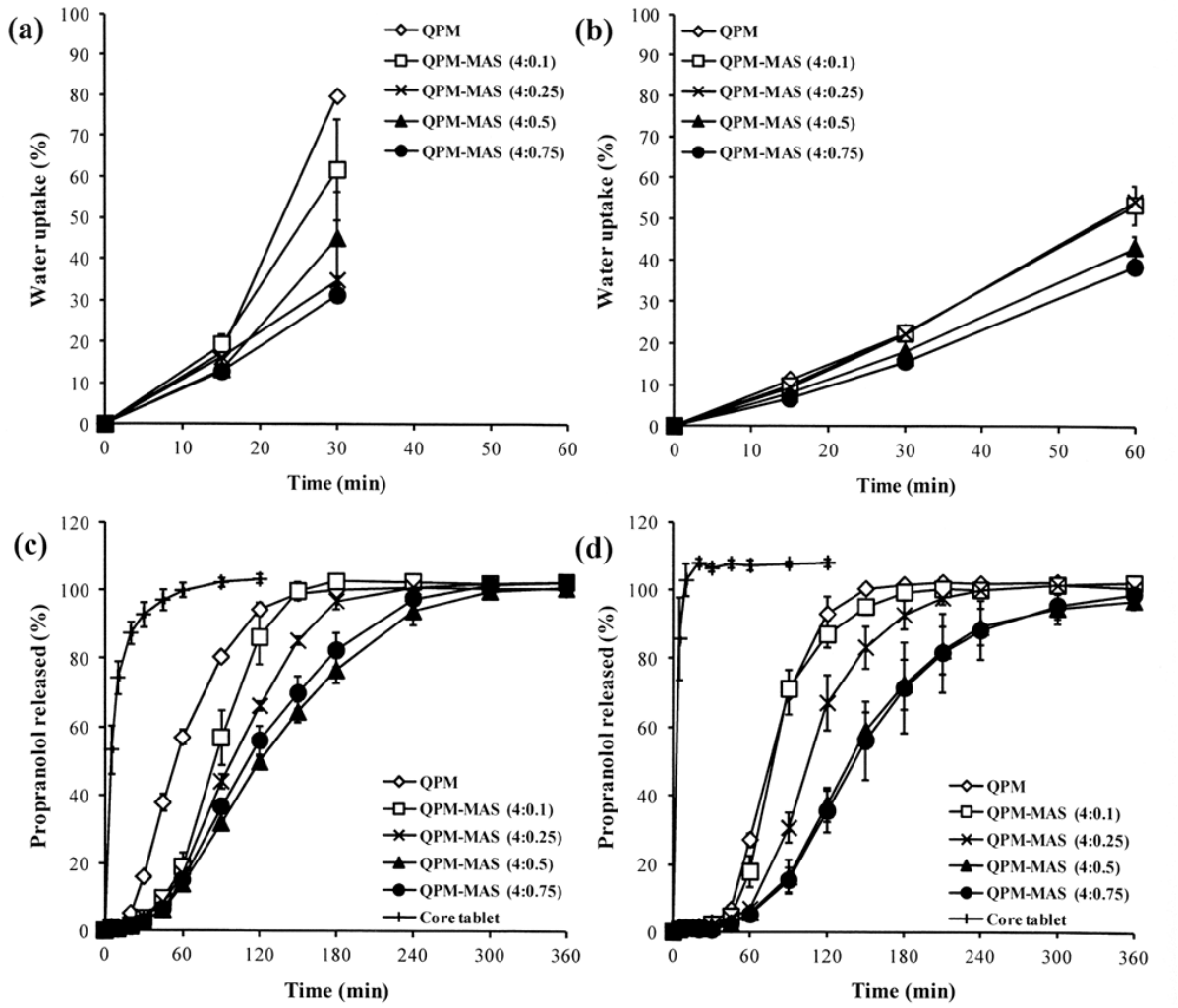


**Figure 2.** Effect of the QPM-MAS ratio on water uptake (a,b) and drug release (c,d) of PPN coated tablets at coating level of 13.1 ± 0.94 mg $cm^{-2}$ in 0.1 M HCl (a,c) and pH 6.8 phosphate buffer (b,d). Mean values ± SD are indicated, n=3.

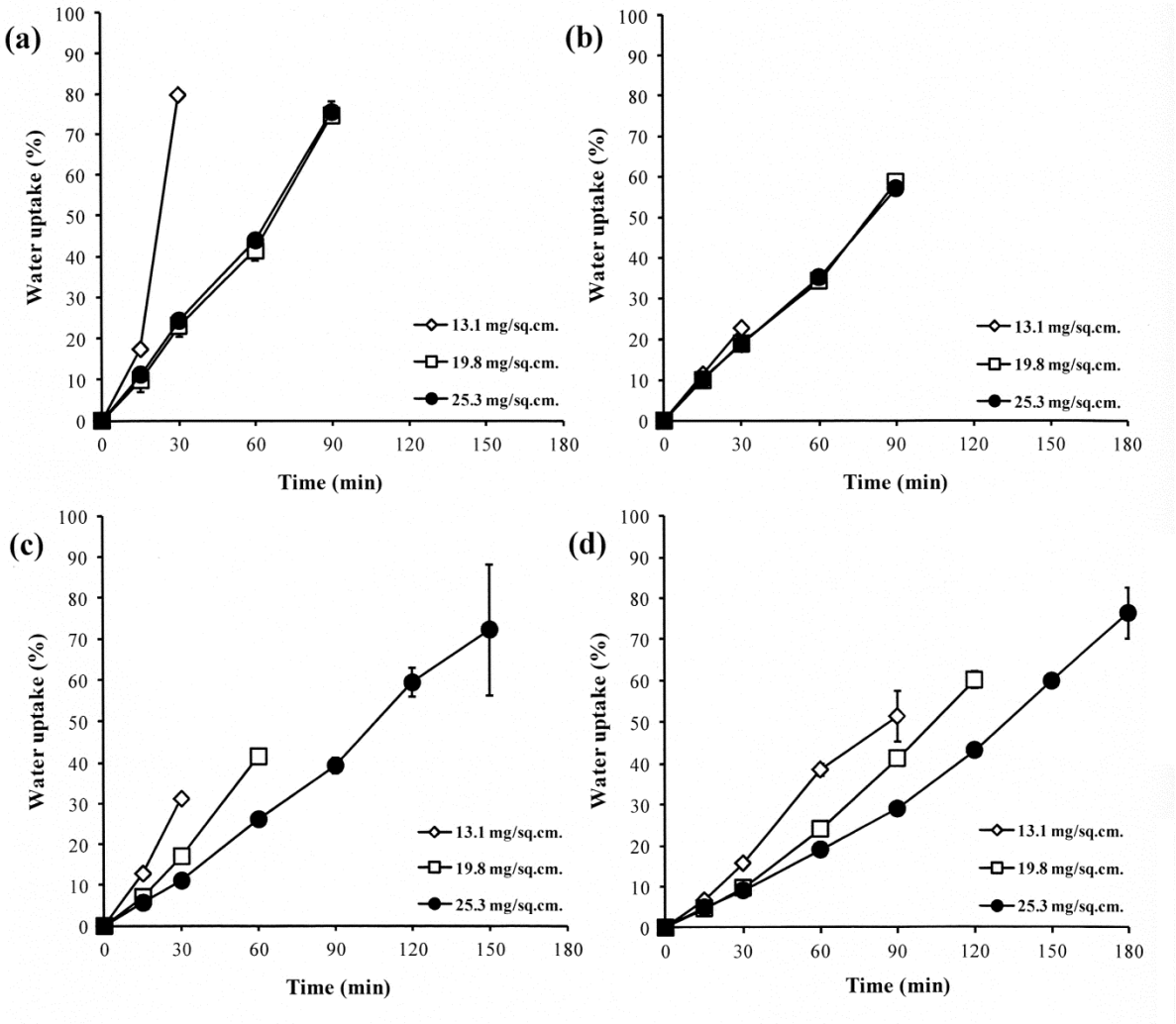


**Figure 3.** Effect of coating level on water uptake of PPN tablets coated with QPM film (a,b) and QPM-MAS (4:0.75) films (c,d) in 0.1 M HCl (a,c) and pH 6.8 phosphate buffer (b,d). Mean values ± SD are indicated, n=3.

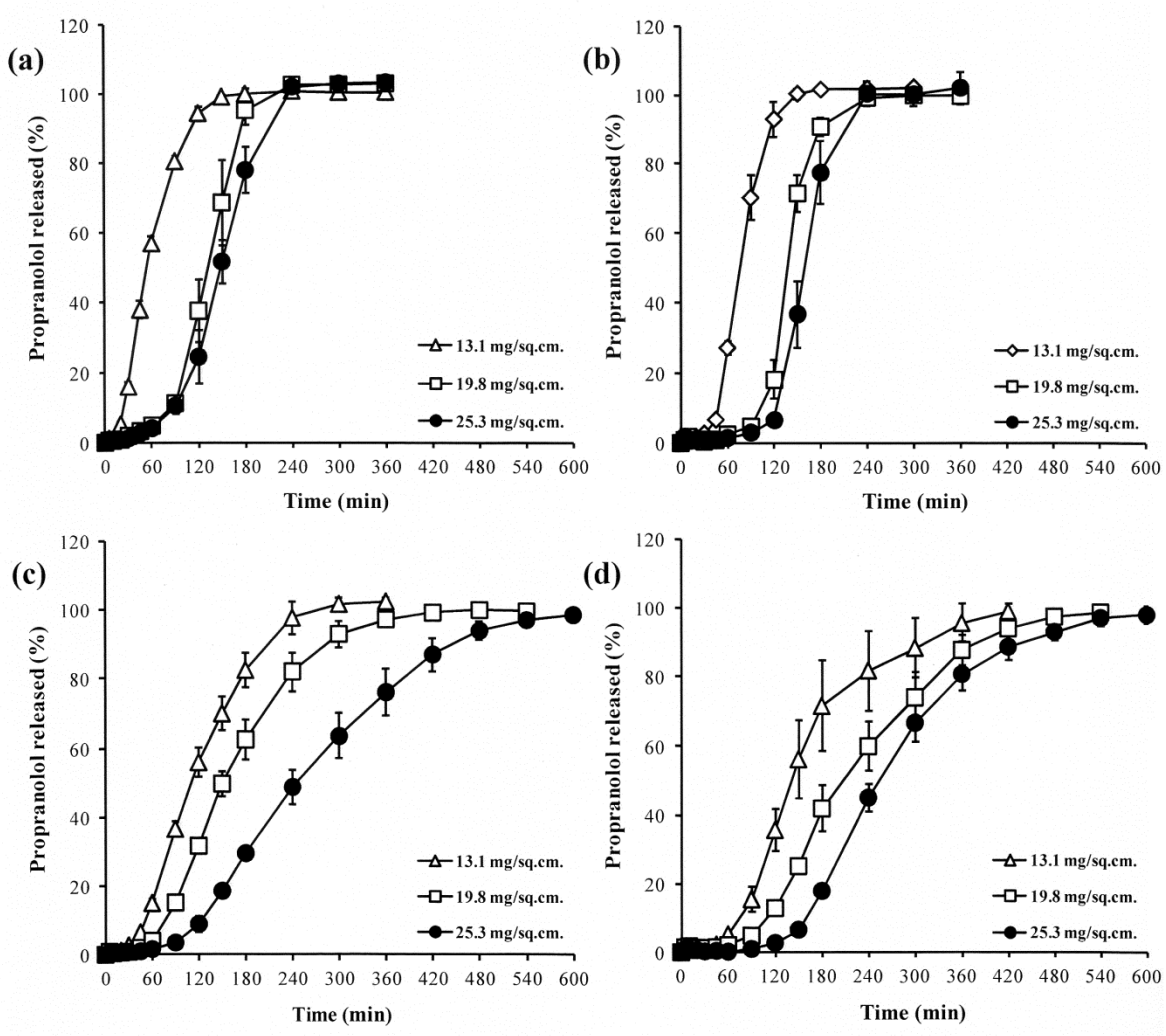


**Figure 4.** Effect of coating level on drug release of PPN tablets coated with QPM film (a,b) and QPM-MAS (4:0.75) films (c,d) in 0.1 M HCl (a,c) and pH 6.8 phosphate buffer (b,d). Mean values ± SD are indicated, n=3.

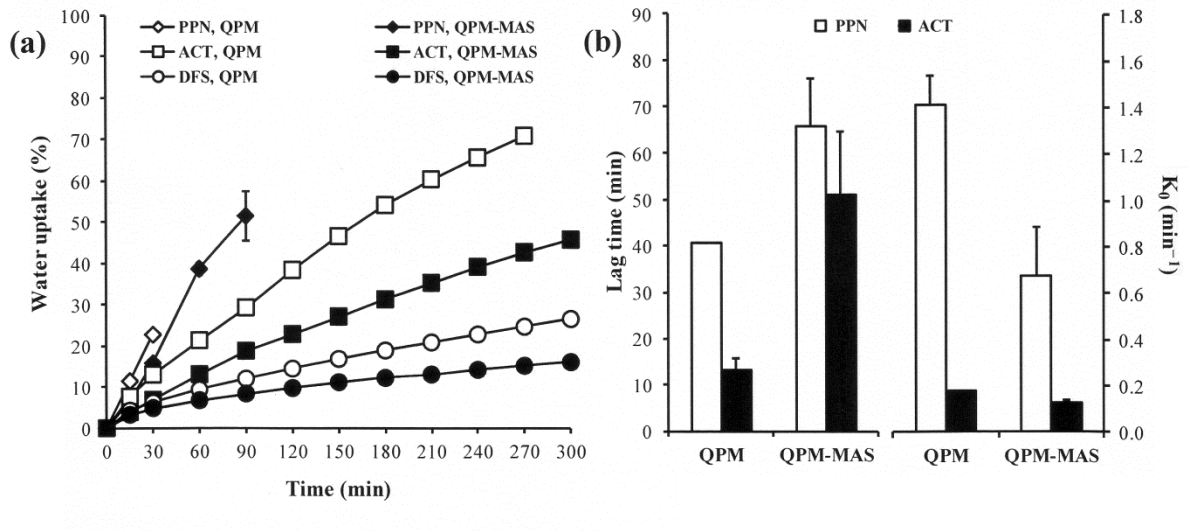


**Figure 5.** Effect of drug type on water uptake (a) and drug release parameters of QPM- and QPM-MAS (4:0.75) tablets in pH 6.8 phosphate buffer. Mean values ± SD are indicated, n=3.

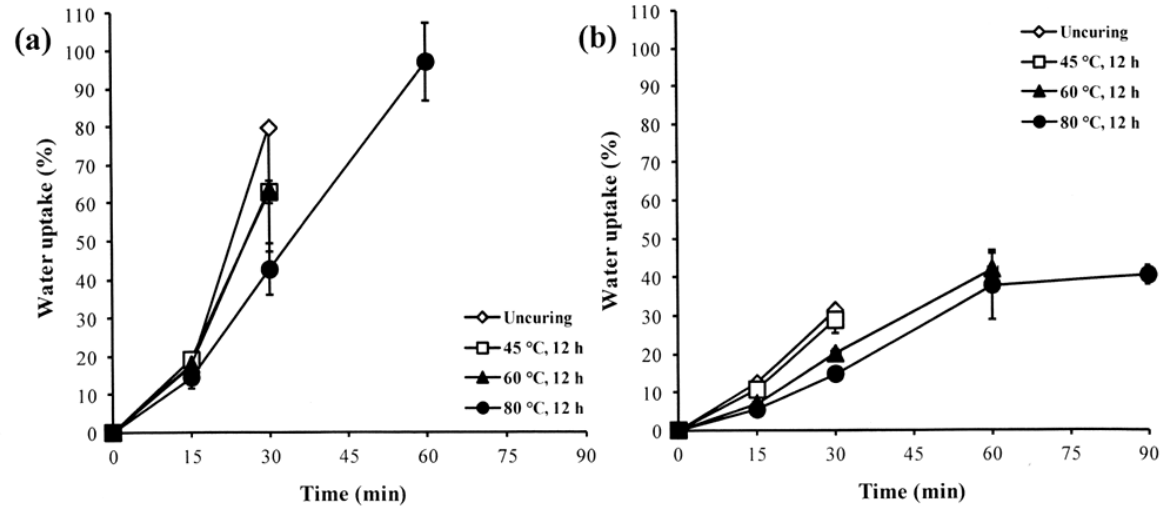


**Figure 6.** Effect of curing temperature on water uptake of PPN tablets coated with QPM (a) and QPM-MAS (4:0.75) films (b) in 0.1 M HCl. Mean values ± SD are indicated, n=3.

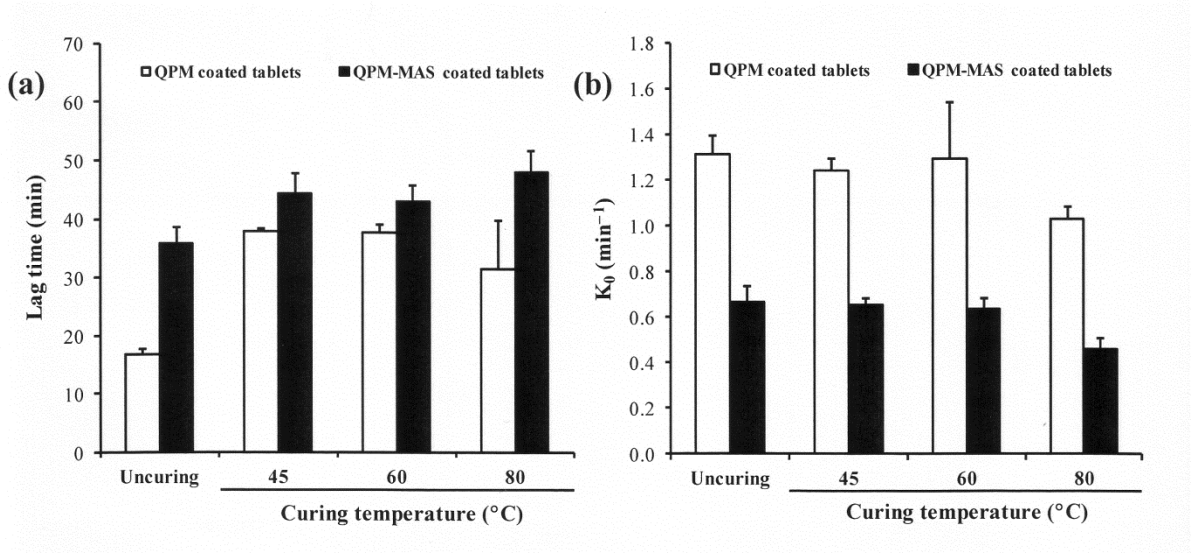


**Figure 7.** Effect of curing temperature on drug release parameters of PPN tablets coated with QPM and QPM-MAS (4:0.75) films in 0.1 M HCl. Mean values ± SD are indicated, n=3.

**Table 1.** PPN release parameters of QPM and QPM-MAS coated tablets at different QPM-MAS ratios and coating levels.

| Investigation factors | 0.1 M HCl | | pH 6.8 phosphate buffer | |
|---|---|---|---|---|
| | Lag time (min) | $K_0$ ($min^{-1}$) | Lag time (min) | $K_0$ ($min^{-1}$) |
| Effect of QPM-MAS ratio | | | | |
| 4:0 | 16.63 ± 1.00 | 1.31 ± 0.08 | 40.47 ± 0.06 | 1.41 ± 0.12 |
| 4:0.1 | 31.54 ± 0.65 | 0.91 ± 0.15 | 44.42 ± 1.41 | 1.52 ± 0.04 |
| 4:0.25 | 35.49 ± 4.94 | 0.79 ± 0.05 | 55.05 ± 1.69 | 1.00 ± 0.14 |
| 4:0.5 | 34.01 ± 1.67 | 0.56 ± 0.03 | 67.04 ± 6.77 | 0.71 ± 0.01 |
| 4:0.75 | 35.85 ± 2.56 | 0.67 ± 0.07 | 65.66 ± 10.32 | 0.68 ± 0.21 |
| Effect of coating level | | | | |
| QPM | | | | |
| 13.1 mg $cm^{-2}$ | 16.63 ± 1.00 | 1.31 ± 0.08 | 40.47 ± 0.06 | 1.41 ± 0.12 |
| 19.8 mg $cm^{-2}$ | 78.91 ± 1.61 | 0.95 ± 0.20 | 91.75 ± 2.18 | 1.11 ± 0.09 |
| 25.3 mg $cm^{-2}$ | 77.92 ± 4.72 | 0.68 ± 0.07 | 116.03 ± 1.88 | 1.18 ± 0.13 |
| QPM-MAS (4:0.75) | | | | |
| 13.1 mg $cm^{-2}$ | 35.85 ± 2.56 | 0.67 ± 0.07 | 65.66 ± 10.32 | 0.68 ± 0.21 |
| 19.8 mg $cm^{-2}$ | 60.18 ± 4.37 | 0.53 ± 0.06 | 96.49 ± 5.09 | 0.51 ± 0.10 |
| 25.3 mg $cm^{-2}$ | 89.89 ± 7.80 | 0.35 ± 0.05 | 133.63 ± 2.58 | 0.41 ± 0.04 |

Data are mean ± SD, n=3.